

Some pages of this thesis may have been removed for copyright restrictions.

If you have discovered material in AURA which is unlawful e.g. breaches copyright, (either yours or that of a third party) or any other law, including but not limited to those relating to patent, trademark, confidentiality, data protection, obscenity, defamation, libel, then please read our [Takedown Policy](#) and [contact the service](#) immediately

SYNTHESIS AND CHARACTERISATION
OF HYDROGEL POLYMERS
FOR MEDICAL APPLICATIONS

RICHARD ALEXANDER YOUNG

Doctor of Philosophy

ASTON UNIVERSITY

September 1998

This copy of the thesis has been supplied on condition that anyone who consults it is understood to recognise that its copyright rests with its author and that no quotation from the thesis and no information derived from it may be published without proper acknowledgement.

ASTON UNIVERSITY

SYNTHESIS AND CHARACTERISATION
OF HYDROGEL POLYMERS
FOR MEDICAL APPLICATIONS

RICHARD ALEXANDER YOUNG

Submitted for the Degree
of Doctor of Philosophy

September 1998

SUMMARY

A fundamental if poorly understood problem that hydrogels display is the tendency of these contact lens materials to dehydrate, causing certain complications of the corneal epithelium. However, recent studies have indicated that the evaporation rate of water from different hydrogel lenses is the same and the severity of conditions such as corneal staining is controlled by the states of water in the material. A study was therefore undertaken which concluded that increased corneal desiccating staining occurred as the proportion of water existing in the bound state decreased. The possibility of using dehydrated hydrogels as packaging materials with desiccating properties has also been investigated. As hydrogels have a high affinity for water they have adequate ability to function as a moisture scavenger in an enclosed atmosphere. It was concluded that this ability is maximised by a high total water content and an increase in the proportion of this water existing in the bound state for the material when it is fully hydrated.

N-vinyl pyrrolidone has a low reactivity in vinyl polymerisation reactions which results in polymers with local domains of the same chemical type which can lead to deposition. As contact lenses comprising of this monomer are susceptible to deposition, a monomer with a higher reactivity in vinyl polymerisations is acryloylmorpholine and its incorporation in favour of NVP is encouraged. Unfortunately a large proportion of high EWC hydrogels are mechanically weak and attempts to increase this property by increasing hydrophobicity or cross-linking results in a decrease in EWC. Monomers with the potential to carry a positive charge were incorporated into a high EWC, AMO-HEMA copolymer and the physical properties were investigated. Although EWC increased mechanical properties decreased only slightly. Therefore simultaneous incorporation of a positively charged monomer and a negatively charged monomer was investigated. The resulting copolymers showed increased water content and increased initial modulus.

A technique for measuring the coefficient of friction of contact lenses during lubrication has been developed. Experiments using artificial tear solutions and multipurpose contact lens cleaning solutions indicate that friction increases with increasing static surface tension

Keywords: hydrogel, corneal staining, cationic, ampholytic, coefficient of friction

To my family

ACKNOWLEDGEMENTS

I would like to take this opportunity to thank the following

Firstly, my supervisor Professor Brian Tighe for his advice and encouragement throughout the course of this project.

All the members of the Biomaterials Research Unit, past and present, who have made my time at Aston a very enjoyable experience including, Ais for her single-minded approach to work even in the face of free alcohol, Andy for his inspirational dedication to work, Bev for showing us the pitfalls of being disorganised, Fi for her long hour commitment to work, Steve for his stamina in extreme drinking sessions, Matt for his puzzle solving ability and many other drinking colleagues and flatmates.

Dr Lyndon Jones for the clinical data regarding corneal staining levels in contact lens wearers.

Dr Vincient Rebeix for dynamic surface tension measurements on ophthalmic solutions.

Smithkline Beecham and EPSRC for their financial support under the Total Technology Scheme.

Finally Melissa Fleming for her patience and support during the period I have been writing up this thesis.

LIST OF CONTENTS

<u>TITLE</u>	<u>PAGE</u>
TITLE PAGE	1
SUMMARY	2
DEDICATION	3
ACKNOWLEDGMENTS	4
LIST OF CONTENTS	5
LIST OF TABLES	14
LIST OF FIGURES	16
LIST OF ABBREVIATIONS	22
CHAPTER 1 INTRODUCTION	23
1.1 Hydrogels	24
1.2 Interpenetrating Polymer Networks	24
1.3 Swelling of Hydrogels	26
1.4 The Structure of Water	26
1.5 Hydrogels as Contact Lenses	28
1.6 Techniques for Studying Water Binding of Hydrogels	30
1.6.1 Differential Scanning Calorimetry	30
1.6.2 Nuclear Magnetic Resonance	32
1.6.3 Ultrasonic Sound	33
1.6.4 Dielectric Spectroscopy	33
1.6.5 Specific Conductivity	34

1.6.6	Dilatometry	34
1.7	Biocompatibility	34
1.8	Wettability	36
1.9	Contact Angle Measurements	39
1.9.1	Dehydrated Surfaces	40
1.9.2	Hydrated Surfaces	41
1.9.2.1	Hamilton's Method	41
1.9.2.2	Captive Air Bubble Method	43
1.10	Mechanical Properties of Hydrogels	44
1.11	Coefficient of Friction	45
1.12	Copolymer Sequence Distribution	46
1.12.1	The Terminal Model of Copolymerisation	47
1.12.2	Computer Simulation of Sequence Distribution	48
1.12.3	The Alfrey-Price Q-e Scheme	49
1.13	The Use of Hydrogels as Desiccant Packaging Materials	50
1.14	Water Sorption	51
1.15	Scope and Objectives	52
CHAPTER 2	MATERIALS AND EXPERIMENTAL TECHNIQUES	54
2.1	Reagents	55
2.2	Preparation of Membranes	60
2.3	Solution Polymerisation	61
2.4	Equilibrium Water Content	63
2.5	Dynamic Vapour Sorption	63
2.6	Differential Scanning Calorimetry	65

2.7	Mechanical Properties	67
2.8	Contact Angles	69
2.8.1	Sessile Drop Technique	69
2.8.2	Hamilton Method	70
2.8.3	Captive Air Bubble Technique	70
2.8.4	Dynamic Contact Angle Measurement	70
2.9	Static Surface Tension	72
2.10	Dynamic Surface Tension	73
2.11	Coefficient of Friction	74
2.12	Copolymer Sequence Distribution	75
CHAPTER 3	HYDROGEL CONTACT LENSES - WATER BINDING AND CORNEAL STAINING	79
3.1	Introduction	80
3.2	Techniques to Study the Water Structuring of Hydrogel Contact Lenses	83
3.3	Materials and Methods	85
3.4	Clinical Protocol	85
3.5	Physical Properties	87
3.6	Results	89
3.7	Investigation of Contact Lenses Cleaned in “ReNu” Multipurpose Solution	89
3.8	Investigation of Contact Lenses Cleaned in a Peroxide Based System	92

3.9	Effect of Solution Characteristics on Water Structuring for Contact Lenses	96
3.10	Conclusions	98
CHAPTER 4	HYDROGELS WITH DESICCATING PROPERTIES FOR PHARMACEUTICAL PACKAGING	101
4.1	Introduction	102
4.2	Experimental	105
4.3	Preliminary Evaluations	105
4.3.1	Materials	105
4.3.2	Results	106
4.3.3	Discussion	109
4.3.4	Conclusions	112
4.4	Evaluation of Contact Lenses	112
4.4.1	Materials	113
4.4.2	Results	115
4.4.3	Discussion	115
4.4.4	Conclusion	116
4.5	Evaluation of Specifically Designed Formulations	116
4.5.1	Materials	116
4.5.2	Results	116
4.5.3	Discussion	118
4.5.4	Conclusions	121
4.6	Effect of Incorporation of Interpenetrant	122
4.6.1	Materials	122

4.6.2	Results	123
4.6.3	Discussion	123
4.6.3.1	Moisture Absorbency	123
4.6.3.2	Water Structuring	125
4.6.3.3	Mechanical Properties	126
4.6.4	Conclusions	127
4.7	Chapter Conclusions	128
CHAPTER 5	HIGH EQUILIBRIUM WATER CONTENT ACRYLOYLMORPHOLINE HYDROGELS INCORPORATING BASIC MONOMERS	130
5.1	Introduction	131
5.2	Acryloylmorpholine as a New Hydrophilic Monomer	132
5.2.1	Reactivity and Sequence Distribution	132
5.2.2	Physical Properties	135
5.3	Charged Monomers	136
5.4	Materials and Methods	138
5.5	Effect of Incorporation of Cationic Monomers on the Water Structuring of AMO:HEMA Hydrogel Copolymers	139
5.5.1	Results and Discussion	139
5.5.2	Conclusions	145
5.6	Effect of Incorporation of Cationic Monomers on the Mechanical Properties of AMO:HEMA Hydrogel Copolymers	146
5.6.1	Introduction	146
5.6.2	Results and Discussion	147

5.6.3	Conclusions	151
5.7	Effect of Incorporation of Cationic Monomers on the Surface Properties of AMO:HEMA Hydrogel Copolymers	152
5.7.1	Introduction	152
5.7.2	Surface Properties of Dehydrated Hydrogels Containing Cationic Monomers	152
5.7.3	Surface Properties of Hydrated Hydrogels Containing Cationic Monomers	154
5.7.4	Advancing and Receding Contact Angles for Hydrogels Containing Cationic Monomers	156
5.7.5	Conclusions	158
5.8	Summary Conclusions	158
CHAPTER 6	HIGH EQUILIBRIUM WATER CONTENT ACRYLOYLMORPHOLINE HYDROGELS INCORPORATING BASIC AND ACIDIC MONOMERS	160
6.1	Introduction	161
6.2	Materials and Methods	164
6.3	Water Binding Properties	164
6.3.1	Effect of Incorporation of NVI and Itaconic Acid on Water Binding Properties in a AMO:HEMA (70:30) Copolymer	165
6.3.2	Effect of Incorporation of NVI and SPI on Water Binding Properties in a AMO:HEMA (70:30) Copolymer	167

6.3.3	Effect of Incorporation of NVI and Methacrylic Acid on Water Binding Properties in a AMO:HEMA (70:30) Copolymer	169
6.3.4	Conclusions	170
6.4	Mechanical Properties	171
6.4.1	Effect of Incorporation of NVI and Itaconic Acid on Mechanical Properties in a AMO:HEMA (70:30) Copolymer	171
6.4.2	Effect of Incorporation of NVI and SPI on Mechanical Properties in a AMO:HEMA (70:30) Copolymer	173
6.4.3	Effect of Incorporation of NVI and Methacrylic Acid on Mechanical Properties in a AMO:HEMA (70:30) Copolymer	175
6.4.4	Conclusions	177
6.5	Surface Properties	178
6.5.1	Surface Properties in a AMO:HEMA (70:30) Copolymer Containing NVI and Itaconic Acid in the Dehydrated State	178
6.5.2	Surface Properties in a AMO:HEMA (70:30) Copolymer Containing NVI and Itaconic Acid in the Hydrated State	180
6.5.4	Conclusions	182
6.6	Summary Conclusions	183

CHAPTER 7	COEFFICIENT OF FRICTION OF ACUVUE CONTACT LENSES	186
7.1	Introduction	187
7.2	Lubrication	189
7.3	Coefficient of Friction	190
7.4	Measurement of Coefficient of Friction of Contact Lenses	190
7.5	Development of Equipment for Measuring Coefficient of Friction of Contact Lenses	194
7.6	Multipurpose Solutions	197
7.6.1	Introduction	197
7.6.2	Components	197
7.6.3	Materials	199
7.6.4	Methods	200
7.6.5	Results	200
7.6.6	Discussion	201
7.6.7	Conclusions	205
7.7	Artificial Tear Solutions	205
7.7.1	Introduction	205
7.7.2	The Precorneal Tear Film	206
7.7.3	Tear Film Abnormalities	206
7.7.4	Tear Substitutes	207
7.7.5	Materials	208
7.7.6	Methods	209
7.7.7	Results	210
7.7.8	Discussion	210

7.7.9	Conclusion	214
7.8	Chapter Conclusions	214
CHAPTER 8	CONCLUSIONS AND SUGGESTIONS FOR FURTHER WORK	216
8.1	Conclusions	217
8.2	Suggestions for Further Work	225
	LIST OF REFERENCES	227
	APPENDICES	237

LIST OF TABLES

Table 1.1	Some terms used in water binding studies	27
Table 1.2	Polar and dispersive components for water and diiodomethane	41
Table 2.1	Molecular weights and suppliers of reagents used	55
Table 2.2	Example of summary table for sequence distribution simulation	78
Table 3.1	FDA classification of commercially available contact lenses	84
Table 3.2	Suppliers and characteristics of hydrogel contact lenses used in this study	85
Table 3.3	Grading system for corneal staining	87
Table 4.1	Compositions and results for first set of samples	106
Table 4.2	Composition of the second set of samples	113
Table 4.3	Composition and water uptake for third set of samples	117
Table 4.4	Water binding and mechanical properties of third set of samples	117
Table 5.1	Composition of some commercially available high EWC contact lenses	131
Table 5.2	Reactivity ratios for copolymers of N-containing monomers and HEMA	133
Table 5.3	Sequence simulation results for copolymers of HEMA:nitrogen containing monomer (70:30) for AMO, NVP and NNDMA	133
Table 5.4	The feed ratio and actual ratio of monomers in a number of HEMA copolymers	135
Table 7.1	Surface chemistry and frictional properties of ophthalmic polymer solutions	191
Table 7.2	Composition of multipurpose solutions investigated	200

Table 7.3	Biotribology and surface chemistry results for multipurpose solutions	201
Table 7.4	Compositions of artificial tear solutions investigated	209
Table 7.5	Biotribology and surface chemistry results for artificial tear solutions	210

LIST OF FIGURES

Figure 1.1	Schematic representation of a differential scanning calorimeter	31
Figure 1.2	Advancing and receding contact angle situations	37
Figure 1.3	Hysteresis cycle for Polybutadiene	38
Figure 1.4	Hysteresis cycle for dehydrated poly(HEMA)	38
Figure 1.5	Individual components of the solid surface free energy	40
Figure 1.6	Individual free energy components for Hamiltons method	42
Figure 1.7	Individual free energy components for the captive air bubble technique	43
Figure 2.1	Structures of reagents used	56
Figure 2.2	Diagram of a membrane mould	60
Figure 2.3	Solution polymerisation apparatus	62
Figure 2.4	Schematic diagram of DVS flow stream of controlled humidity	64
Figure 2.5	An example of a thermogram obtained from DSC	66
Figure 2.6	Dimensions of a hydrogel sample for mechanical testing	67
Figure 2.7	An example of a stress-strain curve obtained from the tensometer	68
Figure 2.8	Schematic diagram of the dynamic contact angle analyser	71
Figure 2.9	Diagram of a dynamic contact angle hysteresis curve, illustrating a two immersion cycle	72
Figure 2.10	Apparatus for measurement of the coefficient of friction of contact lenses	75
Figure 2.11	Example of a sequence simulation for a hydrogel copolymer	77
Figure 3.1	The EWC and centre thickness for hydrogel contact lenses	88

Figure 3.2	Mean stain score and centre thickness (Tc) for contact lenses cleaned in ReNu multipurpose solution	89
Figure 3.3	Mean stain score and EWC for contact lenses cleaned in ReNu multipurpose solution	90
Figure 3.4	EWC/centre thickness and inverse stain score for contact lenses cleaned in ReNu multipurpose solution	91
Figure 3.5	Percent fraction of bound water and mean stain score for contact lenses cleaned in ReNu multipurpose solution	92
Figure 3.6	Mean stain score and centre thickness (Tc) for contact lenses cleaned in a peroxide based cleaning system	93
Figure 3.7	Mean stain score and EWC for contact lenses cleaned in a peroxide based cleaning system	94
Figure 3.8	Mean stain score and percent fraction of bound water for contact lenses cleaned in a peroxide based cleaning system	94
Figure 3.9	The percentage of the EWC present as bound water for contact lenses cleaned in ReNu after soaking in a range of solutions	96
Figure 3.10	The percentage of the EWC present as bound water for contact lenses cleaned in a peroxide based system after soaking in a range of solutions	97
Figure 4.1	Diagram of product vial	104
Figure 4.2	Moisture uptake profile for first set of hydrogels	107
Figure 4.3	Sustained exposure of hydrogel samples	108
Figure 4.4	Moisture uptake of hydrogel over extended relative humidity	110
Figure 4.5	Moisture uptake/loss profile of hydrogel over a range of relative humidities	111

Figure 4.6	Moisture uptake profile for second set of hydrogels	114
Figure 4.7	The structure of the urethane unit	123
Figure 4.8	Comparison of moisture absorption/desorption isotherms for IPN hydrogels	124
Figure 4.9	Water structuring properties for a desiccating hydrogel with increasing polyurethane interpenetrant content	126
Figure 4.10	Mechanical properties for a desiccating hydrogel with increasing polyurethane interpenetrant content	127
Figure 5.1	The resonance stabilisation structure of AMO and NNDMA	134
Figure 5.2	The equilibrium water content of AMO:HEMA (70:30) copolymers containing increasing amounts of cationic monomers	140
Figure 5.3	The total water expressed per mole of polymer in AMO:HEMA (70:30) copolymers with increasing amounts of cationic monomers	141
Figure 5.4	The water binding properties of AMO:HEMA (70:30) copolymers containing increasing amounts of NVI	142
Figure 5.5	The water binding properties of AMO:HEMA (70:30) copolymers containing increasing amounts of DMAEMA	142
Figure 5.6	The water binding properties of AMO:HEMA (70:30) copolymers containing increasing amounts of DMAEA	144
Figure 5.7	The water binding properties of AMO:HEMA (70:30) copolymers containing increasing amounts of pyridine-N-oxide	144
Figure 5.8	The water binding properties of AMO:HEMA (70:30) copolymers containing increasing amounts of 4-vinyl pyridine	145

Figure 5.9	The mechanical properties of AMO:HEMA (70:30) copolymers containing increasing amounts of NVI	148
Figure 5.10	The mechanical properties of AMO:HEMA (70:30) copolymers containing increasing amounts of DMAEMA	149
Figure 5.11	The mechanical properties of AMO:HEMA (70:30) copolymers containing increasing amounts of DMAEA	149
Figure 5.12	The mechanical properties of AMO:HEMA (70:30) copolymers containing increasing amounts of pyridine-N-oxide	150
Figure 5.13	The mechanical properties of AMO:HEMA (70:30) copolymers containing increasing amounts of 4-vinyl pyridine	151
Figure 5.14	The surface free energy of dehydrated AMO:HEMA (70:30) copolymers containing increasing amounts of cationic monomers	153
Figure 5.15	The components of the surface free energy for AMO:HEMA (70:30) copolymer with increasing amounts of NVI in the hydrated state	155
Figure 5.16	The polar and dispersive components of the surface free energy for AMO:HEMA (70:30) copolymer with increasing amounts of DMAEMA and DMAEA in the hydrated state	155
Figure 5.17	The hysteresis of AMO:HEMA (70:30) copolymers containing increasing amounts of cationic monomers	157
Figure 6.1	The water binding of AMO:HEMA (70:30) copolymers containing different ratios of NVI and itaconic acid at 5% w/w	165
Figure 6.2	The water binding of AMO:HEMA (70:30) copolymers containing NVI and itaconic acid in a ratio of 1:2 at various incorporation levels	167

Figure 6.3	The water binding of AMO:HEMA (70:30) copolymers containing different ratios of NVI and SPI at 5% w/w	168
Figure 6.4	The water binding of AMO:HEMA (70:30) copolymers containing different ratios of NVI and methacrylic acid at 5% w/w	169
Figure 6.5	The mechanical properties of AMO:HEMA (70:30) copolymers containing different ratios of NVI and itaconic acid at 5% w/w	172
Figure 6.6	The mechanical properties of AMO:HEMA (70:30) copolymers containing NVI and itaconic acid in a ratio of 1:2 at various incorporation levels	173
Figure 6.7	The mechanical properties of AMO:HEMA (70:30) copolymers containing different ratios of NVI and SPI at 5% w/w	175
Figure 6.8	The mechanical properties of AMO:HEMA (70:30) copolymers containing different ratios of NVI and methacrylic acid at 5% w/w	176
Figure 6.9	The total surface free energy of dehydrated AMO:HEMA (70:30) copolymers containing different ratios of NVI and itaconic acid at 5% w/w	179
Figure 6.10	The total surface free energy of dehydrated AMO:HEMA (70:30) copolymers containing NVI and itaconic acid in a ratio of 1:2 at various incorporation levels	180
Figure 6.11	The surface properties of hydrated AMO:HEMA (70:30) copolymers containing different ratios of NVI and itaconic acid at 5% w/w	181

Figure 6.12	The surface properties of hydrated AMO:HEMA (70:30) copolymers containing NVI and itaconic acid in a ratio of 1:2 at various incorporation levels	181
Figure 6.13	The initial modulus as a function of EWC for AMO:HEMA (70:30) copolymers containing various charged monomers	185
Figure 7.1	Typical Stribeck curve for metal surfaces	190
Figure 7.2	Determination of the static coefficient of friction between a RGP contact lens and a corneal model	192
Figure 7.3	Schematic diagram of original testing equipment	194
Figure 7.4	Schematic diagram of 1 st modification of testing equipment	195
Figure 7.5	Schematic diagram of final modification of testing equipment	196
Figure 7.6	Static surface tension values and dynamic surface tension as a function of rate of bubble formation for multipurpose contact lens solutions	202
Figure 7.7	Biotribology properties and surface tension values for a range of multipurpose contact lens solutions	204
Figure 7.8	Static surface tension values and dynamic surface tension as a function of rate of bubble formation for tear substitutes	211
Figure 7.9	Biotribology properties and surface tension values for a range of artificial tear solutions	213

LIST OF ABBREVIATIONS

AMO	Acryloylmorpholine	AZBN	Azo-bis-isobutyronitrile
CCLRU	Cornea and Contact Lens Research Unit	DMAEA	Dimethylaminoethyl acrylate
DMAEMA	Dimethylaminoethyl methacrylate	DSC	Differential Scanning Calorimetry
DST	Dynamic Surface Tension	DVS	Dynamic Vapour Sorption
EEMA	Ethoxyethyl methacrylate	EGDMA	Ethylene glycol dimethacrylate
EWC	Equilibrium Water Content	FDA	Food & Drug Administration
HEMA	2-Hydroxyethyl Methacrylate	IPN	Interpenetrating Polymer Networks
ITA	Itaconic acid	MAA	Methacrylic acid
MPEGMA	Methoxy polyethylene glycol methacrylate	MEMA	Methoxyethyl methacrylate
MMA	Methyl methacrylate	NMR	Nuclear Magnetic Resonance
NNDMA	N, N-dimethylacrylamide	NVI	N-vinyl imadazole
NVP	N-vinyl pyrrolidone	PNO	Pyridine-N-oxide
PEGDMA	Polyethylene glycol dimethacrylate	RH	Relative Humidity
SPI	Sulphopropyl ester of itaconic acid (K salt)	SST	Static Surface Tension
4-VP	4-Vinyl pyridine	Tc	Centre thickness
θ	Contact Angle	μ	Coefficient of friction
γ	Surface Tension		

CHAPTER 1

INTRODUCTION

1.1 Hydrogels

Hydrogels are cross-linked, hydrophilic polymer networks that become highly swollen in the presence of water or biological fluids. The preparation of synthetic hydrogels was first reported by Wichterle and Lim¹ who observed the unique behaviour of these materials and their potential for use as biomaterials. The characteristics of a hydrogel are highly dependent on the amount of water that it absorbs, giving specific mechanical, surface and permeability properties. For a specific hydrogel, the combination of these properties is extremely important in selecting a material's suitability for any particular application.

The amount of water absorbed by a hydrogel can be controlled in three basic ways giving properties most suited to a particular application.

1. Copolymerisation of the main hydrophilic monomer with other monomers which possess different levels of hydrophilicity.
2. Altering the cross-linking density.
3. Altering the conditions under which the polymer is formed.

More sophisticated methods for increasing the mechanical strength of these materials include the formation of interpenetrating polymer networks², fibre reinforcement, composites³ and reinforcement via crystallite formation.

Although the properties of hydrogels have been exploited most successfully in their use as soft contact lenses, this is not their only commercial application. In recent years there has been a great amount of interest in hydrogels for biomedical and pharmaceutical applications⁴⁻¹³. To date these include synthetic articular cartilage⁸, drug delivery systems⁹, wound dressings¹⁰, artificial muscles and tendons¹¹, and membranes for reverse osmosis and kidney dialysis¹².

1.2 Interpenetrating Polymer Networks

Interpenetrating Networks (IPN's) have been defined as a combination of two polymers each in network form, at least one of which has been synthesised and/or

cross-linked in the presence of the other². Varying methods are used to synthesise IPN's and this, in turn, determines the class of IPN produced. These methods are:-

1. Monomer I is polymerised and cross-linked to give a polymer which is then swollen with monomer II plus its own cross-linker and initiator. Polymerisation of monomer II *in situ* produces a true IPN.
2. If only one polymer in the system is cross-linked the network formed is called a semi-IPN.
3. Simultaneous polymerisation of a solution of both monomers with their cross-linkers and initiators, by two different, non-interfering methods produces a simultaneous-IPN or SIN.

Although these materials are known as interpenetrating polymer networks, it is only if there is total mutual solubility that full intermolecular interpenetration occurs. In most IPN's there is some phase separation, although this may be reduced by chain entanglement between the polymers.

The synthesis used for the hydrogel semi-IPN's prepared in this work is where a preformed linear polymer is dissolved in a hydrophilic monomer and cross-linking agent mixture which is subsequently polymerised. In this way a synthetic hydrogel network is formed around a primary polymer chain with the non cross-linked polymer modifying the behaviour of the hydrogel. The use of interpenetration techniques provides an interesting way of modifying the properties of hydrogels. The most obviously beneficial effects relate to mechanical behaviour but, water binding and surface properties are also affected. The initial solubility of the polymer and matrix monomer governs the first essential step in semi-IPN formation. This process can be assisted by the use of non-reactive solvents that are subsequently removed, but this has no beneficial effect on the compatibility of matrix and polymer in the dehydrated state. As compatibility is increased, initial phase separation takes place later during the polymerisation of the second component. As a consequence greater mixing of the two networks takes place, and more interpenetration on a molecular scale may be found in the final product. Compatibility considerations in the hydrated semi-IPN's are quite separate, involving water as the essential third component. Translucence in the hydrated systems is generally due to preferential water clustering around the more hydrophilic moieties to the exclusion of hydrophobic blocks.

Although high water content, optically clear semi-IPN's would be useful in ophthalmic applications, translucent or opaque materials are of potential value in applications such as wound dressings and synthetic articular cartilage. The marked effect that semi-IPN formation has in increasing initial modulus and tensile strength at the expense of elasticity is of considerable interest, since these are the characteristic ways in which biological composite hydrogels differ from their homogeneous synthetic counterparts.

1.3 Swelling of Hydrogels

The total amount of water that a hydrogel absorbs is expressed as the equilibrium water content (EWC) and it is defined as

$$\text{EWC} = \frac{\text{Weight of water in the gel}}{\text{Total weight of the hydrated gel}} \times 100 \quad \text{Equation 1.1}$$

The EWC is probably the most important property of a hydrogel as it dictates the particular mechanical, transport and surface properties that a specific hydrogel will possess. However, it has been observed with calorimetric techniques that at low temperatures only part of the water in the hydrogel network freezes¹³. A proportion of water exists in a state of high mobility that readily freezes at low temperatures while the remainder does not freeze as temperature is lowered.

1.4 The Structure of Water

Water molecules form a continuous network with between four and five mutually associated molecules arranged in the form of strongly hydrogen bonded tetrahedral clusters¹⁴. Each cluster also has strained or broken hydrogen bonds with other water molecules. This system undergoes continuous topological rearrangements with water molecules fluctuating between the clusters and the rest of the network. This fluctuation of water molecules can be affected by changes in temperature and by addition of solutes.

To describe the structure and dynamics of water surrounding biomolecules, protein chemists refer to the adjacent interfacial water layer as the “hydration A-shell”. In this layer, water is primarily associated with polar groups. This represents the minimal amount of water required to maintain the activity and native conformation of proteins¹⁵. Water molecules that are at a transition between the “A-shell” and the bulk water is called the “B-shell”. The water molecules in the A-shell are not permanently attached to the proteins due to the continuous rearrangements but they are hydrogen bonded strongly enough as to be unable to act as solvent for other molecules. Only bulk water and water molecules in the B-shell, have the motion to transport hydrated solutes.

Different terms are adopted by polymer chemists to describe the properties of water in the polymeric environment, some of which are shown in table 1.1 below. Water in polymer systems corresponding to the A-shell and bulk water are described as “bound” and “free” respectively, while the terms intermediate or interfacial are used for the B-shell¹³. The term bound water is associated with water molecules which have direct hydrogen bonding with the polar groups of the polymer or, water molecules that strongly interact with ionic residues of the polymer matrix. Free water molecules do not interact with the polymer matrix and have the same level of hydrogen bonding as pure water. Intermediate water freezes at a lower temperature than pure water and this temperature varies depending on the amount of water present. Many techniques have been used to study the water within hydrogels and it has been found to exist in a continuum of states between the extremities of bound and free¹⁶⁻³⁸.

Table 1.1 Some terms used in water binding studies

Bound Non-freezing		Free Freezing	
Bound	Intermediate	Free	
Primary bound	Secondary bound		
Tightly bound	Interfacial	Bulk	
A-shell	B-shell		

1.5 Hydrogels as Contact Lenses

Hydrogels have been used extensively as a material for contact lenses due to the unique properties that these materials possess. Although numerous papers have been written about the use of hydrogels as contact lenses and the performance and patient comfort of lenses, very few papers have examined the frictional characteristics of hydrogel contact lenses³⁹. Since these lenses dehydrate during wear⁴⁰, it would also be advantageous to investigate frictional changes during dehydration and to look at how hydrogel structure affects both dehydration and hydration.

Dehydration of contact lenses during wear is a phenomenon that can have significant effects upon the hydrogel material. These effects include changing lens optics and lens mass⁴¹, refractive index⁴², curvature, power and fit⁴³. Lens dehydration can also account for epithelial defects, especially in wearers of thinner, high water content contact lenses^{44,45} and these place the patient at risk from corneal infection. These defects, evidenced by corneal dehydration or desiccation staining and erosions, limit the development of these lens types. Nevertheless, for extended wear applications, thin, high water content lenses provide higher levels of oxygen to the cornea, resulting in decreased overnight edema⁴⁶. As a result, lens dehydration has been the subject of studies aimed at identifying the factors that control the dehydration process⁴⁰⁻⁵⁸. Attempts have been made to find a correlation between water content and the extent of lens dehydration on the eye during wear⁴⁷⁻⁴⁹. However lens water content is only a crude predictor of a materials ability to dehydrate during wear since marked departures from the expected correlation have been observed⁵⁷. It has been suggested that there is a material dependent component to lens dehydration⁵⁸.

Hydrogel contact lenses are prepared by polymerisation of monomers containing hydrophilic groups, the polymer may contain either one, or several monomer types. Cross-linking agents used in the process also influence the physiochemical properties. The resulting polymer has two important characteristics. First is the loose, flexible three-dimensional structure of the polymer backbone, attributed to the presence of relatively few cross-links. The second is the strong affinity of the polymer for water, attributed to the presence of hydrophilic groups on the polymer chains. The ability of

the polymer material to absorb and hold water is a result of these features. Water has a strong affinity for hydrogel materials because it can penetrate the flexible matrix and interact with or hydrate the hydrophilic groups.

A number of factors influence water evaporation from hydrogel lenses⁵⁷, including lens thickness, ambient environment, tear film characteristics, eyelid position, time of wear and blink rate as well as individual patient factors. The great patient-to-patient variability of lens dehydration may be the result of variations in the concentrations of lipids and proteins in tears⁴¹.

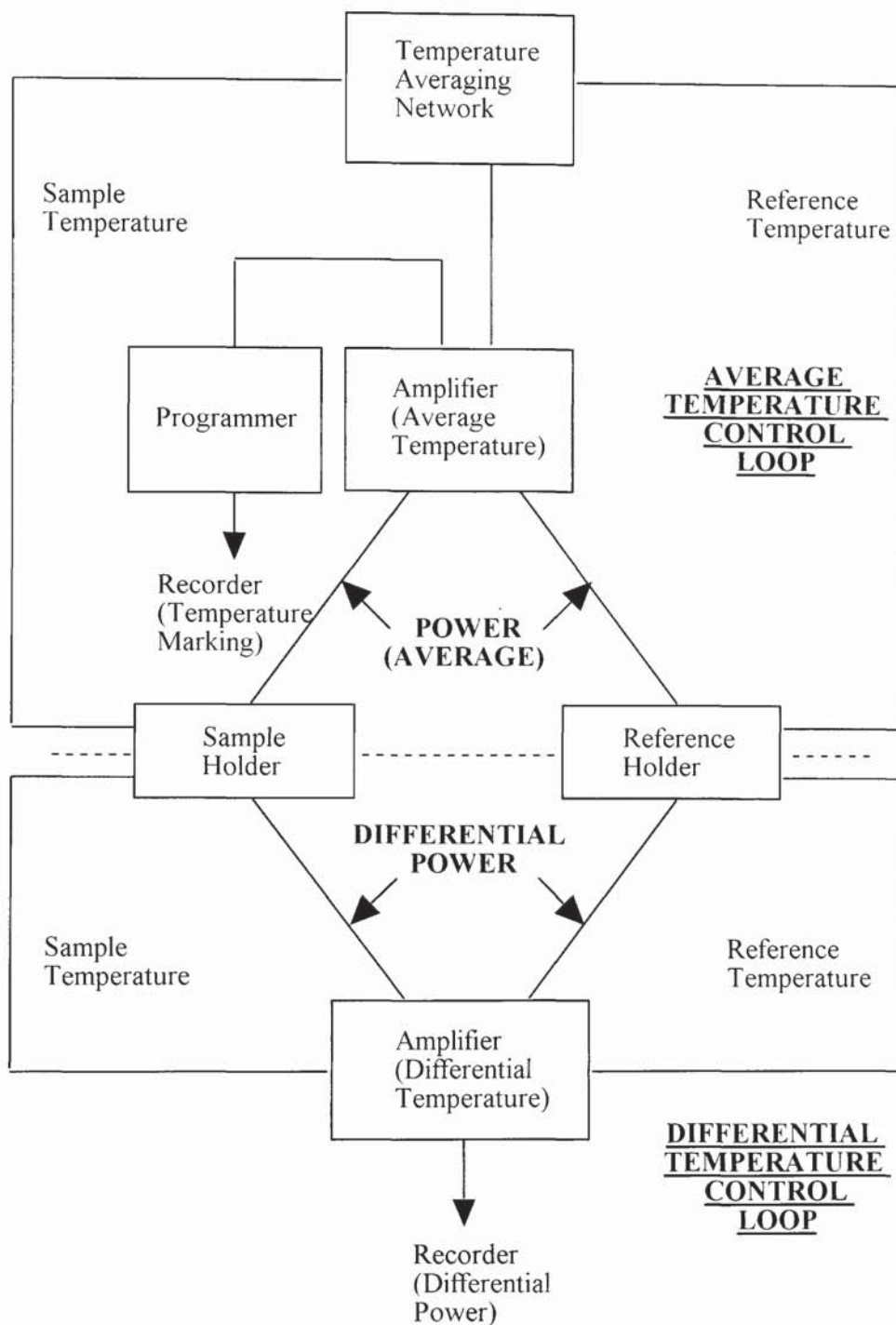
It is possible to selectively vary the water content of hydrogel lenses over a considerable range by varying the composition of the monomers. The number and distribution of cross links also affects the water content of the lenses. It is therefore reasonable to expect that the degree of water loss during wear will be influenced by these factors. As a generalisation, it is expected that a lens with a low water content to contain relatively tightly bound water because, for a low ratio of water molecules to hydrophilic groups, each water molecule will necessarily be close to a hydrophilic group. A lens with a high water content would contain fully hydrated groups, but would also contain water molecules in regions slightly removed from the hydrophilic groups of the matrix. Since the water molecules are constantly in motion, each water molecule spends some fraction of its time in a "bound" state on the polymer chain and the remainder of its time in a "free" state away from the polymer chain. As the ratio of water molecules to hydrophilic groups increases, the relative fraction of bound water molecules is expected to decrease, and the water is expected to become less tightly bound on average. This argument suggests that a correlation between lens dehydration and water content should exist, however, this trend would also be influenced by the structural features of the polymer.

1.6 Techniques for Studying Water Binding of Hydrogels

1.6.1 Differential Scanning Calorimetry

It has been shown by the use of several calorimetric techniques¹⁶⁻¹⁹ that when a polymer network that contains water is cooled to very low temperatures only part of the water within the material freezes. One of these techniques, differential scanning calorimetry (DSC) which was developed by Perkin-Elmer in 1964, allows the ratio of freezing to non-freezing water to be calculated as well as exhibiting information about the water binding sites within the polymer. In DSC the energy required to maintain both the sample and a reference holder at the same temperature is measured as shown in figure 1.1. For endothermic transitions the energy input to the sample is increased while for exothermic transitions energy input is increased to the reference holder. When a transition occurs a peak is displayed and the energy input to the sample or reference holder is measured directly as the area under the peak. Work has shown that the heat of fusion for water associated with polymers is the same as that for pure water. Therefore the amount of freezing water and subsequently non freezing water for a polymer sample can be determined.

Figure 1.1 Schematic representation of a differential scanning calorimeter



1.6.2 Nuclear Magnetic Resonance

NMR relaxational studies have been used to characterise the state of water in swollen hydrogels¹⁹⁻²⁹. Sung et al¹⁹ measured the ¹H spin-spin and spin-lattice relaxation times of water in poly(HEMA) hydrogels. It was found that both the T₁ and T₂ values of the water in the hydrogels were lower than the corresponding values for pure water due to a reduction in mobility. The results were interpreted in terms of a three-state model in which the water was considered to be bound, intermediate or free. The NMR relaxation results were in good agreement with differential scanning calorimetry data used to determine the fraction of bound water. Hatakeyema et al²⁰ used similar studies to characterise water in poly(vinyl alcohol) hydrogels and found that both T₁ and T₂ decreased as the cross-link density was increased.

Yamada-Nosaka et al²¹ investigated the spin-spin and spin-lattice relaxation times of water in poly(HEMA) hydrogels, and compared the results to those of the more hydrophobic hydrogels of poly(MMA). The magnitude, temperature dependence and frequency dependence of the T₁ and T₂ values for the water differed considerably between the two materials. The poly(HEMA) membranes contained more than twice as much bound and intermediate water as the poly(MMA) membranes.

Quinn et al^{22,23} have used NMR techniques to study the states of water in a poly(N-vinyl-2-pyrrolidone/methyl methacrylate) hydrogel and a poly(2-hydroxyethyl methacrylate) hydrogel both in the hydrated states. It was found that although poly(HEMA) is less hydrophilic than poly(NVP/MMA), the relative fraction of bound water is significantly higher for poly(HEMA). For both of these materials, pulsed NMR relaxation data reveals that a significant part of the water is nonfreezable or bound. Consideration of the T₂ component intensities allow the estimation of relative fractions of three distinguishably different types of water in the hydrogels. The bound water can be resolved into a mobile component characterised by a long T₂ (type A) and a component of lower mobility that combines with plasticised polymer to form an intermediate T₂ (type B). In samples with a water content in excess of 70 % there is also bulk like water that freezes in the vicinity of 273K. Parallel DSC measurements

predict a lower estimate for the amount of non-freezable water which correlates well with the amount of type A water present.

1.6.3 Ultrasonic Sound

The mechanical properties of a hydrogel such as elasticity, compressibility and rigidity are affected by the states of water in a gel. Adiabatic compressibility is evaluated from sound velocity and density data. As the compressibility is sensitive to changes in the states of water in the hydrogel, the sound velocity gives information on hydration or the water absorbed in the hydrogel³⁰. The states of water in a hydrogel can be studied using the Brillouin scattering method³¹. The amount of bound water is estimated from the Brillouin shift observed in the gigahertz region. Although the Brillouin scattering method is unsuitable for measuring the sound velocity in an opaque sample, the pulse method is suitable for measuring the sound velocities in many polymers even if they are not transparent. The sound velocity increases with decreasing water content.

1.6.4 Dielectric Spectroscopy

Dielectric permittivity and loss data are generally measured by supercooling followed by heating over the temperature range 77-273K. The permittivity and loss data are acquired for supercooled water in the hydrogel sample and the size and strength of relaxations taking place at phase changes, are compared to the strength of the relaxation transitions of supercooled water^{32,33}. Differences in the shapes and sizes of relaxation transitions of water in the hydrogel and pure water have enabled the water in the hydrogel to be classified into three phases, interfacial, bound and free water. Free water readily crystallises and the former two states readily supercool without crystallisation. The greater the size of the relaxation of crystallised water the greater the amount of free water within the hydrogel.

The development of the dielectric time domain spectroscopy (TDS) method has provided a useful experimental technique since the dielectric relaxation time gives direct information on the reorientational mobility of the water dipoles³⁴. Dielectric relaxation time of bound water in materials is characterised by two dispersion regions

around 100MHz and 10GHz in the dielectric spectrum. The high frequency dispersion is attributed to free water while the low frequency dispersion is interpreted as due to bound water.

1.6.5 Specific Conductivity

Water in polymers has been studied by specific conductivity, κ , measurements^{37,38}. The specific conductivity of the hydrogel is measured over the temperature range 258-297K with a sharp discontinuity being shown at the melting point of water in a plot of $1/T$ versus $\log \kappa$. The types of water in the gel are illustrated by the size and shape of the transition point when compared to the transition point of pure water.

1.6.6 Dilatometry

Dilatometry has been used to determine the characteristics of water in hydrogels^{37,38}. Heating and cooling curves over the temperature range 240-300K are used to determine the specific volume change with temperature of the hydrogel sample. Comparison with the specific volume change for pure water and the shapes of the cooling and heating curves are used to determine the state of water in the polymer.

1.7 Biocompatibility

Since materials were first used for biomedical applications, a great deal of research has been carried out into the factors that contribute to biocompatibility. This is concerned with the interactions that take place between synthetic materials and the body fluids which they are in contact with. The majority of research has centred around the consequences of surface energy, although it is important to also consider the effect of molecular architecture and monomer sequence distribution on biocompatibility. An understanding of biocompatibility is required to enable the design of materials which are accepted by the bodily environment and do not undergo adverse reactions which result in rejection, or failure of the material in its application. One such example is the formation of deposits on contact lenses which results in a decrease in optical clarity and a reduction in comfort and can ultimately lead to infections within the eye. Protein

deposition onto the surface of the synthetic substrate is usually the first stage of this type of interaction illustrating that the surface properties of a material control its biocompatibility.

Biological fluids such as tears contain proteins which are found to exist in aqueous solution. When in contact with another phase proteins tend to accumulate at the interface resulting in adsorption onto any surfaces present such as the surface of a contact lens. A review of protein deposition onto surfaces has been compiled by Baker and Tighe⁵⁹. Protein adsorption is caused by the resultant interactions of polar and dispersive components acting across the interface. The surface energy of a material and the interfacial tension between the material and the biological environment are also highly influential factors.

Baier et al⁶⁰ suggested that for a material to exhibit non-thrombogenic (blood compatible) characteristics it should have a critical surface tension in the region of 20-30 mN/m. Exceptions to this theory were found at a later date. Andrade⁶¹ proposed the theory of minimum interfacial energy. This states that to improve biocompatibility, a minimum interfacial tension should exist between an implant material and its environment. However, later work carried out by the same research workers on a range of hydrogel copolymers produced results that could not be explained in terms of this hypothesis⁶². Ratner et al⁶³ concluded that a balance of polar and non-polar groups enhanced blood compatibility.

The composition and relative hydrophilicity of regions on the surface are also important in controlling the blood compatibility of a material. It has been shown that regions of hydrophilicity and hydrophobicity at the polymer surface control the composition of the absorbed proteins from the biological fluid. Globulin and fibrinogen adhere to hydrophobic domains while albumin adheres to domains that are hydrophilic in nature⁶⁴. The formation of ordered areas of adsorbed proteins is thought to suppress platelet adhesion.

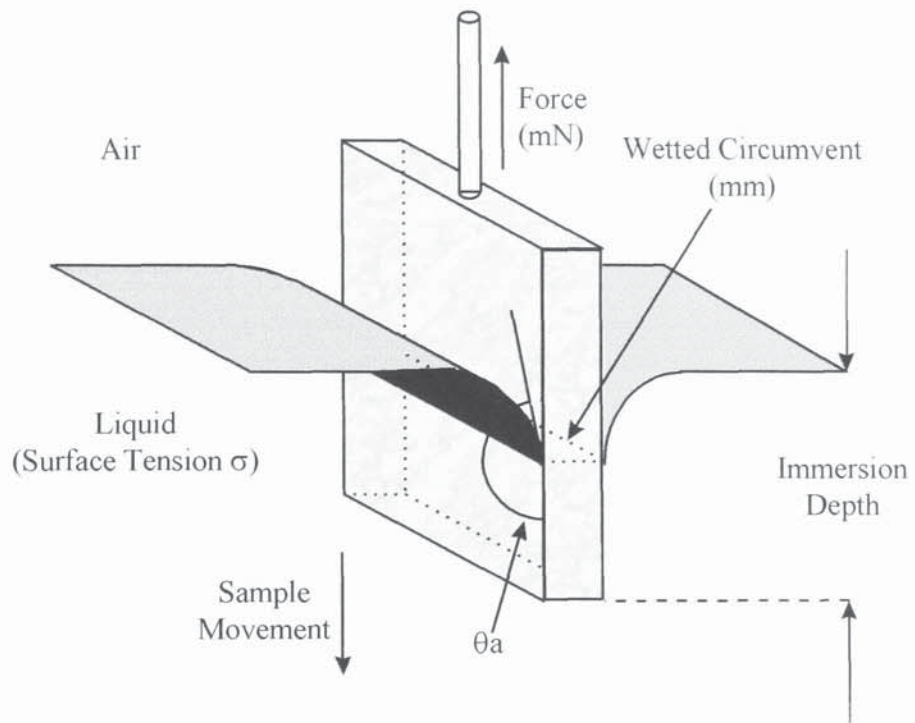
1.8 Wettability

This is the ability of a liquid to adhere to a solid and spread over its surface to varying degrees. It is considered to be a surface property as opposed to hydrophilicity which is thought of as a bulk property. For the fabrication of medical devices that come into contact with blood and tissue, it is usually desirable to utilise materials that exhibit very high degrees of wettability. This is due to the fact that most of the internal biological environment with the exception of lipids are hydrophilic in nature and biocompatibility appears to correlate directly with the degree of hydrophilicity that a surface exhibits³⁸. Thus the practice of incorporating hydrophilic materials into the design of medical devices to enhance their wettability has arisen.

The property of wettability can be characterised by several methods including the measurement of contact angles and the surface tension of solids and liquid. The measured value of the contact angle will vary depending on whether the liquid is advancing initially over a dry surface or receding from a wetted surface (figure 1.2). This is referred to as the contact angle hysteresis and the values of the receding and advancing contact angles may vary by as much as 50° . The divergence of these two values is enhanced by surface heterogeneity and surface roughness.

Many polymer systems display some degree of contact angle hysteresis, which is defined as the difference between the advancing and receding contact angle. Extensive studies on contact angle hysteresis were reported by Smith et al^{65, 66} who employed the Wilhelmy technique. Their equipment consisted of a mechanical testing device, a balance system and an x-y plotter. The result for a sample of polybutadiene can be found in figure 1.3. As the stage is raised, the sample is immersed in the test fluid. When the sample first touches the fluid surface, a meniscus is formed and, as immersion of the sample into the liquid continues, the contact angle levels off giving a constant slope on the x-y recorder, which is a measure of the advancing contact angle. After immersion to 2.5-3.0cm, the process is reversed, the wetting liquid is lowered, and a constant slope due to a receding angle is observed on the recorder.

Advancing Contact Angle



Receding Contact Angle

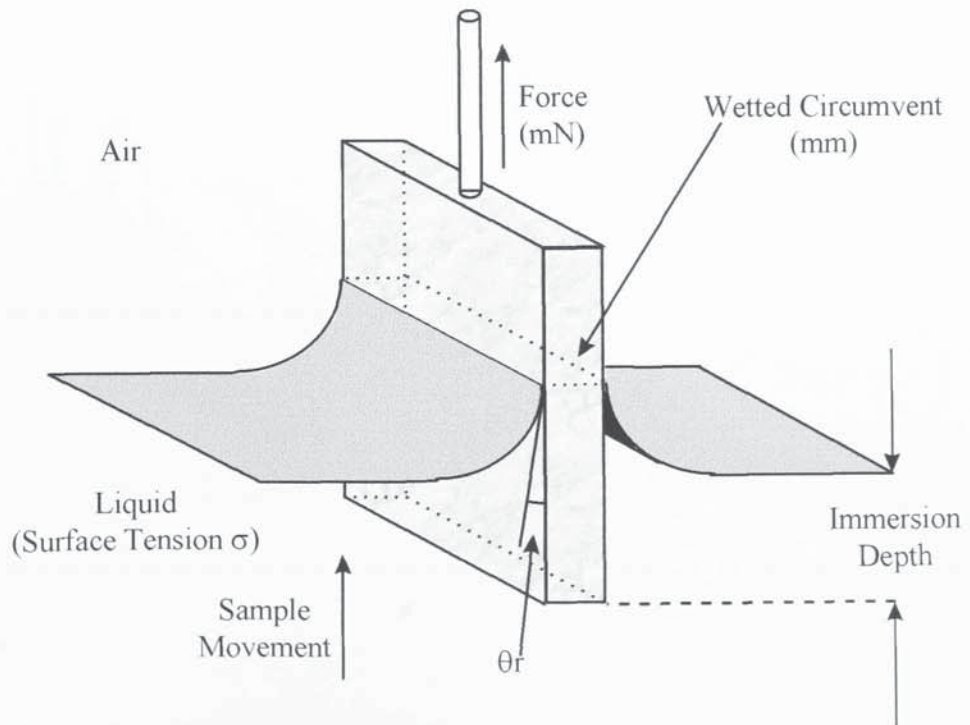


Figure 1.2 Advancing and receding contact angle situations

Generally, a straight-line approximation of the advancing and receding slopes is made and extrapolated to zero depth of immersion. The basic equations for determining the advancing (θ_a) and receding contact angles (θ_r) are given by:

$$F_a = \gamma L \cos \theta_a \quad \text{Equation 1.2}$$

$$F_r = \gamma L \cos \theta_r \quad \text{Equation 1.3}$$

where F_a and F_r represent the observed forces at zero depth immersion of samples at the advancing and receding cycle, respectively, γ is the surface tension of the wetting liquid (water $\gamma = 72.6$ dyne/cm at 20°C) and L is the peripheral of the immersed sample.

The contact angle hysteresis can be classified into two groups:

1. Thermodynamic hysteresis, where the hysteresis curve is reproducible over many cycles and is independent of time and frequency.
2. Kinetic hysteresis, where the hysteresis curve changes with time and circumstances.

Figure 1.3 Hysteresis cycle for Polybutadiene

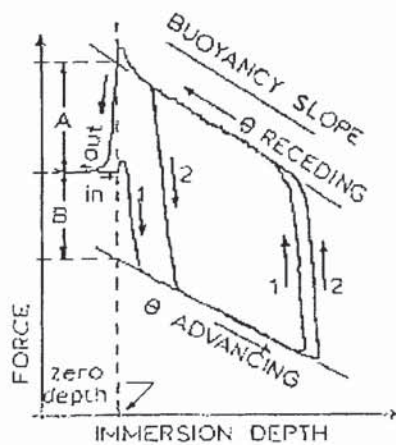
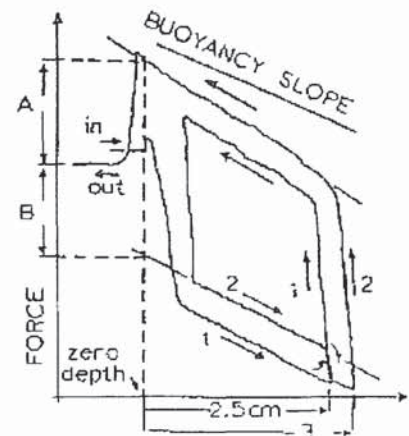


Figure 1.4 Hysteresis cycle for dehydrated poly(HEMA)



The hysteresis observed for the Wilhelmy plate measurement on the poly(butadiene) surface is mainly due to thermodynamic hysteresis. An example of the Wilhelmy plate measurement for a poly(HEMA) hydrogel is shown in figure 1.4. Here the contact angle hysteresis is due to kinetic or time-dependent effects. In this particular case a dehydrated poly(HEMA) gel was immersed in water and the Wilhelmy plate experiment carried out. During the experiment, the gel swells and its mass dimensions and wettability also change. The result is that the recorded force increases with time in contact with the water. On the second cycle the gel was immersed a short distance beyond the immersion distance for the first cycle, i.e., the dry gel is seeing water for the first time.

In the work carried out in this thesis, the experiment was performed on the hydrogel in its fully hydrated state. If the experiment is carried out quickly enough the hydrogel will not dehydrate during the course of the experiment. This results in the observation of a thermodynamic hysteresis with the curve being reproducible over a number of cycles. Thus, the accuracy of the results is validated by the fact that the results are consistent for a set number of runs.

1.9 Contact Angle Measurements

Contact angle measurements provide information about the characteristics of a hydrogel surface. Forces are resolved at a three phase interface of a drop of wetting liquid or vapour on a solid surface. Results from these measurements enable the surface free energy of solids in both the hydrated and dehydrated states to be determined. The surface free energy can be split into polar and dispersive components and it is these that influence the blood compatibility and biotolerance of the material. The polar component is of great interest as it determines the wettability of a material which is an important parameter in the evaluation of a materials suitability for use as a contact lens.

Results are obtained via the resolution of the forces at a three phase interface. The three phase interface is formed either by a drop of liquid on a solid surface in air or by

a drop of liquid or vapour on a solid surface immersed in a liquid. The theory for using contact angle measurements to determine the surface energy of a polymer is shown below.

1.9.1 Dehydrated Surfaces

In 1805 Young⁶⁷ derived an equation to resolve the forces at the point of contact of a sessile drop of liquid on a solid surface as shown in figure 1.5.

$$\gamma_{sv} = \gamma_{sl} + \gamma_{lv} \cos \theta \quad \text{Equation 1.4}$$

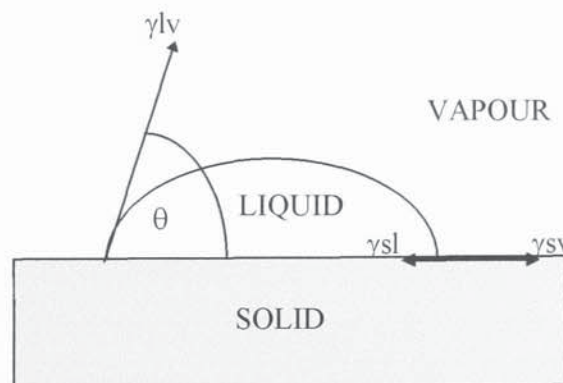
Sixty years later Dupre⁶⁸ deduced that the reversible work of adhesion of a liquid and solid, W_a could be expressed as

$$W_a = \gamma_s + \gamma_{lv} - \gamma_{sl} \quad \text{Equation 1.5}$$

These equations are combined to give the Young - Dupre equation.

$$W_a = (\gamma_s - \gamma_{sv}) + \gamma_{lv} (1 + \cos \theta) \quad \text{Equation 1.6}$$

However if polar forces act across the interface this equation is not detailed enough to deal with this situation.



where

- γ_{lv} = liquid-vapour interfacial free energy
- γ_{sl} = solid-liquid interfacial free energy
- γ_{sv} = solid-vapour interfacial free energy

Figure 1.5 Individual components of the solid surface free energy

Owens and Wendt⁶⁹ resolved the polar and dispersive forces to give the following expression for the determination of the surface free energies of dehydrated polymer surfaces

$$1 + \cos \theta = (2/\gamma_{lv}) \{ (\gamma_{lv}^d \gamma_s^d)^{0.5} + (\gamma_{lv}^p \gamma_s^p)^{0.5} \} \quad \text{Equation 1.7}$$

This equation relates the contact angle to the polar and dispersive forces of the solid. Therefore, if the polar and dispersive components for two wetting solutions are already known, the same components for the solid can be found by the solution of simultaneous equations. The total free surface energy can be found by adding the values of the polar and dispersive components.

$$\gamma_s^t = \gamma_s^d + \gamma_s^p \quad \text{Equation 1.8}$$

The wetting liquids generally used are distilled water and diiodomethane⁷⁰. This is because of their high total surface free energies and their balance of polar and dispersive components. This is shown in the following table

Liquid	γ_s^d (mN/m)	γ_s^p (mN/m)	γ_s^t (mN/m)
Water	21.8	51.0	72.8
Diiodomethane	48.1	2.3	50.8

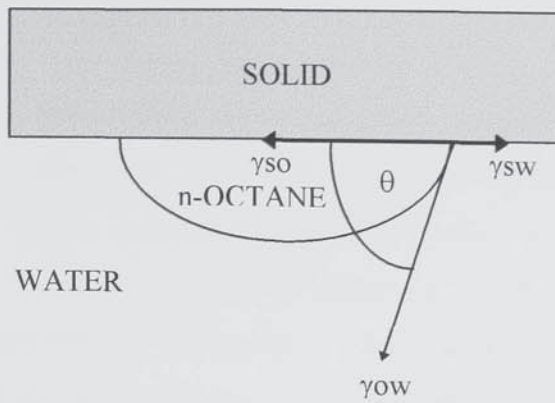
Table 1.2 Polar and dispersive components for water and diiodomethane

1.9.2 Hydrated Surfaces

With hydrated surfaces, problems arise in the determination of surface energies in air as reproducibility of the removal of excess water is difficult and dehydration from the polymer surface often occurs. Two techniques have been developed which overcome these problems and allow surface energies in the fully hydrated state to be determined.

1.9.2.1 Hamilton's Method

Hamilton's method involves measuring contact angles of n-octane drops on a solid surface while it is immersed in water^{71, 72} as shown in figure 1.6.



where

- γ_{sw} = solid-water interfacial free energy
- γ_{so} = solid-octane interfacial free energy
- γ_{ow} = octane-water interfacial free energy

Figure 1.6 Individual free energy components for Hamilton's method

The equation developed by Fowkes⁷³ for the work of adhesion at the solid-liquid interface is given by

$$\gamma_{sl} = \gamma_s + \gamma_{lv} - 2 (\gamma_{lv}^d \gamma_s^d)^{0.5} \quad \text{Equation 1.9}$$

This equation does not take into account the polar forces acting across the interface. It was not until Tamei et al⁷⁴ modified the equation to take account of the polar contribution to the stabilisation of a solid surface to give

$$\gamma_{sl} = \gamma_s + \gamma_{lv} - 2 (\gamma_{lv}^d \gamma_s^d)^{0.5} - I_{sl} \quad \text{Equation 1.10}$$

where

$$I_{sl} = 2 (\gamma_{lv}^p \gamma_s^p)^{0.5} \quad \text{Equation 1.11}$$

The dispersive components γ_{lv}^d of water and n-octane are identical and n-octane has no polar component. Therefore it is possible to combine equation 1.4 and 1.10 to produce equation 1.12 which corresponds to the polar stabilisation energy between water and the solid.

$$I_{sw} = \gamma_{wv} - \gamma_{ov} - \gamma_{ow} \cos \theta \quad \text{Equation 1.12}$$

where

I_{sw} = Polar stabilisation energy between water and the solid

γ_{wv} = Surface tension of n-octane saturated water

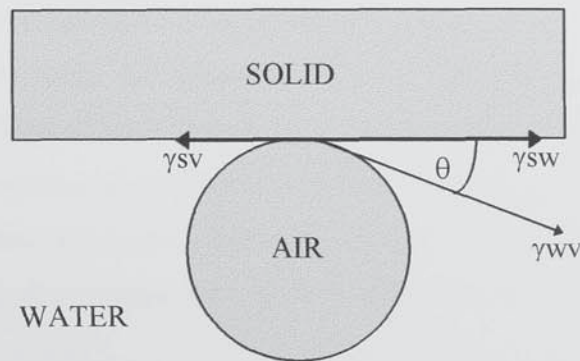
γ_{ov} = Surface tension between n-octane and its vapour

γ_{ow} = Surface tension between n-octane and water

The components γ_{ov} and γ_{ow} are determined experimentally as shown in figure 1.6. After I_{sw} (I_{sl}) has been calculated, its value is placed into equation 1.11, enabling the polar component of the surface free energy to be determined.

1.9.2.2 Captive Air Bubble Method

This technique uses the same experimental procedure as Hamilton's method, using a bubble of air instead of a drop of n-octane on the solid surface as shown in figure 1.7⁷⁵. Using data from both Hamilton's and the captive air bubble techniques, values for γ_{sv} , γ_{sv}^p , γ_{sv}^d and γ_{sw} can be determined⁷⁶.



where

γ_{sv} = solid-water interfacial free energy

γ_{sv} = water-vapour interfacial free energy = surface tension of water

γ_{sv} = solid-vapour interfacial free energy = γ_s = solid surface free energy

Figure 1.7 Individual free energy components for the captive air bubble technique

Application of Youngs equation to the captive air bubble technique

$$\gamma_{sv} - \gamma_{sw} = \gamma_{wv} \cos \theta \quad \text{Equation 1.13}$$

As γ_{wv} is equal to the surface tension of water, 72.8 mN/m, and θ is obtained from the measurement shown in figure 1.7, it is possible to determine $\gamma_{sv} - \gamma_{sw}$.

The polar stabilisation component, derived as Equation 1.12 is

$$I_{sw} = \gamma_{wv} - \gamma_{ov} - \gamma_{ow} \cos \theta$$

For the captive air bubble technique $\gamma_{wv} = 72.8$ mN/m, $\gamma_{ov} = 21.8$ mN/m and $\gamma_{ow} = 51.0$ mN/m then

$$I_{sw} = 51.0(1 - \cos \theta) \quad \text{Equation 1.14}$$

Combining and rearranging equations 1.10 and 1.13, it is possible to determine the dispersive component of the hydrogel γ_{sv}^d .

$$\gamma_{sv}^d = [\{ (\gamma_{sv} - \gamma_{sw}) - I_{sw} + \gamma_{wv} \} / 2(\gamma_{wv}^d)^{0.5}]^2 \quad \text{Equation 1.15}$$

The polar component of the hydrogel is obtained by rearranging equation 1.11 to give

$$\gamma_{sv}^p = I_{sw}^2 / (4 \gamma_{wv}^p) \quad \text{Equation 1.16}$$

Using a computer program with the relevant equations enables $(\gamma_{sv} - \gamma_{sw})$, I_{sw} , γ_{sv}^d , γ_{sv}^p , γ_{sv} and γ_{sw} to be calculated from contact angle measurements for hydrogels.

The dispersive component of the surface free energy of hydrated hydrogels can also be determined by using the Owens and Wendt equation (equation 1.7). The polar component obtained from Hamilton's method together with the water / air contact angle are substituted into the Owens and Wendt equation which permits the calculation of the dispersive component. The results obtained from this method and from equation 1.15 are in good agreement to within 0.2 mN/m of each other⁷⁹.

1.10 Mechanical Properties of Hydrogels

In the dehydrated state hydrogels, such as poly(HEMA), are hard and brittle materials similar to perspex or poly(methyl methacrylate). However in the hydrated state poly(HEMA) is soft and rubber-like, properties which give the material the potential for use as a biomaterial.

Unlike the majority of polymers that are tested mechanically, swollen hydrogels are typically extremely weak materials which can exhibit poor mechanical strength. This

weakness and the requirement that the sample does not dehydrate during testing requires unique measurement procedures⁸⁰. Standard test conditions and specimen geometry for use with the Hounsfield tensometer have been established by Trevett and Tighe⁸¹. The values obtained cannot be regarded as absolute as different methods will give varying results but, in this work all test conditions remained the same for each sample so the results give comparative information. It has been found that tensile testing of hydrogels is sensitive to small changes in both composition and sample preparation.

1.11 Coefficient of Friction

The surfaces of materials such as metals and ceramics possess very ordered structures that exhibit relatively little movement of constituent particles. The surfaces of polymeric materials, on the other hand, exhibit high degrees of molecular mobility in the rotational and translational modes. Driven by a thermodynamic tendency to minimise interfacial energy, polymeric surfaces are in continuous motion until this requirement is achieved. The dynamic nature of these surfaces makes analysis difficult and more difficult still is the analysis of hydrophilic surfaces.

In fabricating medical devices, hydrophilic materials are used to, impart lubricity, regulate diffusion and to improve biocompatibility⁸². The force of friction associated with surfaces in contact with each other arises from a number of interactions occurring at both the macroscopic and microscopic level. Friction is the force required to rupture these interactions as the solid surfaces slide over one another. Lubrication of surfaces has been used traditionally to reduce friction and the subsequent wear occurring between moving parts in contact with each other. For medical devices the need for lubricating surfaces is necessary to minimise the trauma sustained by tissue in contact with devices such as angioplasty catheters and contact lenses. By using hydrophilic materials, the surface friction of a device can be significantly reduced⁸³.

The force of friction (F) existing between two surfaces is proportional to the applied load (N), and is fairly independent of the area of contact. This results in the following equation where (μ) is the coefficient of friction.

$$F = \mu N$$

Equation 1.17

The force required to start motion is referred to as the static force of friction and the force necessary to maintain motion at a constant velocity is the kinetic force of friction. The static force of friction and its coefficient are greater than the kinetic force of friction and its coefficient.

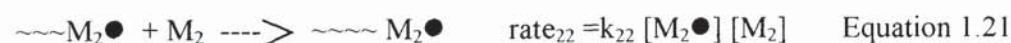
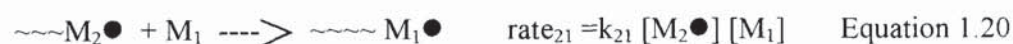
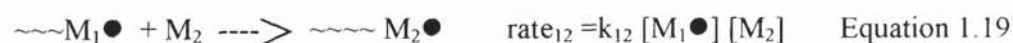
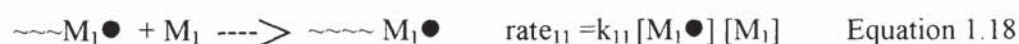
The coefficient of friction is a useful value in characterising the frictional properties of a medical device. Due to the intricacy of their design however, evaluating frictional properties can be quite challenging. Contact lenses with their parabolic shape and limited surface area, are probably the most difficult device to be evaluated for this property. An ASTM standard test exists for both static and dynamic coefficients of friction and apparatus to carry out this test was modified so that contact lenses could be evaluated. The details of this can found in Chapter 7.

1.12 Copolymer Sequence Distribution

It is evident from the research cited above that for biocompatibility a careful balance of chemical structure and surface energies is required. Work carried within this group has shown that synthetic polymers with large irregular domains of the same chemical type, have a greater tendency to show non specific protein adsorption than polymers with regular chemical variations. It would be useful to predict the order of chemical constituents at different compositions in a copolymer so that the formation of blocks of one component are avoided. This resulted in the development of a computer simulation program which allows the sequence distribution to be predicted for copolymerisation reactions, based on the concentration and reactivity ratios of the monomers used. Although the reactivity ratios for a pair of monomers are fixed, optimisation of the concentration of monomers of specific reactivity ratios enables copolymers with short repeat units to be produced.

1.12.1 The Terminal Model of Copolymerisation

The standard kinetic treatment of free radical polymerisation is the terminal model of copolymerisation^{84, 85}. In this model the reactivity of an active centre is dependent only on the monomer unit in the copolymer chain on which the radical is located. For two monomers the growth of the polymer chain and the consumption of monomer is illustrated by four propagation steps:



where:

- M = monomer
- M● = monomer radical
- k = rate constant
- [] = concentration of individual species

The rate of consumption of the monomers can be expressed as:-

$$d[M_1]/dt = k_{11} [M_1\bullet] [M_1] + k_{21} [M_2\bullet] [M_1] \quad \text{Equation 1.22}$$

$$d[M_2]/dt = k_{12} [M_1\bullet] [M_2] + k_{22} [M_2\bullet] [M_2] \quad \text{Equation 1.23}$$

$\frac{d[M_1]/dt}{d[M_2]/dt}$ is the mole ratio of the monomers in the copolymer. This gives

$$\frac{d[M_1]/dt}{d[M_2]/dt} = \frac{k_{11} [M_1\bullet] [M_1] + k_{21} [M_2\bullet] [M_1]}{k_{12} [M_1\bullet] [M_2] + k_{22} [M_2\bullet] [M_2]} \quad \text{Equation 1.24}$$

If a steady state is reached instantly after polymerisation is started, the total concentrations of $M_1\bullet$ and $M_2\bullet$ will remain constant and the rate of conversion of $M_1\bullet$ to $M_2\bullet$ will equal the rate of conversion of $M_2\bullet$ to $M_1\bullet$ i.e.:-

$$k_{21} [M_2\bullet] [M_1] = k_{12} [M_1\bullet] [M_2] \quad \text{Equation 1.25}$$

If k_{11}/k_{12} is defined as r_1 , the reactivity ratio of monomer M_1 and k_{22}/k_{21} is defined as r_2 the reactivity ratio of monomer M_2 then equation 1.24 reduces to the copolymer equation

$$\frac{d[M_1]}{d[M_2]} = \frac{[M_1] (1 + r_1[M_1] / [M_2])}{[M_2] (r_2 + [M_1] / [M_2])} \quad \text{Equation 1.26}$$

The monomer reactivity ratios r_1 and r_2 are the ratios of the rate constant for a given radical adding to its own monomer compared to that for the addition to the other monomer. They are a measure of which monomer a particular radical has a preference to react with, thus if $r_1 > 1$ radical $M_1\bullet$ prefers to add to monomer M_1 and if $r_1 < 1$, radical $M_1\bullet$ prefers to add to monomer M_2 . The relative values of r_1 and r_2 will therefore determine the mechanism of polymerisation of the copolymer.

If $(r_1) \times (r_2) = 1$, the situation is referred to as an ideal copolymerisation in that the radicals have the same preference of addition to each of the monomers. The units of the two monomer types are arranged completely at random along the chain. When $r_1 = r_2 = 0$, each radical shows a strong preference for cross propagation which results in the monomers alternating regularly regardless of the monomer feed ratio until one monomer is completely consumed. In the situation of $r_1 = r_2 = 1$ neither radical centre shows a preference for either monomer and the rates of consumption are determined by the relative concentrations of monomer in the initial feed. If r_1 is much greater than r_2 the polymerisation produces large blocks of M_1 with small clusters of M_2 between the blocks until M_1 is consumed.

1.12.2 Computer Simulation of Sequence Distribution

The terminal model is very useful for explaining the structure of copolymers prepared from various vinyl monomers whose reactivity ratios are known. A computer program based on this model provides an illustration of the sequence distribution of copolymers whilst allowing alterations in key parameters such as monomer type and initial feed

concentration. The approximate sequence distributions of various copolymers can be determined easily without the need for producing the polymer and performing detailed structural analysis required for determination of the sequence distribution.

Computer simulation of sequence distributions is carried out using two computer programs. The 'COPOL' program allows the simulation of the sequence distribution for binary systems whilst the 'TERPOL' program allows ternary systems to be studied. Ashraf⁸⁶ has provided experimental evidence for the accuracy of the simulations using these two programs.

1.12.3 The Alfrey-Price Q-e Scheme

The reactivity ratios of monomers must be known to allow the computer simulations described previously to be utilised. For many monomers the reactivity ratios have been determined experimentally but there are still a number of monomers for which this process has not been carried out. To overcome this problem without the need to carry out lengthy experimental work, an approximation technique known as the Alfrey-Price Q-e scheme has been employed^{87, 88}. This scheme quantifies reactivity by consideration of the polar and resonance stabilisation effects of the monomer and the influence these have on the copolymerisation process.

The two reactants in the copolymerisation were assigned values e_1 and e_2 to represent their charges, identical charges being assumed for a monomer and its radical. The reactivities of the monomers and radicals were then denoted by Q and P respectively. The rate of reaction was considered to be dependent on the four quantities P, Q, e_1 and e_2 as indicated in equation 1.27.

$$k_{12} = P_1 Q_1 \exp(-e_1 e_2) \quad \text{Equation 1.27}$$

Four of these equations are obtained from the propagation steps outlined previously in equations 1.18-1.21, which were then combined and rearranged to give:-

$$r_1 = (Q_1/Q_2) \exp [-e_1(e_1-e_2)] \quad \text{Equation 1.28}$$

and

$$r_2 = (Q_2/Q_1) \exp [-e_2(e_1-e_2)] \quad \text{Equation 1.29}$$

Combination of these equations gives

$$r_1 r_2 = \exp [-(e_1 - e_2)^2] \quad \text{Equation 1.30}$$

Thus the Q-e scheme enables predictions of the reactivity ratios to be made for a pair of vinyl monomers which have not been studied experimentally.

1.13 The Use of Hydrogels as Desiccant Packaging Materials

Over thirty years ago Beecham made a major breakthrough in the pharmaceutical industry by identifying and isolating the penicillin nucleus 6-APA, which enabled the production of semi-synthetic penicillins. The range of these semi-synthetic penicillins has been extended with the manufacture of clavulanic acid, an enzyme inhibitor which increases the effectiveness of penicillins. For Smithkline Beecham the biggest of these products is Augmentin which is a clavulanate potentiated sodium amoxicillin which is currently in use in the non-crystalline form. It is however desirable that the crystalline form of sodium amoxicillin is adopted because of production difficulties and since this product state offers better performance. The formulation of interest for this project is the intravenous form in which the product is present as a powder in an injection vial. Water is added to the vial to make a reconstituted solution which is injected into the patient. Before the solution is reconstituted, any moisture present will render the powder in the injection vial useless if it is in the crystalline form. This is since the crystalline form of sodium amoxicillin is less able to scavenge excess moisture than the existing form. The principle idea therefore is to include a desiccant within or attached to the injection vial or stopper of the vial to scavenge excess moisture as this will increase the shelf life of the amoxicillin if the crystalline form is adopted. This has to be achieved without any change in the dimensions of the vial and the design incorporated must allow the removal of the reconstituted solution from the bottle by use of standard equipment.

Hydrogels possess the necessary properties to make them useful for this particular application. They have a high affinity for water and should absorb moisture at the low relative humidity levels that are encountered within the sample vial. As they are used to an extent already within the human body there should be no toxicity problems.

Aston university's involvement arises from previous work on anti-mist coatings and the novelty of using this class of materials for pharmaceutical applications.

1.14 Water Sorption

Virtually all materials are sensitive to the presence of water vapour or moisture. They can retain water by bulk absorption, surface adsorption, chemical reaction, formation of a solution or a combination of these mechanisms. Many of the water sorption problems commonly encountered are associated with the storage, processing, and chemical or biological activity of these material types. A material's moisture content is directly dependent on the partial vapour pressure of water, commonly referred to as the relative humidity (RH), in the sample environment. An important fundamental relationship which provides a meaningful description of the water sorption processes is the water sorption isotherm - the dependency of the equilibrium moisture content of a material and % relative humidity.

In conventional moisture absorption experimental techniques, the moisture uptake of a sample is monitored by gravimetric techniques. The procedure involves placing the sample in cabinets of controlled relative humidity for a period of time after which they are weighed to see if the sample has gained or lost water. As well as requiring many manual measurements over a long period of time, the method can be prone to inaccuracies caused by moving the sample from cabinet to balance at a different humidity to that of the cabinet. Also other environmental factors such as temperature and differing humidities from day to day can result in inconsistent results.

In dynamic vapour sorption (DVS), the sample to be investigated is placed on a microbalance which is exposed to a continuous flow of air with a predetermined and constant relative humidity. This is achieved by mixing two air flow streams, one dry and one at 100% humidity, at a particular ratio in order to achieve the desired combined humidity. As the humid air passes over the sample a zone of constant relative humidity is established around the sample. This zone allows the rapid establishment of water vapour sorption or desorption equilibrium, by maximising the mass transport of water vapour into and out of the sample. By monitoring the sample

mass as a function of time, and by varying the relative humidity of the air, a wide range of physicochemical facets of moisture behaviour can be studied.

1.15 Scope and Objectives

The work in this thesis is concerned with several aspects of hydrogel characteristics and how these can be improved for a range of applications.

A significant problem for hydrogel contact lenses that are used for extended wear applications is that they dehydrate during wear. A number of viewpoints suggest a wide range of differing factors which may contribute to the rate and degree of dehydration of a lens while it is in the eye. To evaluate the validity of one of these theories, results from a clinical study of complications that arise from lens dehydration were compared to the ratios of different types of water present in a number of contact lens materials. In a separate area of work, the factors that affect the rates of hydration of hydrogel materials in the dehydrated state was also studied.

Although some contact lenses contain ionic groups, only a small number of charged monomers have been used in their manufacture. Incorporation of charged groups has a number of effects, the most noticeable being a large increase in the water content of the resulting material. A consequence of inclusion of charged monomers into a materials composition is that it may also effect the mechanical properties of the material although there has been little investigation into this. It was therefore decided to incorporate monomers that have the potential to carry a positive charge into hydrogels in the hope that the charge can form weak interactions with the polymer chain. Investigations where a pair of monomers that carry positive and negative charges were incorporated in a hydrogel, were also carried out to see if improvements in mechanical properties would be observed. It would also be beneficial if the amount of water that exists in the bound state increases with incorporation of charged monomers.

An important property for which no current, generally available measurement technology exists is the coefficient of friction for hydrogel contact lenses. In fact to measure this property for hydrogels in sheet form is itself experimentally demanding. Therefore apparatus designed to measure the coefficient of friction for materials has been modified to measure this property for hydrogels in both sheet and contact lens form. The equipment uses a tensiometer to provide the mechanical movement that is required to measure the resistance encountered when a surface slides over another. The measurement can be, and usually is, carried out in the presence of a lubricating solution. It has been found that the method is sensitive both to different types of contact lenses and different lubricating solutions.

CHAPTER 2

MATERIALS AND EXPERIMENTAL TECHNIQUES

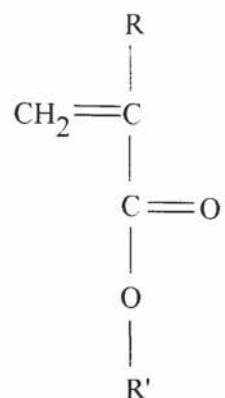
2.1 Reagents

The reagents used in this work are shown in the following table 2.1. The structures of the reagents are shown in figures 2.1. All monomers were purified by the method of reduced pressure distillation⁸⁹ before use and were stored in a refrigerator.

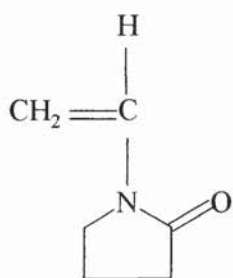
Table 2.1 Molecular weights and suppliers of reagents used.

Reagent	M.Wt	Abbreviation	Supplier
2-Hydroxyethyl methacrylate	130	HEMA	Vista
N-vinyl pyrrolidone	111	NVP	Vickers
Acryloylmorpholine	141	AMO	Vista
N, N-dimethylacrylamide	99	NNDMA	Dajac
Methyl methacrylate	100	MMA	Vickers
Methoxyethyl methacrylate	158	MEMA	Ubichem
Ethoxyethyl methacrylate	144	EEMA	Ubichem
Dimethylaminoethyl methacrylate	157	DMAEMA	Aldrich
Dimethylaminoethyl acrylate	143	DMAEA	Aldrich
N-vinyl imidazole	94	NVI	Aldrich
Sulphopropyl ester of itaconic acid (potassium salt)	450	SPI	Raschig
Methacrylic acid	86	MAA	Aldrich
Itaconic acid	130	ITA	Aldrich
Pyridine-N-oxide	95	PNO	Aldrich
4-vinyl pyridine	105	4VP	Aldrich
Ethyleneglycol dimethacrylate	198	EGDMA	BDH
Azo-bis-isobutyronitrile	164	AZBN	BDH
Polyethylene glycol 200 dimethacrylate	374	PEG200	Polysciences
Polyethylene glycol 1000 dimethacrylate	1166	PEG1000	Polysciences
Methoxy polyethylene glycol 200 methacrylate	320	MPEG200	Polysciences

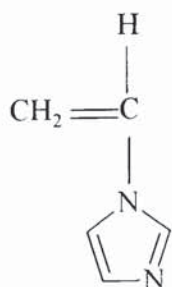
Figure 2.1 Structures of reagents used



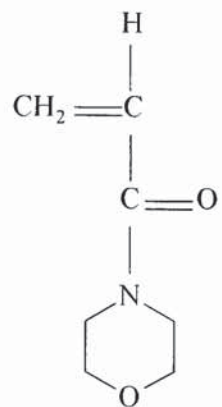
R=CH ₃ R'=CH ₂ CH ₂ OH	2-Hydroxyethyl methacrylate	HEMA
R=CH ₃ R'=CH ₃	Methyl methacrylate	MMA
R=CH ₃ R'=CH ₂ CH ₂ N(CH ₃) ₂	Dimethylaminoethyl methacrylate	DMAEMA
R=H R'=CH ₂ CH ₂ N(CH ₃) ₂	Dimethylaminoethyl acrylate	DMAEA
R=CH ₃ R'=(CH ₂) ₂ OCH ₂ CH ₃	Ethoxyethyl methacrylate	EEMA
R=CH ₃ R'=(CH ₂) ₂ OCH ₃	Methoxyethyl methacrylate	MEMA



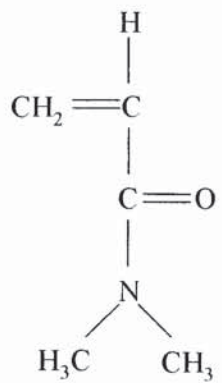
N-vinyl pyrrolidone (NVP)



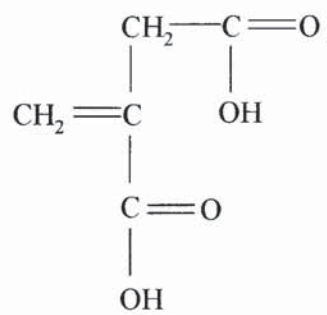
N-vinyl imidazole (NVI)



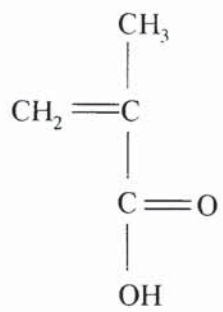
Acryloylmorpholine (AMO)



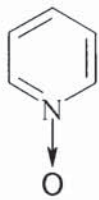
N,N-dimethyl acrylamide (NNDMA)



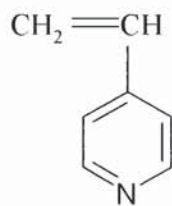
Itaconic acid (ITA)



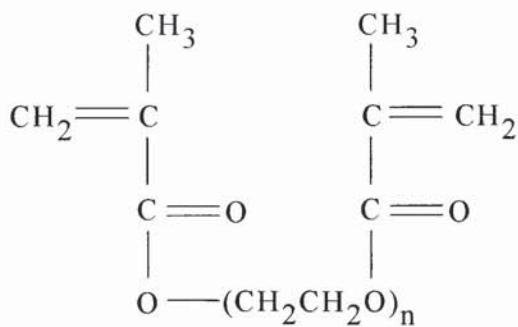
Methacrylic acid (MAA)



Pyridine-N-oxide (PNO)



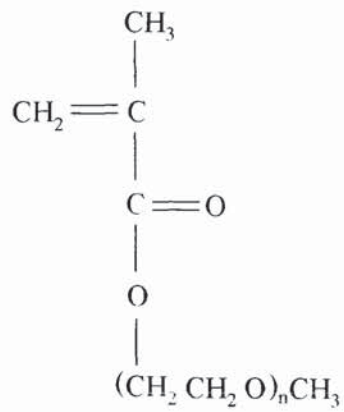
4-vinyl pyridine (4-VP)



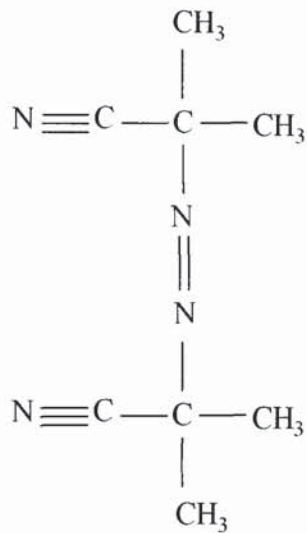
n=1 Ethylene glycol dimethacrylate

n=4 Polyethylene glycol 200 dimethacrylate

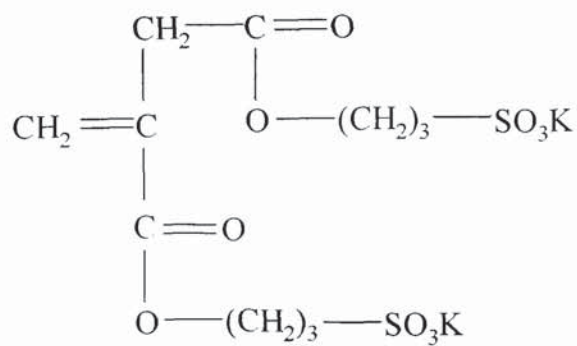
n=22 Polyethylene glycol 1000 dimethacrylate



n=4 Methoxy polyethylene glycol 200 methacrylate



Azo-bis-isobutyronitrile (AZBN)

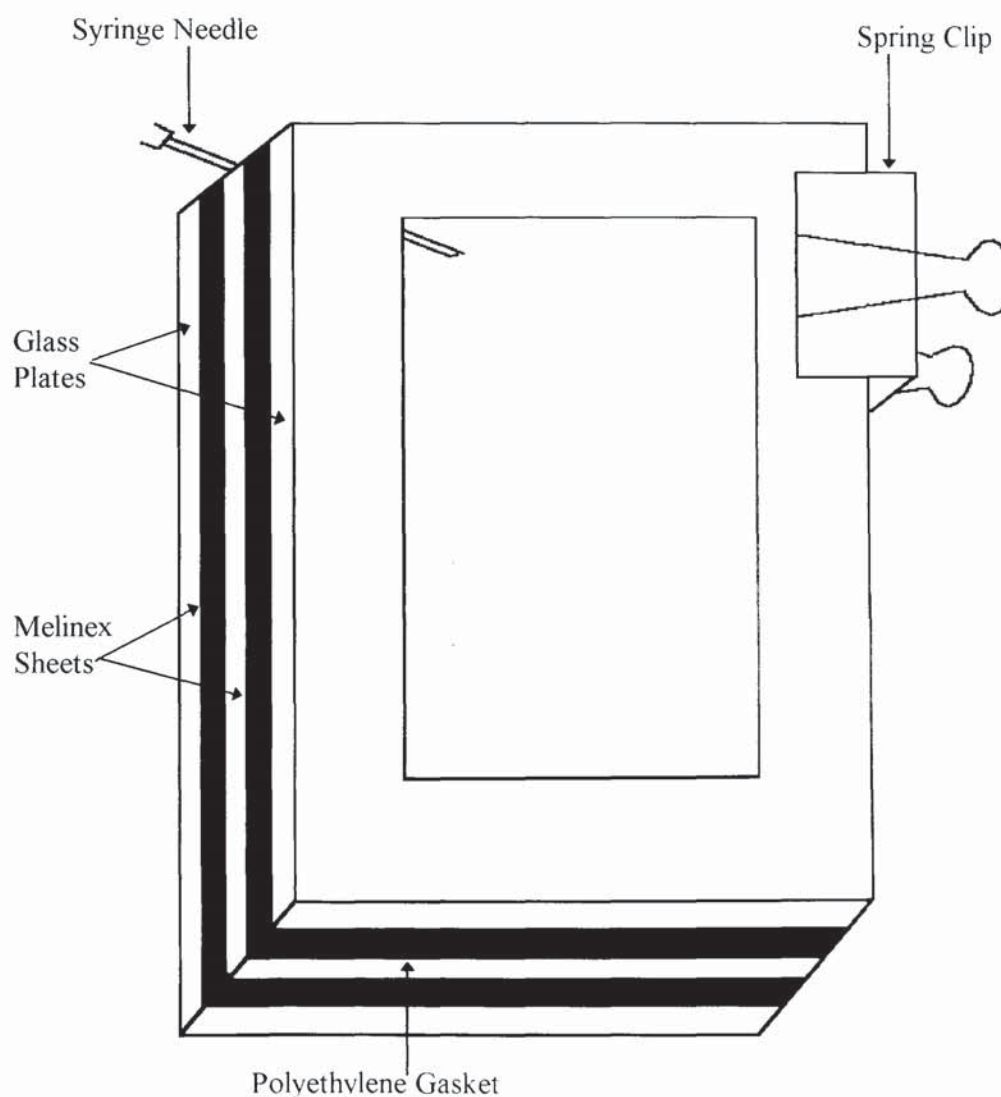


Sulphopropyl ester of itaconic acid (potassium salt) SPI

2.2 Preparation of Membranes

Membranes are produced by the free radical polymerisation of the monomer mixture in a glass mould as shown in figure 2.2. Two glass plates (15cm x 10cm) were each covered by a Melinex (polyethylene terephthalate) sheet to permit easy separation of the polymer membrane from the plates. The covered plates were placed face to face and separated by two polyethylene gaskets (each 0.2 mm thick). Spring clips were used to hold the mould together, leaving sufficient space for the insertion of a G22 syringe needle for the injection of the monomer mixture into the mould cavity.

Figure 2.2 Diagram of a membrane mould

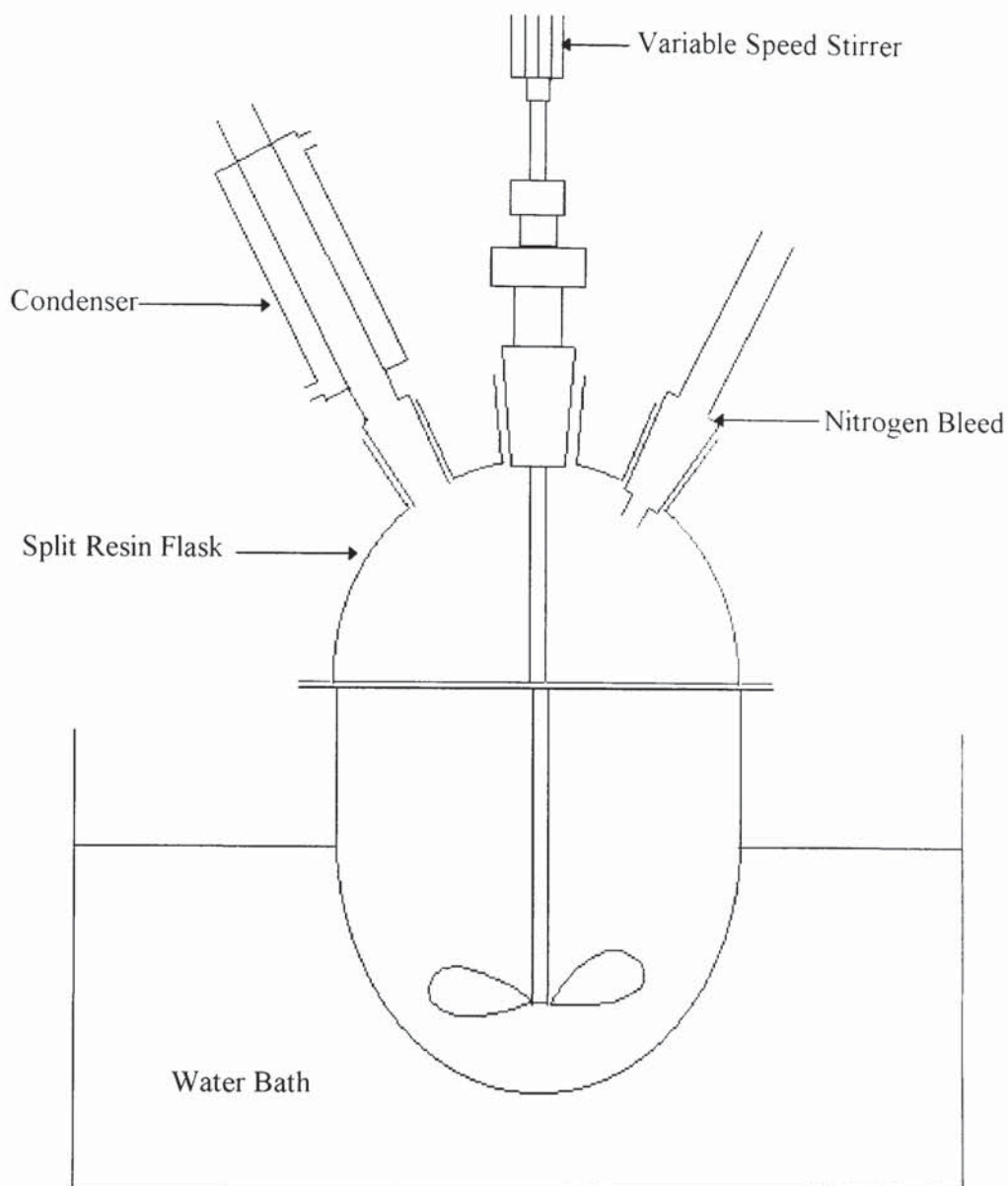


In a typical copolymer composition, the monomers were mixed together to obtain a homogeneous solution to which is added ethylene glycol dimethacrylate cross linker 1.0% (w/w) and azo-bis-isobutyronitrile initiator 1.0% (w/w). The mixture was outgassed with nitrogen before injection into the mould. The mould was then placed in an oven at 60 °C for three days followed by a three hour postcure at 90 °C. The spring clips were removed and, after opening the mould, the membrane was separated from the Melinex sheets, then placed in distilled water to hydrate for two weeks. Studies with a variety of monomer combinations have shown in the past that provided the hydration medium was changed daily, constant values of equilibrium water content were reached in four or five days. The experience with systems such as this, is that the period of time was sufficient both to reach equilibrium hydration and to extract any of the water soluble monomer residuals (as detected by the appropriate g.l.c. technique used in initial assessments of monomer purity).

2.3 Solution Polymerisation

The desired ratio of monomers to be used are dissolved in the required solvents usually in a monomer to solvent ratio of between 1:2 and 1:4. To this solution, 1% by weight of monomers of t-butyl cyclohexyl perdicarbonate is added as the initiator to the polymerisation reaction. The solution is purged with nitrogen and then put in a split resin flask with a stirrer, condenser and nitrogen bleed attached as shown in figure 2.3. After turning the condenser on the apparatus is placed in a water bath at 50°C and the solution is stirred for twenty four hours under a blanket of nitrogen. At the end of this period the solution is made ready for use by the addition of a cross-linker.

Figure 2.3 Solution polymerisation apparatus



To produce thin membranes that could be tested using the dynamic vapour sorption technique, a Melinex sheet is placed on a large glass plate and a small amount of the coating solution is spread thinly on the Melinex using a purpose made spreader. This is then left to air dry since if it is placed in the oven straight away, loss of solvent may cause the appearance of bubbles in the membrane. After the membrane has been air dried for around twenty four hours it is placed in an oven for three hours to dry further and to cross-link. From this small samples could be cut out and sent for analysis.

2.4 Equilibrium Water Content

The equilibrium water content (EWC) was calculated by weight difference of the hydrated and dehydrated samples. Small samples were cut from a hydrated sheet of the hydrogel using a size seven (diameter 13mm) cork borer with any surface water being removed by blotting with filter paper. The samples were weighed then dehydrated for 10 minutes in a microwave oven before being weighed again. The EWC was calculated using equation 1.1 below and the final value is an average of at least three determinations.

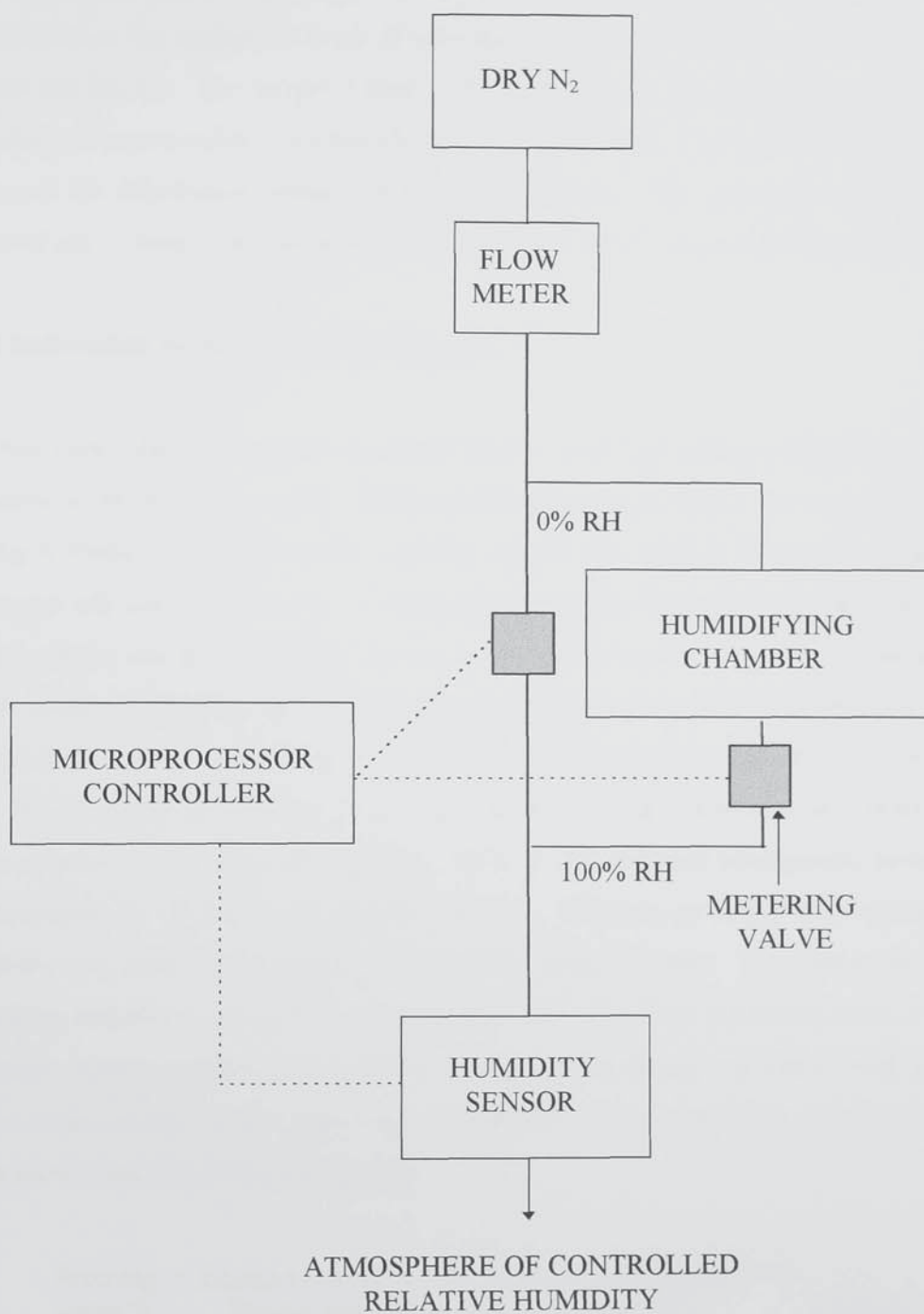
$$\text{EWC} = \frac{\text{Weight of water in gel}}{\text{Total weight of hydrated gel}} \times 100 \quad \text{Equation 1.1}$$

2.5 Dynamic Vapour Sorption (DVS)

The apparatus consists of a highly sensitive Cahn microbalance that is located within sealed glassware. Within the sealed unit the microbalance can be exposed to an air flow of constant relative humidity. This is achieved by mixing a stream of dry air with a stream of air at 100% relative humidity at a specific ratio in order to obtain the desired humidity level as shown in figure 2.4. The balance is linked to a computer in order that changes in mass over long periods of time can be recorded. The humidity level is also computer controlled and so investigations with humidity level changes can be pre-programmed before the experiment begins.

For investigations of moisture uptake in dehydrated hydrogels, the samples were obtained initially in the hydrated state and were then activated immediately prior to assessment by complete dehydration in a microwave oven. The moisture uptake behaviour of samples were evaluated in a standardised 24 hour cycle on the Dynamic Vapour Sorption (DVS-1) apparatus. The samples were prepared and placed at a nominal 0% relative humidity (actual 2%) for four hours to complete activation. The R.H. was then raised to a nominal 10% (actual 12%) for 1000 minutes and then returned to 0% for a further 200 minutes completing the 24 hour cycle. Data was normalised to allow for any weight loss during the initial 4 hour activation stage.

Figure 2.4 Schematic diagram of DVS flow stream of controlled humidity



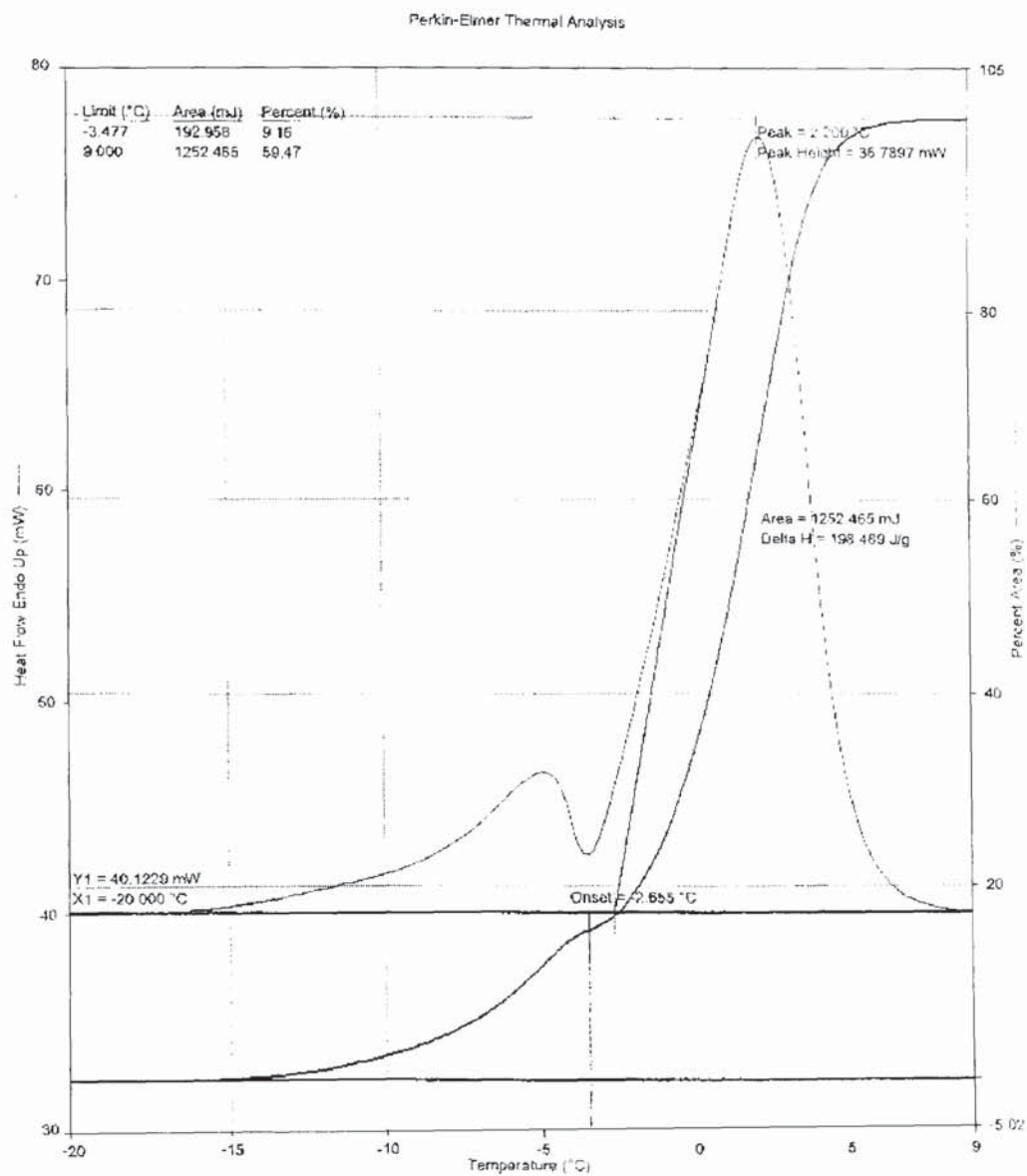
For investigations into the dehydration of hydrogels, samples are used in the fully hydrated state. Small samples are cut from the hydrogel sheet and the surface water is removed carefully by blotting with filter paper. Before the sample is placed on the microbalance the equipment is set to its maximum level of humidity and allowed to reach equilibrium. The sample is held at this humidity just long enough for the mass reading to become stable. The humidity is then lowered to the desired level in order to observe the dehydration characteristics of the hydrogel. The procedure can also be carried out to observe the dehydration characteristics of actual hydrogel contact lenses.

2.6 Differential Scanning Calorimetry (DSC)

In this work, DSC was used for the determination of the percentage of freezing water present in the hydrogel sample. Thermograms as shown in figure 2.5 were obtained using a Perkin Elmer differential scanning calorimeter, DSC 7 fitted with a liquid nitrogen sub ambient accessory. Small samples were cut from the hydrated hydrogel sheet using a size one cork borer and any surface water was removed by blotting with filter paper. Each individual sample was then weighed and sealed in an aluminium pan before being placed in the sample holder of the thermal analyser. The sample is cooled to -70°C to ensure the freezing of any supercooled water and allowed to equilibrate for five minutes. The sample was heated to -25°C at $20^{\circ}\text{C}/\text{min}$ and subsequently to room temperature at $10^{\circ}\text{C}/\text{min}$. A heating rate of $10^{\circ}\text{C}/\text{min}$ produced well separated endothermic peaks in the region of the melting point of water. The area under the resulting endotherm corresponds to the energy required to melt the frozen water in the sample. As the weight of the sample is known and the energy required to melt 1g of pure water is known, the percentage of freezable water within the sample can be calculated using the following equation.

$$\text{Freezing water \%} = \frac{\text{Energy required to melt water in 1g of sample} \times 100}{\text{Energy required to melt 1g of pure water}} \quad \text{Equation 2.1}$$

Figure 2.5 An example of a thermogram obtained from DSC



2.7 Mechanical Properties

The mechanical properties of the hydrogel samples was investigated using a Hounsfield HTi tensometer which was interfaced to an IBM 55SX computer. The tensometer was fitted with a 10N load cell which was attached to the instruments crosshead which moved in a vertical direction. Values for a set of parameters were entered into the program to control the crosshead speed and to allow the calculation of specific properties for the sample under test. The crosshead was raised at the entered speed until the sample broke completely.

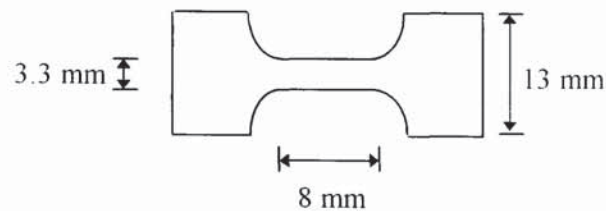


Figure 2.6 Dimensions of a hydrogel sample for mechanical testing

Samples were cut from a hydrated sheet into dumbbell shaped test pieces of gauge length 8mm and width 3.3mm using a metal cutter. The dimensions of a test piece are shown in figure 2.6. The test pieces were equilibrated in distilled water prior to testing to ensure complete hydration. A micrometer allows the thickness of each individual test piece to be measured before it is placed into the jaws of the tensometer. A standard test speed of 10mm min^{-1} was used at the conditions of room temperature and pressure. This speed has been found to be slow enough to allow the chains of the polymer to uncoil thus giving a representative result of the materials mechanical properties⁹⁰. To maintain complete hydration (100% humidity) the samples were sprayed before and during the test cycle with a fine spray of distilled water. The force of this spray is small enough as to not induce the sample to break prematurely. The computer program calculated the Youngs modulus (E), tensile strength at break (Ts) and elongation at break (Eb) using the following equations.

$$\text{Youngs (E) modulus} = \frac{\text{stress}}{\text{strain}} \quad \text{Equation 2.2}$$



where

$$\text{stress } (\epsilon) = \frac{\text{load}}{\text{cross-sectional area}} \quad \text{Equation 2.3}$$

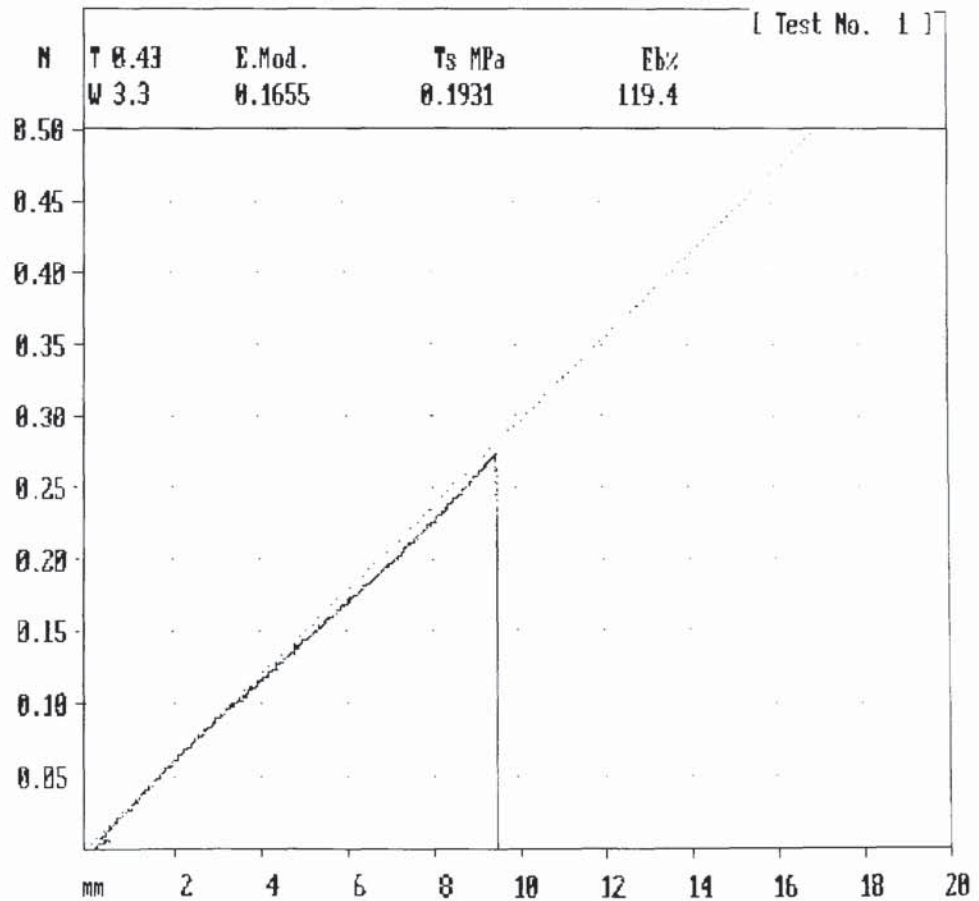
and

$$\text{strain } (e) = \frac{\text{extension of gauge length}}{\text{original gauge length}} \quad \text{Equation 2.4}$$

$$\text{Tensile strength } (T_s) = \frac{\text{load at break}}{\text{cross-sectional area}} \quad \text{Equation 2.5}$$

$$\text{Elongation at break } (E_b) = \frac{\text{extension of gauge length} \times 100}{\text{original gauge length}} \quad \text{Equation 2.6}$$

Figure 2.7 An example of a stress-strain curve obtained from the tensometer



2.8 Contact Angles

The surface energies of the hydrogels in the dehydrated state were obtained using the sessile drop technique and in the hydrated state obtained using the Hamilton and captive air bubble methods. The theory used to determine surface energies from contact angle measurements has already been presented in chapter one.

2.8.1 Sessile Drop Technique

Disks were cut from the hydrated polymer membrane using a size seven cork borer. The surface of the discs was cleaned with Teepol detergent solution after which they were rinsed thoroughly and allowed to soak overnight in distilled water. The discs are then dehydrated in a microwave for ten minutes and then placed in a dessicator. The discs are mounted horizontally on a microscope slide.

The contact angles are measured using a GBX contact angle measuring system. The system consists of a computer controlled stage, above which sits an automated syringe which is again controlled by the computer. A video camera located within the instrument is used to view the stage and syringe tip with the image being sent to the computer. The system can be set to take an instantaneous image after a drop is placed on the surface of the material. The contact angle can then be measured from the image visible on the computers monitor using the programs software.

By the use of an automated syringe, the drop that is formed can be set to always be of the same volume. The computer controlled stage ensures that the drop formed by the syringe is placed on the material with a reproducible force. As the software is used to calculate the contact angle there is no reliance on the judgement of the operator. Thus the method is more user friendly and eliminates the variability from user to user that is seen with conventional goniometers. The equipment can also measure the contact angle automatically, and this permits experiments where a change in the contact angle is observed as the drop is absorbed into the surface to be undertaken.

2.8.2 Hamiltons Method

Using a size seven cork borer discs were cut from the hydrated hydrogel membrane. Surface water was removed from one side of the hydrogel sample by blotting with a filter paper. The sample is mounted on a glass slide and suspended in an inverted position in a glass cell with optically perfect sides. The cell was filled with distilled water with a drop of n-octane being placed on the surface of the hydrogel sample using a G25 syringe needle. The point of the needle had been removed to ensure that the drop that formed on the surface of the hydrogel was symmetrical. The contact angle between the hydrogel sample and the octane bubble was measured again using the GBX system.

2.8.3 Captive Air Bubble Technique

This technique was carried out in the same way as the Hamilton method but with bubbles of air being used instead of droplets of n-octane.

2.8.4 Dynamic Contact Angle Measurement

Dynamic contact angles for hydrogel membranes were obtained using a DCA 300 series analyser from Cahn instruments which was interfaced to an IBM computer. A schematic representation of the instrument is shown in figure 2.8.

The instrument was used to determine the values of the advancing and receding contact angles of hydrated hydrogel samples. Hydrogel membranes were polymerised by the method described earlier. After the required period of hydration the samples were cut into strips of length 10 mm and width 3.3 mm using a cutter. The thickness of the strips of sample were measured with a digital micrometer and the values recorded.

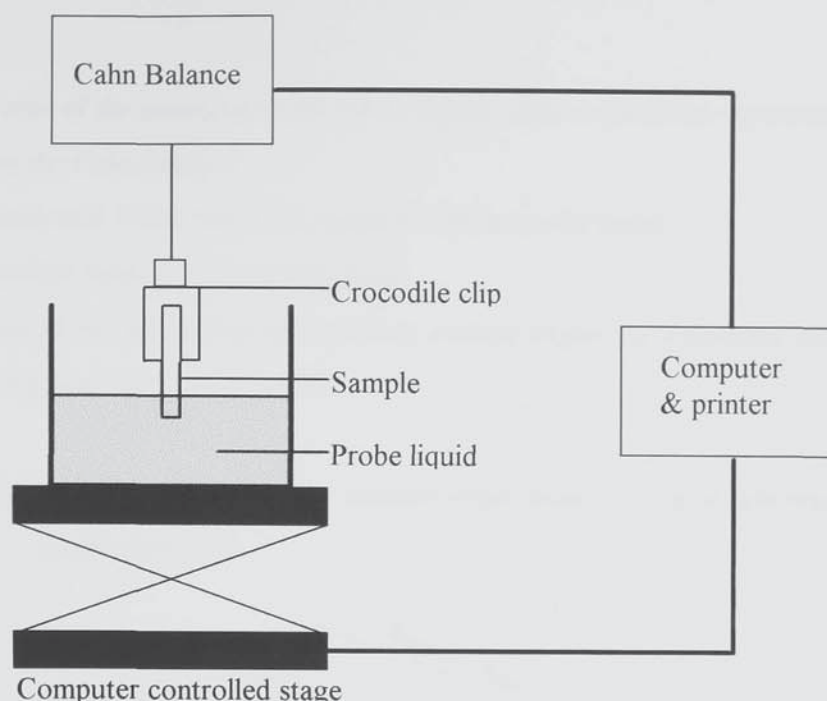


Figure 2.8 Schematic diagram of the dynamic contact angle analyser

The hydrated sample was suspended from the Cahn balance by a connecting wire and a small crocodile clip and held in a vertical position with the lowest edge 3mm above the level of the liquid. Prior to sample preparation the instrument had the depth of immersion and number of immersion cycles programmed into the computer. Once the sample was in place and the required information entered, the sample was lowered into the probe liquid at a rate of 0.1mm s^{-1} to a depth of 7mm. The sample was immediately raised at the same rate until it returned to the starting height. At this point, it was ensured that the sample made no contact with the meniscus of the probe liquid (nominally 2-3mm below the sample). This dipping procedure was repeated for the required number of immersion cycles; a minimum number of three cycles were performed for each sample. The computer program plotted the results obtained as force versus immersion depth, a typical dynamic hysteresis profile is illustrated in figure 2.9. A simple equation relates the wetting force to the cosine of the contact angle :-

$$\cos \theta = F / L \gamma \quad \text{Equation 2.7}$$

where

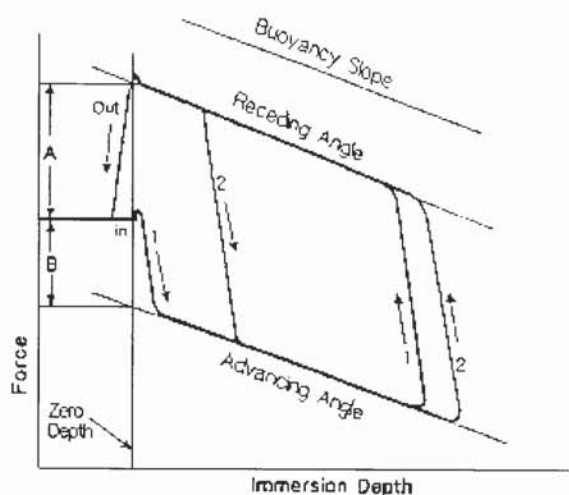
F = force of the meniscus at the solid / liquid / vapour interface, measured directly by the Cahn balance

L = perimeter of the sample in contact with the probe liquid

γ = surface tension of the probe liquid

The values of the advancing and receding contact angles are calculated automatically by the computer using this equation.

Figure 2.9 Diagram of a dynamic contact angle hysteresis curve, illustrating a two immersion cycle.



2.9 Static Surface Tension (SST)

Static Surface Tension is calculated at the equilibrium state and can be measured using either the DuNouy ring or the Wilhelmy plate. These methods are based on the forces involved at the air-liquid interface and record the maximum force acting on the ring or the plate. The DuNouy ring is suspended from the Cahn balance used for dynamic contact angle measurement and immersed in the probe liquid. The computer controlled stage is then lowered slowly until the ring pulls clear of the liquid. As the ring pulls clear of the liquid, the force required to raise it reaches a maximum and is displayed on the balance as a static surface tension. The static surface tension measurements in this work were repeated several times to enable an average value to be obtained.

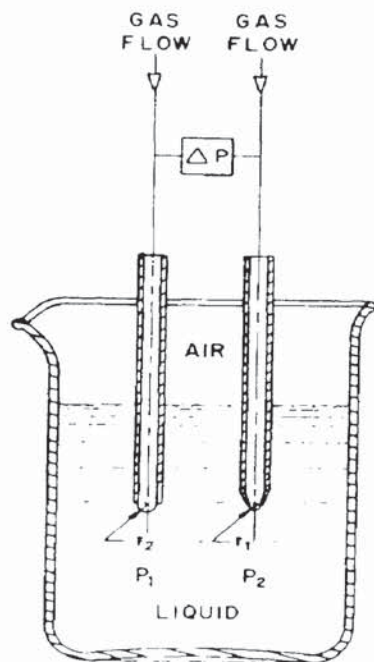
2.10 Dynamic Surface Tension (DST)

This technique is based on the measurement of the maximum pressure obtained within an air bubble formed in a liquid. Two probes of different radii are immersed in the liquid, and a flow of an inert gas passes through these probes. The pressure inside the probe is given by the Laplace equation as shown below.

$$P = \rho gh + 2\gamma / r + P_0 \quad \text{Equation 2.8}$$

where P_0 is the atmospheric pressure.

By the use of two probes, the experiment is independent of the depth of immersion, and of the atmospheric pressure. From the pressure difference of the probes, the surface tension of the solution using equation 2.9 can be calculated.



$$\gamma = \frac{\Delta P}{2 \left(\frac{1}{r_1} - \frac{1}{r_2} \right)} \quad \text{Equation 2.9}$$

γ = dynamic surface tension

ΔP = pressure difference between the two probes : $P_1 - P_2$

r_1 = radius of probe 1

r_2 = radius of probe 2

P_1 = pressure in probe 1

P_2 = pressure in probe 2

For a pure solution, the surface tension will be independent of the gas flow, i.e. of the bubble rate. However for a lubricating solution, the measurement is dependent on the flow used for the experiment. The flow is recorded as the frequency of bubble formation at the small probe, given in bubbles / s. The bubble rate can also be converted into length formed per second in order to correlate these measurements with those obtained in frictional studies. The conversion is :

$$1 \text{ bubble / s} = \pi / 4 \text{ (mm s}^{-1}\text{)} \quad \text{Equation 2.10}$$

By the modification of bubble rate, we can measure :

- the behaviour of surfactant DST.
- the solution efficiency in dynamic rather than in static conditions,
- i.e. lubrication level during blinking.

2.11 Coefficient Of Friction

Apparatus to measure the coefficient of friction for large sheet samples has been modified to measure this property for contact lenses as displayed in figure 2.10. For accurate measurements it is essential that the friction between the Nylon and the glass surfaces is kept to a minimum. Therefore all surfaces that come into contact with each other are thoroughly cleaned with methanol as is the surface of the Melinex sheet. A contact lens is placed on the convex mould which is then upturned and placed upon the polyethylene terephthalate sheet. A small amount of the lubricating solution that is being investigated is added to the trough before testing can begin.

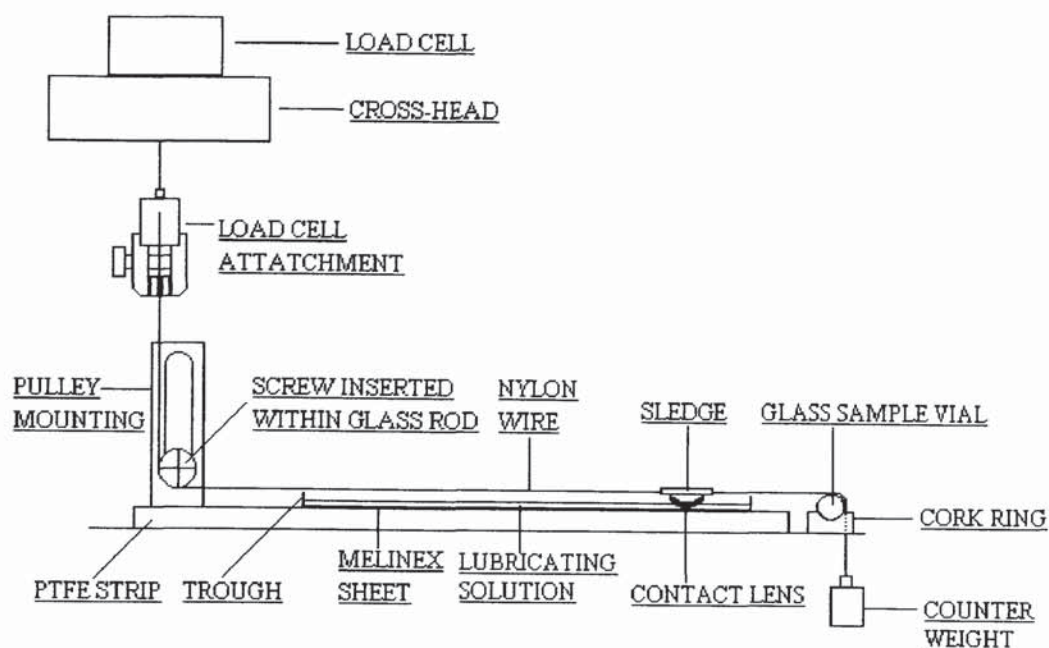
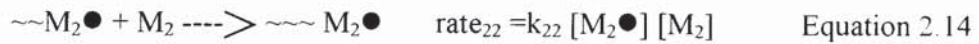
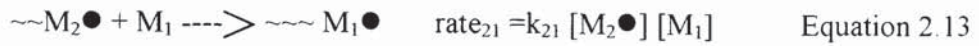
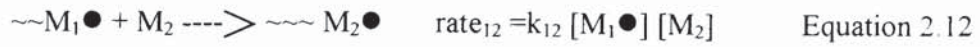
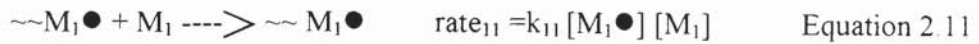


Figure 2.10 Apparatus for measurement of the coefficient of friction of contact lenses

Different weights can be placed upon the sledge to stimulate a range of pressures during blinking which typically are between $35\text{-}40\text{g cm}^{-2}$ in value⁹¹. The experiments are carried out at 0.83cm s^{-1} , a maximum for the apparatus. These details are entered into the computer program to enable the calculation of the frictional force.

2.12 Copolymer Sequence Distribution

The effect of monomer reactivity on sequence distributions was studied using a computer simulation model. The program uses the Monte Carlo method of statistical trials⁹², which constructs a random process for the solving of computational mathematical problems. The development of the model, upon which the computer simulation is based, was constructed using the basic free radical polymerisation model. The statistical hypothesis for the reaction kinetics of this model is that the reactivity of the radical centre is governed by the monomer unit upon which the active radical centre is located. Four propagation steps for the reaction are possible:-



where:

M	=	monomer
M \bullet	=	monomer radical
k	=	rate constant
[]	=	concentration of individual species

Considering the reactions which involve polymer chains ending with a M₁ radical, gives an overall rate for these reactions of :-

$$R_1 = \text{rate}_{11} + \text{rate}_{12} \quad \text{Equation 2.15}$$

and the fraction of these polymer chains that will add a further unit of M₁ at the radical end will be given by:-

$$f_{11} = \text{rate}_{11} / R_1 \quad \text{Equation 2.16}$$

where f₁₁ is the fraction of polymer chains ending in an M₁ radical adding to another unit of M₁. Substitution of the above equations into equation 2.16 gives :-

$$f_{11} = k_{11} [A] / (k_{11} [A] + k_{12} [B]) \quad \text{Equation 2.17}$$

where A is monomer 1 and B is monomer 2. This equation simplifies to :-

$$f_{11} = 1 / (1 + k_{12} [B] / k_{11} [A]) \quad \text{Equation 2.18}$$

The individual reactivity ratios of M₁ and M₂ are defined as the ratio of the rates of reaction of a polymer chain ending in a radical of one type adding itself to the rate of its reaction with the second monomer in the copolymer system. Therefore :-

$$r_1 = k_{11} / k_{12} \quad \text{Equation 2.19}$$

and

$$r_2 = k_{22} / k_{21} \quad \text{Equation 2.20}$$

where r₁ and r₂ are the reactivity ratios of the monomers M₁ and M₂ respectively.

Substitution of equation 2.19 into equation 2.18 gives :-

$$f_{11} = 1 / (1 + 1/r_1 \cdot [B] / [A]) \quad \text{Equation 2.21}$$

Similarly it follows that :-

$$f_{22} = 1 / (1 + 1/r_2 \cdot [A] / [B]) \quad \text{Equation 2.22}$$

Therefore if the initial concentrations of the monomers and their reactivity ratios are known then the fraction of the polymer chains ending in the radical M_1 that add to unreacted monomer M_1 will be given by f_{11} . Similarly, the fraction of polymer chains ending in M_1 that add to unreacted monomer M_2 will be given by f_{12} .

The computer simulation generates a random number (RN) after each addition step, in the range 0 to 1 and compares this to the value of f_{11} generated from initial concentrations and reactivity ratios. If $f_{11} > RN$ then the simulation adds an M_1 monomer unit onto the growing free radical polymer chain. If $f_{11} < RN$ then to the growing chain an unreacted M_2 monomer unit is added. After the addition of a M_2 monomer unit, the simulation considers addition of the two monomers onto a growing polymer chain ending with an M_2 radical. This procedure continues until there is 100% conversion of the monomers into polymer.

Ashraf⁸⁶ studied the viability of using these computer simulation programs. Computer simulations as shown in figure 2.11, were prepared using a number of methacrylate based comonomer systems together with the experimental preparation of the same copolymers. It was found that the sequence lengths determined using the methods of ¹³C NMR and elemental analysis were within 3% of the sequence lengths produced by the computer simulation. It is therefore assumed that the computer simulation is accurate enough to simulate the reactivity of comonomers in a free radical polymerisation.

Figure 2.11 Example of a sequence simulation for a hydrogel copolymer

70% of Monomer A = HPMA

30% of Monomer B = AMO

$r(AB) = 0.409$

$r(BA) = 0.102$

CHAPTER 3

HYDROGEL CONTACT LENSES - WATER BINDING AND CORNEAL STAINING

3.1 Introduction

The work discussed in this and the following chapter examines the dehydration and hydration characteristics of hydrogel systems. This chapter is concerned with the dehydration of hydrogel contact lenses, a fundamental if poorly understood problem with materials of this type. The process may be dependent on both the material structure and water binding properties of the hydrogel which may enable materials susceptible to dehydration to be identified. The following chapter examines the hydration characteristics and water binding properties of a number of hydrogel formulations which would be expected to be influenced in a similar way.

Hydrogel contact lenses can cause reversible damage to the corneal epithelium by a number of different processes. Wearers of thin, high water content lenses are particularly prone to certain complications, apparently indicating the increased effect of dehydration as a consequence of increasing water content and decreasing thickness. This manifests itself as “corneal desiccation staining” which is one of the clinical problems impeding the development of successful extended wear hydrogel materials. The loss of water from the surface of a lens, followed by the movement of water through the lens from the epithelium, leads ultimately to localised corneal drying and epithelial damage. However a number of research groups have hypothesised that corneal staining is independent of lens dehydration, a point which is discussed in detail later in this chapter. Many research groups attempted unsuccessfully to find correlations between changes in the water content of hydrogels during wear and various lens wear conditions^{51, 54}. It became clear to these researchers that a better understanding of the physiochemical properties of hydrogel materials would be required before a reliable model predicting the extent of hydrogel lens dehydration could be constructed⁵⁸.

Holden et al⁴⁵ reported that corneal desiccation was avoided by using thicker contact lenses or those of lower water content, or by increasing ambient relative humidity. This suggests that an evaporative process is the main factor in causing damage to the corneal epithelium. The effect of humidity was not clear in that study since humidity, temperature, and oxygen tension varied simultaneously in the micro-environment in

front of the eye. An evaporative process may not be the sole mechanism underlying the corneal damage as a subsequent clinical report found no relationship between ambient humidity and corneal staining⁴⁴. Fatt⁹³ presented a theoretical model as a framework to understand the possible mechanisms underlying these clinical observations. In this model it was proposed that the depth to which dehydration penetrated from the anterior lens surface was a causative factor in corneal epithelial damage. In his analysis, the blink characteristics and the physical properties of the hydrogel governed the extent to which the cornea was affected by the penetrating dehydration of the contact lens.

Mirejovsky et al⁵³ carried out a study to determine the propensity of a given material to induce corneal staining. They postulate that materials containing a higher amount of water with the properties of bulk water would be more prone to water loss and hence induce corneal desiccation more readily than materials with the same water content but a larger proportion of water interacting strongly with the polymer. Another factor of the epithelial damage is that the loss of free water from the contact lens leads to a reduction in oxygen transport to the cornea. This reduction may be of the order of 7 Dk units⁹⁴ for high EWC contact lenses. Therefore, the corneal epithelial damage may be due to alterations in the metabolism of the corneal epithelial cells.

Andrasko⁵⁷ reported that a single lens displayed a relative loss of water content of 11.4% after 30 minutes of closed eye wear and 13.2% after the same period of open eye wear. It was found that the time course of dehydration during the first 30 minutes of wear is a function of lens thickness, in that the water content of a thin lens decreases more rapidly than lenses of a greater thickness. This study however is limited in that it was a low water content lens worn for 30 minutes by one subject. Brennan et al⁵⁴ carried out a similar study on seven subjects with a variety of lens types during a seven hour wear period where the results are applicable to the typical extended wear situation. In this study, subjects used a hand refractometer to measure the dehydration of hydrogel lenses of different water contents and thickness under normal daytime and overnight wearing conditions. Only a single measurement was obtained after each period of wear as the lenses continue to dehydrate after removal from the eye and repeated measurements would have resulted in an underestimation of the true *in vivo*

water content. It was found that the absolute decrease in water content was not predictable on the basis of the initial water content of the lens. The results also indicated that thickness did not play a role in determining the equilibrium water content after seven hours of wear. It was therefore hypothesised that thicker lenses display a slower initial rate of dehydration, but ultimately reach the same equilibrium water content as thinner lenses. The unexpected result of this study however, was that there was no significant difference between the amount of dehydration observed in closed eye wear compared to that of open eye wear.

To account for the above results, the factors which control dehydration from a hydrogel contact lens will be outlined. There are a number of competing environmental influences whose contribution is variable and difficult to predict. The dehydration of hydrogel contact lenses is known to be affected by temperature increase⁵², evaporation⁹⁵, osmolarity and changes in pH⁹⁶. During the closed lid situation a decrease in water content would be expected since pH decreases⁹⁷ and temperature increases⁹⁸. Conversely, evaporation is virtually eliminated and tears become relatively hypotonic⁹⁹, the result of which would be a decrease in dehydration compared to that of open-eye conditions. Considering these factors, several reasons may be offered to explain the similarity between open and closed eye lens dehydration. A relatively minor influence on lens water content is expected for the difference in pH and osmolarity known to exist between the open and closed eye. Also the principal competing influences of increased temperature and decreased evaporation under the closed lid may counterbalance.

In the majority of the literature corneal desiccation and lens dehydration are discussed interchangeably but it has been shown that they are not always related. It was found that the incidence of corneal epithelial disruption found with thin high water content lenses could not be correlated with the degree of dehydration of the lens¹⁰⁰. The degree of equilibrium swelling of a hydrogel is dictated by the chemical potential of the water used which itself is determined by the nature and concentration of solutes present. The chemical potential of water within tears will therefore control the water content that a lens equilibrates to when placed into the eye. The main role of lipids in tears is to prevent the evaporation of water by lowering the activity at the tear

interface. Therefore a high water lens will be affected more by a change in the chemical potential of water than a low water lens. In actual fact the higher the content of free water in the lens the greater the effect of the water activity of the tears. Lens dehydration is seen as an equilibrium process rather than a simple loss of water from the hydrogel by evaporation. This view is further supported by data showing the same degree of dehydration in closed and open eye wear.

Corneal desiccation is controlled by the ability of water to move through the contact lens. It has been determined that the initial rate of evaporation of water from various lenses was in the same range regardless of material type or water content and was the same rate as the evaporation of pure water. The same rate of evaporation for high and low water content lenses indicates that the evaporation of water can not be the cause of lens dehydration or corneal staining, since high water content lenses suffer more from these complications than lenses of low water content.

3.2 Techniques to Study the Water Structuring of Hydrogel Contact Lenses

Various techniques and studies have been undertaken over the last few years to study the dehydration of contact lenses during both open and closed eye wear and to correlate these results to properties that are easily measurable. The hand held refractometer has proved to be a useful clinical tool for measuring the water content of hydrogel contact lenses¹⁰¹. Unfortunately this easily operable instrument gives no information on the precise structure of the water within the lens. Larsen et al⁴⁰, correlated *in vivo* lens dehydration to water mobility using proton NMR relaxation. A different approach to predict *in vivo* lens dehydration based upon swelling pressure and the calculation of water transport coefficients in hydrogels was proposed by Fatt¹⁰². In both these studies, for high and low water content hydrogels substantial differences in water properties were found. It is not clear however whether these approaches are sensitive enough to predict *in vivo* desiccation induced by materials with similar water contents but slightly different compositions.

Mirejovsky et al⁵³ used both differential scanning calorimetry and the permeabilities of glucose and water to investigate the states of water in commercially available contact

lenses. Some polymers exhibit multiple melting endotherms when DSC is used. The portion showing a sharp melting endotherm at 0°C corresponds to free water while the portion exhibiting a broad melting pattern between -30°C and 0°C corresponds to intermediate water. To investigate the water structuring within a hydrogel contact lens, permeability measurements can also be used. Water is used to determine whether the dominant transport process is that of viscous flow or diffusive flow. The permeability of glucose is then used to determine the relative magnitude of bulk water involved in transport processes. Glucose can only diffuse through hydrogel regions containing water available for its solubilisation, i.e. intermediate and free water. Thus the results obtained from DSC have been confirmed by an independent technique.

The purpose of the work summarised in this chapter is to see if corneal staining itself can be correlated with the states of water in commercially available contact lenses. Thus, investigation of the complex dehydration process for a hydrogel contact lens on the eye is avoided. Other physical factors such as centre thickness of the lens and equilibrium water content will also be taken into account.

When investigating the properties of contact lenses it is important to distinguish between the various classes of contact lenses. The lenses are categorised into specific classes as directed by the Food & Drug Administration (FDA). These groups are shown in table 3.1.

Table 3.1 FDA classification of commercially available contact lenses.

F.D.A. Classification	Characteristics
I	Low water, non-ionic
II	High water, non-ionic
III	Low water, ionic
IV	High water, ionic

3.3 Materials and Methods

In order to evaluate a materials capability to induce corneal staining, a clinical study was carried out on a range of hydrogel contact lenses that were also investigated by differential scanning calorimetry. The characteristics of the lenses that were used in the study are shown in table 3.2.

Table 3.2 Suppliers and characteristics of hydrogel contact lenses used in this study

Lens	Manufacturer	EWC %	Group	Disposable	Centre thickness mm
Z6	Hydron	38	I	No	0.06
DR40	Vista Optics	40	I	No	0.06
Classic	PBH	43	I	No	0.06
Focus	Ciba Vision	55	IV	Yes	0.10
Surevue	Vistakon	58	IV	Yes	0.11
Excelens	Ciba Vision	64	II	No	0.12
Medalist 66	Baush + Lomb	66	II	Yes	0.10
ES70	Lunelle	70	II	No	0.14
Rythmic	Lunelle	73	II	Yes	0.15
Precision UV	PBH	74	II	Yes	0.14

3.4 Clinical Protocol

Each lens type was worn by a minimum of ten subjects for twenty eight days resulting in a minimum of twenty data points. Two systems were employed by subjects for the cleaning of lenses, a peroxide based system and a multipurpose solution. A number of lens types were cleaned using both systems to see if this would affect a lenses capability to induce corneal staining.

Lenses were soaked in the relevant cleaning solution for a minimum of three days prior to investigation by differential scanning calorimetry. This procedure also applied when the lenses were evaluated in their packing solution as well as in saline and distilled water. Thermograms were obtained as described in section 2.6.

All slit-lamp examinations were undertaken on a Nikon FS3 zoom photo-slit lamp, with 20x eye-pieces at magnifications ranging from 7.5-30x. Fluorescein examinations were undertaken with a blue excitation filter and yellow barrier filter (Kodak Wratten #12) in order to enhance the contrast of any staining. Observation of the clinical signs in this study was used to ensure that no untoward complications were occurring with the lens/care system combination under test

Findings such as blood vessel infiltration into the cornea can be measured using a graticule eye-piece and multiple findings such as epithelial microcysts and stromal striae can be counted. However, the majority of clinical findings cannot be recorded in this way. The generally accepted recording technique for use with features which cannot be measured depends upon the practitioner assigning scales to their clinical observations. Each observation may be regarded as part of a continuous scale which is assigned a grade based on the clinical observation. This grade serves as a standard by which any future observation can be judged.

Confidence limits must be ascertained which will provide an indication as to the likely probability that a second observation will result in a grade which is different from the first when, in fact, no real change has occurred. Confidence limits depend upon the clinicians consistency in assigning grades. Where possible, dividing the ocular structure of interest into specific quadrants will enhance such scales, as each area can be assigned a severity scale and all areas added together to give a global score. The advantage of this scoring system is that the principal area of staining, in addition to its extent, can be ascertained. The use of picture scales (particularly when used with a decimalised scoring system) reduces inter and intra-observer variability. The publication of such findings has resulted in the recent release of picture-based grading scales utilising photographs from the CCLRU in conjunction with Vistakon.

These studies used an adaptation of the CCLRU grading scale which is described in Table 3.3

Table 3.3 Grading system for corneal staining

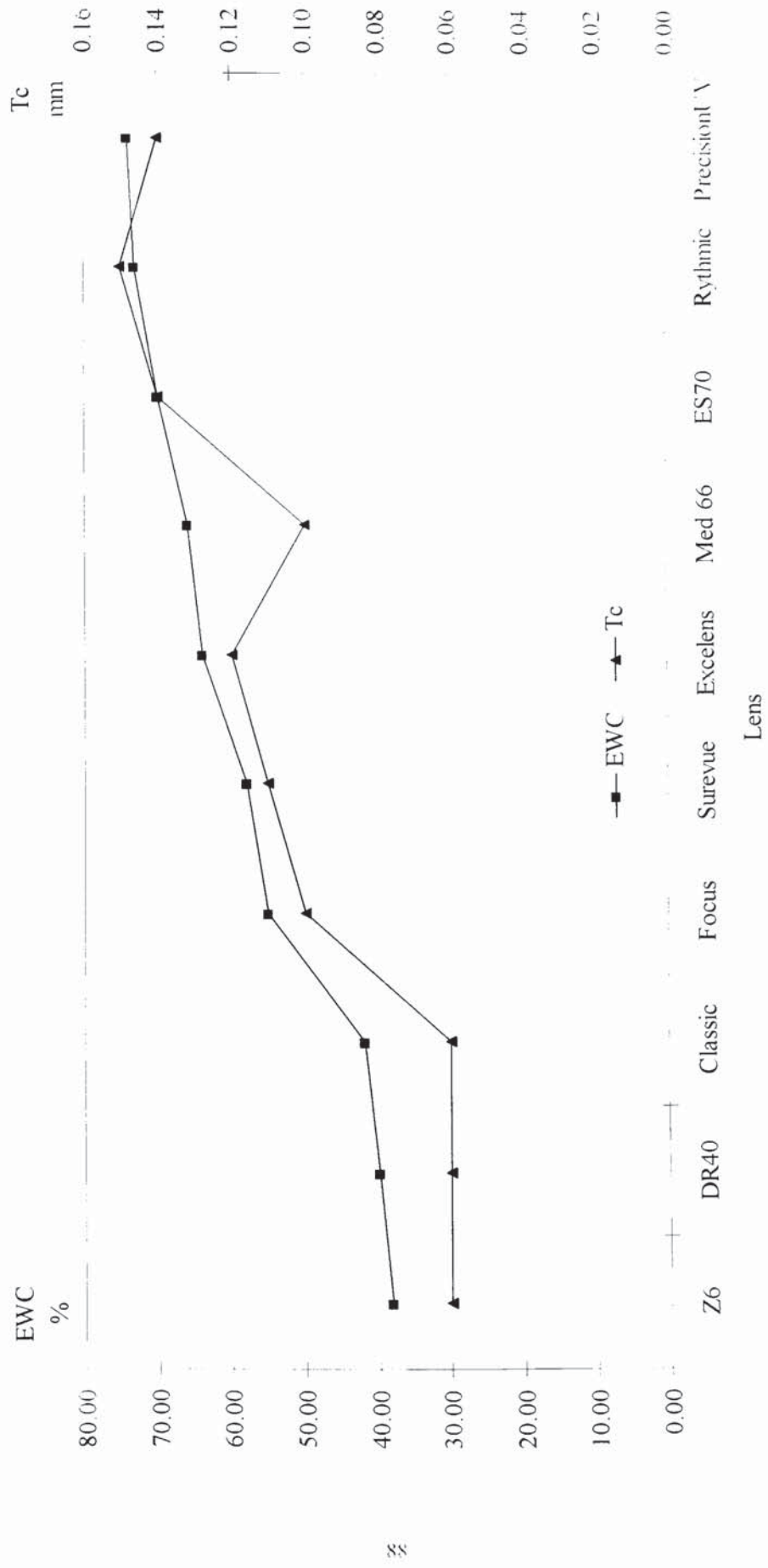
EXTENT	DEPTH	AREA
0)None	0)None	A = Superior
1)1-20 punctate spots	1)Not stromal	B = Nasal
2)21-40 punctate spots	2)Stromal, slow diffusion	C = Inferior
3)Light confluent area	3)Immediate, moderate stromal diffusion	D = Temporal
4)Abrasion/ulcer	4)Widespread stromal diffusion	E = Central

The grading system was scored by taking the staining score for each area (extent x depth) and adding all five areas together to achieve a global score.

3.5 Physical Properties

Although the detailed water structure of various contact lens materials have been obtained it is important to also consider the bulk properties of the contact lens. Factors such as equilibrium water content and lens thickness will have an influence on lens dehydration and consequently the degree of corneal staining. In figure 3.1 it can be seen that as the EWC of the contact lens material increases, the centre thickness of the contact lens also rises. This is a consequence of the hypothesis that corneal staining is reduced by use of thicker lenses or by using materials with a lower equilibrium water content. The EWC of lenses at a certain lens thickness falls into a band which causes some irregularities as seen in figure 3.1.

Figure 3.1 Equilibrium water content and centre thickness (Tc) for a range of contact lenses

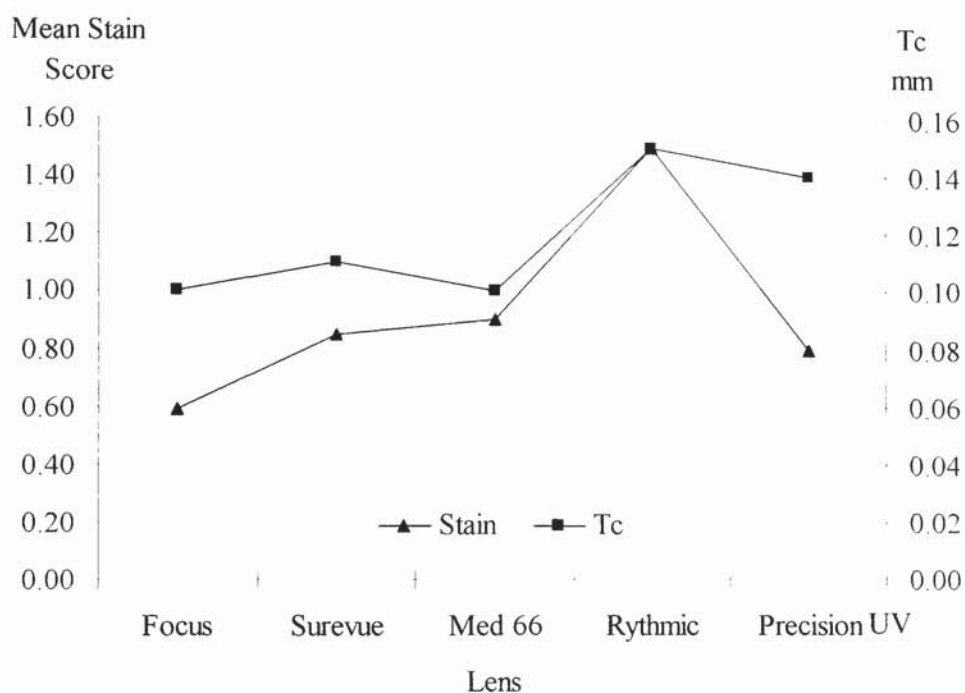


3.6 Results

The results are presented graphically in figures 3.2-3.10 and can also be found in appendix I.

3.7 Investigation of Contact Lenses Cleaned in “ReNu” Multipurpose Solution

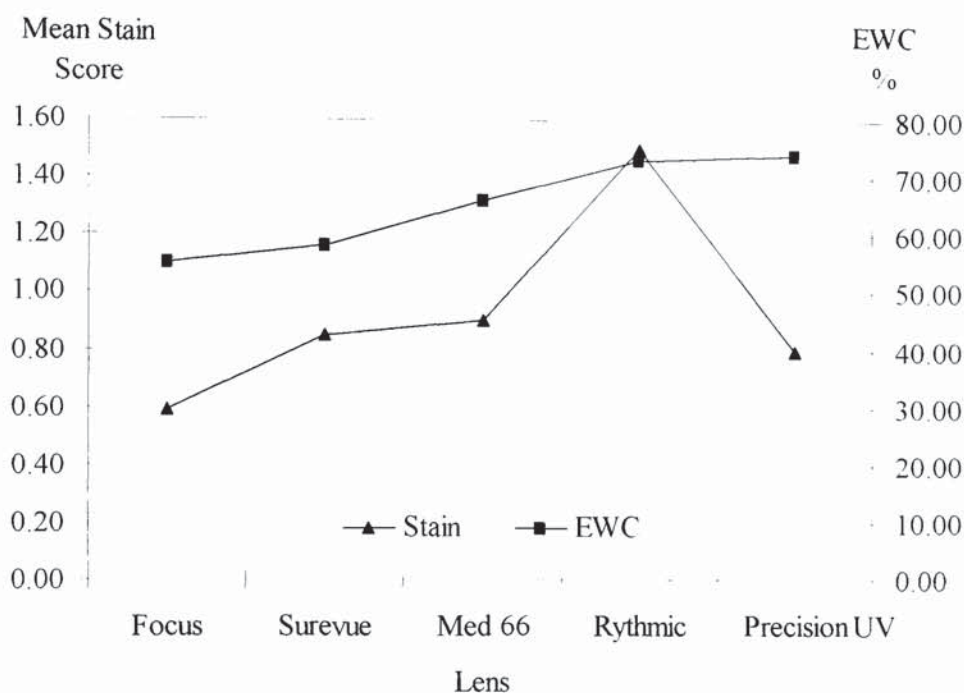
Figure 3.2 Mean stain score and centre thickness (Tc) for contact lenses cleaned in ReNu multipurpose solution



For the lenses cleaned using ReNu multipurpose solution, the mean stain scores can be plotted against the physical properties of the contact lens before the proportions of free and bound water are considered. Figure 3.2 shows mean stain score and centre thickness for these lenses. There are similarities between the two plots but marked differences exist between some of the values as displayed in the results for the precision lens. As the EWCs increase in proportion to the centre thickness of the contact lens, a plot of mean stain score and EWC would be expected to display similar trends and this is illustrated in figure 3.3. Here the plots again show similar trends but there are discrepancies in the values for some of the lenses. The mean stain scores for the Rythmic and Precision UV lenses appear respectively, too high and too low.

However, if the standard deviations are taken into account, the results can be tailored to display almost any desired trend. Therefore as a large number of data points were collected, the mean stain scores will be considered absolute.

Figure 3.3 Mean stain score and EWC for contact lenses cleaned in ReNu multipurpose solution

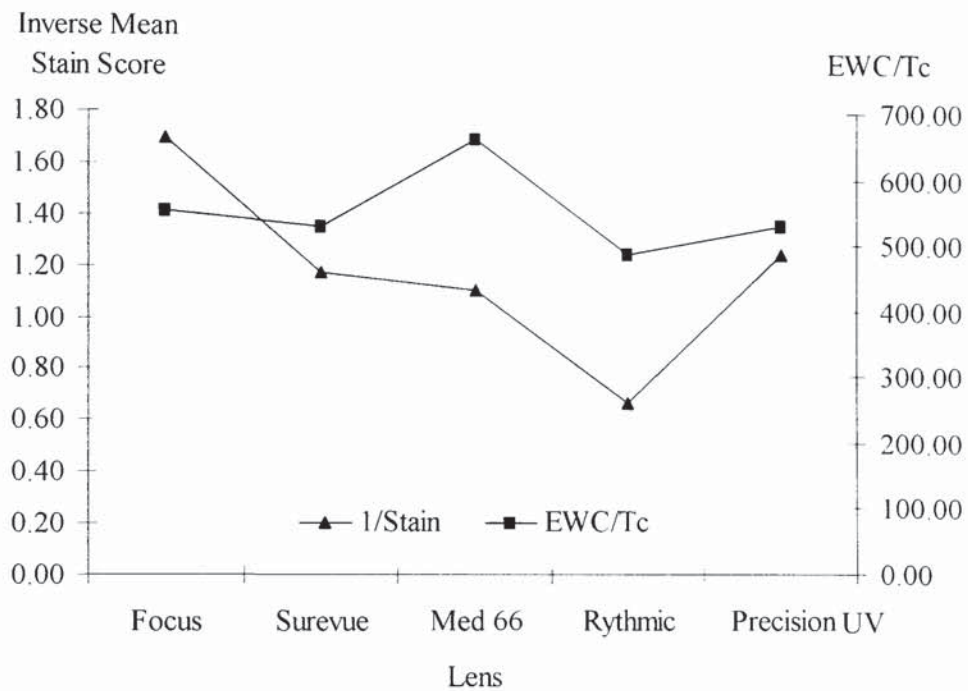


The mean stain scores appear to show similar trends to both the EWC and the centre thickness of the contact lens. In order to evaluate how correct this statement was EWC/centre thickness, was plotted together with the stain scores as in figure 3.4. In this plot the inverse of the mean stain score was used as this would illustrate better any similarities between the two sets of data. It can be seen that the mean stain scores are not dependent on either the EWC or the centre thickness of the lens but are probably influenced by these properties.

Differential scanning calorimetry allows the percentages of a samples weight present as free and intermediate water to be obtained. As the total amount of water in the sample, the EWC, is known, the amount of bound water expressed as a percentage of the samples weight can be determined easily. The contact lenses that were cleaned using the ReNu multipurpose solution were investigated using DSC, and the

proportions of each type of water present in the lens was found. The amount of bound water when expressed as a percentage of the weight of the lens is similar for all the lenses cleaned in ReNu, but this is due to the water structuring within hydrogels.

Figure 3.4 EWC centre thickness and inverse stain score for contact lenses cleaned in ReNu multipurpose solution

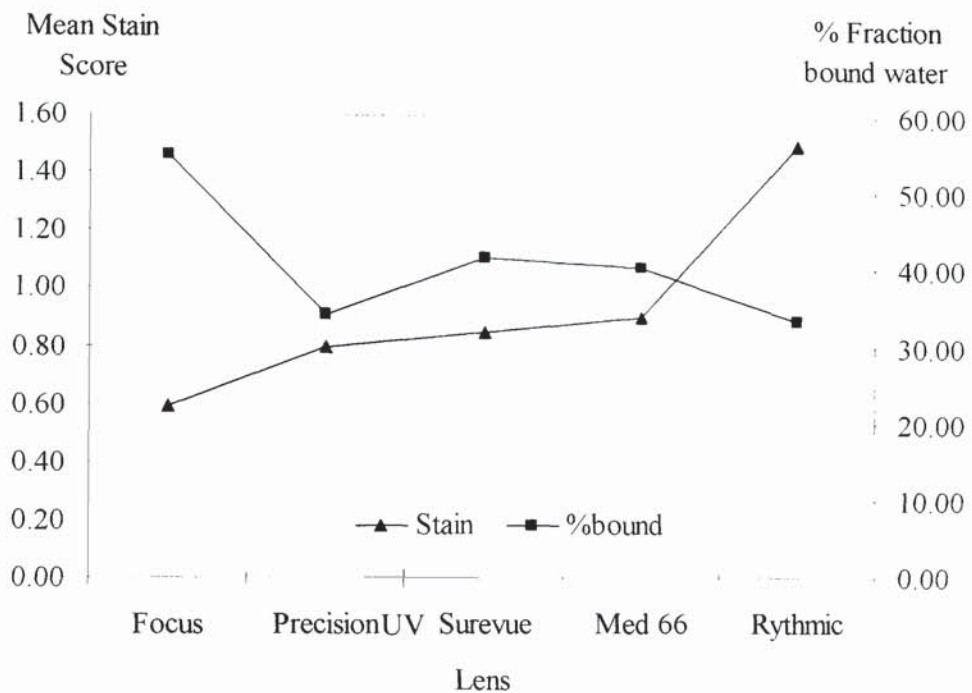


At a low level of water content, almost all the water in hydrogels is present as bound water. This is a consequence of the availability of sites for hydrogen bonding and strong ion-dipole interaction. As the water content increases, intermediate water appears when all the sites available for strong interaction have been occupied. As the water content increases even more, free water appears when there are no sites left for any interactions. The lenses in this study have an FDA classifications of being high water content lenses and so water within these materials is present in all three states.

The bound water is more usefully expressed as a percentage of the total water present within the contact lens. This gives the relative proportion of bound to free water within the material and allows investigation of a possible relationship with the mean stain scores. Figure 3.5 shows this for lenses cleaned in ReNu that were also stored in ReNu prior to testing by DSC. A link between these appears to exist for all the lenses

in this part of the study with the exception of the Precision UV lens whose mean stain score appears to be lower than would be expected. As mentioned previously the standard deviations for these results are quite large when compared to the magnitude of the stain scores. Taking this into account, the subjects selected to wear the Precision UV lenses may have provided results which underestimated the degree of corneal staining.

Figure 3.5 Percent fraction of bound water and mean stain score for contact lenses cleaned in ReNu multipurpose solution

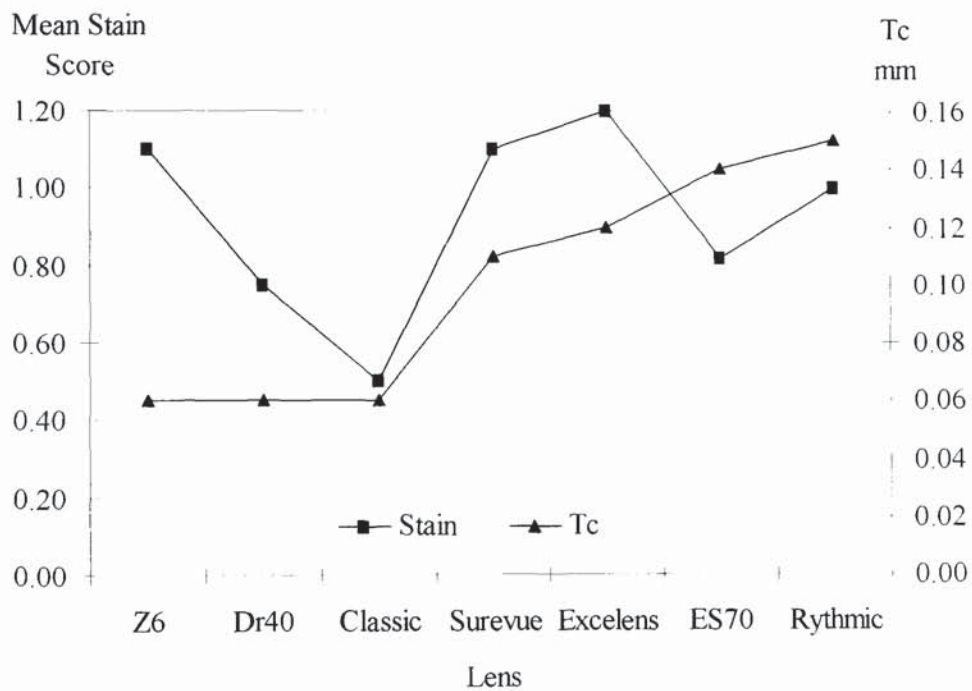


3.8 Investigation of Contact Lenses Cleaned in a Peroxide Based System

For lenses cleaned in peroxide, the possibility of the existence of similar trends can also be explored. If the water binding properties are examined after the lenses have been soaked in peroxide, they will give misleading results, a point which is discussed further in section 3.9. The results presented in this section are for the lenses which have been soaked in saline prior to investigation by DSC, but were cleaned in a peroxide based system during the clinical evaluation.

When the mean stain score is plotted together with the centre thickness of the contact lenses as in figure 3.6, there appears to be no correlation between these two properties. As equilibrium water content has been shown to follow a similar trend as the centre thickness of the contact lens, it would be expected that no correlation will exist in a plot of this property with the mean stain score. This is illustrated in figure 3.7.

Figure 3.6 Mean stain score and centre thickness (Tc) for contact lenses cleaned in a peroxide based cleaning system



The lenses that were cleaned in the multipurpose solution ReNu, were all high water content lenses some of which were also ionic. As the water contents of these lenses are of a similar order of magnitude, comparisons of the stain scores can be carried out relatively easily. The lenses cleaned in peroxide include low water content lenses and so comparisons are less straightforward.

Figure 3.7 Mean stain score and EWC for contact lenses cleaned in a peroxide based cleaning system

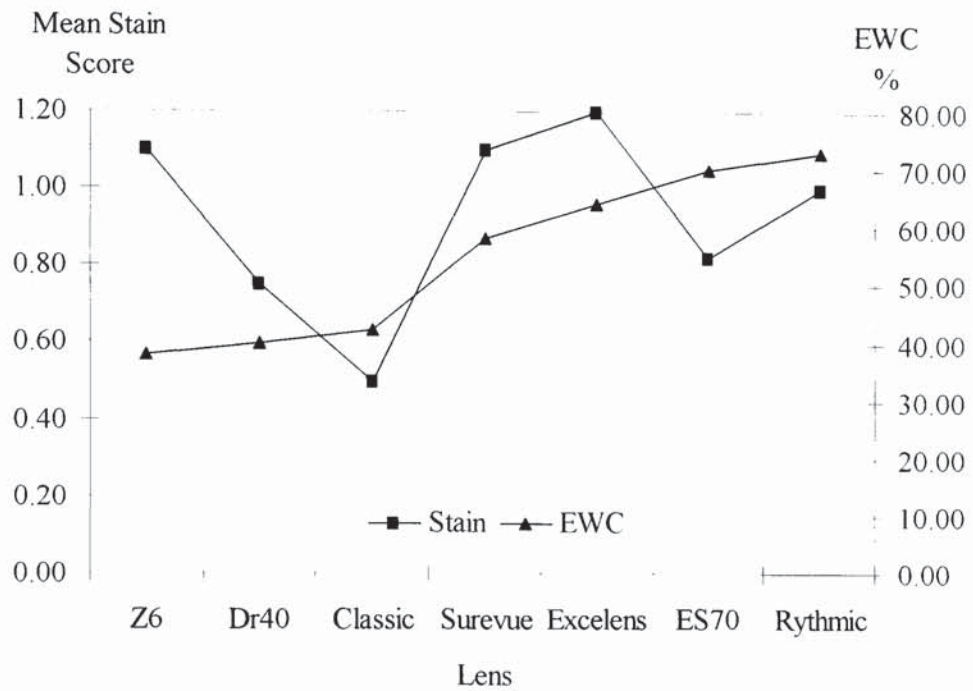
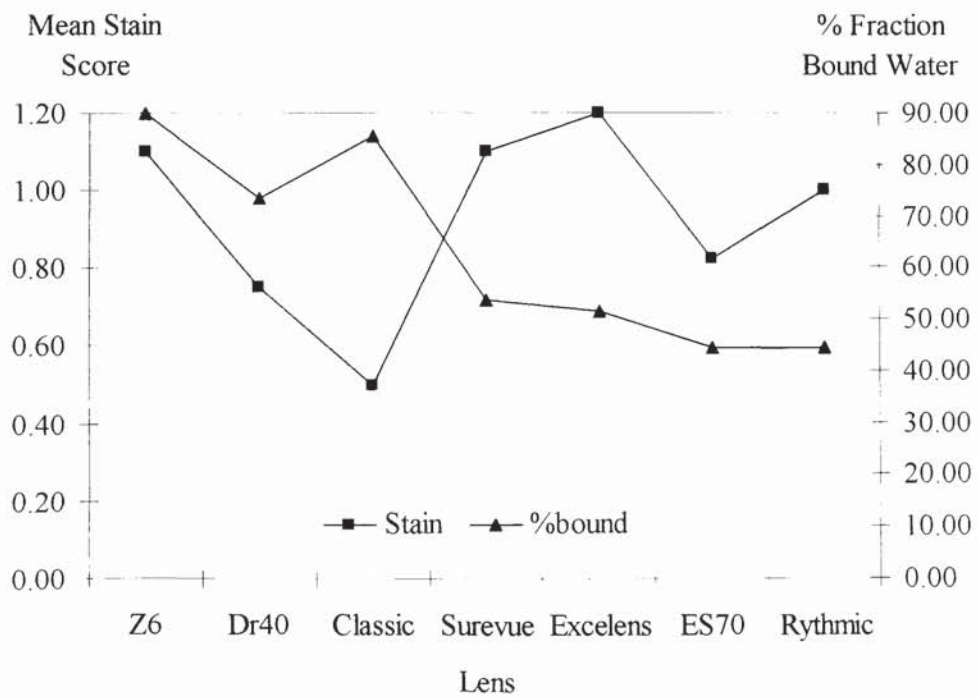


Figure 3.8 Mean stain score and percent fraction of bound water for contact lenses cleaned in a peroxide based cleaning system



The amount of equilibrium water content present as bound water and expressed as a percentage can be plotted with the mean stain score as shown in figure 3.8. On first inspection of this plot there appears to be no correlation between the two sets of data. The lenses can be divided into specific classes which make the results more meaningful. The Z6 lens is a polymer of 2-hydroxyethyl methacrylate (HEMA). This monomer, when polymerised has been shown to produce polymers with low equilibrium water contents and thus the water present is held tightly. A consequence of this is a higher proportion of water present as bound water than in polymers of N-vinyl pyrrolidone which is a constituent in the majority of the other lenses. A comparison of this lens when examining possible trends between bound water and stain scores with other lenses would therefore be misguided.

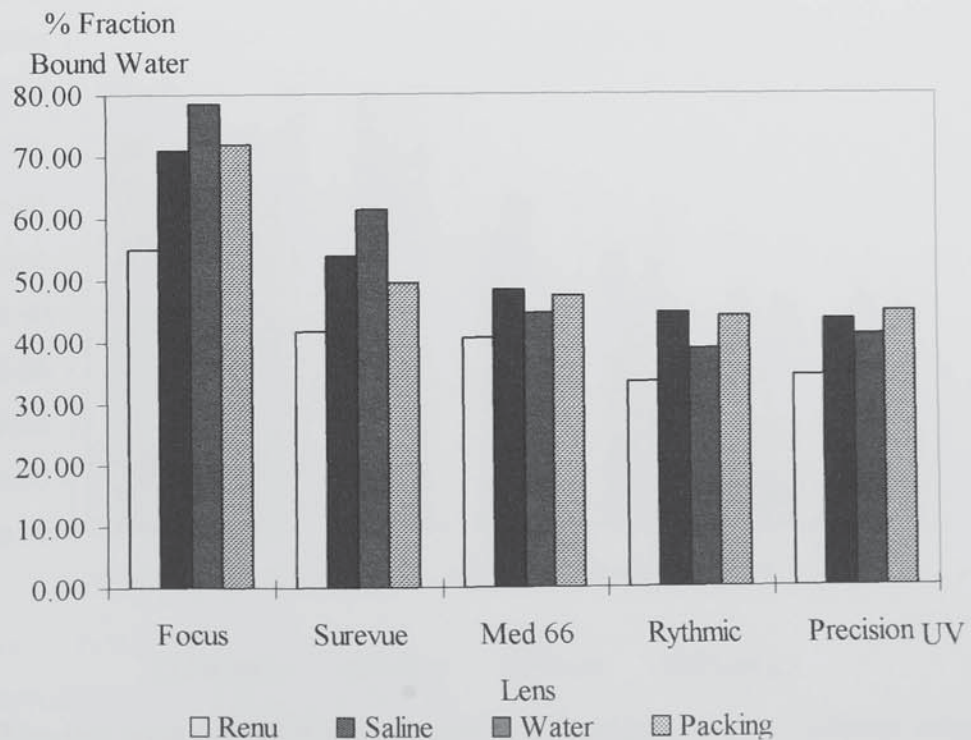
The Classic and DR40 lenses are both comprised of a copolymer of HEMA together with other vinyl monomers. They also both have the FDA classification of being low water content lenses. When the fraction of water present as bound water is compared to the mean stain score, it can be seen that the classic lens which has a higher bound water content also gave subjects a lower stain score. The Lunelle ES70 lens and the Rythmic lens are both copolymers of N-vinyl pyrrolidone and methyl methacrylate and have the FDA classification of being non-ionic, high water content lenses. The ES70 lens has a slightly lower water content and so the fraction of water present within this material as bound water is slightly higher. This is reflected in the stain score where this lens has a lower mean stain score than the Rythmic lens.

The Surevue and Excelens lenses are both of similar water contents although they are comprised of different copolymers and have different FDA classifications with the Surevue lens being ionic. Their water contents are of a medium order of magnitude when compared to the other materials and so they can be examined together. The proportion of bound water in the Surevue lens is greater than the Excelens lens which could be a consequence of the higher EWC of the Excelens material. The Surevue lens gave a mean stain score that is lower than Excelens and so the pattern of a lower stain score being accompanied by a higher proportion of bound water is again illustrated.

3.9 Effect of Solution Characteristics on Water Structuring for Contact Lenses

The solution in which the contact lens is stored prior to investigation by DSC will have a significant effect on the proportion of bound water found within the material. Figure 3.9 displays for various solutions, the percentage of the EWC present as bound water for lenses cleaned with the ReNu multipurpose system. The saline solution used in these experiments has a pH of 7.0 and is isotonic. The majority of the packing solutions also have these same characteristics and thus the results for both of these solutions are in agreement, within experimental error. The packing solutions and saline both contain a small amount of salt. The sodium ions within these contain a positive charge and water molecules form weak bonds with these ions. The result is that the amount of bound water observed with these solutions is higher than when the lenses are examined after storage in water. These results are consistent for all the contact lenses that are non-ionic.

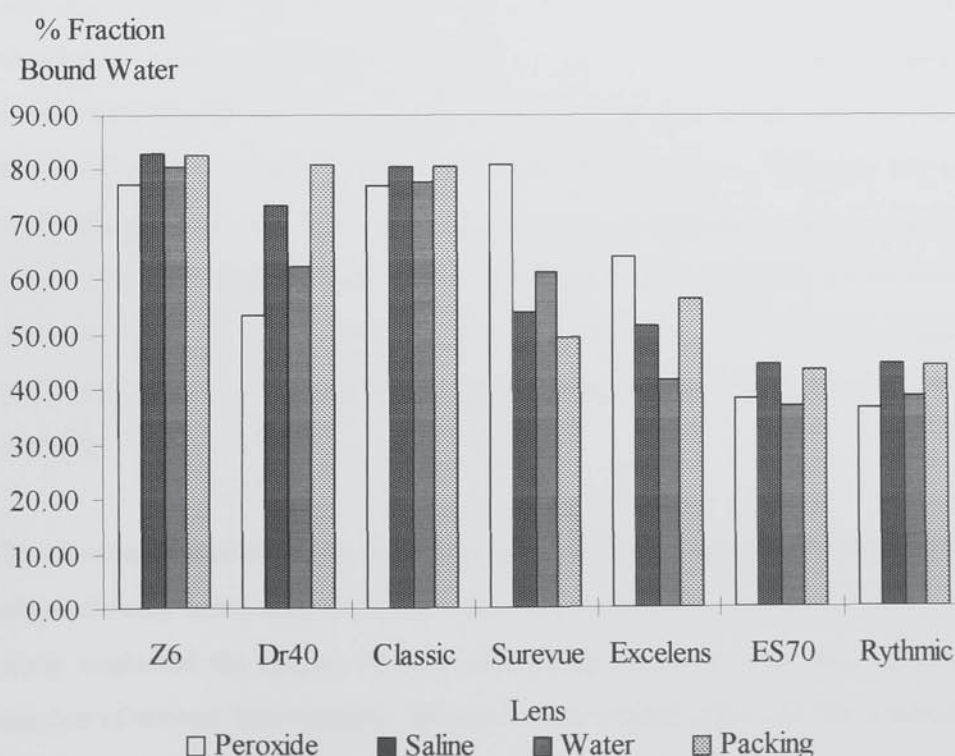
Figure 3.9 The percentage of the EWC present as bound water for contact lenses cleaned in ReNu after soaking in a range of solutions



The Focus and Surevue lenses both belong to the FDA classification of being ionic and having a high water content. As these contain acid groups, the ions in the saline and packing solutions are attracted to these more strongly than they are to water molecules. The ions therefore form weak bonds to the acid groups on the polymer chain and this prevents any water molecules from binding strongly with these hydrophilic sites. The result is that the amount of water existing in the bound state for these ionic lenses is greater when they are stored in water compared to when they are stored in saline.

The ReNu solution is isotonic and has a pH of 7.4, the same as natural tears and also contains a surfactant to reduce its surface tension and enhance its cleaning ability. This results in a reduction in bound water content as the ions present in the solution also interact with some of the groups on the polymer.

Figure 3.10 The percentage of the EWC present as bound water for contact lenses cleaned in a peroxide based system after soaking in a range of solutions



Lenses that were cleaned in the peroxide based system also show different values for the amount of water in the bound state for each type of solution they were soaked in before investigation as shown in figure 3.10. The trends outlined above can also be

observed for both the ionic and non-ionic lenses in saline, water and the packing solution for each lens type.

When the lenses are soaked in peroxide before evaluation by DSC the amount of water existing in the bound state in the non-ionic lenses is approximately the same as that with water. However for the only ionic lens in this set, Surevue, the bound water content is greatly increased with peroxide when compared to the other three solutions. As this material contains a small amount of methacrylic acid, the presence of peroxide can cause a change in the degree of ionisation of the monomer. This results in a dramatic increase in the proportion of water existing in the bound state, although this is actually caused by the large decrease in the free water content.

3.10 Conclusion

It is of widespread belief that hydrogel contact lenses dehydrate during wear although the precise contribution of various controlling factors is unclear. It is also thought that this dehydration of the lens is a major causative factor in the condition of corneal staining and other complications of contact lens wear. For all contact lenses it would be expected that the dehydration process will be the same and the contribution that this dehydration has on corneal staining will also be the same. Therefore any variations seen with different contact lenses would be due to differences in the actual material used. The main reason for this study was to see if corneal staining could be correlated with the states in which the water in a hydrogel exists. Thus the investigation and understanding of the complex dehydration process for a contact lens on the eye is avoided.

The first section of the study was concerned with five high water content lenses, two of which were ionic, that were cleaned using ReNu multipurpose solution. A clinical study evaluated the degree of corneal staining observed with each lens type for a number of contact lens wearers. When the lenses were soaked in this solution prior to investigation by DSC., a correlation between the percentage of water present in the bound state and degree of corneal staining was found. An increase in the extent of

corneal staining is observed as the percentage of the total water present, that exists in the bound state decreases.

A number of lenses were cleaned using a peroxide based system instead of the multipurpose solution and the bound water in these systems was again investigated after the lenses had been soaked in peroxide, saline, water and the lens packing solution. The results for these lenses after they had been soaked in peroxide would give misleading information if any attempts to correlate this information with the corneal staining data were made. Therefore comparisons were made with the proportions of bound water for the lenses after they had been soaked in water. When this group of lenses are divided into groups based on both their water contents and the main hydrophilic monomer used in their compositions, the results follow the trends outlined above. The corneal staining appears to be inversely proportional to the percentage of lens water existing in the bound state.

The solution in which a lens is stored prior to investigation of its free water content by means of DSC will have a significant effect on the value of both this and the bound water content. For neutral or non-ionic lenses a solution that contains salt ions will give an increased level of bound water when compared to the value obtained with water. However if the lens is an ionic lens, the amount of bound water found with solutions such as saline or the lens packing solution is lower than that found with water.

It must be noted that in this study large patient to patient variations were found for the extent of corneal staining observed for each particular lens type. This is probably due to variations in the concentrations of lipids and proteins in tears. Higher solute concentrations lower water activity which in turn results in greater lens dehydration. Additionally, the adsorption of tear components inside the hydrogel and the persistence of these solutes will also affect hydration. It has been observed that the presence of lysozyme in high water/ionic lenses reduces hydration⁹⁴. The variations between patients can lead to difficulties in identifying any particular trends or links between different sets of data. As the standard deviations found were so large, it was decided to take the mean values as absolute.

Desiccation staining depends on many variables including individual tear film characteristics, lens thickness, lens design, lens fit and ambient humidity. Also, desiccation is not the sole cause of corneal staining and it is therefore difficult to differentiate this from other types of staining. This could therefore also lead to inaccuracies in the findings of the clinical investigation

The extent of corneal desiccation is determined by the capacity of water to move through the hydrogel lens. However the mechanism of this movement is as yet unclear. The evaporation of water from various hydrogel lenses has been found to be in the same range, regardless of water content and material type, being the same as that for pure water⁵³. Since high water content lenses suffer more from lens dehydration and corneal staining, evaporation of water from the lens cannot be the cause of these processes. The results presented here appear to agree with the theory presented by Mirejovsky⁵³. It is postulated that the evaporation of water from tears between blinks lowers the activity of water at the lens/tear interface. The water activity gradient between the surface and the lens interior will give rise to transport of water towards the interface. Therefore a steeper gradient, or a larger amount of water with a high activity inside the lens (i.e. free water) will lead to a greater incidence of corneal desiccation staining.

CHAPTER 4

HYDROGELS WITH DESICCATING PROPERTIES FOR PHARMACEUTICAL PACKAGING

4.1 Introduction

Hydrogel materials are used in a number of applications that take advantage of the particular water structuring properties that this class of materials display. However one specific use for these materials utilises the properties that hydrogels display in their dehydrated state. Anti-mist or anti-cloud coatings are used to treat a number of articles to render them resistant to becoming cloudy in situations where excess moisture is encountered. Articles that could utilise such coatings include safety visors, safety goggles, prescription glasses and household items such as mirrors and windows.

A lens becomes cloudy when a large number of microscopic water droplets adhere to its surface. An “anti-cloud” coating is one which can prevent microscopic water droplets from sticking to its surface. Two fundamentally different approaches to achieve this situation are as follows. The first is to change the microscopic water droplets into a thin layer of water by reducing the contact angle between the material and water droplets. The second is to absorb the moisture that appears on the surface of the substrate. It is this process that is utilised in the application of pharmaceutical packaging materials that display desiccant properties.

Hydrogel materials possess the necessary attributes for use as a water scavenging packing material. They are highly hydrophilic materials that will readily absorb moisture at the low humidity levels that would be encountered in this application. As they are used widely in applications where a degree of biocompatibility is required, there will be no toxicity problems. Hydrogel formulations that have been used in anti-fog coatings will be of particular interest as they will possess the necessary properties required for desiccant applications.

A hydrogel with desiccating properties is believed to be one which when hydrated, incorporates a major amount of the hydrating water as non-freezing or bound water. This is a consequence of the hypothesis that the larger the proportion of water present in the bound state, the lower the evaporation and hence the better absorbency of moisture. Contact lenses comprising mainly of 2-hydroxyethyl methacrylate generally have lower free to bound ratios than lenses of comparable water contents based on N-

vinyl pyrrolidone. It is therefore believed that there is less water evaporation from lenses of this type.

A number of authors have studied the swelling characteristics of dehydrated hydrogels using methods such as gravimetric techniques¹⁰³, magnetic resonance imaging¹⁰⁴ and ultrasound¹⁰⁵. They concluded that the penetration of a solvent into a stiff polymer sample is usually described as the result of two different processes, the diffusion of the solvent into the swollen matrix, and the advancement of the swollen-unswollen boundary as a consequence of the stress induced in the polymer. When the rate determining step is the first process there is a linear dependence between the solvent uptake at a particular time t when plotted versus $t^{1/2}$, and the system is said to exhibit Fickian behaviour. However, if the advancement of the swollen-unswollen boundary is slower than the diffusion of the solvent in the swollen polymer, zero order kinetics are observed and the water uptake increases linearly with swelling time.

In all the studies reported above, the swelling experiments are carried out in an environment of 100% relative humidity. Also the geometry of the experiment is such that a one dimensional water sorption process is assumed. Under these conditions it was found that in dehydrated hydrogels and for the first 200 minutes, the swelling process is characterised by Fickian behaviour. However for this application, the environmental condition of interest is a relative humidity of only 10% and so the swelling characteristics may be very different from those above.

The requirements for any candidate material that can be used for a desiccant application are as follows:-

1. Withstand sterilisation by heat or gamma irradiation. The former is a distinct possibility for a cycle of three hours at 135 °C for hydrogel structures.
2. Very low or zero extractables and the experience at Aston has shown that all monomer and solvent residues can be removed by simple washing. Also required is a resistance to hydrolysis especially at the alkaline pH's that the reconstituted products produce.
3. Desiccating capacity. The higher the capacity the more the desiccant implant size can be reduced.

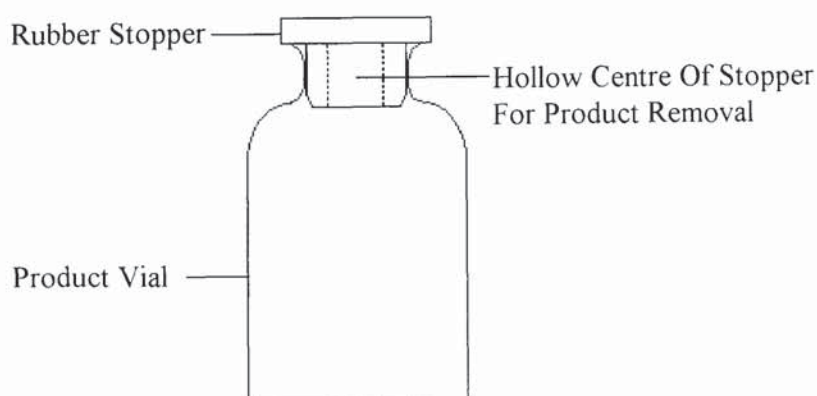
4. Controlled rate of moisture uptake. A relatively slow pick-up will be adequate for product protection and will minimise loss of desiccant capacity during handling and packaging.
5. Appropriate handling properties. Processing and mechanical handling of hydrogels is a major consideration

Various ways of incorporating the desiccant material within or attached to the sample vial have been suggested. This must be achieved without a change to the dimensions of the sample vial which is shown in figure 4.1. This is a consequence of the fact that the reconstituted solution is removed from the vial by equipment that is an international standard. The incorporation of the hydrogel can be achieved in one of the following forms.

- Desiccant film as the inside wall of sample vial.
- Desiccant film as the inner layer of blister packs.
- Hydrogel pellet insert into the rubber stopper.
- Two-part vial stopper in which the entire skirt is replaced with hydrogel.
- Complete replacement of stopper with hydrogel.

The overall requirement is for an inexpensive material at the commercial scale and this will depend on the establishment of a simple manufacturing process and the actual cost of goods used.

Figure 4.1 Diagram of product vial



Previous work carried out at Aston in the area of anti-fog coatings utilised solution polymerisation for the production of polymer systems. After completion of the polymerisation process, the polymer in solution form could be used to treat the substrate by either dip or spray coating. As the method of incorporation of the hydrogel was initially undecided, it was decided to become familiar with this method of polymerisation as the resulting polymer solution could easily be used to coat the inside of the sample vial. An advantage of solution polymerisation is that the cross-linker can be added either during the polymerisation process or when the substrate is to be coated. The latter increases the shelf life of the polymer in solution and the cross-linker is simply dissolved in the solution before the substrate is coated. The coated object is then placed in the oven to cross-link.

4.2 Experimental

All the samples in this chapter were subjected to evaluation by dynamic vapour sorption apparatus as well as examination by other standard methods. These include evaluation of the water binding properties in the hydrated state and mechanical testing again in the hydrated state.

4.3 Preliminary Evaluations

To provide initial indications into the possibility of using hydrogels as desiccant materials, a number of copolymer compositions were examined using dynamic vapour sorption apparatus. These covered a broad range of typical compositions used in a range of applications including contact lenses. Also a number of control samples were included whose compositions were such that they should absorb a minimal amount of moisture.

4.3.1 Materials

Seven samples (including two control samples) were produced for testing and these covered a wide range of hydrogel formulations whose compositions are shown in table 4.1.

Table 4.1. Compositions and results for first set of samples

Sample	Components	Composition	EWC (%)	Free (%)	Bound (%)
1	NVP:MMA	70:30	61.6	27.9	33.7
2	HEMA:AMO	50:50	63.2	41.4	21.8
3	HEMA:AMO	90:10	41.1	8.9	32.2
4	HEMA:NVP	90:10	38.7	7.3	31.4
5	HEMA:NNDMA	90:10	43.5	13.1	30.4
6	MEMA:EEMA	50:50	-	-	-
7	MEMA:EEMA	70:30	-	-	-

4.3.2 Results

The moisture uptake profiles of the samples are shown in figure 4.2 and, as expected, the two control samples did not absorb any moisture. Data for the equilibrium water content and proportions of water existing in bound and free states for each sample can also be found in table 4.1. As samples 6 and 7 were prepared by solution polymerisation, water binding properties were not investigated as the samples were never fully hydrated.

To evaluate whether the samples had reached a stable equilibrium at the end of the holding time at 10% RH (relative humidity), two samples with different profiles in testing were held for 24 hours at 0% RH followed by a rise to 10% RH for 45 hours as illustrated in figure 4.3. This confirmed that the maximum moisture uptake was achieved within 1000 minutes and therefore an equilibrium with the environment had probably been reached for all the samples in the first experiment.

Figure 4.2 Normalised Moisture Uptake Data for First Set of Hydrogels

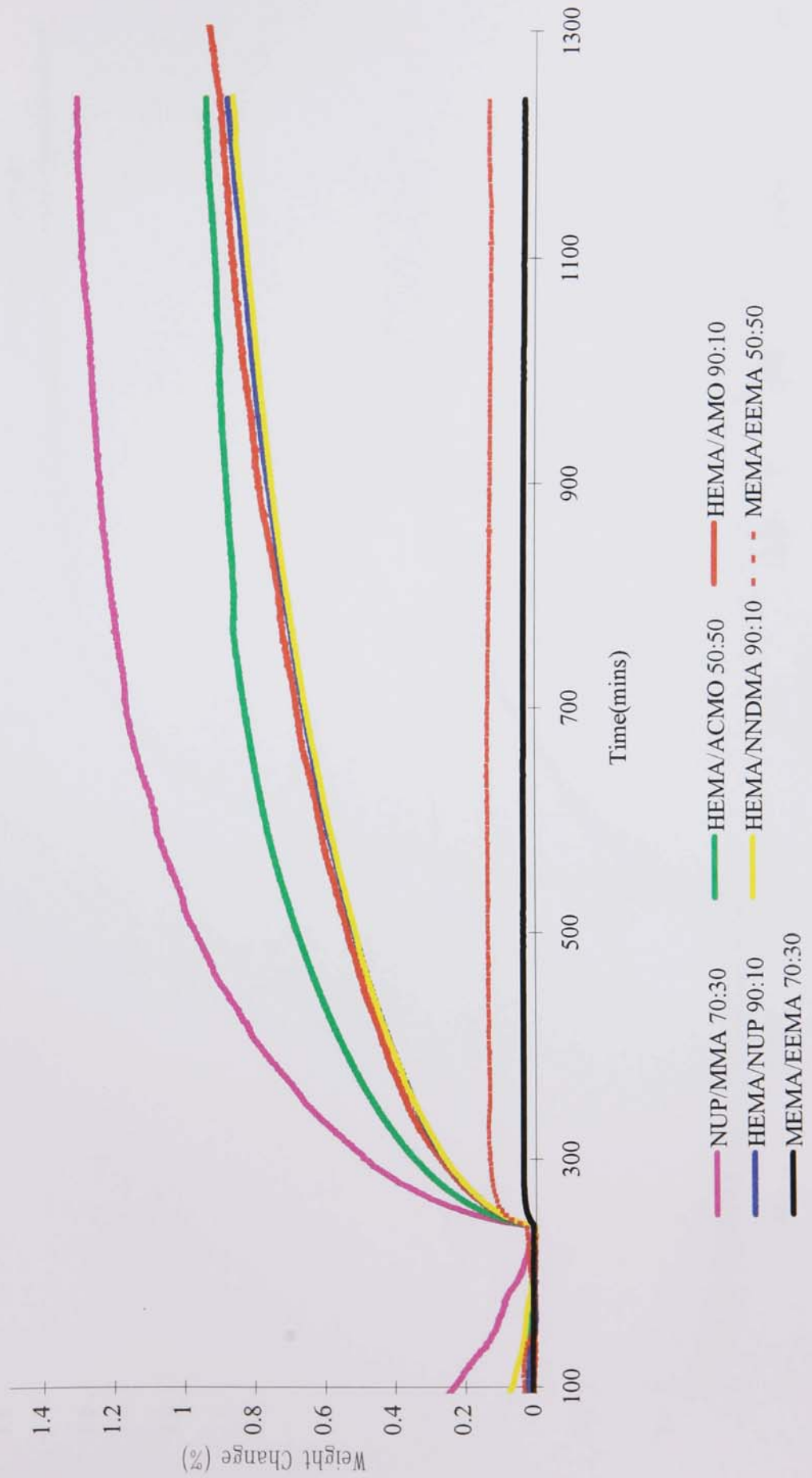
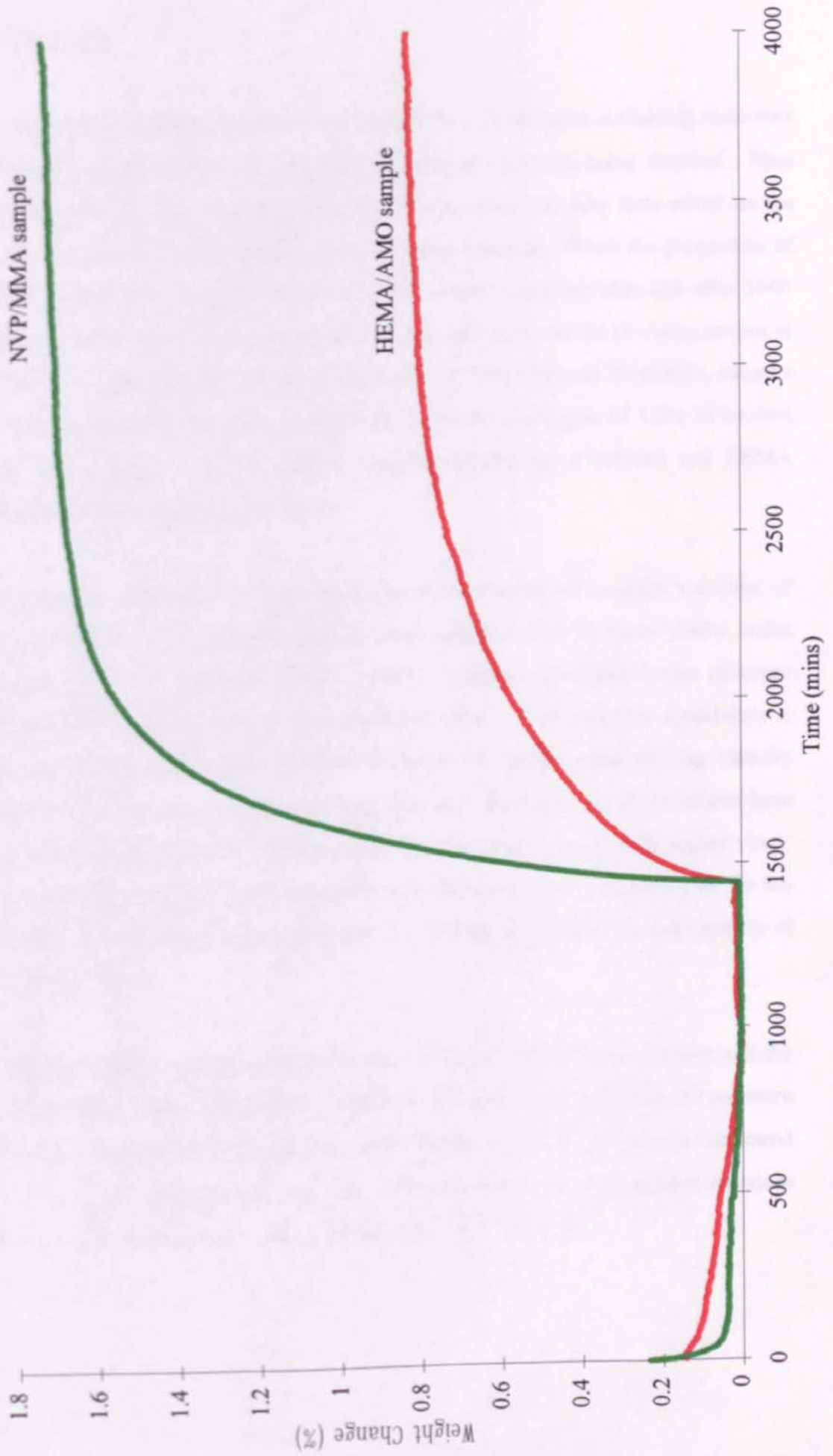


Figure 4.3 Sustained Exposure of Hydrogel Samples



4.3.3 Discussion

The compositions containing 90% HEMA and 10% of a nitrogen containing monomer all showed the same moisture uptake with the absorption charts being identical. Thus the component which is present at such a low proportion has very little effect on the amount and profile of water uptake of the resulting material. When the proportion of AMO is increased to 50%, the rate of moisture uptake increases although after 1000 minutes the total amount of moisture absorbed is similar to the 90:10 compositions at around 0.9%. The material with the composition of 70%NVP and 30%MMA shows a much increased rate of moisture uptake with a total moisture gain of 1.2% of its own weight. As expected, the two control samples comprising of MEMA and EEMA absorbed a minimal amount of moisture.

If the moisture absorbency is compared to the water binding information a number of trends can be seen. The formulations at compositions of 90:10 show similar water binding properties to each other which would be expected, given the similar structure and hydrophilicity of the nitrogen containing monomers. The moisture absorbency is again very similar which would be expected given the similar water binding capacity and structure of monomers used in the compositions. The other two formulations have similar water contents with the HEMA:AMO (50:50) having the slightly higher value. However, the proportion of this water present in the bound state is much higher for the NVP:MMA (70:30) and it is this material that has the much higher rate and capacity of moisture absorbency.

The moisture uptake appears to be dependent on the amount of water present and the state in which this water exists. For materials with similar water contents, the moisture absorbency is greatest for the material with the higher proportion of water in the bound state. For compositions with similar free to bound water ratios the greater moisture uptake is seen in the material with the higher total water content.

Figure 4.4 Moisture Pick Up of Hydrogel over Extended Relative Humidity Profile

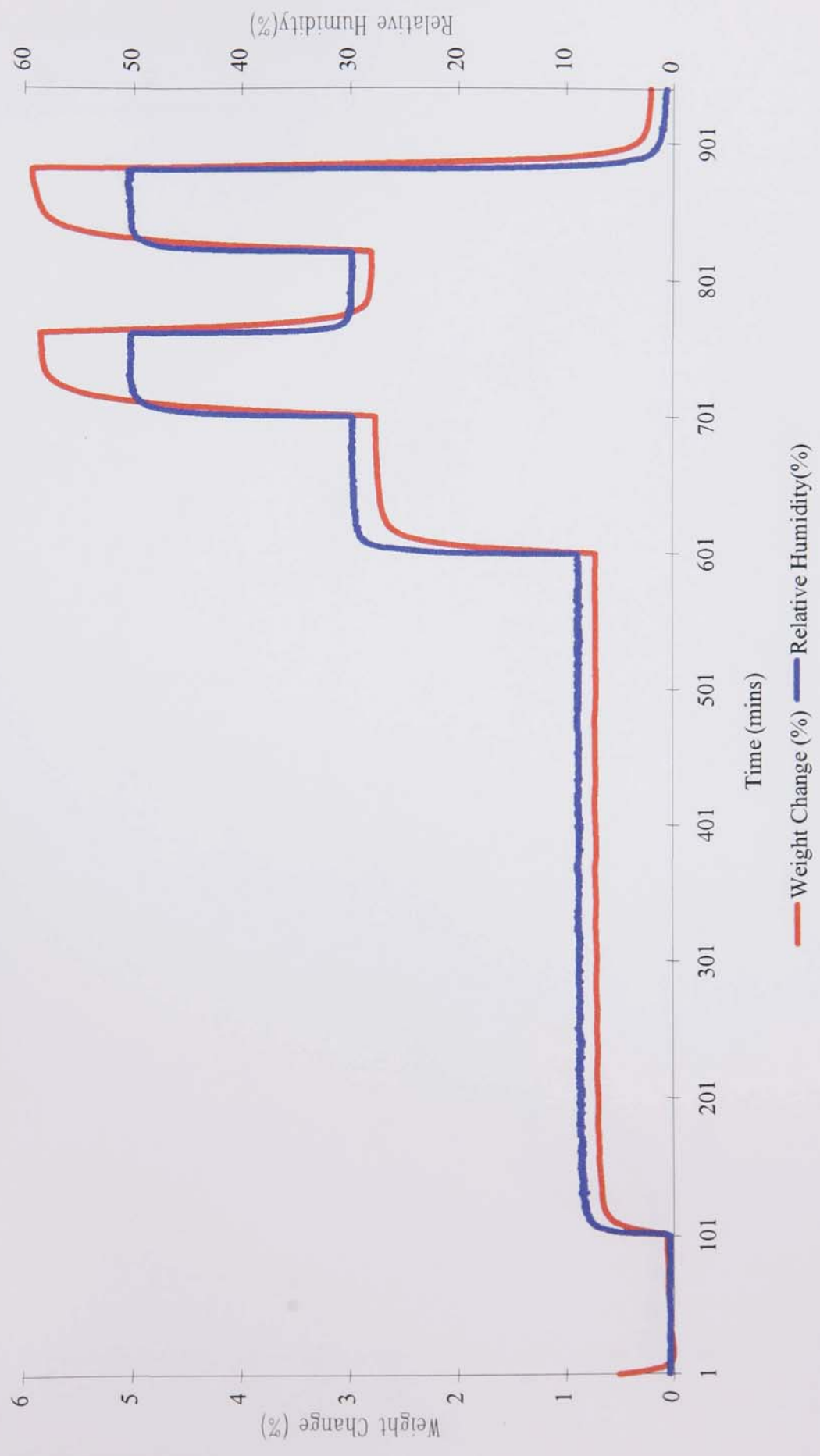
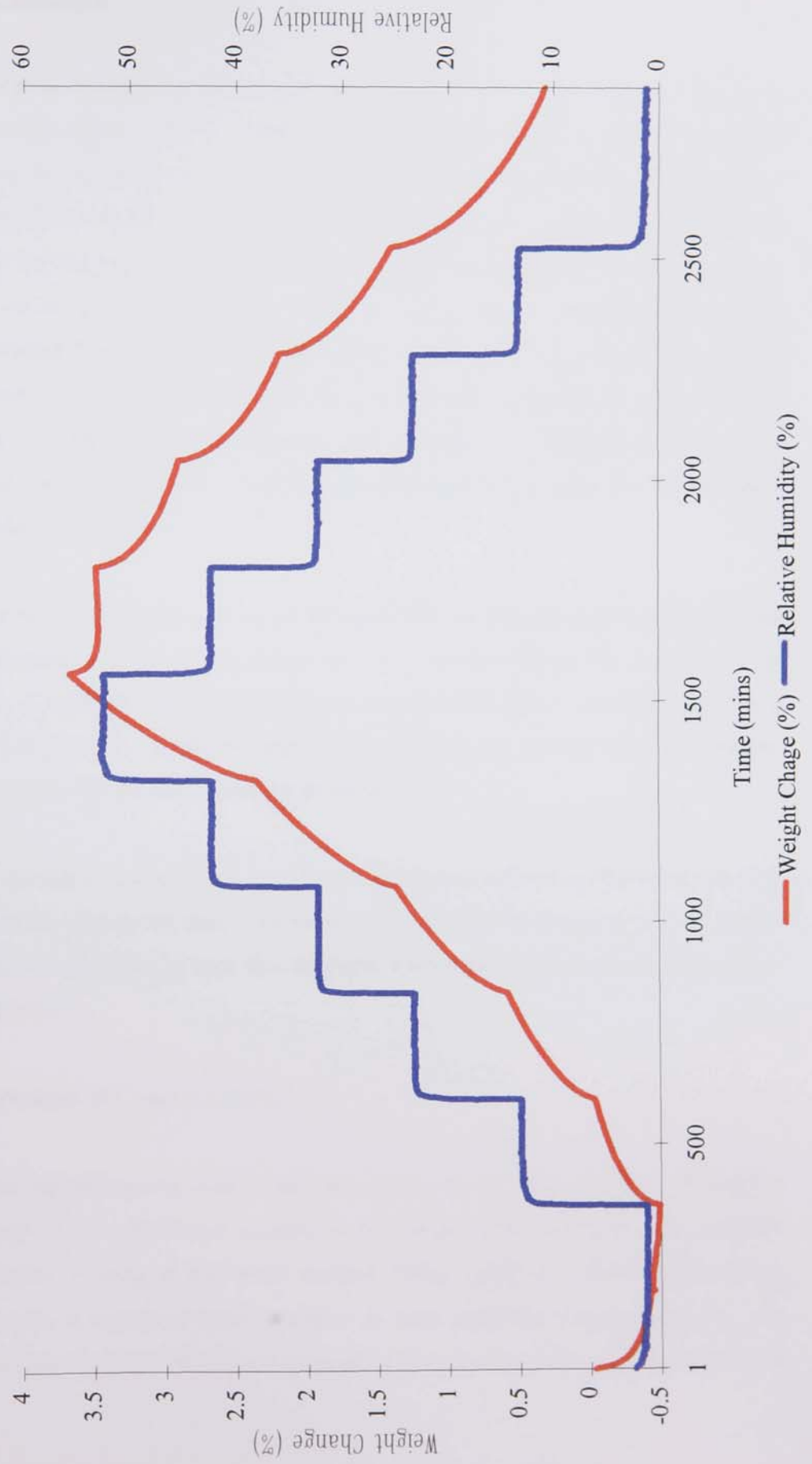


Figure 4.5 Moisture Uptake/Loss Profile of Hydrogel over a range of Relative Humidities



4.3.4 Conclusions

The relative humidity profile graph (figure 4.4) shows that moisture uptake is considerably higher at 30% RH (normal handling conditions) than at the 10% necessary to keep below to achieve the desired stability of the product. As the uptake at higher RH is readily reversible at the lower RH as seen in figure 4.5, it would be possible for hydrogels equilibrated at the normal handling humidity to act as a water source rather than a sequestrant at the lower humidity level. Also, equilibration with environmental humidities at the normal ambient conditions is a very rapid phenomenon. Therefore if hydrogels are to be used for this particular application, it will be vital to store and handle them under extremely low humidity. An alternative to very low humidity handling would be to activate the hydrogels in situ after the vial has been filled with the product.

For this type of application, it would be permissible for the desiccation process in the finished pack to occur over a period of 2 to 3 weeks without any serious loss of activity. A hydrogel formulation which had a significantly slower rate of pick up, but a good final capacity, would be expected to achieve the desired level of moisture sequestration with far fewer handling problems.

All the samples examined had undesirable physical properties in that they are very brittle in the dehydrated state. As expected the samples also expand as they absorb moisture and this must be kept to a minimum if these materials are to be successful in this application.

4.4 Evaluation of Contact Lenses

As water content appears to be a controlling factor on the degree and rate of moisture absorption, it was decided to examine some contact lenses that belong to the FDA classification of being of high water content. These would also include some lenses that possess a degree of ionic character as they contained methacrylic acid. As compositions based on HEMA are believed to contain water that is predominantly in

the bound state, the lenses would contain predominant amounts of this hydrophilic monomer.

It is believed that the rate of evaporation of moisture from contact lenses is dependent on another factor of monomer structure, the energy barrier to rotation of the carbon backbone. The magnitude of this property is dependent on the size and nature of the pendent groups that are attached to the carbon main chain. If this structural feature affects the evaporation of moisture, it would also be expected to affect moisture uptake which is the reverse process of evaporation. It was therefore decided to include a material that contained a methacrylate monomer as the other materials examined contained the same monomer in the form of the acrylate derivative. Whereas an acrylate only contains a hydrogen attached to the α -carbon atom, the methacrylate contains a methyl group at the α -carbon atom. This imparts a greater steric hindrance to rotation in the resulting polymer about its carbon backbone.

4.4.1 Materials

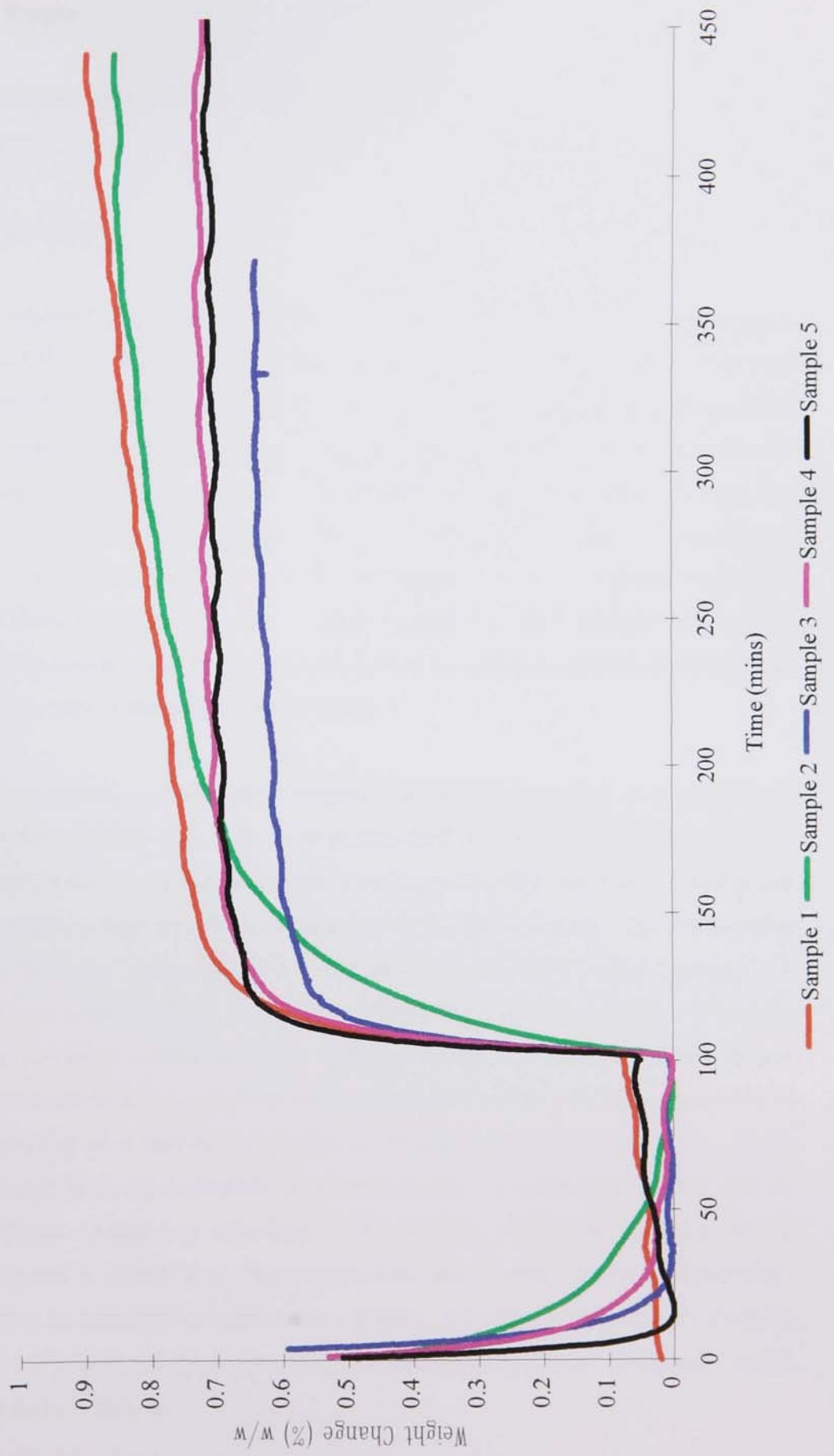
The materials that were examined consist of HEMA copolymerised with various different polyethylene glycol acrylates of different molecular weights, with one material containing polyethylene glycol methacrylate. Two of the materials also contained a small proportion of methacrylic acid which gave the material a degree of ionic character. The compositions of the lens materials used are shown in the following table.

Table 4.2. Compositions of the second set of samples

Sample	%PEG>1000	%PEGA<1000	%HEMA	%MAA	EWC%
1	45(A)	0	55	0	70
2	15(MA)	0	85	2	60
3	25(A)	15	60	0	62
4	45(A)	0	55	2	70
5	35(A)	12	53	0	65

where (A)= Polyethylene Glycol Acrylate (MA)=Polyethylene Glycol Methacrylate

Figure 4.6 Moisture Uptake Data for Second Set of Hydrogels



4.4.2 Results

The moisture uptake profiles of the contact lens samples are presented graphically in figure 4.6.

4.4.3 Discussion

With reference to the moisture uptake of the samples in graphical form (figure 4.6), it can be seen that the initial rate of absorbency is much greater than that in the first set of samples. Samples 4 and 5 have profiles that are almost identical to each other with both similar rates and capacity for their moisture absorbency. For sample 4, the inclusion of methacrylic acid in the formulation would be expected to raise the moisture capacity to a level higher than that of sample 5. However, incorporation of smaller molecular weight PEG acrylates in sample 5 results in a greater number of water binding sites than sample 4 which contains just PEG acrylates of a higher molecular weight. Thus the inclusion of methacrylic acid in sample 4 raises its capacity level to a value comparable to that of sample 5.

The most significant result in these samples is the profile of sample 2. It's initial rate of absorption, although high, is far more gradual than the other samples in this set. It is this sample that contains PEG groups in the form of methacrylates as opposed to the other samples which contain these groups in the acrylate derivative. The final capacity of this particular sample however is comparable to the other samples examined. It could be concluded that the rate of absorbency is dependent on the degree of rotation of the polymer's carbon backbone. More precisely the controlling factor to this process could be the energy barrier to rotation which will be the only consequence of the inclusion of a methacrylate group as compared to an acrylate group. In the dehydrated state, the hydrophilic groups are buried within the polymer bulk and the hydrophobic groups are expressed at the surface. When the humidity of the environment is raised, it is thermodynamically more favourable for the hydrophilic groups to be orientated towards the air interface. Therefore rotation occurs along the carbon main chain and this is more difficult and slower in polymers containing a methyl group at the α position.

4.4.4 Conclusions

The mechanical properties of the second set of samples are more desirable for this particular application than the first set. This is because in the dehydrated state, the second set of samples are far less brittle than the first set. The more brittle the material in the dehydrated state, the more difficult the production process as care must be taken in order to prevent cracking or breakage of the final product. Also ease of handling of the final product will also be dependent primarily on these mechanical properties. It is thought that the improved mechanical properties that this set of materials show over the first set of materials are due to the plasticising nature of the derivatives of PEG that are used in these compositions.

4.5 Evaluation of Specifically Designed Formulations

It was decided to formulate a new set of materials based on a range of hydrophilic monomers that have been used in contact lens applications. These formulations will utilise various derivatives of PEG in order to improve the mechanical properties of these materials in the dehydrated state.

4.5.1 Materials

The composition of samples produced as described in Chapter 2, are shown in table 4.3. The water binding and moisture absorbency of the samples were investigated by differential scanning calorimetry and dynamic vapour sorption techniques.

4.5.2 Results

The moisture uptake of the samples are presented in table 4.3, with values for the equilibrium water content and amounts of free and bound water, and mechanical properties displayed in table 4.4.

Table 4.3. Compositions and water uptake for third set of samples

Sample	Monomers	Ratio %	% Weight Uptake After (mins)		
			100	200	300
1	Peg200:NVP:MAA	60:30:10	0.6	0.75	0.8
2	Peg200:NVP:MAA	50:40:10	0.55	0.8	0.96
3	Peg200:NVP:MAA	40:50:10	0.55	0.75	0.85
4	Peg1000:NVP:MAA	60:30:10	0.45	0.6	0.7
5	Peg1000:NVP:MAA	50:40:10	0.55	0.65	-
6	Peg1000:NVP:MAA	40:50:10	0.6	-	-
7	Mpeg200:NVP:MAA	50:40:10	-	-	-
8	Peg1000:AMO:MAA	50:40:10	0.55	0.75	0.85
9	Peg200:AMO:MAA	50:40:10	0.27	0.38	-
10	Peg200:AMO:MAA	40:50:10	0.38	0.46	0.5
11	Peg1000:HEMA:MAA	50:40:10	0.28	0.44	0.47
12	Peg200:HEMA:MAA	50:40:10	0.27	0.42	-

Table 4.4. Water binding and mechanical properties of third set of samples

Sample	EWC %	Free %	Bound %	Elastic Modulus Mpa	Tensile Strength MPa	Elongation %
1	59.7	31.9	27.8	0.48	0.15	32.1
2	67.1	39.6	27.5	0.47	0.13	29.8
3	65.9	34.7	31.2	0.45	0.13	31.2
4	64.7	34.9	29.8	0.39	0.08	21.6
5	62	32.5	29.8	0.50	0.13	26.2
6	67.3	31.9	35.4	0.33	0.12	39.1
7	66	38.3	27.7	-	-	-
8	64.9	41.6	23.3	1.30	0.16	23.2
9	62.8	40.5	22.3	1.32	0.16	11.32
10	66.3	46.7	19.6	0.96	0.26	27.5
11	46.9	16.1	30.8	1.13	0.43	43.4
12	46.7	16.6	30.1	1.14	0.41	42.8

4.5.3 Discussion

All the samples in this section contained 10% by weight of methacrylic acid as shown in table 4.3. The first three samples were based on different ratios of PEG200 dimethacrylate to NVP. Going from a ratio of 60:30 to a ratio of 40:50, the total water content of the polymer increases (within experimental error), as does the amount of bound water. However if the bound water is expressed as a percentage of the total water content, no significant increase is seen. The moisture uptake profiles for these three samples look very similar, therefore, to observe any differences the samples are expressed as the % weight uptake after 100, 200 and 300 minutes. When the moisture uptake is presented this way, the samples again show similar water absorbency although sample two does possess the highest capacity. This is surprising when it is noted that it is this sample that has the greatest proportion of its total water content in the free state.

As the proportion of NVP is increased the water content increases and this is expected given that NVP is more hydrophilic than PEG200 dimethacrylate. It is the presence of NVP and methacrylic acid which are mainly responsible for the moisture uptake with the PEG 200 dimethacrylate giving the material a degree of flexibility in the dehydrated state. As would be expected the moisture uptake rises with an increase in the NVP content which is accompanied by an increase in the total water content.

Samples 4-6 were of the same composition as samples 1-3 respectively, however these samples contained PEG dimethacrylate with a molecular weight of 1000. This will effect both the water binding and mechanical properties of the resulting copolymers as well as their moisture absorbency. In the hydrated state, these materials show similar tensile strengths as the PEG 200 DMA samples but a reduced initial modulus. As the molecular weights of the dimethacrylate monomers are so different, there will be far more of the 200 molecular weight units in its copolymers than 1000 molecular weight units in its copolymers. This results in the PEG 200 dimethacrylate having a greater initial modulus than the PEG 1000 derivative.

Changing the molecular weight of the PEG dimethacrylate does not have any significant effects on the total water content and relative proportions of free and bound water in the resulting copolymers. Even though the two sets of copolymers have different numbers of PEG units, they contain similar numbers of polyethylene chains and thus the water binding properties of the hydrated polymers is similar.

As the ratio of NVP:PEG is changed from 30:60 to 50:40, the total water content of the copolymer increases very slightly. The amount of this water that exists in the bound state also increases as the number of polar hydrophilic sites becomes greater. This is a consequence of the higher NVP content. The rate of moisture uptake also increases with increasing NVP content and as such this could be correlated with the proportion of water that exists in the bound state when the material is at complete hydration. However a correlation with total water content could also be drawn which is also the case for the first three samples. In the first set of samples a correlation with the bound water proportion cannot be made.

Sample 7 is a single example where the PEG methacrylate has been replaced by methoxy PEG methacrylate. This has no significant effect on the water binding properties of the material when it has reached its equilibrium level of hydration. The moisture uptake of this sample is however very different from all the other hydrogel samples that were examined by this method. The water absorbency reaches a maximum after less than 100 minutes after which the water in the sample begins to be lost back to the atmosphere. After falling steadily for a period of about 400 minutes the sample settles at a stable level of hydration.

Sample 8 has the same composition as sample 5 except that NVP has been replaced by AMO. This slightly increases the total water binding properties of the resulting copolymer, however there is a decrease in the proportion of this water that exists in the free state. The rate of moisture absorption is higher in this sample than in the NVP analogue and this could be a consequence of the higher total water content that this sample possesses in the fully hydrated state. The mechanical properties of the AMO copolymers, especially the elastic modulus are better than for the NVP copolymers of

the same composition. This is due to the higher energy barrier to rotation that polyAMO has when compared to polyNVP.

The next sample, 9, has the same composition as the previous sample except the PEG dimethacrylate used has a molecular weight of 200 as opposed to the 1000 derivative which is present in sample 8. This does not change the water binding properties significantly but does lower the rate of moisture uptake greatly. This is surprising as with NVP, the PEG 200 dimethacrylate shows a greater rate of water absorbency than the PEG 1000 dimethacrylate.

If the ratio of Peg 200 dimethacrylate to AMO is changed from 50:40 to 40:50, the total water content of the fully hydrated polymer increases as can be seen in sample 10. Accompanying this increase is a fall in the proportion of the water that is present in the bound state. As the proportion of the hydrophilic monomer is increased, the rate of moisture uptake increases but it is still at a far lower level than the copolymers containing the larger molecular weight PEG dimethacrylate.

NVP has a relatively low reactivity in vinyl polymerisation reactions which result in large blocks of NVP along the polymer chain. These blocks could be responsible for the high level of moisture uptake seen with the NVP copolymers. AMO has a higher reactivity in vinyl polymerisations and so has smaller blocks of hydrophilic monomers. When the PEG dimethacrylate of molecular weight 1000 is used, the number of units used is relatively low and so the size and amount of hydrophilic blocks remains high. However, when the PEG dimethacrylate of molecular weight 200 is incorporated in the polymer, a much larger number of units are incorporated in the polymer. This has the effect of splitting the hydrophilic blocks into smaller sections which have a reduced moisture absorption ability.

In samples 11 and 12, the hydrophilic monomer NVP which is used in all the other samples has been replaced by the less hydrophilic monomer HEMA. In contact lenses where the material is present in the fully hydrated state, it is thought that a lower rate of evaporation occurs in materials based on HEMA when compared to those based on NVP. The inclusion of HEMA would also be expected to lower the total water

content of the material and increase the proportion of this water that is present in the bound state.

With a ratio of PEG1000 dimethacrylate to HEMA of 50:40 which is seen in sample 11, the total water content of the copolymer when compared to the NVP analogue has fallen by approximately 20% to an EWC of 47%. However, as expected, the proportion of this water present in the bound state has increased dramatically. With the lower water content the material has, the tensile strength has also increased and with the reduction in the free water proportion, the stiffness of the material has also increased. The rate of moisture uptake has also decreased in comparison to the NVP samples with the final capacity also being much reduced.

Sample 12 is based on the same composition as the previous sample with the exception of incorporation of PEG dimethacrylate of molecular weight 200 as opposed to 1000. This has virtually no effect on either the materials total water content or the states in which the water in the material exists. It is therefore unsurprising that the rate of moisture absorbency for both these samples is the same. As HEMA is highly reactive in polymerisation reactions, there are no relatively large hydrophilic blocks to influence the water uptake ability of the sample. The result is little change in water uptake as the molecular weight of the PEG is decreased.

4.5.4 Conclusions

The moisture absorbency of the samples appears to be influenced by the water binding properties in the same way as the samples investigated in the first two sets of experiments. Samples with the highest bound and total water contents display the largest capacity of moisture uptake. The hydrophilicity of the main monomer controls the total water content of the resulting polymer which is further enhanced by the presence of methacrylic acid. When NVP, which is used in the majority of the compositions, is replaced with HEMA an increase in the proportion of water in the polymer existing in the bound state is observed. However, this is accompanied by a substantial decrease in the total water content of the polymer and so a greatly reduced moisture absorbency capacity is observed. The incorporation of PEG dimethacrylate

lowers the total water content of the hydrogel copolymer but its presence improves mechanical properties in the dehydrated state and reduces dimensional changes observed as moisture is absorbed.

The samples produced in this section show good moisture absorbency and improved mechanical properties in the dehydrated state. However, it was felt that a further improvement in the mechanical properties of these samples was required. As the principle moisture absorbency properties of the hydrogel must be retained, interpenetrating polymer network techniques were identified as offering the greatest potential for the improvement in mechanical properties required.

4.6 Effect of Incorporation of Interpenetrant

The incorporation of a preformed polymer in the monomer mixture before polymerisation results in the formation of an interpenetrating polymer network. In the hydrated state these types of polymers have greatly improved mechanical properties when compared to conventional hydrogels. However the unique properties of the hydrogel, such as its affinity for water and the transport characteristics that this water imparts, are still preserved in these composite materials. The amount of interpenetrant will affect the total water content as well as the relative proportions of free and bound water and this would be expected to have some effect on the materials water uptake profile.

4.6.1 Materials

Increasing amounts of a polyurethane interpenetrant were incorporated within one of the compositions that shows a good degree of moisture absorbency. The level to which this incorporation was investigated is up to 20% by weight of the monomer mixture. The composition that was used for this investigation was the same as that used to prepare sample 2 of the previous set of samples. All standard test methods were used to evaluate the properties of the resulting polymers. The unit that gives polyurethane its name is the basic urethane structure shown in figure 4.7. However the overall structure of the polymer is much more complicated. Two basic polyurethanes

exist and these are the polyether-urethanes and the polyester-urethanes. The polyurethane that was used for this investigation was an aromatic polyester based polyurethane (Estane resin 5706 F).

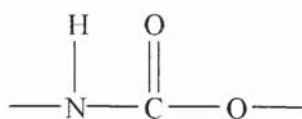


Figure 4.7. The structure of the urethane unit

4.6.2 Results

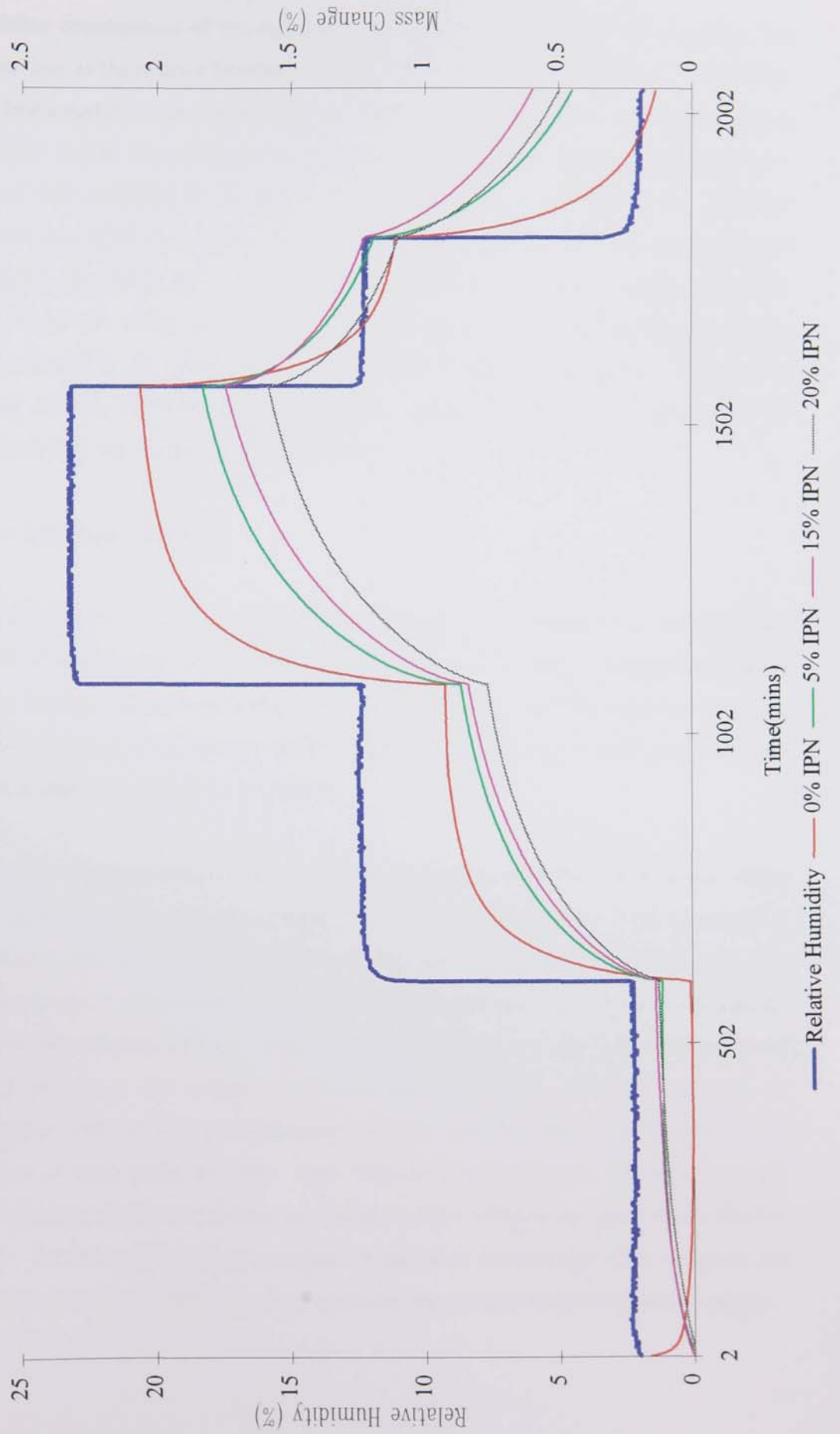
The moisture absorbency profiles of each of the samples containing an interpenetrant are shown in figure 4.8. Also the water binding and mechanical properties are shown in figures 4.9 and 4.10 respectively.

4.6.3 Discussion

4.6.3.1 Moisture Absorbency

When the relative humidity in the air around the samples is increased by 10% all the samples show an increase in weight which is attributed to an absorption of moisture. The sample without any interpenetrant displays a very fast level of moisture uptake reaching its maximum of around 0.95% within around 300 minutes. When the interpenetrant is added to the system, the rate of moisture uptake is much slower and the final capacity is still rising 500 minutes after the initial increase in relative humidity. The magnitude of the final capacity is still comparable to that of the copolymer with no interpenetrant and reaches a level of 0.85%. These levels could be similar because the incorporation of the interpenetrant lowers the total water content, but the amount of water in the sample that exists in the bound state increases. As the amount of interpenetrant in the copolymer system is increased, only small effects are observed in the moisture uptake profile. With increasing interpenetrant content both the rate of moisture uptake and the final moisture capacity of the copolymer decrease. However, these decreases are very small in magnitude, with the difference in capacity between 5 and 20% interpenetrant content being less than 0.1% by weight.

Figure 4.8 Comparison of Moisture Absorption/Desorption Isotherms for IPN Hydrogels



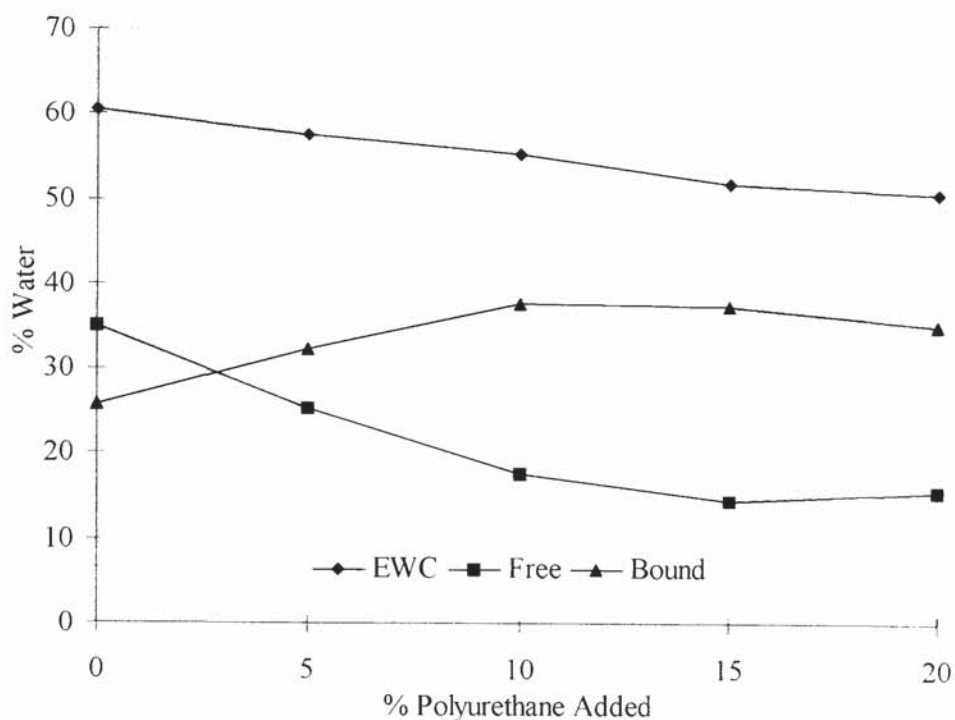
Another consequence of the incorporation of an interpenetrant is the effect on the water loss as the relative humidity is lowered by 10%. For the composition containing no preformed polymer, the decrease in weight seen in this sample as it loses moisture is rapid and all the moisture that was held in the sample is almost completely lost. When the interpenetrant is added, the rate of moisture loss that occurs with the decrease in humidity is greatly reduced. Also 200 minutes after the humidity level is dropped, the sample still contains approximately 0.5% moisture by weight which is far more than the sample containing no interpenetrant. As the amount of polyurethane incorporated in the copolymer is increased, no significant changes are observed in either the rate of moisture loss, or in the moisture capacity of the copolymer 200 minutes after the humidity level is lowered.

4.6.3.2 Water Structuring

As the amount of the polyurethane interpenetrant in the copolymer is increased, the EWC of the polymer decreases as shown in figure 4.9. This is expected as there is more hydrogel material in contact with the polyurethane and this increases the steric hindrance around the hydrogel chains. The result of this is less water molecules can pack in and around the polymer chains.

When the interpenetrant is added to the system, a large increase in the amount of water that exists in the bound state is observed. Also, as the proportion of interpenetrant is increased, the bound water increases slightly while the amount of water in the free state decreases. The inclusion of the polyurethane increases the amount of hydrophilic sites in the resulting polymer. This causes the observed increase in the level of bound water present in the system. However, the total water content of the polymer decreases with increasing interpenetrant content, and the result is a decrease in the amount of water in the free state. Any water present will interact with sites of strong hydrophilicity until all these sites are occupied, after which it can only exist in the free state. As the amount of interpenetrant is increased the amount of free space in the polymer decreases which is the main cause for the decrease in the total water content.

Figure 4.9 Water structuring properties for a desiccating hydrogel with increasing polyurethane interpenetrant content



4.6.3.3 Mechanical Properties

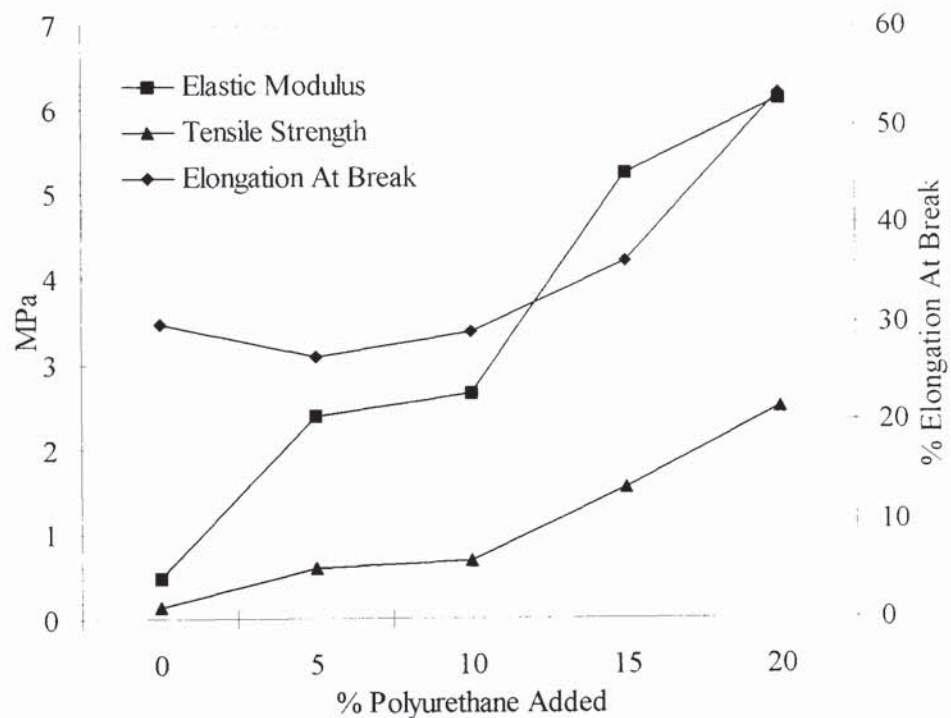
The incorporation of an interpenetrant also has a noticeable effect on the mechanical properties of the copolymer in the hydrated state. As more of the interpenetrant is added to the copolymer system, a large increase in both the tensile strength and elastic modulus for the resulting copolymers is observed as illustrated in figure 4.10. On moving from the unmodified copolymer to the lowest level of interpenetrant incorporation which is 5%, a fall in elongation at break is observed. However on raising the incorporation level, an increase in elongation at break is also seen.

The inclusion of the interpenetrant at small concentrations increases the elastic modulus far more than it increases the tensile strength of the material. This results in the small decrease in elongation at break which is observed. As its inclusion is increased, both the tensile strength and the elastic modulus of the copolymer increases and this results in the increase in elongation at break which is also seen. The inclusion

of the preformed polymer results in the formation of a rigid network which imparts a large degree of stiffness in the resulting copolymer.

In the dehydrated state the IPN materials are very tough possessing a high elastic modulus and tensile strength. As they are based on a rigid polyurethane network, they also retain a degree of dimensional stability when they are hydrated even up to their maximum hydration capacity. Thus these materials possess mechanical properties that allow them to be processed in either the hydrated or dehydrated state and their dimensional change as they absorb moisture is kept to a minimum.

Figure 4.10 Mechanical properties for a desiccating hydrogel with increasing polyurethane interpenetrant content



4.6.4 Conclusions

The inclusion of a preformed, interpenetrant polymer within a hydrogel formulation displaying good moisture absorbency, has significant effects on the mechanical properties of the resulting IPN copolymer. Increasing interpenetrant content also affects the water binding and absorbency capacity of the material. The total water content of the IPN copolymer decreases slightly although the amount of water existing

in the bound state actually increases. With increasing interpenetrant content, a slight decrease in the dehydrated materials capacity for moisture uptake is observed. However as the environmental humidity is decreased to zero, materials containing some interpenetrant polymer retain some of the moisture the material previously absorbed. This is a beneficial property that the simple hydrogel copolymer does not display.

The mechanical properties of the IPN copolymer in the hydrated state are considerably better than those for the same copolymer without any interpenetrant. With increasing preformed polymer content, dramatic increases in both elastic modulus and tensile strength are observed. As the material is dehydrated dimensional changes of the material are kept to a minimum. In the dehydrated state the materials are less brittle, possessing the necessary properties to allow mechanical processing.

4.7 Chapter Conclusions

The work reported within this chapter has shown that hydrogels possess the necessary properties which make them suitable for use as pharmaceutical packaging products that perform a desiccating function. They have a high affinity for water, can be sterilised easily and as they are used extensively in biomedical applications should not pose any toxicity problems in this application. The properties of the hydrogel that are utilised for this application are the same as those for so called “anti-mist” coatings for glasses.

In the dehydrated state the hydrogel copolymers prepared in this work absorb moisture at a rapid rate when the environmental humidity is raised from 0 to 10%. The equilibrium capacity is reached relatively quickly and depends on the total water content and the relative proportions of this water that exists in the bound state. The higher the equilibrium water content, the larger the moisture uptake. For materials with similar water contents, the moisture absorbency is greatest for the material with the higher proportion of water in the bound state. Absorbency capacity must be maximised to enable the size of the desiccant hydrogel implant within the product vial to be minimised.

The simple hydrogel copolymers produced for this application have adequate moisture absorbency but suffer from undesirable mechanical properties. The materials are employed in the dehydrated state for this particular application and it was found that the initial hydrogels produced were extremely brittle in this state. Although the incorporation of monomers to increase flexibility in the dehydrated state resulted in polymers with improved properties, the flexibility of the polymer was still not considered sufficient to allow easy mechanical processing. Also substantial dimension changes were observed as the sample absorbed moisture.

Interpenetrating polymer network technology was employed to increase flexibility in the dehydrated state and improve dimensional stability as the hydrogel absorbs moisture. A polyurethane polymer is added to the hydrogel monomer mixture prior to the polymerisation process. As incorporation increases the water content of the resulting copolymer decreases while a dramatic increase in mechanical properties is observed. However, the absorbed moisture capacity decreases only slightly and the materials containing an interpenetrant retain a significant amount of moisture when humidity is lowered back to zero, a property not observed in the conventional hydrogels.

The ideal hydrogel formulation for this application would therefore incorporate all the points identified above. A simple hydrogel based on a highly hydrophilic monomer would produce a high EWC polymer and methacrylic acid can also be added to the system to increase the water content further. Copolymerisation with other monomers can manipulate the hydrogels water binding properties such that the proportion of water existing in the bound state is maximised. Finally a small percentage of polyurethane interpenetrant (e.g. Estane resin 5706 F) is added to the system to impart a degree of flexibility to the hydrogel in the dehydrated state.

CHAPTER 5

HIGH EQUILIBRIUM WATER CONTENT ACRYLOYLMORPHOLINE HYDROGELS INCORPORATING BASIC MONOMERS

5.1 Introduction

The eye is a unique human body site possessing an unrivalled combination of biochemical complexity and ease of access. It therefore provides an opportunity for testing aspects of material biocompatibility with relative ease and without the need for invasive surgery. The fact that hydrogels are used extensively as contact lenses, which maybe produced relatively easily, enables the ocular biocompatibility of new polymer structures to be evaluated quickly. However the range of materials that may be investigated for ophthalmic applications is relatively limited, as there is a need for specific mechanical, surface and permeability properties as dictated by the ocular environment.

For contact lenses within Group II of the FDA classification (EWC >55%, non-ionic), the number of monomers used is relatively small. This is a consequence of the level of hydrophilicity required to produce a material with a high water content whilst still retaining adequate mechanical strength. Table 5.1 shows the composition of some commercially available high EWC lenses.

Table 5.1 Composition of some commercially available high EWC contact lenses

Name	Manufacturer	Components	EWC%
Focus	Ciba	HEMA,PVP,MAA	55
Medalist 66	Bausch & Lomb	HEMA,VP	66
Igel-68	Igel Optics	MMA,VP,CMA	68
Lunelle ES70	Lunelle	MMA,VP	70
Omniflex	Hydron	MMA,VP	70
Sauflon-70	Contact Lens Manufacturing	MMA,VP	70
Permalens	Pilkington Barnes-Hind	HEMA,VP,MMA	71
Frequency 73	Aspect	HEMA,VP	73
Rythmic	Lunelle	MMA,VP	73
Calender	Pilkington Barnes-Hind	MMA,VP	74
Permafex	Pilkington Barnes-Hind	MMA,VP	74
Precision UV	Pilkington Barnes-Hind	MMA,VP	74
Cristelle	Lunelle	MMA,VP	78

The hydrophilic monomer N-vinyl pyrrolidone (NVP) is widely used to produce high water content contact lenses as seen in table 5.1. However despite extensive commercial success its performance fails to reach a level of ideality. NVP is relatively unreactive in free radical vinyl polymerisation, thus producing polymers with local domains of the same chemical type. It has been found that polymers with this block-type structure are more susceptible to biochemical and biological deposition than polymers with small alternating monomer sequences¹⁰⁶. This is a significant problem as deposition on the surface of the synthetic material can result in incompatibility between the material and the biological environment which it is in contact with.

5.2 Acryloylmorpholine As A New Hydrophilic Monomer

Acryloylmorpholine (AMO) was first synthesised by Parrod and Elles in 1957 and has been used to synthesise hydrophilic gels¹⁰⁷. The structure of AMO has similarities with NVP and has evolved from that of another hydrophilic monomer acrylamide. However even though acrylamide has been used widely in contact lens formulations¹⁰⁸ and possesses a high K_p/K_t for polymerisation reactions, it is susceptible to hydrolysis. The mono-substituted derivatives of acrylamide such as N-isopropyl acrylamide are more stable but can undergo enzymatic hydrolysis. It is therefore a di-substituted derivative of acrylamide, N, N-dimethyl acrylamide (NNDMA), which is used in contact lens compositions as its structure prevents any hydrolysis reactions. The presence of a ring in AMO also prevents hydrolysis as no hydrogen atoms are bonded to the nitrogen atom in its structure. AMO, NVP and NNDMA have comparable levels of hydrophilicity and their relative advantages are now presented.

5.2.1 Reactivity and Sequence Distribution

To produce sequence distributions, copolymerisation simulations are performed on 2-hydroxyethyl methacrylate (HEMA) with each of the nitrogen containing monomers. The reactivity ratios of the monomers are obtained from experimentally determined literature values or from the Q and e scheme when experimental values have not been determined and are shown in table 5.2.

Table 5.2 Reactivity ratios for copolymers of N-containing monomers and HEMA

Monomer 1	Monomer 2	r_1	r_2
HEMA	NVP	4.43	0.04
HEMA	NNDMA	1.56	0.34
HEMA	AMO	3.79	0.21

Computer simulations for the sequence distribution of copolymers of 30 mole% N-containing monomer and 70 mole% HEMA were carried out for AMO, NVP and NNDMA and can be found in appendix II. The sequences represent reaction to 100% conversion and the results are summarised in table 5.3.

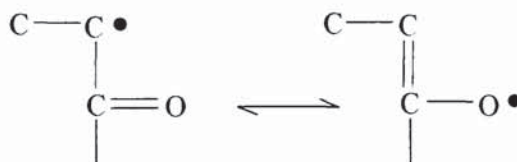
Table 5.3. Sequence simulation results for copolymers of HEMA:nitrogen containing monomer (70:30) for AMO, NVP and NNDMA

Sequence Length	Number of Sequences		Number of Sequences		Number of Sequences	
	HEMA	NNDMA	HEMA	AMO	HEMA	NVP
1	130	319	73	214	75	244
2	83	60	62	44	37	19
3	67	15	24	12	27	1
4	31	9	31	3	23	1
5	20	1	9	3	19	0
6	18	1	17	1	16	0
7	18	0	10	1	12	0
8	10	1	9	0	8	0
9	9	0	2	0	5	0
10	5	1	7	0	7	0
11	5	0	4	0	6	0
12	3	0	6	0	3	0
13	2	0	4	0	8	0
14	2	0	3	0	3	0
15	2	0	3	0	2	0
51	0	1				
120			0	1		
345					0	1

The reactivity of the nitrogen containing monomers are a function of both steric and polar effects as well as resonance stabilisations. Steric and polar effects are important in both the reacting radical and the monomer and must be considered simultaneously. It would be expected that the steric and polar effects for the three monomers would be similar as the structures and size of the constituents within their structures are comparable. The resonance stabilisation energy however which occurs when monomer is converted to radical is more important than the reactivity of the radical. A high resonance stabilisation energy for the radical will result in a lowering of the activation energy for the reaction which in turn leads to a higher rate of reaction for the monomers addition to the radical.

The radicals of AMO and NNDMA have a higher resonance stabilisation energy than the radical of NVP, due to the formation of the resonance structure shown in figure 5.1.

Figure 5.1 The resonance stabilisation structure of AMO and NNDMA



This resonance stabilisation energy does not occur with the radical of NVP as its structure will not allow the formation of the radical structures. It would therefore be expected that AMO and NNDMA will add to HEMA at a greater rate than NVP due to the lower activation energy that results from the formation of the resonance structures. AMO and NNDMA will have a higher reactivity than NVP to vinyl polymerisation with HEMA and this is reflected in the results of the simulation of the sequence distribution. NNDMA and AMO are consumed at a faster rate in the copolymerisation reaction than NVP which is consumed in the latter stages of the reaction and forms a large terminal block.

Another consequence of the reactivity ratios is the difference in composition of the resulting copolymer compared to the initial feed ratio of monomers. Ma¹⁰⁹ reported that elemental analysis of copolymers prepared by solution polymerisation showed marked differences when compared to feed ratios.

Table 5.4 The Feed ratio and actual ratio of monomers in a number of HEMA copolymers

Copolymer Composition	Initial Feed Ratio (weight%)	Actual Weight Ratio (weight%)
HEMA:NVP	90:10	95:5
	70:30	83:17
	50:50	61:39
HEMA:NNDMA	90:10	91:9
	70:30	71:29
	50:50	50:50
HEMA:AMO	90:10	92:8
	70:30	73:27
	50:50	52:48

5.2.2 Physical Properties

Acryloylmorpholine, when copolymerised with 2-hydroxyethyl methacrylate, produces hydrogels with similar water contents as copolymers of HEMA with N-vinyl pyrrolidone. These two copolymer series also possess similar proportions of water existing in both freezing and non-freezing forms. However, although these series display similar polar and dispersive components of surface free energy, the protein and lipid adsorption of HEMA-NVP copolymers is greater than for HEMA-AMO copolymers. The lower protein deposition that AMO copolymers exhibit is due to the improved sequence distribution these copolymers have over NVP copolymers. The higher lipid adsorption that the NVP copolymers display is unsurprising when it is noted that pyrrolidone has been used as a skin permeation enhancer.

Polymers of NVP and NNDMA have a lower glass transition temperature than the polymer of AMO which indicates that AMO has a higher energy barrier to rotation.

The tensile strength of NVP and AMO copolymers are very similar with the value for NNDMA being much lower. This is a consequence of NNDMA's susceptibility to chain transfer reactions during copolymerisation, which are caused by hydrogen abstraction from the pendant methyl groups. This produces imperfect networks with lower than expected mechanical properties.

It would be expected that the higher energy barrier to rotation that AMO possesses would give rise to copolymers with improved mechanical properties when compared to similar copolymers incorporating NVP. However the mechanical properties of copolymers incorporating these two monomers are very similar. This is a consequence of the improved water structuring of the AMO copolymer owing to its more regular sequence distribution. The NVP copolymer has longer sequences of HEMA units and as it is a less hydrophilic monomer than the nitrogen containing monomers these segments are slightly stiffer. The longer the segments of HEMA, the greater the mechanical properties. The AMO copolymer has shorter HEMA segments and so the improvement in mechanical properties due to the higher energy barrier to rotation is offset by the reduction in stiff segments when compared to the NVP copolymer.

Obviously, hydrogels possessing a high water content generally have poor mechanical properties due to the large amount of water present within their structure. Therefore it is desirable to improve the mechanical properties of hydrogels that have large degrees of hydrophilicity without reducing the water content.

5.3 Charged Monomers

Investigation of the potential use of ion containing monomers in hydrogel contact lenses has received little attention in published literature. A fact which is surprising when it is noted that methacrylic acid is always present in both the monomer and polymer of HEMA. It is a product of a disproportionation reaction which makes it almost impossible to obtain 100% pure HEMA.

For applications including solute separation and controlled release of solutes, hydrogels which show significant swelling changes in response to external stimuli such as pH, have received considerable attention¹¹⁰⁻¹¹⁹. In these investigations, monomers containing ionisable groups are included in the copolymer composition. Initially monomers that were used for this application were only weakly ionisable and included methacrylic and acrylic acids¹¹⁰⁻¹¹². More recently, sulphonate monomers used for so called “superabsorbant” polymers have emerged that contain a greater degree of charge¹¹³⁻¹¹⁷. Zwitterionic monomers which contain an inner salt, have been investigated widely for the above applications^{118, 119}. However the incorporation of cationic monomer in hydrogels for ophthalmic applications has received very little attention.

The possibility of using basic, potentially cationic monomers in conventional hydrogel compositions has only been investigated to a very limited degree. Fushimi et al¹²⁰, studied the states of water in cationically charged poly(vinyl alcohol) membranes using DSC and NMR spectroscopy, but no comment was made on the effect of the cationic monomer on the states of water present. French¹²¹ looked at the effect of incorporation of positively charged monomers into poly(HEMA) hydrogels on the physical properties of the resulting copolymers. It was observed that the EWC was relatively unaffected although the proportion of bound water increased slightly. Mechanical properties increased very slightly while surface properties were relatively unaffected.

The inclusion of ions within the polymer will be expected to affect the mechanical properties of the resulting hydrogel. In the dehydrated state, these materials should have a greater tensile strength and initial modulus due to the clustering of the ionic groups which act as physical cross-links. However in the hydrated state, the ions increase the water content, and as the water acts as a plasticiser a reduction in mechanical properties may be expected if this increase in water content is sufficiently large. Therefore optimisation of ion content, to give a balance between the expected increase in water content and any possible reduction in mechanical properties, must be attained.

The work presented in this chapter deals with the effect of incorporation of monomers with the potential to carry a positive charge on the physical properties and the surface energy of the resulting hydrogel copolymer. It is desirable that the incorporation of such monomers will improve the mechanical properties of AMO copolymers without having a detrimental effect on their surface properties. Evaluation of improvements in mechanical properties will be difficult as increased incorporation of monomers with charged groups will be accompanied by an increase in the EWC and subsequently a decrease in mechanical strength.

5.4 Materials and Methods

Hydrogel membranes were produced as described in Chapter 2 and are all based on a copolymer of AMO and HEMA in a ratio of 70:30. This composition produces polymers with high water contents as both monomers are relatively hydrophilic. Thus the incorporation of monomers possessing charged groups will have a relatively small effect on the water content and will allow improvements in mechanical properties to be displayed. The monomers that were incorporated into this composition were N-vinyl imidazole (NVI), dimethylaminoethyl methacrylate (DMAEMA), dimethylaminoethyl acrylate (DMAEA), pyridine-N-oxide (PNO) and 4-vinyl pyridine (4VP). Each of these monomers whose structures are shown in Chapter 2, were incorporated at 2.5, 5, 7.5 and 10 % w/w in the AMO:HEMA copolymer.

The above monomers are basic monomers with the potential to show cationic character at certain pH ranges. The pH of the hydration water for all the hydrogels was in the range of 6 and at this range although the monomers do not carry a formal charge, there is a degree of charge at the basic units. Unbuffered water was used throughout the work as osmotic effects were not desired. It is known that phosphate and borate buffers produce different mechanical properties in hydrogels with a variety of functional groups although this has not been studied extensively.

The equilibrium water content and water binding properties of the hydrogels were obtained as were values for the mechanical properties. The surface properties were also investigated and evaluated by contact angle measurements.

5.5 Effect of Incorporation of Cationic Monomers on the Water Structuring of AMO:HEMA Hydrogel Copolymers.

5.5.1 Results and Discussion

The equilibrium water content of a series of copolymers for increasing amounts of cationic monomers is shown in figure 5.2. As the amount of cationic monomer present in the copolymer increases, the EWC increases. This would be expected since the cationic monomers possess polar groups which attract water molecules to a greater degree than the hydrophilic monomers already present. This increase in EWC may not be as great as expected for some of these monomers however as steric factors may dominate the water binding ability of the monomer. In addition, the magnitude of any increase in EWC will be small due to the high water content possessed by the AMO:HEMA copolymer.

For increasing proportions of DMAEA and DMAEMA, the resulting values for the EWC are very similar and increase as the proportion of cationic monomer increases. This would be expected as these two monomers are structurally similar with DMAEMA possessing an α -methyl group which limits the mobility of the polymer chain. The values for NVI and PNO are also similar which indicates the two monomers have a similar balance of polar and steric effects. However an increase in the proportion of 4-vinyl pyridine present in the copolymer results in a decrease in its EWC.

Expressing the water contents as percentages illustrates clearly the changes that occur when the composition of the hydrogel is altered. However in high water content systems such as these, results presented this way can obscure possible trends in the values of each water type present. Expressing each water type in the form of moles of water present per mole of polymer gives an indication of the water binding ability of each individual repeat unit. This is necessary as each monomer is incorporated at specific weight percentages and for varying molecular weights, varying numbers of repeat units will be incorporated in the resulting copolymer.

Figure 5.2 The equilibrium water content of AMO:HEMA (70:30) copolymers containing increasing amounts of cationic monomers

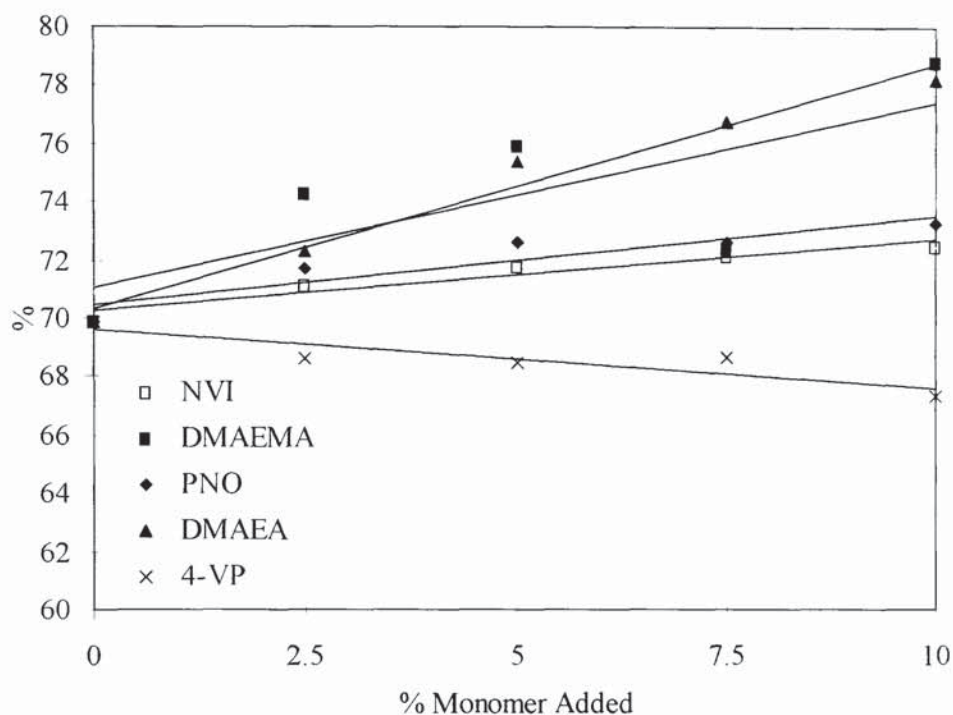
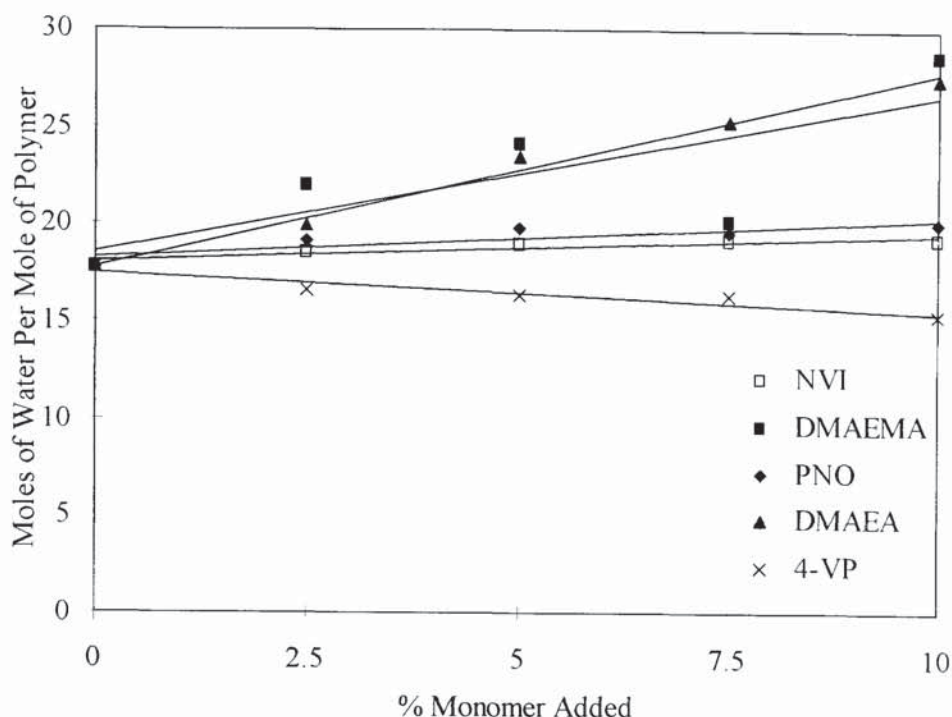


Figure 5.3 shows the change in EWC for increasing proportions of monomer added for a range of cationic monomers expressed as moles of water per mole of polymer. The most significant changes are that increasing the amount of NVI or PNO present in the copolymer does not have any significant effect on the proportion of water present. Increasing the amount of 4-VP in the copolymer decreases the amount of water present in the hydrogel only slightly. Little change is seen in the plots for DMAEA and DMAEMA as these monomers possess similar molecular weights as HEMA and AMO and so changing the way the results are expressed has little effect on the magnitude of each data point.

Figure 5.3 The total water expressed per mole of polymer in AMO:HEMA (70:30) copolymers with increasing amounts of cationic monomers



For increasing amounts of each cationic monomer the EWC can be displayed together with the amount of free and bound water present in the resulting hydrogel. Figure 5.4 shows these properties for NVI. It can be seen that as the amount of NVI is increased, the total water present increases slightly, but little change is seen in the proportion of free water. The increase in total water is therefore mainly due to an increase in the proportion of bound water present and this is illustrated in the plot. NVI is a polar and therefore hydrophilic monomer which possesses a bulky ring structure in its side group. This imparts a degree of steric hindrance which effectively limits the availability of space for the interaction of water molecules. Thus the overall water content does not increase significantly when the amount of this monomer present in the copolymer is increased. As the NVI content is increased, a higher proportion of the water is strongly associated with the polymer. This indicates that NVI can promote hydrogen bonding of water molecules to the polymer chain. Thus as the amount of NVI increases, the amount of water held tightly to the polymer chain increases due to the polarity of the monomer but the total number of water molecules associated with the polymer does not increase due to the bulky nature of the monomers side group.

Figure 5.4 The water binding properties of AMO:HEMA (70:30) copolymers containing increasing amounts of NVI

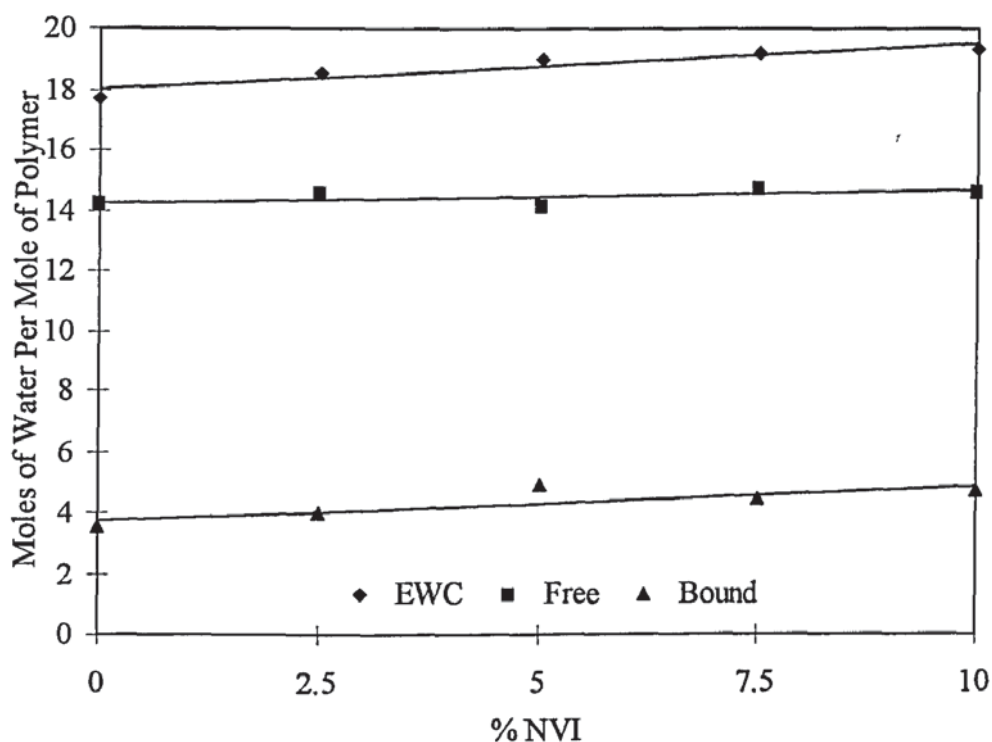


Figure 5.5 The water binding properties of AMO:HEMA (70:30) copolymers containing increasing amounts of DMAEMA

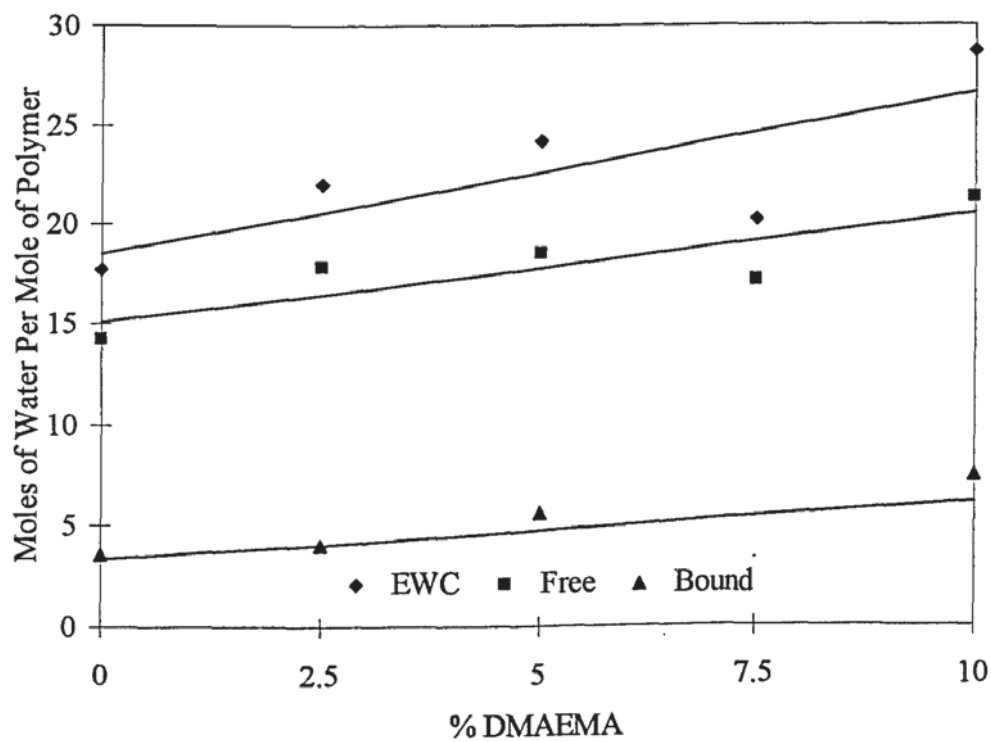


Figure 5.5 shows the proportions of each type of water present as the amount of DMAEMA in the copolymer is increased. As the cationic monomer content is increased, a large increase in the total amount of water present in the sample is seen. The proportion of bound water is again seen to increase due to the polar nature of the monomer. However the proportion of free water is also seen to increase with increasing DMAEMA content. The results indicate that DMAEMA is slightly more polar than NVI as more water molecules can closely associate with the polymer chain. Also as more free water within the polymer is observed, the monomer must have a less bulky side chain than NVI. Thus as DMAEMA content is increased, the bound water increases due to the monomers polar nature which also promotes more free water within the polymer as there is no significant increase in steric hindrance.

Figure 5.6 shows the EWC and proportions of free and bound water for increasing amounts of DMAEA. The values for DMAEA are very similar for the values for the similar monomer DMAEMA. The α -methyl group that DMAEMA possesses does not appear to reduce its polarity or increase the magnitude of its steric hindrance to any extent. The water binding properties of these two monomers appear to be the same within experimental error.

Figure 5.7 illustrates the water binding properties for increasing amounts of pyridine-N-oxide. As the amount of cationic monomer increases, the total amount of water present increases slightly. The bound water proportion is seen to remain relatively unaffected by this increase, however the proportion of free water is seen to account for this slight increase. The results suggest that the PNO monomer has a similar hydrophilicity as HEMA and AMO as the proportion of bound water is seen to remain relatively static. However, PNO does not contain a vinyl double bond at which it can undergo a polymerisation reaction. It therefore acts only as a diluent, a fact further illustrated by the gels blue appearance after production, which was lost during the hydration period by leeching.

Figure 5.6 The water binding properties of AMO:HEMA (70:30) copolymers containing increasing amounts of DMAEA

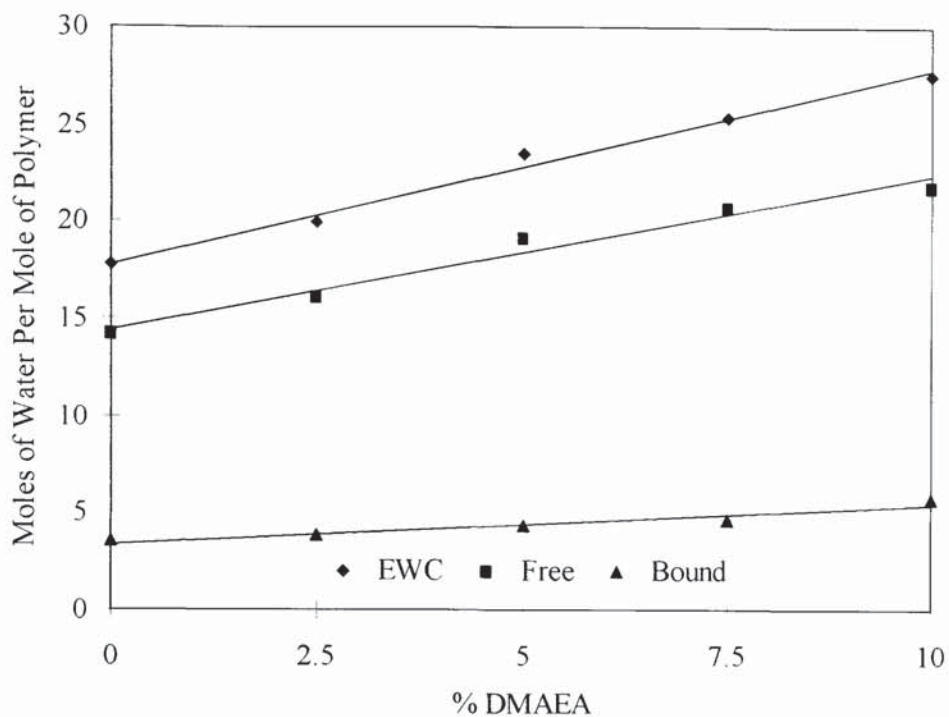


Figure 5.7 The water binding properties of AMO:HEMA (70:30) copolymers containing increasing amounts of pyridine -N-oxide

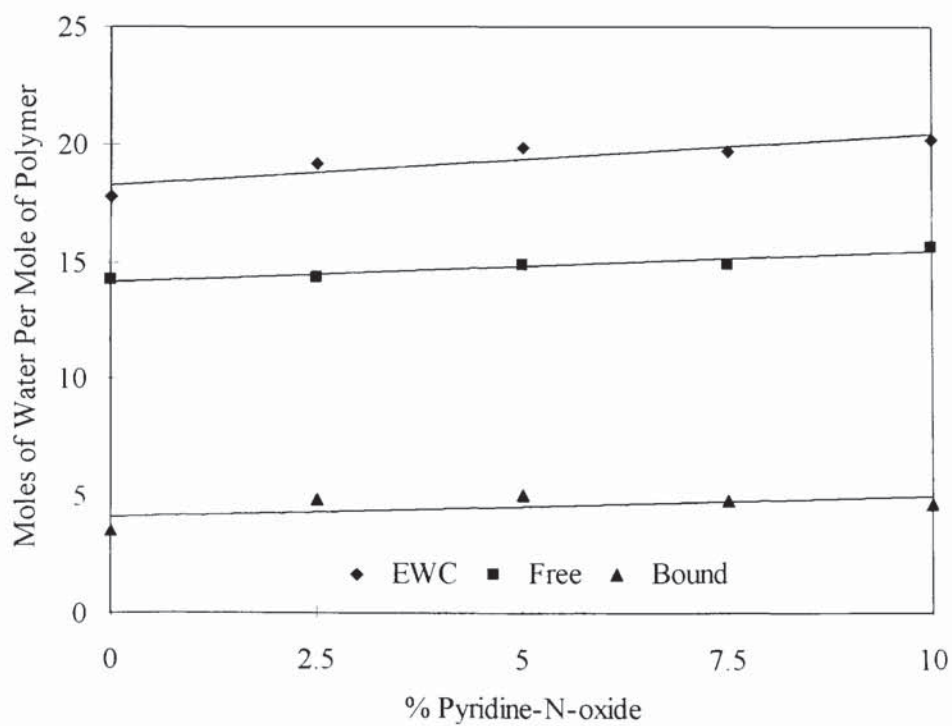
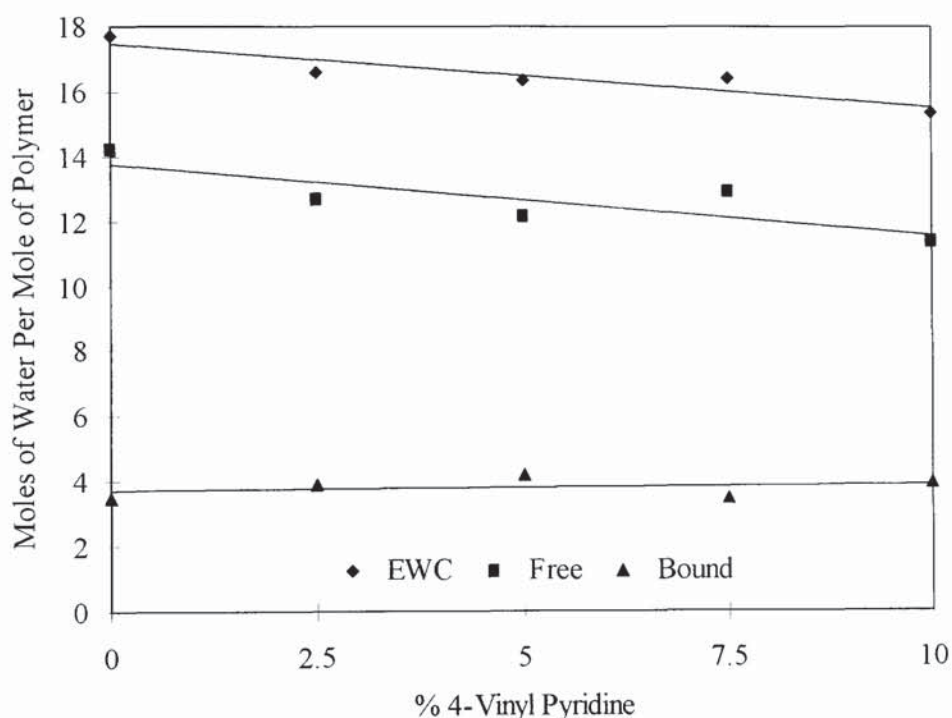


Figure 5.8 shows the EWC and proportions of free and bound water for increasing amounts of 4-vinyl pyridine in the HEMA:AMO copolymer. As the amount of cationic monomer is increased, the total amount of water present in the polymer decreases. The proportion of bound water is the same despite the addition of the monomer, however the amount of free water is seen to decrease in the same manner as the total water. This implies that 4-VP has a similar degree of hydrophilicity as AMO and HEMA but conveys a relatively increased steric hindrance.

Figure 5.8 The water binding properties of AMO:HEMA (70:30) copolymers containing increasing amounts of 4-vinyl pyridine



5.5.2 Conclusions

The results show that incorporation of cationic monomers, which have the potential to attain a positive charge, increases the EWC of AMO:HEMA copolymers. This is mainly due to the greater degree of hydrophilicity that these monomers display in comparison to the two monomers that make up the copolymer in which the charged monomers were incorporated.

For the majority of the cationic monomers investigated, the rise in EWC is caused by an increase in both the free and bound water proportions. However the rise in EWC for polymers incorporating NVI is attributed to a rise in the proportion of water that is bound. This results in the production of polymers with lower proportions of freezing water and this is the water that plasticises the copolymer. This factor enables the design of copolymers which possess smaller amounts of freezing water in the hope that their mechanical properties will be improved.

5.6 Effect of Incorporation of Cationic Monomers on the Mechanical Properties of AMO:HEMA Hydrogel Copolymers.

5.6.1 Introduction

The relatively poor mechanical properties that hydrogels display has limited their use as biomaterials. It is reasonable to expect hydrogels to become mechanically weaker as their water content is increased, but other factors will also affect a materials strength and stiffness. Monomer structure, cross-link density and inter-chain forces in the form of polar, ionic and steric interactions will have major implications on the elastic behaviour and rigidity of a material. Mechanical strength will be affected by these properties but for typical copolymers is mainly controlled by the state of water present within the polymer.

As water content increases, the mechanical strength decreases due to the plasticising effect of the imbibed water. As the results have shown that EWC increases with increased amounts of cationic monomer, it is necessary to investigate changes in mechanical properties. More specifically, it is necessary to compare mechanical properties to the relative proportion of each state of water, as the free water acts as an internal plasticiser. This has been explained by the theory of polymer networks using the following equation which relates the modulus of the material G , to other properties of the polymer network.

$$G = (1-2/f) \cdot \nu RT \cdot \langle r^2 \rangle / \langle r^2 \rangle_0 \quad \text{Equation 5.1}$$

where f is the functionality of crosslinks

ν is the molar number of elastically effective network chains per unit volume

R is the gas constant

T is the temperature

$\langle r^2 \rangle$ is the mean square end to end distance of the chains in the network

$\langle r^2 \rangle_0$ is the mean square end to end distance of the chains, in uncrosslinked state

When the EWC and consequently the degree of swelling is increased, ν is seen to vary inversely and thus the modulus G decreases. It would be expected however that ionic charges will produce hydrogels that deviate from this behaviour.

Little attention in literature has been paid to the effect of basic monomers on the mechanical properties of hydrogels. Previous work at Aston has investigated the mechanical properties of polyHEMA with incorporation of up to 20% of a basic monomer. Ma¹⁰⁹ reported that incorporation of NVI up to 2% increased the tensile strength while from 2-5% a gradual decrease to a tensile strength below that of polyHEMA was observed. However French¹²¹ reports a gradual increase in tensile strength as incorporation of NVI is increased from 0-20%.

5.6.2 Results and Discussion

The effect of increasing cationic monomer incorporation on the mechanical properties of the AMO:HEMA copolymer can also be examined. The tensile strength and initial modulus for increasing charged monomer content can be presented graphically for each individual monomer. Figure 5.9 displays this information for NVI. As charged monomer content is increased, the tensile strength increases while the initial modulus decreases only very slightly. If the water structuring is examined, the increase in EWC with increasing cationic monomer content is almost entirely due to an increase in bound water while the free water content increases only very slightly. With the increase in bound water, the number of water molecules around the polymer chain

increases and this raises its energy barrier to rotation. As there is no increase in the amount of plasticising water the overall consequence is an increase in the polymer's tensile strength. The initial modulus decreases very slightly in the same way as the free water increases. This illustrates the plasticising effect of the free water on the polymer and the effect that it has on the material's stiffness.

Figure 5.9 The mechanical properties of AMO:HEMA (70:30) copolymers containing increasing amounts of NVI

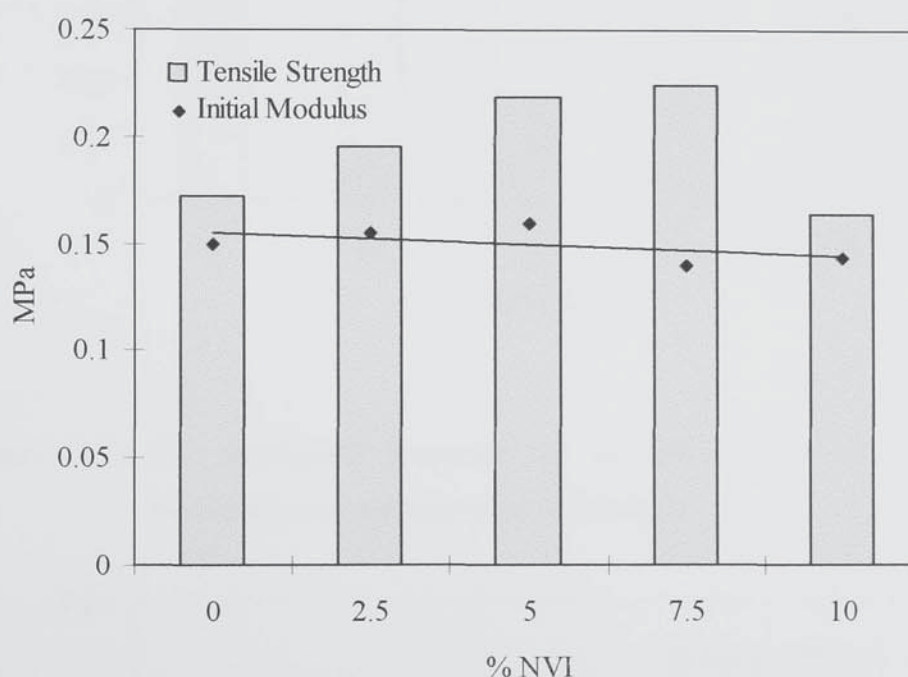


Figure 5.10 displays the tensile strength and initial modulus for the copolymer with increasing DMAEMA content. Both these properties decrease when the proportion of DMAEMA is increased and to understand this behaviour the water structuring properties must again be examined. As the EWC increases, the bound and free water fractions both increase, with the increase in the free water being quite substantial. Although the bound water increases, raising the energy barrier to rotation the free water proportion also increases and this increase in plasticising water offsets the rise in the energy barrier to rotation. This reduces tensile strength, while the decrease in initial modulus is again reflected by the increase in free water.

Figure 5.10 The mechanical properties of AMO:HEMA (70:30) copolymers containing increasing amounts of DMAEMA

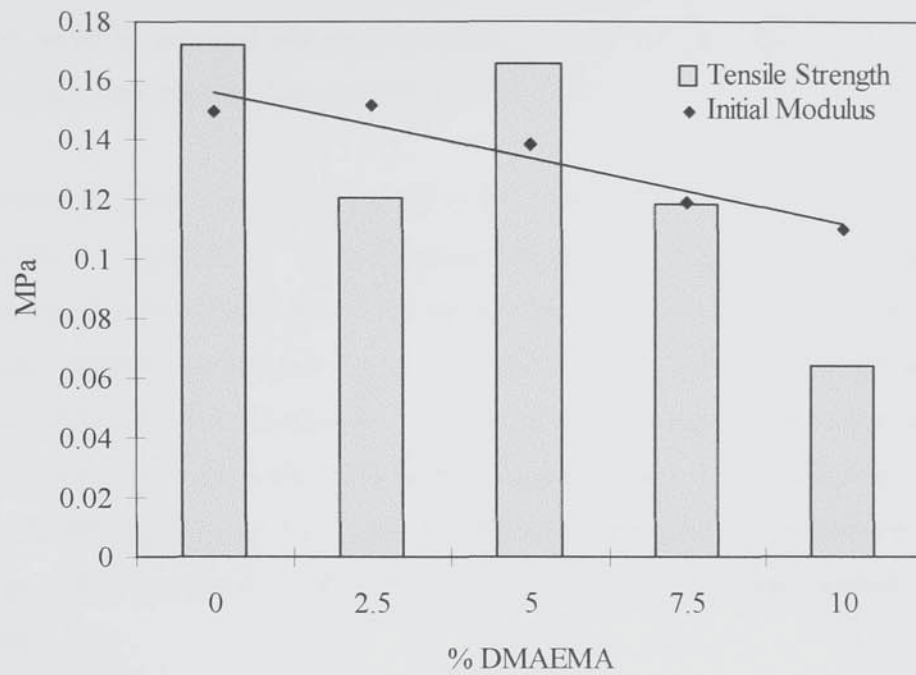
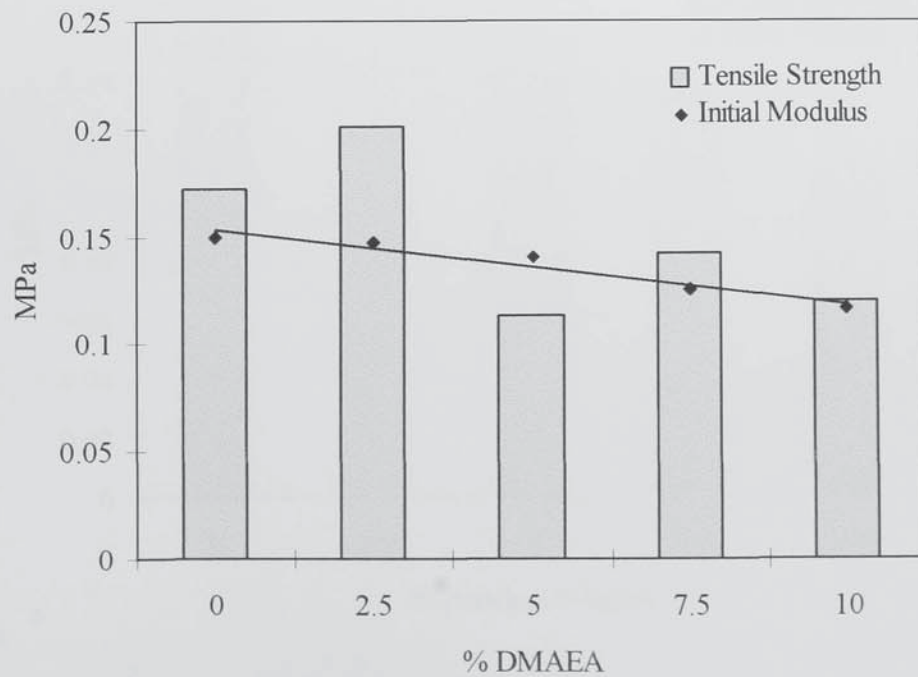


Figure 5.11 The mechanical properties of AMO:HEMA (70:30) copolymers containing increasing amounts of DMAEA



The mechanical properties for increasing proportions of DMAEA in the AMO:HEMA copolymer are shown in figure 5.11. The tensile strength and initial modulus of the materials follow the same behaviour as the structurally similar monomer DMAEMA. This would be expected and can be explained by the fact that DMAEA also possesses the same water binding characteristics as DMAEMA.

For increasing amounts of pyridine-N-oxide in the polymer, the mechanical properties are shown in figure 5.12. Both the tensile strength and initial modulus of the material decrease with increasing amounts of cationic monomer added. Inspection of the water binding properties show the increase in EWC is accompanied by an increase in both free and bound water proportions. The increase in free water is mirrored as previously by a similar decrease in the value of the initial modulus. This increase in free water also causes the value of the tensile strength to decrease, but as this increase is not as large as for the previous monomers, the fall in value of the tensile strength is not as great.

Figure 5.12 The mechanical properties of AMO:HEMA (70:30) copolymers containing increasing amounts of pyridine-N-oxide

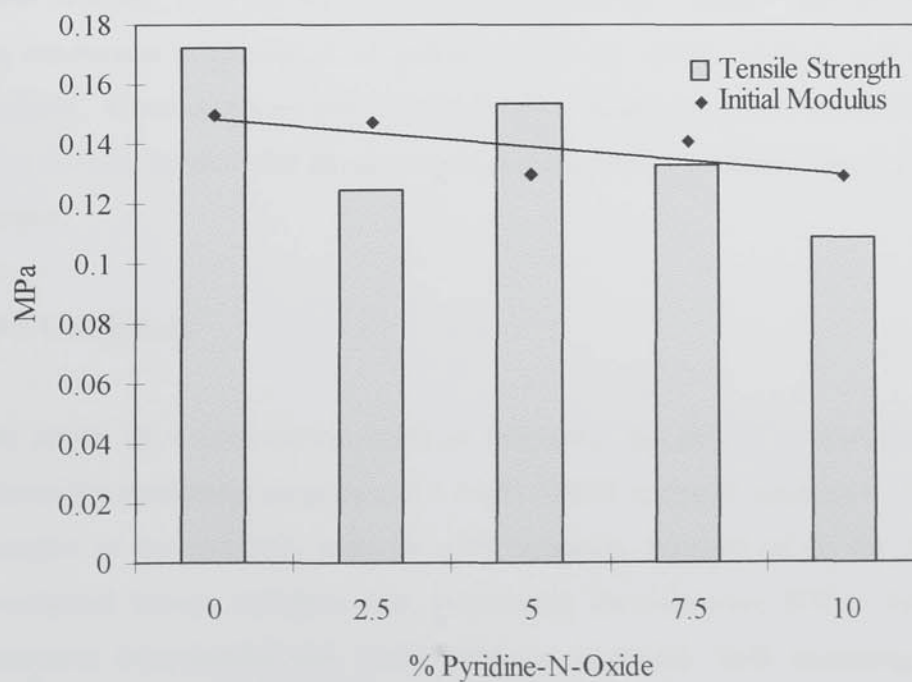
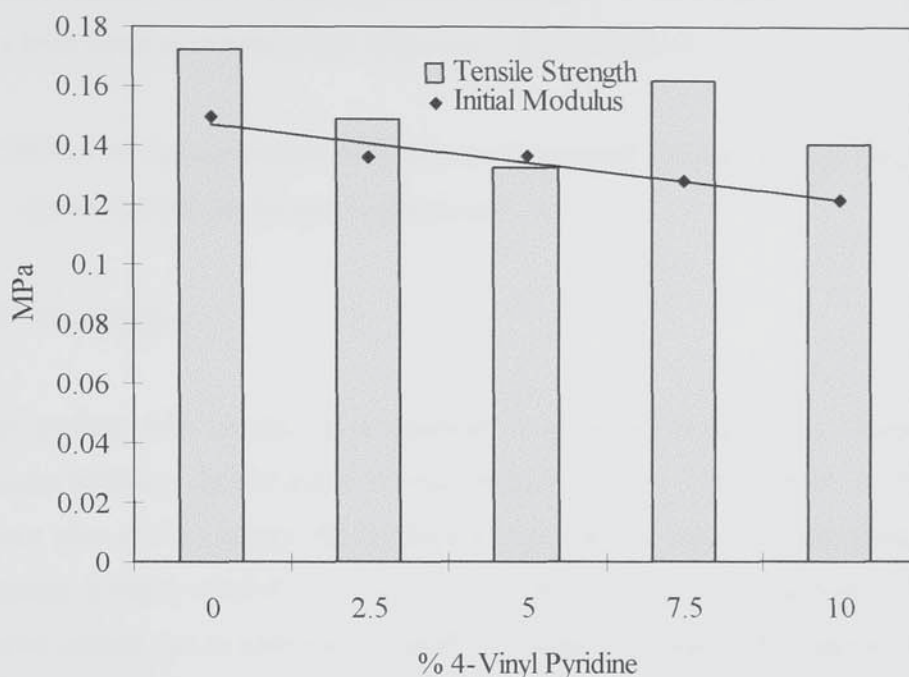


Figure 5.13 The mechanical properties of AMO:HEMA (70:30) copolymers containing increasing amounts of 4-vinyl pyridine



Mechanical properties for increasing proportions of 4-vinyl pyridine are illustrated graphically in figure 5.13. As the amount of monomer increases, the EWC and free water decrease, while the bound water remains relatively stable. The effect of this on the mechanical properties is to decrease both the tensile strength and the initial modulus. These decreases are however small in magnitude which would be expected given the way in which the states of water are affected by increasing charged monomer content.

5.6.3 Conclusions

The results show that incorporation of increasing amounts of a cationic monomer reduces the mechanical properties of a AMO:HEMA hydrogel copolymer. The tensile strengths of the materials decrease with increasing amounts of all the monomers investigated except polymers that incorporate the monomer NVI. For all the monomers investigated, the initial modulus decreases with increasing charged monomer content. The results for the initial modulus show a great degree of consistency along a graphical line of best fit, however the tensile strength results are

slightly more erratic. The elongation at break appears to follow a more unusual pattern. For each monomer, as its degree of incorporation is increased, the elongation at break initially rises to a maximum value between 5-7.5% incorporation before falling to a level equal to or below that of the unmodified copolymer.

5.7 Effect of Incorporation of Cationic Monomers on the Surface Properties of AMO:HEMA Hydrogel Copolymers.

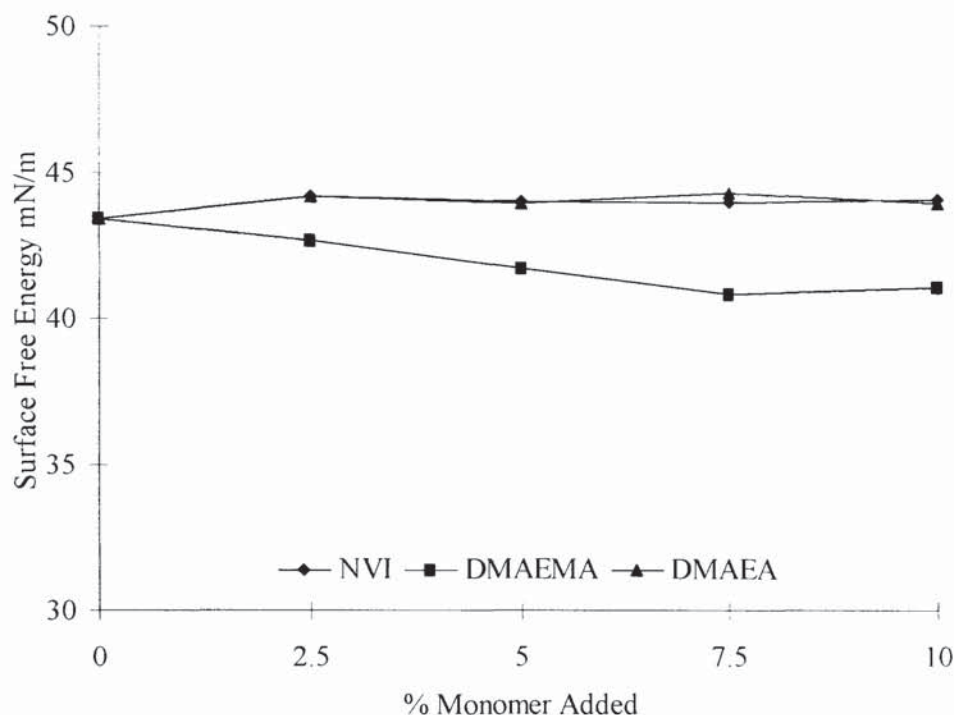
5.7.1 Introduction

The surface free energy of a material is a major property in determining its biocompatibility. As the major application of hydrogels is in the field of biomaterials where they are in contact with biological fluids and tissue, the measurement of this property is highly desirable. Surface energy measurements as described in Chapter 2 can be carried out in both the hydrated and dehydrated state. This allows the values for the total surface free energy and the dispersive and polar components to be determined for the hydrogel materials.

5.7.2 Surface Properties of Dehydrated Hydrogels Containing Cationic Monomers

The measured surface free energies of the dehydrated polymer surface are a function of the interactions that take place both at the surface and in the bulk of the polymer. The orientation of the groups at the polymer surface will be affected by the nature of the adjacent phase and this will affect the value of the surface free energy. The determination of accurate and consistent values for the surface free energy in the dehydrated state is a very difficult process. Rapid hydration in ambient relative humidity and the interaction of this water with the wetting liquid are the major causes of inaccuracies.

Figure 5.14 The surface free energy of dehydrated AMO:HEMA (70:30) copolymers containing increasing amounts of cationic monomers



The effect of incorporating increasing proportions of NVI, DMAEMA and DMAEA on the surface free energy in the dehydrated state is shown in figure 5.14. As the amount of NVI is increased, the total surface free energy increases very slightly. With the incorporation of the charged monomer the polar component of the surface free energy stays at a minimal value. This observation is consistent with the effect of hydrophobic group expression at the air interface and the orientation of the hydrophilic groups towards the polymer bulk. This results in the surface of the polymer being dominated by hydrophobic groups and the value of the surface energy being dominated by the dispersive component. The effect of incorporation of the charged monomer has little effect on the total surface free energy but does raise its value slightly. It should be noted that with increasing NVI content, the EWC only changes slightly and therefore, it is not surprising that the change in total surface energy is small.

For DMAEMA and DMAEA similar trends to those of NVI can also be seen. The surface in the dehydrated state is completely dominated by the dispersive component and the total surface free energy only changes slightly with increasing ionic monomer content.

5.7.3 Surface Properties of Hydrated Hydrogels Containing Cationic Monomers

The determination of surface energies in the dehydrated state provides useful information about the surface of the polymer. However when hydrogel materials are swollen as they are in biomedical applications, the surface energies change dramatically. The determination of contact angles of hydrated hydrogels is a difficult process due to dehydration of the polymer surface during measurement. However the use of inverted droplet methods has eliminated these problems.

The effect of incorporation of increasing amounts of NVI on the polar and dispersive components of the surface free energy of the AMO:HEMA copolymer is shown in figure 5.15. When the results are compared to the dehydrated situation it can be seen that a large polar component has arisen while the dispersive component is greatly reduced. As these materials have high water contents, the values of the two components are similar to those of pure water. With increasing NVI content it can be seen that while the polar component increases slightly, no significant change in the dispersive component is observed. The increase in the polar component is caused by the increased polar character that NVI possesses compared to AMO and HEMA.

Figure 5.16 displays the polar and dispersive components of the surface free energy of the AMO:HEMA copolymer containing increasing amounts of DMAEMA and DMAEA. For the two sets of copolymers containing these structurally similar monomers the values of the polar and dispersive components are almost identical. It may be expected that the acrylate monomer would possess a higher surface free energy than the methacrylate monomer. However the polar character that these basic monomers show is large and masks the effect the α -methyl group has on lowering the rotation about the carbon backbone in the methacrylate monomer. As with NVI the polar character increases while the dispersive component remains unaffected.

Figure 5.15 The components of the surface free energy for AMO:HEMA (70:30) copolymer with increasing amounts of NVI in the hydrated state

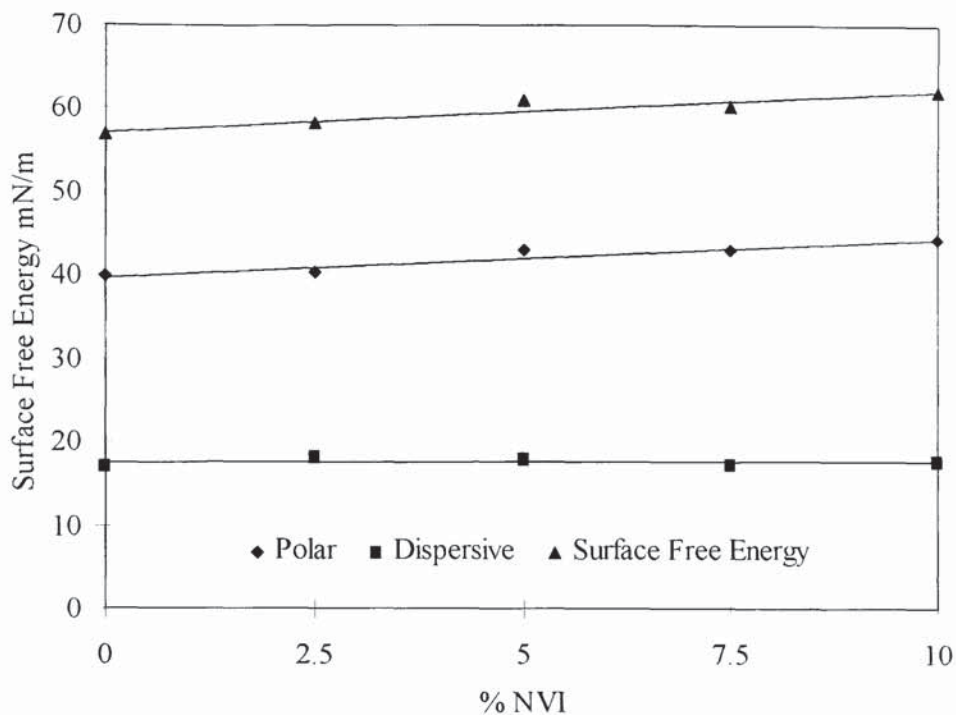
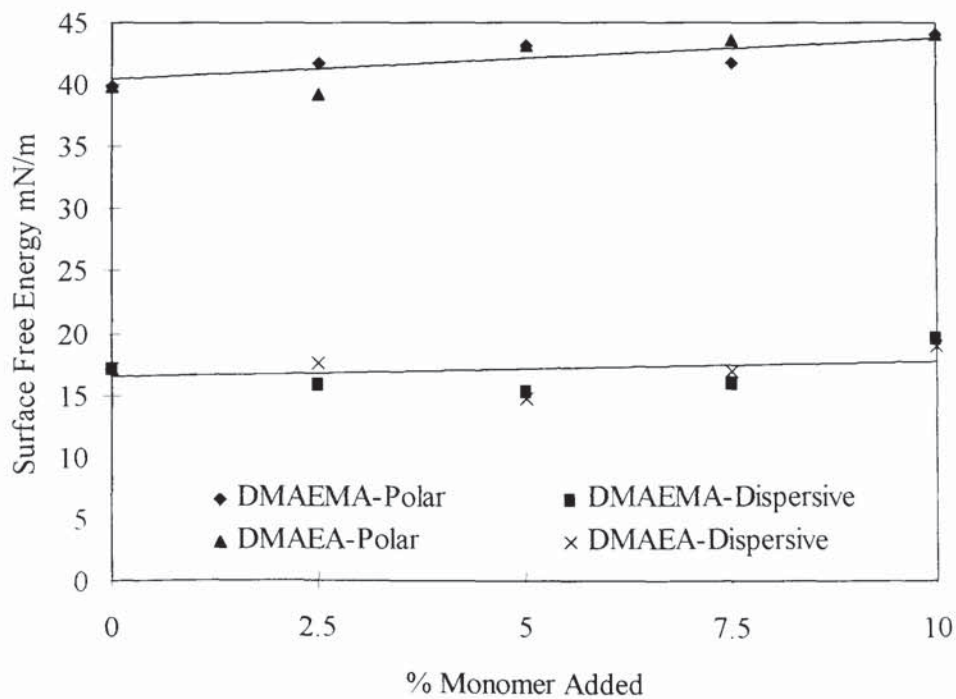


Figure 5.16 The polar and dispersive components of the surface free energy for AMO:HEMA (70:30) copolymer with increasing amounts of DMAEMA and DMAEA in the hydrated state



5.7.4 Advancing and Receding Contact Angles for Hydrogels Containing Cationic Monomers

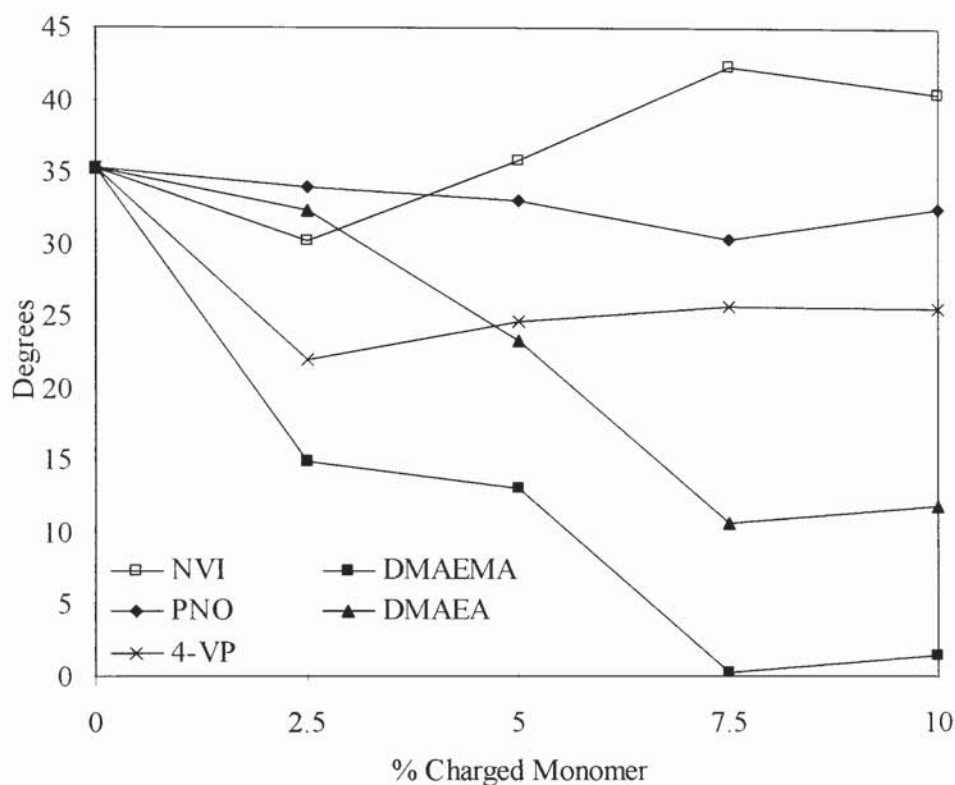
In hydrogels, there are both hydrophilic and hydrophobic groups situated on the polymer's carbon backbone. As this backbone is made up of single carbon to carbon bonds, it has a large degree of rotational mobility about its axis. This enables the polymer to present the groups at the surface which are energetically more favourable to the surrounding environment. Thus, as a hydrogel is removed from water the hydrophilic groups are orientated so that they are buried within the material while the hydrophobic groups are presented at the polymer surface. The interfacial tension is minimised by the formation of van der Waals interactions. The contact angle at the surface in this situation is known as the receding contact angle. When the hydrogel is lowered back into the hydrating medium, the backbone rotates to present the hydrophilic groups at the polymer surface as this is the more thermodynamically favourable position. Hydrogen bonding occurs between these polar hydrophilic groups and the bulk solution, dramatically reducing the interfacial tension. This situation gives rise to the value for the advancing contact angle. The difference in the value of the contact angle in these two situations is known as the contact angle hysteresis.

The contact angle hysteresis gives an indication of the degree of rotational mobility about the carbon backbone. The lower the hysteresis, the less the carbon chain can rotate to reach a thermodynamically favourable situation. If the hysteresis is high the difference between the advancing and receding contact angle is large which indicates that the chains can rotate freely to lower the interfacial tension.

For the five charged monomers that have been incorporated in the HEMA:AMO copolymer, it can be seen in figure 5.17 for increasing charged monomer content the change in the contact angle hysteresis follows a number of different patterns. Pyridine-N-oxide shows little change as its incorporation is increased, which indicates that the polymer chain does not lose any of its rotational mobility. This is as expected when it is noted that both the water content and the initial modulus of the material do not change to any great degree. NVI also shows no specific change in the value of the contact angle hysteresis with a broader variation than that in pyridine-N-oxide.

Although NVI may possess a bulky side group, it does not seem to affect the ease of rotation about the carbon main chain.

Figure 5.17 The hysteresis of AMO:HEMA (70:30) copolymers containing increasing amounts of cationic monomers



Materials containing 4-vinyl pyridine show a reduced contact angle hysteresis as incorporation of the monomer within the copolymer is increased. However the nature of this decrease appears to follow an unusual trend that does not allow any definite conclusions to be drawn. DMAEA and DMAEMA on the other hand do show trends in the values of their hysteresis that can be explained in terms of the monomer structure. As the proportion of DMAEA is increased, the value of the hysteresis decreases. Thus, as the difference between the advancing and receding contact angle is decreasing, the mobility about the polymer backbone is therefore decreasing. When the degree of incorporation of DMAEMA is raised, the contact angle hysteresis falls dramatically and to a larger extent than DMAEA. This is due to the extra methyl group that the methacrylate contains when compared to the acrylate. This extra methyl group increases the energy barrier to rotation about the carbon backbone, which in

turn reduces its mobility and results in a very small difference between the advancing and receding contact angle.

5.7.5 Conclusions

The surface free energy of the dehydrated hydrogels remains relatively unaffected by the incorporation of increasing amounts of charged monomers. In this state the surface energy is totally dominated by the dispersive component with the polar component having a value approximately equal to zero. This is due to hydrophobic group expression at the air interface and the orientation of the hydrophilic groups towards the polymer bulk. This results in the surface of the polymer being dominated by hydrophobic groups and the value of the surface energy being controlled by the dispersive component.

In the hydrated situation, the surface free energy is dominated by a large polar component, with a dispersive component much reduced compared to the dehydrated situation. As the incorporation of basic, potentially cationic monomers is raised, the polar component of the surface free energy increases, while the dispersive component remains unaffected. The magnitude of the polar and dispersive components are approximately the same for the three monomers that were investigated in the AMO:HEMA copolymer.

The contact angle hysteresis is dependent on the ability of the carbon main chain to rotate pendant groups to the most thermodynamically favourable position. This has been shown to be dependent on both the size of the pendant group and the presence of any methyl groups upon the α -carbon atom.

5.8 Summary Conclusions

Incorporation of monomers that carry a positive charge into neutral hydrogel copolymers has significant effects on the physical properties of the resulting material. The most dramatic of these is the considerable increase in the EWC of the particular AMO:HEMA copolymer used in this work. This rise is due to the greater degree of

hydrophilicity that these monomers display, which is a result of the increased polarity that the charge induces.

For the majority of the cationic monomers investigated, the rise in EWC is caused by an increase in both the free and bound water proportions. However the rise in EWC for polymers incorporating NVI is singularly attributed to a rise in the proportion of water that exists in the bound state. Polymers can therefore be produced with lower proportions of plasticising water. This enables the design of copolymers which possess smaller amounts of freezing water in the hope that the increase in water content will not result in a decrease in mechanical properties.

The incorporation of increasing amounts of cationic monomer also reduces the mechanical properties of a AMO:HEMA hydrogel copolymer. The tensile strengths of the materials decrease with increasing amounts of all the monomers investigated except polymers that incorporate the monomer NVI. For all the monomers investigated, the initial modulus decreases with increasing charged monomer content. The results for the initial modulus show a great degree of consistency along a graphical line of best fit, however the tensile strength results are slightly more erratic. The elongation at break appears to follow a more unusual pattern. For each monomer, as its degree of incorporation is increased, the elongation at break initially rises to a maximum value between 5-7.5% incorporation before falling to a level equal to or below that of the unmodified copolymer.

In the dehydrated state the surface free energies of the materials produced in this chapter are totally dominated by the dispersive component and the addition of monomers displaying a high degree of polarity has little effect on the magnitude of this value. In the hydrated state the dispersive component is much reduced while a large polar component has arisen whose value increases with a rise in cationic monomer content. These two situations arise through the rotation that occurs along the carbon backbone whose ease is controlled by the size and nature of the pendent groups.

CHAPTER 6

HIGH EQUILIBRIUM WATER CONTENT ACRYLOYLMORPHOLINE HYDROGELS INCORPORATING BASIC AND ACIDIC MONOMERS

6.1 Introduction

Chapter 5 evaluated the consequence of incorporation of a range of cationic monomers on the physical properties of a copolymer comprised of the hydrophilic monomers 2-hydroxyethyl methacrylate and acryloylmorpholine. As expected the charged monomers influenced water binding, mechanical and surface properties. The advantages of incorporation of cationic monomers at low levels include increased mechanical properties and the potential for improved biocompatibility. The possibility of incorporation of anionic monomers in these materials will now be discussed together with the combination of monomers with opposite charges in the same hydrogel polymer.

The effect on physical properties of increasing quantities of negative charge in a poly(HEMA) hydrogel have already been examined by Ma¹⁰⁹. The charged monomers investigated were methacrylic acid and itaconic acid, which at physiological pH of 7.4 cause the surface of a material to be negatively charged. N-(3-sulfopropyl)-N-methacryloxyethyl-N, N-dimethylammonium betaine (SPE), a sulphobetaine monomer which contains a zwitterion or inner salt in its side chain was also examined.

For poly(HEMA), as methacrylic and itaconic acid content is increased from 0-5%, the equilibrium water content increases from 38% to approximately 70%. For SPE the increase in water content is greatly reduced reaching a maximum value of only 40%. This is unexpected as the monomer contains a strong water binding sulphonate group which has higher ionic strength than the carboxylate group and a quaternary nitrogen whose combined effects should produce an EWC comparable to those of the acids. It is however the steric effects that dominate the total water binding ability of this monomer highlighting the importance of steric as well as polar contributions.

The increase in EWC for both methacrylic acid and itaconic acid is dictated by a rise in both free and bound water proportions. The relative proportions of these two water types remains the same for increasing amounts of both of these monomers. At 5% incorporation, the proportions of bound water was 31% for MAA and 36% for ITA. This indicates that using a monomer with two pendent groups as opposed to one,

increases both the EWC and the proportion of bound water. For SPE, the increase in EWC is mainly due to an increase in the bound water proportion. As monomer content is increased steric factors prevent an overall increase in the total amount of water present, however more of the water present is in the bound state.

As the proportion of MAA and ITA incorporated within the poly(HEMA) increases, the rise in water content is accompanied by a decrease in mechanical properties. The initial modulus, tensile strength and elongation at break values all fall substantially as the water content increases. With increasing amounts of SPE, the tensile strength remains relatively unaffected while the initial modulus decreases only slightly which results in an increase in the value of the elongation at break. As the SPE does not affect the water content greatly, the change in mechanical properties must be due to the charged monomer itself and the way it affects the state of the water by increasing the proportion of bound water.

For hydrogels in the dehydrated state, increasing the amount of ionic charge in poly(HEMA) decreased the polar component of the surface free energy. This was consistent with the effect of hydrophobic group expression at the air interface and the orientation of hydrophilic groups towards the polymer bulk. For increasing amounts of itaconic acid however, the polar component of the surface free energy increases because it possesses two carboxyl groups and produces copolymers with a carboxyl group either side of the polymer backbone. Thus a polar group is always expressed at the air interface which contributes to the polar component of the surface free energy.

When hydrated systems are examined, the polar component of the surface free energy due to the polymer was greater than the polymer's dispersive component. This result is consistent with the theory that the molecular motion of the polymer backbone is such that polar groups within the copolymer are orientated towards the water interface.

As the water content increases, the values for the polar and dispersive components of the surface free energy approach those of water which would be expected as water dominates the polymer. Thus the polar and dispersive contributions to the surface energy of the hydrogel which are due to the polymer itself decrease with increasing water content. The ratio of the polar and dispersive components for the polymer indicate that the polymer becomes increasingly polar with increasing amounts of ITA and MAA. Although ITA contains two polar acid groups, these are situated opposite each other and at any time only one can be expressed at the polymer surface. Thus the ratio of polar to dispersive components is similar for both of these monomers. The addition of SPE also causes an increase in the polar character of the polymers surface.

The type of charge that ionic monomers possess will affect the types of proteins that materials which incorporate these monomers will attract. Obviously, monomers carrying a particular charge will be expected to attract proteins that are of opposite charge. Thus polymers can be designed to attract proteins of a specific charge type. SPE contains a zwitterionic structure possessing both a positive and negative charge. With increasing content the resulting polymers attract more negatively charged proteins while the amount of positively charged proteins adsorbed decreases slightly.

The effects of incorporation of positively charged monomers on protein uptake was investigated by French¹²¹ as was the effect of incorporation of both positively and negatively charged monomers. As the content of the positively charged monomer NVI is increased, the amount of positively charged proteins absorbed on the surface decreases while the amount of negatively charged proteins increases slightly. In poly(HEMA) with 5% MAA and 5% NVI, the amount of positively charged proteins absorbed decreases when compared to pure poly(HEMA) while the concentration of negatively charged proteins adsorbed on the surface increases. However the water binding and mechanical properties of these materials were not investigated and it is felt that these types of materials may show improved physical properties when compared to neutral materials or materials containing only one charge type. The simultaneous incorporation of both positively and negatively charged monomers in hydrogel copolymers was therefore investigated.

6.2 Materials and Methods

As in Chapter 5, all investigations were carried out using a basic copolymer of AMO:HEMA at a ratio of 70:30 unless otherwise stated. Hydrogel membranes are produced as described in Chapter 2 and values were obtained for the water binding, mechanical and surface properties of these materials by the methods described again in Chapter 2. The monomers which have the ability to carry a negative charge that were used in the work were methacrylic acid (MAA), itaconic acid (ITA) and SPI. Methacrylic acid is used widely in the contact lens industry and possesses an acid group in its side chain. Itaconic acid has two pendent groups both of which are comprised of carboxylic acid groups. This will allow investigation of the effects of incorporation of a monomer with two pendant groups both of which have the ability to become charged. Similarly SPI again has two pendent groups present within its structure, however, both of these contain sulphonate groups as opposed to carboxylate groups. Investigations were carried out on the di-potassium salt derivative.

The positively charged monomer used in this section was N-vinyl imidazole (NVI) because of the advantages it showed which were illustrated by the results in the previous chapter. It was materials incorporating this monomer alone that showed both increased water contents and improved mechanical properties when compared to the unmodified copolymer.

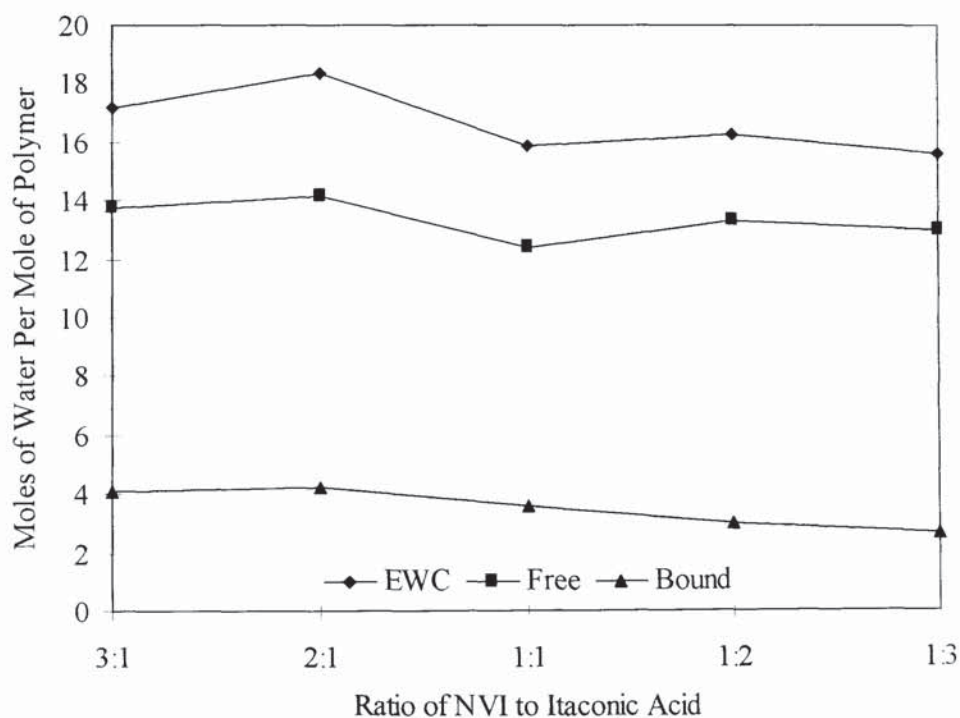
6.3 Water Binding Properties

The water binding properties of the AMO:HEMA (70:30) copolymers containing a pair of monomers of opposite charge are now discussed for each individual pair of monomers.

6.3.1 Effect of Incorporation of NVI and Itaconic Acid on Water Binding Properties in a AMO:HEMA (70:30) Copolymer

Initially different ratios of NVI to ITA were investigated at a total charged monomer content of 5% by weight in the AMO:HEMA copolymer. Figure 6.1 shows the water binding properties for such materials at ratios ranging from 1:1 to 3:1 in favour of either of the charged monomers. As the proportion of NVI is increased, the EWC increases and this is due to an increase in both the free and bound water proportions. When the states of the water are expressed in moles per mole of polymer these trends are also observed. As the proportion of ITA is increased, the total amount of water present remains relatively unaffected. A decrease in the proportion of bound water is seen while a corresponding increase in the proportion of free water is also observed.

Figure 6.1 The water binding properties of AMO:HEMA (70:30) copolymers containing different ratios of NVI and itaconic acid at 5% w w



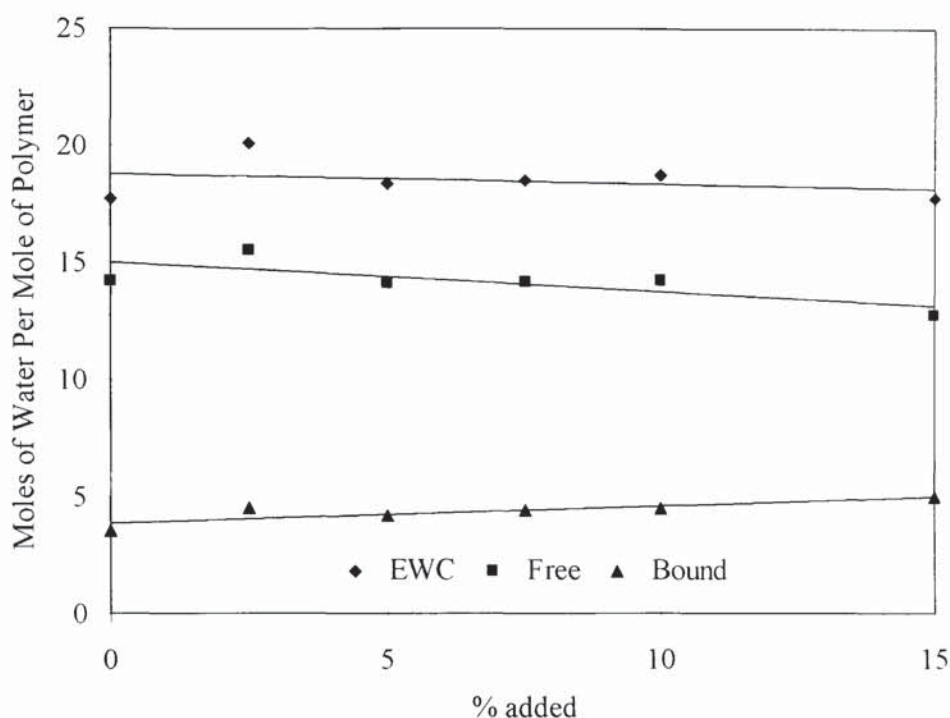
When the original copolymer is compared to the composition containing charged monomers at a ratio of 1:1 a number of differences can be identified. The fraction of water present in the bound state, expressed as moles of bound water per mole of

polymer is the same, however the total water present does decrease. This decrease is accounted for by a decrease in the proportion of water in the free state. This decrease in total water content is unexpected as the total number of hydrophilic sites is expected to have increased. It could therefore be concluded that these hydrophilic sites are interacting with each other which should result in an increase in mechanical properties.

As the ratio of charged monomers is increased in favour of either of these monomers there is a rise in the total water present which would be expected as one charge type becomes more dominant than the other. As the NVI is increased the free and bound water proportions both increase due to the presence of the increasing cationic charge. The charge causes more water to be bound to the polymer chain and also, as there is no increase in steric hindrance the free water proportion increases. As the amount of itaconic acid is increased, the total water content remains relatively unaffected while the proportion of water in the bound state decreases. Accompanying an increase in the monomer with two pendent chains, is an increase in the steric hindrance around the polymer chain. The space for water molecules to be held tightly is reduced but the increase in charge present still attracts water molecules to the polymer chain.

If we examine one particular ratio of NVI to itaconic acid, we can investigate the effect of different incorporation levels on the physical properties of the resulting materials. The effect of incorporation of NVI:Itaconic acid at a 1:2 ratio was examined up to a level of 15%. The water binding properties are illustrated graphically in figure 6.2. As the proportion of charged monomers is increased, the total water content remains relatively unaffected but the proportion of free water is seen to fall. The bound water increases at a similar rate to the fall in free water, and this indicates an increase in the number of sites available for strong interaction with water molecules. As more molecules are held tightly to the polar sites of the polymer, less room is available for water to exist in a free state around the chains and so the total water content remains the same. As the content rises to 15%, the total water content falls very slightly and this is probably due to a small increase in steric hindrance caused by the itaconic acid.

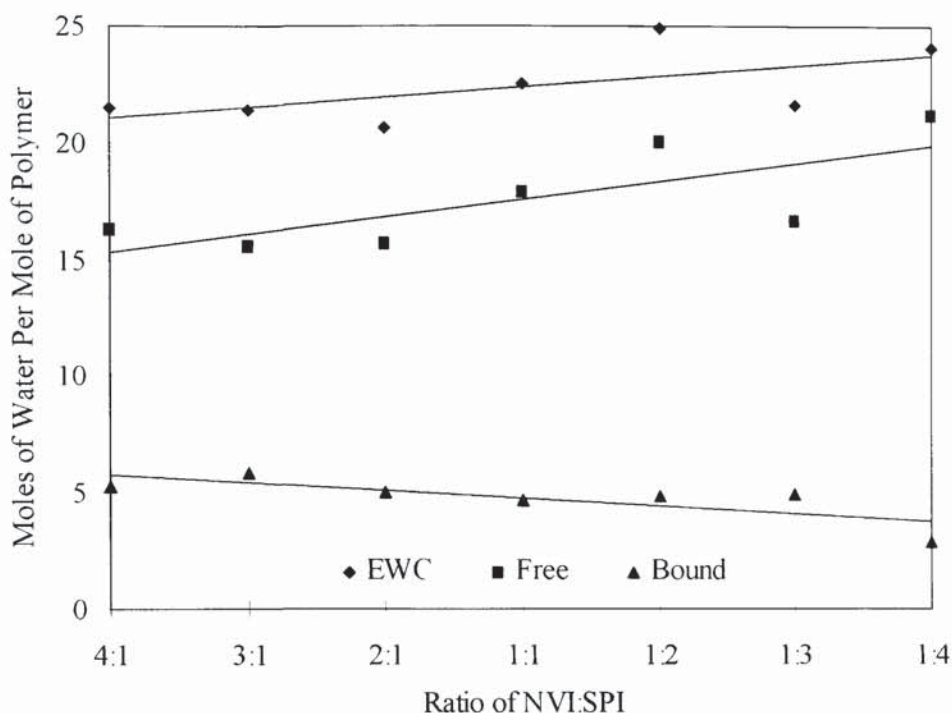
Figure 6.2 The water binding properties of AMO:HEMA (70:30) copolymers containing NVI and itaconic acid in a ratio of 1:2 at various incorporation levels



6.3.2 Effect of Incorporation of NVI and SPI on Water Binding Properties in a AMO:HEMA (70:30) Copolymer

NVI and SPI were incorporated at various ratios at a total content of 5% by weight in AMO:HEMA (70:30) copolymers. The charged monomers were incorporated between ranges of 4:1 in favour of both the monomers as shown in figure 6.3. Comparison of the copolymer containing a 1:1 ratio of the charged monomers with the original copolymer shows large differences in physical properties. The total water content has increased dramatically with the majority of this being accounted for by an increase in the free water proportion. SPI is a large molecule, which results in steric hindrance that prevents water molecules interacting closely with the polymer chain. However the large size of the molecule does allow a large proportion of water to associate around the polymer chains in the free state.

Figure 6.3 The water binding properties of AMO:HEMA (70:30) copolymers containing different ratios of NVI and SPI at 5% w w



As the ratio of NVI:SPI is increased to 4:1, the total amount of water present in the material per mole of polymer decreases. This is caused by a large fall in the free water proportion and a small rise in the proportion of water in the bound state. As the NVI increases, less steric hindrance is present around the polymer chain which allows more water molecules to associate strongly with it. Increasing NVI also results in more polar sites as the molecular weight of NVI is so much less than SPI. However as NVI is much smaller than SPI there is less polymer available for water to associate freely with.

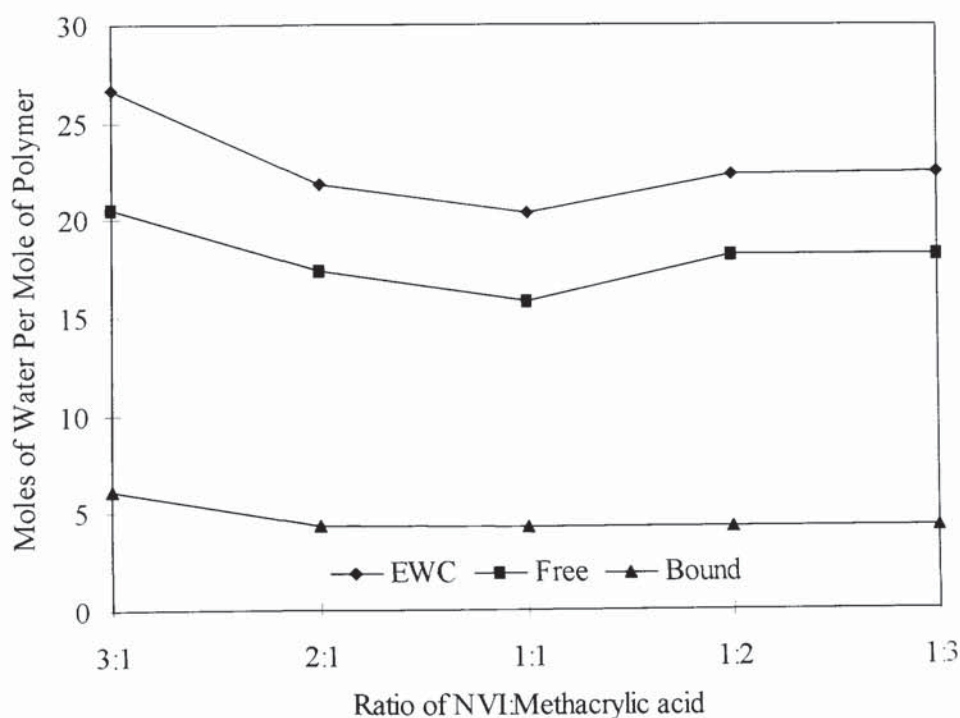
As the proportion of SPI increases, the total amount of water present in the copolymer increases. A rise in the free water content is accompanied by a fall in the proportion of water in the bound state. As the SPI content increases, the number of polar hydrophilic sites on the polymer decreases and the amount of water that can therefore strongly associate with the polymer decreases. As more of the bulky SPI monomer is added to the system, less water molecules can exist close to the polymer and so more water exists in the free state. This increase in free water is larger than the fall in bound

water and so the overall amount of water in the polymer increases with increasing amounts of SPI.

6.3.3 Effect of Incorporation of NVI and Methacrylic acid on Water Binding Properties in a AMO:HEMA (70:30) Copolymer.

NVI and methacrylic acid were incorporated in the AMO:HEMA copolymer at a range of ratios between 3:1 in favour of either of the monomers. The water binding properties of these copolymers, expressed as moles of water type per mole of polymer are illustrated in figure 6.4. At the composition with a ratio of 1:1, the total water present in the system is higher than in the unmodified copolymer. The majority of this increase is due to a rise in the free water proportion although there is a slight rise in the proportion of bound water in the system as well.

Figure 6.4 The water binding properties of AMO:HEMA (70:30) copolymers containing different ratios of NVI and methacrylic acid at 5% w/w



In comparison to the corresponding composition containing itaconic acid, the amount of bound water is similar while the methacrylic acid system contains far more free water which results in a larger total water content. The number of polar acid groups in

the two systems is similar and this accounts for the similar bound water content. However, as the itaconic acid contains two acid groups and is approximately double the molecular weight of methacrylic acid, the increase in steric hindrance with this monomer is large and so the amount of free water is greatly reduced.

As the amount of methacrylic acid is increased to give with NVI a ratio of 3:1, the total amount of water in the system increases. The amount of bound water in the system stays relatively unaffected indicating that the polar nature of methacrylic acid is not sufficiently large enough to increase the ability of the polymer to interact strongly with water. However the amount of free water increases and the result is an increase in the total water content. This is probably due to the increase in charge which occurs in the system as the proportion of one monomer is increased. At an equal ratio the opposite charges may interact with each other which results in less water molecules being able to interact weakly with the polymer.

As the proportion of NVI is increased, an increase in both the free and bound water proportions is observed. As the proportion of NVI is raised, more charged groups exist on the polymer which increases the amount of water molecules that are able to interact with the main chain.

6.3.4 Conclusion

With the incorporation of equal proportions of two monomers of opposite charge, the amount of water in the AMO:HEMA copolymer generally increases. This would be expected given the increase in hydrophilic sites. However, this increase in EWC is mainly caused by a rise in the proportion of water existing in the free state. As the presence of charged groups would be expected to increase the proportion of bound water, it may be concluded that weak ionic bonds are being formed between monomers of opposite charge. When the ratio of monomers is increased in favour of a particular charge type, the total water content of the polymer increases. This unsurprisingly indicates that the presence of an excess amount of one charge type increases the hydrophilicity of the material. The magnitude of the increase is dependent on polar and steric effects which vary for each particular monomer.

As the incorporation of monomers of opposite charge, at a specific ratio, is increased the total amount of water in the AMO:HEMA copolymer is relatively unaffected. However there is an increase in the amount of bound water and a decrease in the amount of water existing in a free state. As the ratio was 2:1 in favour of one of the charged monomers, the increase in the bound water is expected with increasing charge content as these highly polar sites will bind to the water molecules strongly.

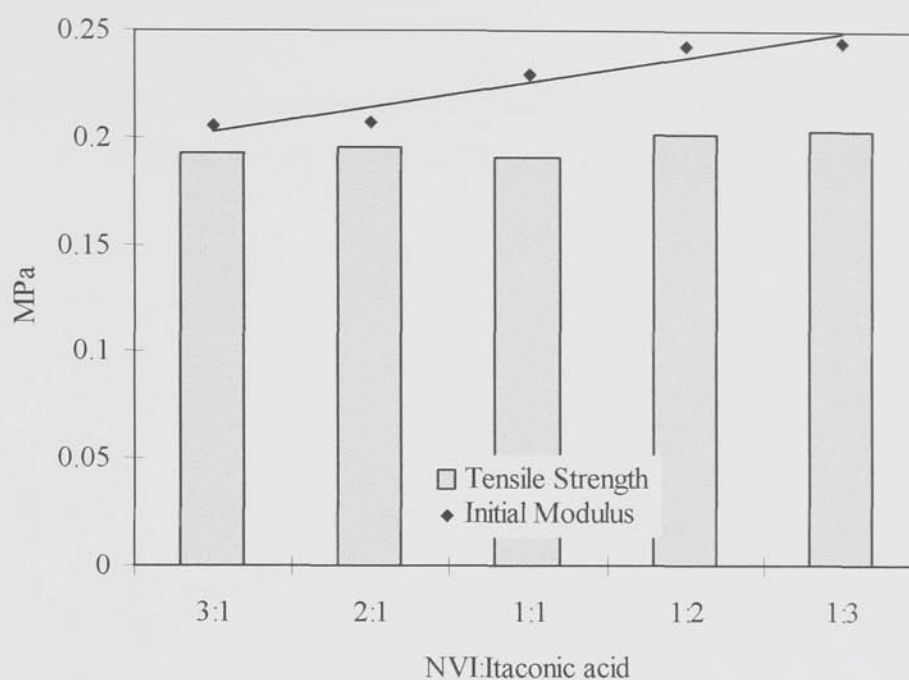
6.4 Mechanical Properties

The mechanical properties of the AMO:HEMA (70:30) copolymers containing a pair of monomers of opposite charge are now discussed for each individual pair of monomers.

6.4.1 Effect of Incorporation of NVI and Itaconic Acid on Mechanical Properties in a AMO:HEMA (70:30) Copolymer.

Different ratios of NVI to Itaconic acid were incorporated at a total concentration of 5% by weight and the effect of this on the mechanical properties of the hydrogel copolymer was investigated. The ratios evaluated covered a range between a value of 3:1 in favour of each of the charged monomers and are illustrated graphically in figure 6.5. Large differences are observed in mechanical properties when the composition containing the monomers at a 1:1 ratio is compared to the original unmodified copolymer. The initial modulus of the AMO:HEMA (70:30) was 0.15MPa while for the composition with a 1:1 ratio of charged monomers, its value was 0.23MPa. The total water content of this material has decreased and given that the number of polar sites has increased with the incorporation of these monomers, it could be concluded that inter-chain attraction occurs and this has increased the stiffness of the material. The tensile strength remained relatively unaffected which would indicate that the integrity of the hydrogel network has not increased.

Figure 6.5 The mechanical properties of AMO:HEMA (70:30) copolymers containing different ratios of NVI and itaconic acid at 5% w/w

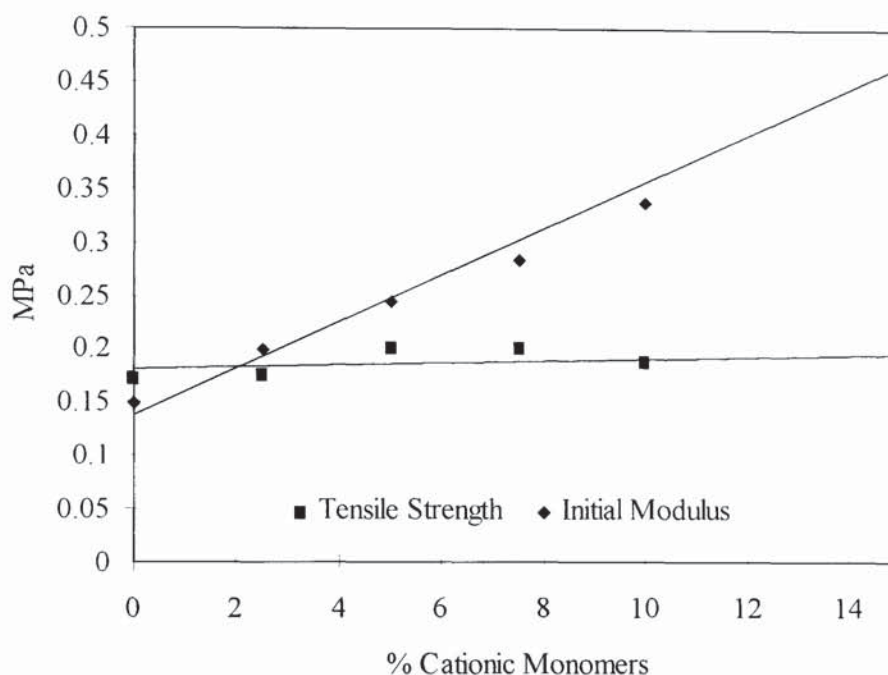


As the compositions change from 3:1 in favour of NVI to 3:1 in favour of itaconic acid, the initial modulus varies inversely with the free water proportion. This would be expected as it is the amount of free water that controls the degree of stiffness of the material. The free water acts as an internal plasticiser within the polymer system and the more of this there is, the greater the flexibility. The tensile strength does not change significantly over this composition range but does appear to be slightly higher as the proportion of itaconic acid is increased. This also corresponds to the compositions where the total water content of the system is lowest.

The mechanical properties of the AMO:HEMA (70:30) copolymer containing up to 15% by weight of NVI:itaconic acid at a ratio of (1:2) were also investigated. As the incorporation of the charged monomers is increased, the initial modulus increases dramatically as shown in figure 6.6. Accompanying this change is a slight increase in the bound water proportion in the polymer. It is surprising that this increase in the bound water proportion is not greater as the amount of polar sites on the polymer has been increased greatly. It must therefore be concluded that the sites of opposite charge are interacting with each other and this causes the observed increase in the stiffness of

the material. This argument appears to be supported by the fact that the total water content is not affected by this composition change when it would be expected to increase.

Figure 6.6 The mechanical properties of AMO:HEMA (70:30) copolymer containing NVI and itaconic acid in a ratio of 1:2 at various incorporation levels



As the incorporation of NVI:itaconic acid (ratio 1:2) in the AMO:HEMA copolymer is increased, the tensile strength remains relatively unaffected. The total water content also remains unaffected by this composition change and it could therefore be concluded that the tensile strength is closely related to the total water present in the system.

6.4.2 Effect of Incorporation of NVI and SPI on Mechanical Properties in a AMO:HEMA (70:30) Copolymer.

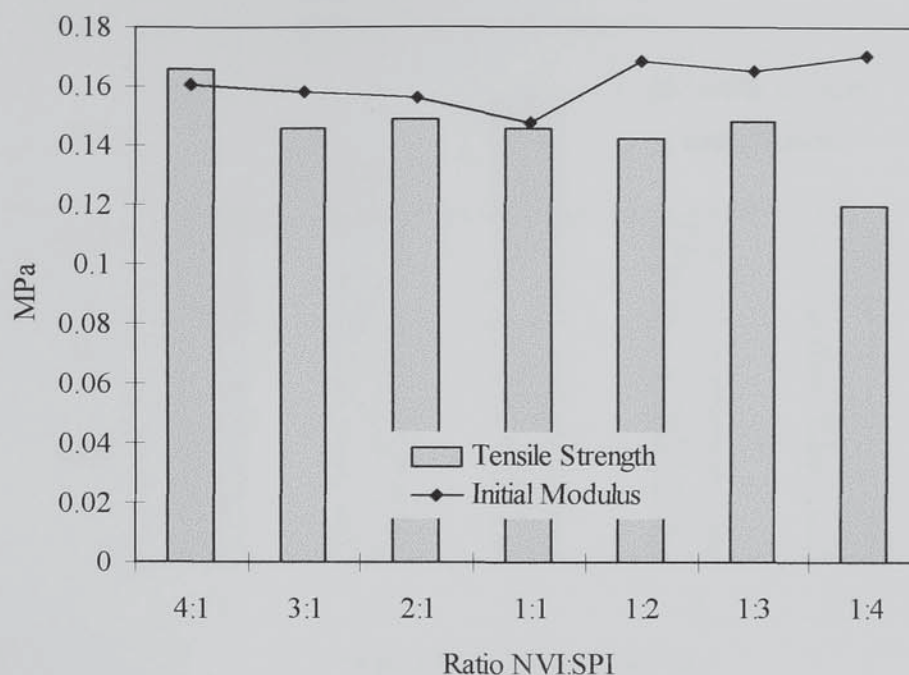
NVI and SPI were incorporated at a ratio of 1:1 in the AMO:HEMA (70:30) copolymer at a total level of 5% by weight. When this composition is compared to the unmodified copolymer, the initial modulus is the same while the tensile strength is greatly reduced. The total water content is greater than in the unmodified copolymer and this results in the decrease in tensile strength that is observed. The bound water

fraction increases but surprisingly no change in the stiffness of the material is observed. As SPI has a far larger molecular weight than NVI, the number of polar sites of each charge type on the copolymer will be unbalanced. The greater number of positive charges that occurs due to the larger number of NVI units results in an increase in the proportion of water in the bound state. However some interaction between charges of opposite type does occur and even though the water content of the polymer increases dramatically, this interaction stiffens the polymer to a level comparable to that of the unmodified copolymer.

The mechanical properties were also investigated when the ratio of NVI:SPI is increased to 4:1 in favour of both monomers, while keeping the level of incorporation at a total of 5% by weight with the results displayed graphically in figure 6.7. As the proportion of NVI is increased, the tensile strength of the material is relatively unaffected. There is however a slight increase in initial modulus which is accompanied by a fall in the total water present in the polymer, attributable mainly to the free water proportion. As the free water proportion is inversely related to the materials stiffness, the initial modulus is seen to increase.

As the proportion of SPI is raised to a level of SPI:NVI at 4:1, a fall in the tensile strength is observed which is accompanied by a rise in the initial modulus. At this composition, a rise in the total water content of the polymer is seen and so a fall in the tensile strength would be expected. However the increase in the initial modulus of the material cannot be attributed to a fall in the free water proportion. It is more likely that this increase is due to the increased incorporation of the SPI monomer. This monomer is extremely large and so its energy barrier to rotation is far higher than any of the other monomers and it is this that results in the polymers increased stiffness.

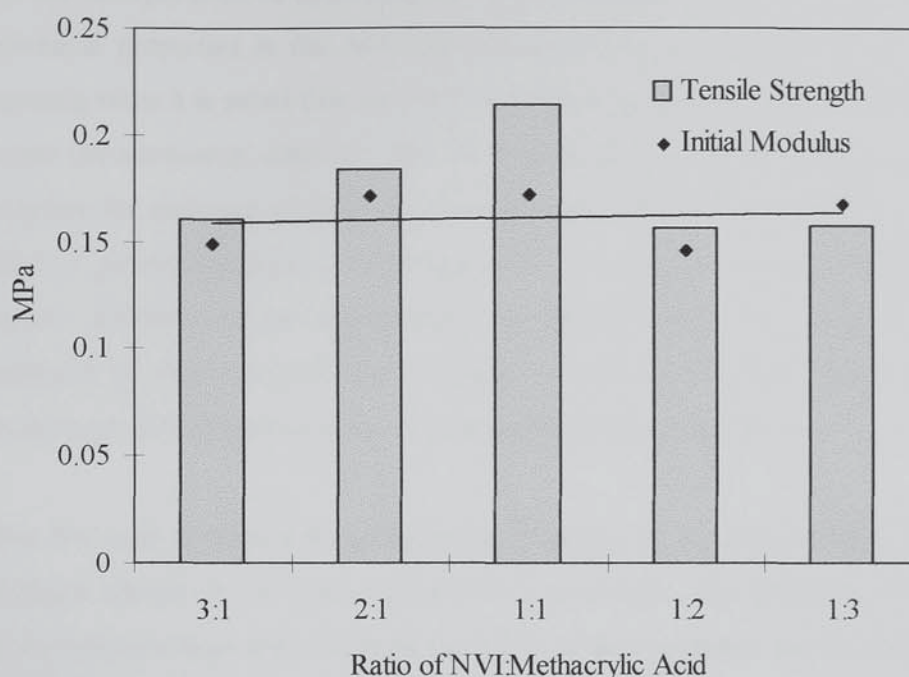
Figure 6.7 The mechanical properties of AMO:HEMA (70:30) copolymers containing different ratios of NVI and SPI at 5% w/w



6.4.3 Effect of Incorporation of NVI and Methacrylic Acid on Mechanical Properties in a AMO:HEMA (70:30) Copolymer.

NVI and methacrylic acid were incorporated in the AMO:HEMA copolymer at a range of ratios between 3:1 in favour of either of the monomers. The mechanical properties of these copolymers are displayed graphically in figure 6.8. In the copolymer containing the monomers at a 1:1 ratio, both the tensile strength and the initial modulus are seen to have increased when compared to the unmodified copolymer. Also a rise in both the total water content and the proportion of this water in the free state are also observed. As the changes in mechanical properties cannot be attributed to the state and amount of water content, some interaction must be occurring between opposite charges on neighbouring polymer chains. This has the effect of increasing both the strength and stiffness of the resulting copolymer.

Figure 6.8 The mechanical properties of AMO:HEMA (70:30) copolymers containing different ratios of NVI and methacrylic acid at 5% w/w



As the ratio of NVI:methacrylic acid is increased to 3:1, the tensile strength and initial modulus both remain relatively unaffected. At the same time a large increase in the total water content and free and bound water proportions are observed. As the amount of NVI is raised an increase in the number of polar sites on the polymer is observed, and as there is not enough methacrylic acid to interact with these sites they cause more water molecules to associate with the polymer. However there remains still some interaction between sites of opposite charge and so although water content is greatly increased, the mechanical properties are similar to those of the unmodified copolymer that possesses a greatly reduced water content.

As the amount of methacrylic acid is increased to a ratio of 3:1 with NVI, the tensile strength and initial modulus are again relatively unaffected. As again the charges are unbalanced an increase in the free and therefore the total water contents are observed although these are not as great as the increased NVI situation. This results in no change in mechanical properties as there is again some interaction of opposite charges, and so the mechanical properties are still greater than the unmodified AMO:HEMA copolymer.

6.4.4 Conclusion

With the incorporation of equal proportions of two monomers of opposite charge, the mechanical properties in the AMO:HEMA copolymer generally increases. This is surprising when it is noted that the EWC of these copolymers also generally increases. Despite the increase in value for both the properties however, the relative mechanical properties for each pair of charged monomers are still inversely related to the EWC. This is a general property for hydrogels that is unavoidable in such homogeneous systems. However as the mechanical properties have either increased or remained unaffected by the increased water content, it may be concluded that weak ionic interactions have formed between the monomers of opposite charge.

When the ratio of monomers is increased in favour of a particular charge type, no significant change in mechanical properties is observed. The presence of an excess amount of one charge type increases the EWC of the copolymer and the magnitude of this increase is dependent on the water binding ability of each particular monomer. This increase in EWC maybe accompanied by a small decrease in mechanical properties, the size of which is dependent on the magnitude of the change in EWC.

As the incorporation of monomers of opposite charge, at a specific ratio, is increased the total amount of water in the AMO:HEMA copolymer is relatively unaffected. However, there is a dramatic increase in the initial modulus of the resulting copolymer, although the tensile strength again remains unaffected. The modulus of the material is a measure of its stiffness and as this increases, it can be concluded that ionic bonds are formed between monomers carrying opposite charge. Since the tensile strength does not increase, the charged monomers may cause the premature termination of polymer chains which results in an imperfect network of reduced tensile strength.

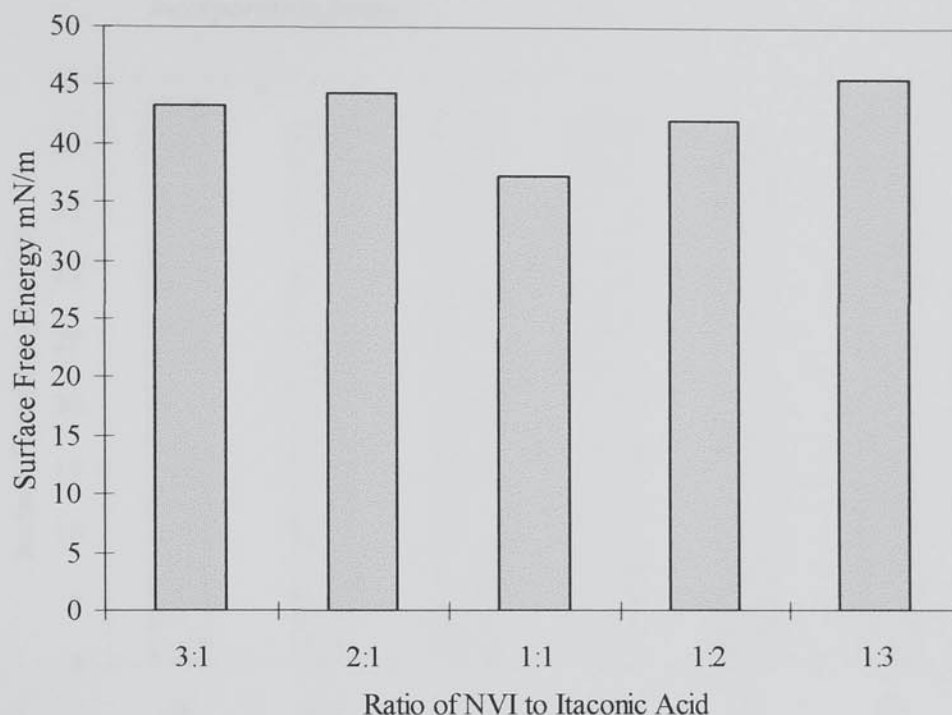
6.5 Surface Properties

The surface properties of the AMO:HEMA (70:30) copolymers containing a pair of monomers of opposite charge are now examined. A number of surface properties were investigated for copolymers containing both NVI and ITA at a range of different ratios. Also the concentration of NVI and ITA at one particular ratio was varied over a wide range up to 15% incorporation. The surface energies and the size of the polar and dispersive components of surface free energy were determined in both the hydrated and dehydrated states and all methods used in this section are detailed in chapter 2.

6.5.1 Surface Properties in AMO:HEMA (70:30) Copolymers Containing NVI and Itaconic Acid in the Dehydrated State.

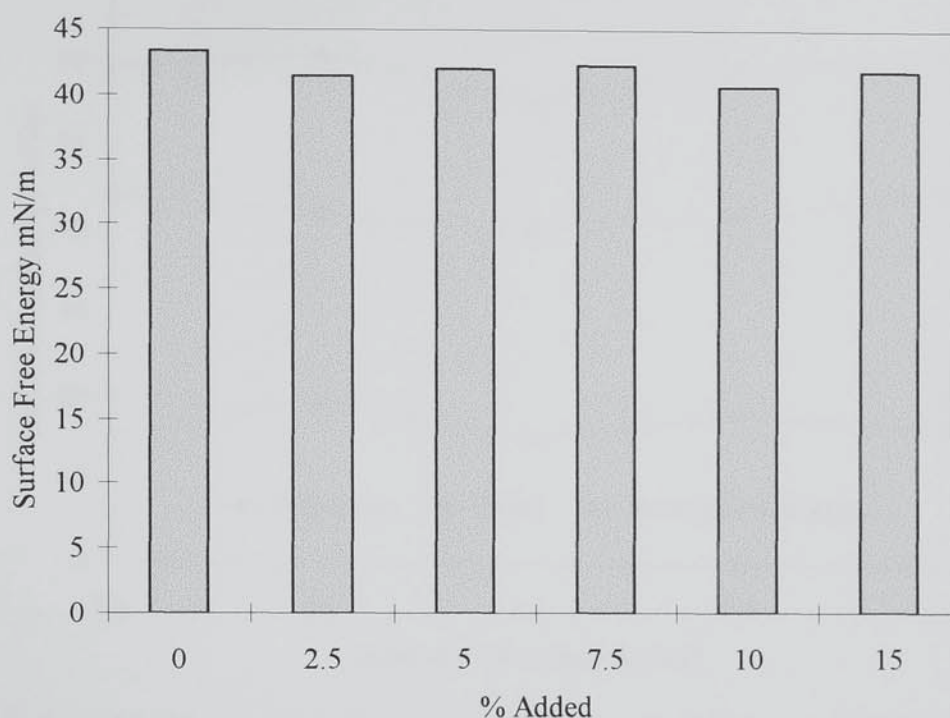
NVI and ITA were incorporated at a number of ratios to each other at a total concentration of 5% by weight. When these two monomers of opposite charge are incorporated at an equal ratio in the AMO:HEMA copolymer, the value of the total surface free energy is very low as shown in figure 6.9. This is since the monomers of opposite charge cancel each other out. When the ratio of incorporation is increased in favour of either of the charged monomers, an increase in the surface free energy of the copolymer is observed. This would be expected given the presence of an excess amount of each charge type as the ratios are adjusted. With reference to appendix V it can be seen that the surface free energy in the dehydrated state is totally dominated by the dispersive component. This is a consequence of the rotation that occurs along the carbon main chain to expose the hydrophobic groups at the interface between the polymer and air. This orientation results in the hydrophilic groups burying themselves within the bulk of the polymer which is the most thermodynamically favourable position.

Figure 6.9 The total surface free energy of dehydrated AMO:HEMA (70:30) copolymers containing different ratios of NVI and itaconic acid at 5%w/w



NVI and itaconic acid at a ratio of 1:2 were incorporated at a range of concentrations up to 15% in the AMO:HEMA (70:30) copolymer. The surface energies in the dehydrated state were again obtained and the results are displayed graphically in figure 6.10. As the incorporation level is increased, the total surface free energy remains relatively unaffected. The total surface free energy is again totally dominated by the dispersive component. However with reference to appendix V, when the incorporation level reaches 15% by weight, a polar component of the total surface free energy does arise. This could be a result of the excess amount of negative charge that will be present in this particular ratio of monomers.

Figure 6.10 The total surface free energy of dehydrated AMO:HEMA (70:30) copolymers containing NVI and itaconic acid in a ratio of 1:2 at various incorporation levels



6.5.2 Surface Properties of AMO:HEMA (70:30) Copolymers Containing NVI and Itaconic Acid in the Hydrated State.

The surface energies of the copolymers were determined in the hydrated state by measurement of contact angles. Figure 6.11 shows the total surface free energy and the polar and dispersive components for the AMO:HEMA copolymer containing different ratios of NVI and itaconic acid. As the ratios are increased in favour of either of the charged monomers the polar component of the surface free energy increases. This is a consequence of the presence of excess polar hydrophilic groups that are not interacting with groups of opposite charge. These groups are therefore presented at the surface of the copolymer and increase the polar character present at the water polymer interface. The dispersive component remains relatively unaffected within experimental error and so the increase in total surface free energy is attributed to the increase in the polar component.

Figure 6.11 The surface properties of hydrated AMO:HEMA (70:30) copolymers containing different ratios of NVI and itaconic acid at 5%w/w

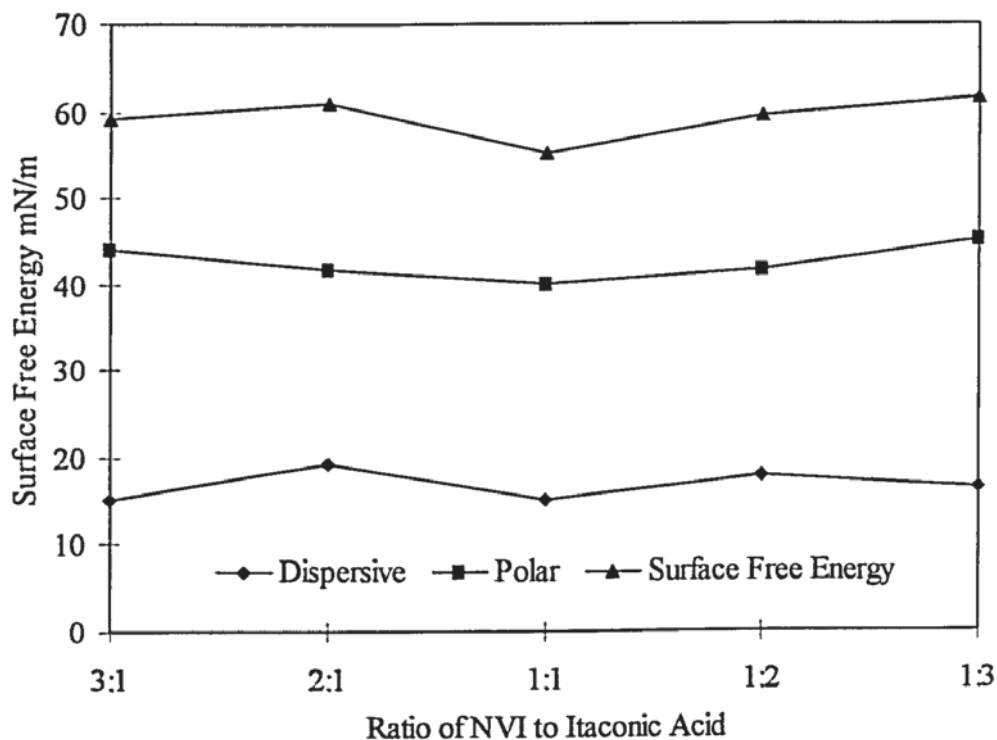
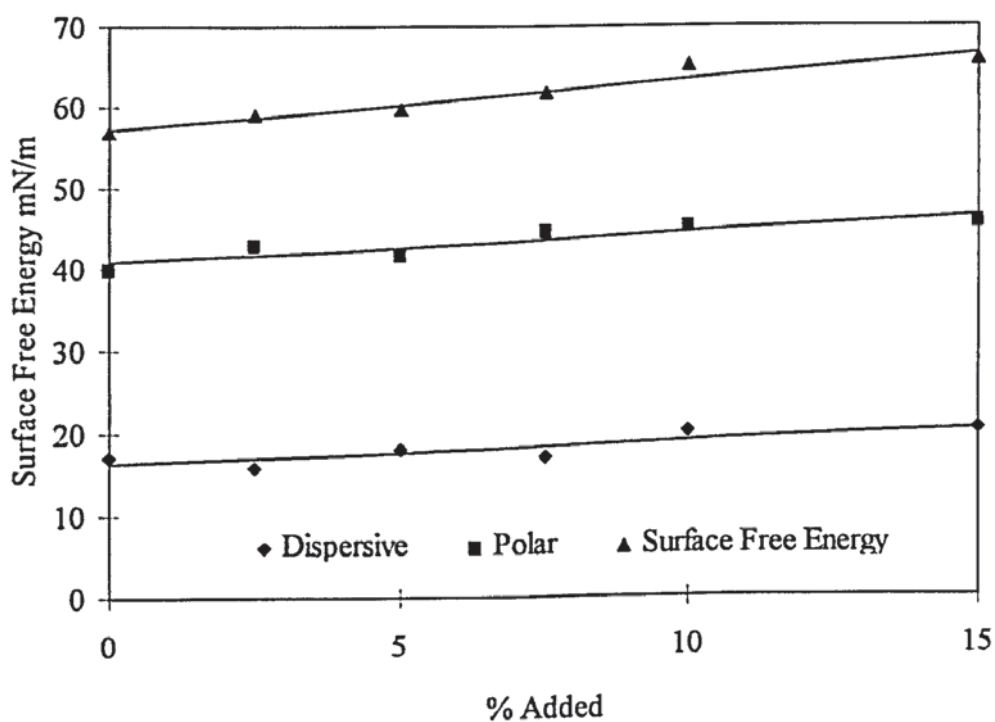


Figure 6.12 The surface properties of hydrated AMO:HEMA (70:30) copolymers containing NVI and itaconic acid in a ratio of 1:2 at various incorporation levels



The consequence of increasing the incorporation level of a particular ratio of NVI to itaconic acid on the surface free energy of the AMO:HEMA copolymer is illustrated graphically in figure 6.12. As the amount of charged monomers increases, a rise in the polar component of the surface free energy is observed. As this ratio contained an excess amount of one charge type, it is further evidence that the polar groups of this charge type are free to express themselves at the surface of the copolymer as they are not interacting with groups of opposite charge. As the incorporation level is increased, more charged groups are present at the surface of the polymer and the polar component of the surface free energy increases. The dispersive component again remains relatively unaffected so the increase in total surface free energy is due to the increase in the polar nature of the surface.

6.5.3 Conclusion

When NVI and ITA were incorporated at a number of ratios to each other in the AMO:HEMA copolymer, the value of the total surface free energy in the dehydrated state is totally dominated by the dispersive component. This is a consequence of the rotation that occurs along the carbon main chain to expose the hydrophobic groups at the interface between the polymer and air. This orientation results in the hydrophilic groups burying themselves within the bulk of the polymer which is the most thermodynamically favourable position. As the degree of incorporation at a particular ratio is raised to up to 15% in the AMO:HEMA (70:30) copolymer, the surface energies in the dehydrated state remains relatively unaffected. The total surface free energy is again totally dominated by the dispersive component. However as the incorporation level reaches 15% by weight, a polar component of the total surface free energy does arise. This is a result of the excess amount of negative charge that is present at this particular ratio of monomers.

When the surface energies of these copolymers are measured in the hydrated state, the surfaces show very different characteristics to those of the dehydrated situation. A large polar component of surface free energy has arisen and the value of the dispersive component is greatly reduced. When NVI and itaconic acid are incorporated into the AMO:HEMA (70:30) copolymer at an equal ratio, the surface characteristics do not

change significantly. However as the ratio of NVI to itaconic acid is increased in favour of either of these monomers, the polar component increases slightly while the dispersive component remains relatively unaffected. The polar groups of opposite charge appear to interact with each other to a certain degree. However as one charge type is present at an excess, it has no groups of opposite charge to interact with and as these groups present themselves at the surface during the hydrated situation the polar nature at the surface is seen to increase. When NVI and itaconic acid are incorporated up to 15% by weight at a ratio of 1:2, an increase in the polar component is again observed while the dispersive component is again unaffected. As this ratio contains an excess of one charge type the increase in the polar component is further evidence that the polar groups have a high degree of mobility and are free to express themselves at the surface.

6.6 Summary Conclusion

A pair of monomers carrying opposite charges were incorporated at different ratios and at different concentration levels in an AMO:HEMA (70:30) copolymer. With incorporation of equal proportions of two monomers of opposing charge, the amount of water in the copolymer increases. The increase is due to a rise in the free water content which is surprising as the presence of charged groups would be expected to increase the bound water proportion. It could therefore be concluded that weak bonds are being formed between the monomers carrying opposite charges. This view is further supported by the increase in mechanical properties that occurs despite the increasing water content. In the dehydrated state the total surface free energy of the copolymer is slightly reduced with the incorporation of equal amounts of a pair of oppositely charged monomers. However this surface is totally dominated by the hydrophobic groups giving rise to a large dispersive component of surface free energy. In the hydrated state, the value of the dispersive component is greatly reduced and the surface free energy is largely dominated by the polar component. The addition of equal ratios of monomers of opposite charge has very little effect on the magnitude of both the dispersive and polar components of the surface free energy. The inclusion of these charge carrying monomers would be expected to increase the polar component

of the surface free energy. However as this is not observed the results can be interpreted as further evidence for the interaction of monomers of opposite charge

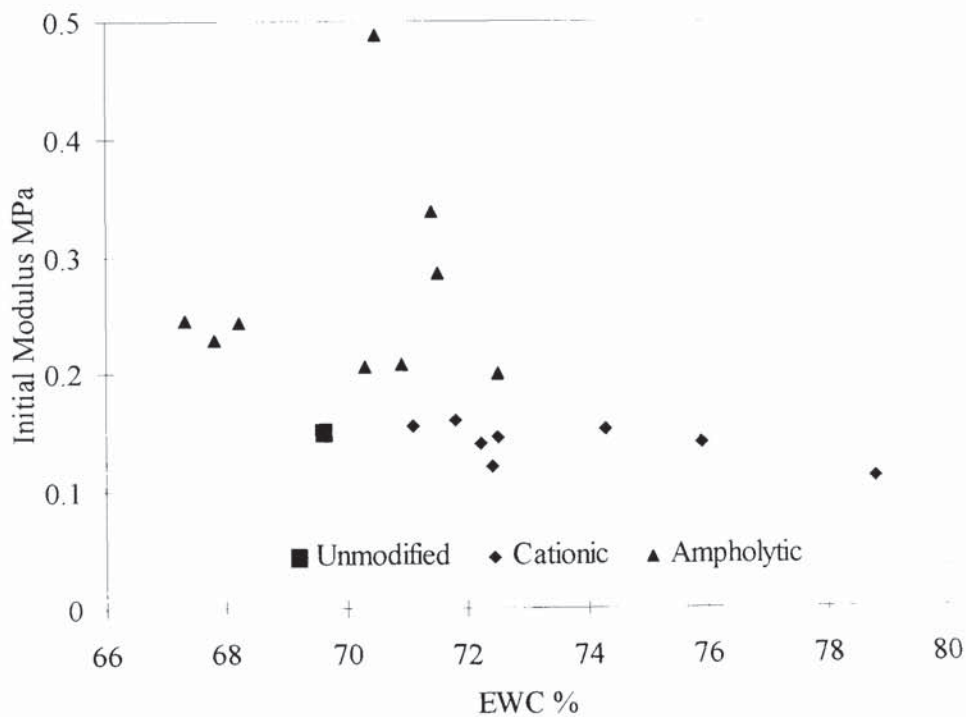
When the proportion of one particular charge type is increased to a level higher than that of the opposite charge, an increase in the total water content of the copolymer is observed. This unsurprisingly indicates that the presence of an excess amount of one charge type raises the hydrophilicity of the resulting material. The magnitude of the increase is dependent on the polar and steric effects of each particular monomer. With the rise in water content there is no significant change in the mechanical properties of the copolymer. In the hydrated state as the proportion of one charge type is increased to an excess, the polar component of the surface free energy increases while the dispersive component is relatively unaffected. The polar groups of the monomer of excess charge type have no groups of opposite charge to interact with and therefore present themselves at the surface during hydration which causes the observed increase in polar character.

As the incorporation of monomers of opposite charge, at a specific ratio, is increased the total amount of water in the AMO:HEMA copolymer is relatively unaffected. However there is an increase in the amount of water in the bound state and a decrease in the amount of water existing in a free state. As the ratio was in favour of one of the charged monomers the increase in bound water is expected given the increase in polar charged sites. A dramatic increase in the initial modulus is also observed although the tensile strength of the resulting copolymer remains unaffected. As the modulus of the material is a measure of its stiffness, it can be concluded that ionic interactions are occurring between monomers carrying opposite charge. As the incorporation level of these monomers of opposite charge at an unequal ratio, is increased, the polar component of the surface free energy increases while the dispersive component is unaffected. The polar groups of the monomer of excess charge type present themselves at the surface during complete hydration and increase the polar nature of the surface.

For the copolymers produced in this and the previous chapter, the values obtained for the initial modulus can be plotted as a function of equilibrium water content. Figure

6.13 shows this for the hydrogels containing only a basic or cationic monomer and for ampholytic hydrogels, i.e. those containing both basic and acidic groups. The neutral unmodified copolymer is also included for comparison purposes. When basic monomers with the potential to show cationic properties are incorporated into the hydrogel the initial modulus remains relatively unaffected, although the water content does increase. When two monomers of opposite charge are included in the copolymer formulation the EWC of the system is close to that of the original AMO:HEMA copolymer with a significant increase in the value of initial modulus. As the degree of incorporation is raised the initial modulus increases considerably as shown by the three data points with the highest values. The inclusion of monomers of opposite charge can therefore increase the mechanical properties of the hydrogel without introducing any hydrophobic character or decreasing water content. It appears that manipulation of charged moieties will enable some degree of independent control of water content and initial modulus to be obtained.

Figure 6.13 The initial modulus as a function of EWC for AMO:HEMA (70:30) copolymers containing various charged monomers



CHAPTER 7

COEFFICIENT OF FRICTION OF ACUVUE CONTACT LENSES

7.1 Introduction

Hydrophilic polymers are presently incorporated in the design of a rich variety of biomedical and pharmaceutical products. Contact lenses, ocular implants, lubricious coatings for less invasive devices, biological adhesives, anti-thrombogenic coatings, soft tissue replacement and permanent implants are some of the current commercial applications that incorporate hydrophilic polymers. They are used at the surface of such devices to augment biocompatibility and reduce trauma to surrounding tissue. Lubrication has been widely considered to be important in biomedical technology. For instance, biomaterials to be used for catheters or endoscopes should have a surface with good handling characteristics when dry, becoming slippery upon contact with body fluids. This would enable easy use of the device and prevent mechanical injury to the mucous membranes and minimise discomfort to the patient.

Until recently, lubrication was considered to be applicable to metals and ceramics, but not to polymers. This is since lubrication always accompanies wear, against which polymers are quite weak, especially under large normal loadings. This poor wear resistance of polymers is due to their low modulus and rigidity compared to metals and ceramics, which is a result of the different molecular structures these materials possess. The smallest units of the constituents of metals and ceramics are associated with each other through primary and secondary bonding at high densities which results in high melting temperatures. However, the repeat units of polymers are constructed through primary bonds only in one direction with very weak lateral bonding. As a result, the constituent units of polymers have a much higher mobility than those of metals and ceramics even when they are cross-linked.

In a typical polymer surface any segment is able to change its position as a result of environmental factors since rotation along the main chain is not restricted as it is in metals and ceramics. However, this high degree of mobility results in poor resistance against wear since these segments may be readily deformed and stripped off from the surface when it is subjected to high mechanical stress. The motion also allows liquid molecules to enter the interstices of the polymer segments, resulting in polymer swelling, even though the density of chemical or physical cross-linking is high. The

characteristics of the polymer surface are therefore greatly influenced by the liquid that is used to swell the polymer.

Although very few man-made materials are known that have slippery surfaces, it is not difficult to find such surfaces occurring naturally. These include slippery surfaces on mucous tissues and organs in animal bodies. The purpose of these surfaces in nature has not yet been fully understood, but it is obvious that the slippery surface greatly reduces the frictional resistance occurring when the surface slides on another solid object. These surfaces contain a large amount of water, and when this water is squeezed out by fingertip touch it acts as a lubricant making the polymer surface slippery. Another feature of such surfaces is to prevent the surface from adhering to other objects with which it is in contact. All of the naturally occurring slippery surfaces are extremely hydrophilic however, synthetic materials such as poly(HEMA) are not nearly as slippery although they are known as hydrophilic polymers.

When the coefficients of friction of various polymers are determined against a glass plate in pure water, it was found that both a very hydrophobic and a strongly hydrophilic surface exhibited very low values¹²². In these extreme cases, the work of adhesion between the polymer and the glass surface is very low. Since the work of adhesion is directly related to the molecular interactions between the surfaces of both substances, the low adhesion values mean that no strong interaction is operative on the hydrophilic or hydrophobic surfaces in water. This seems reasonable because a very hydrophobic polymer such as PTFE has no significant dangling molecular force, while the strong dangling force of a very hydrophilic surface will disappear in a hydrophilic medium such as water. Thus a surface has a low coefficient of friction if its surface energy is either extremely high or low, i.e., if the water contact angle is either very high or low. From a practical point of view, it is easier to achieve an extremely hydrophilic polymer surface than it is to achieve an extremely hydrophobic one. This is since the water contact angle of even the most hydrophobic surface currently available is no larger than about 120 degrees. Thus hydrophilic materials or coatings are the easiest route for the production of lubricating polymer surfaces.

7.2. Lubrication

When the coefficient of friction between two solid surfaces is measured in the presence of a liquid that lowers its value, the liquid is described as a lubricant. This lowering of the friction or lubrication takes place through three different modes : boundary, fluid-film and solid film lubrication. The term fluid-film lubrication also includes hydrodynamic lubrication. The differentiation between the various types of lubrication can be made using a Stribeck curve. In this the variation in the coefficient of friction is plotted as a function of the Sommerfeld number.

The coefficient of friction during lubrication is potentially influenced by sliding speed (v), normal force (N), and solution viscosity (η). In lubrication theory, these three factors often appear as a single quantity called the Sommerfeld number (S).

$$S = \frac{\eta v}{NL} \quad \text{Equation 7.1}$$

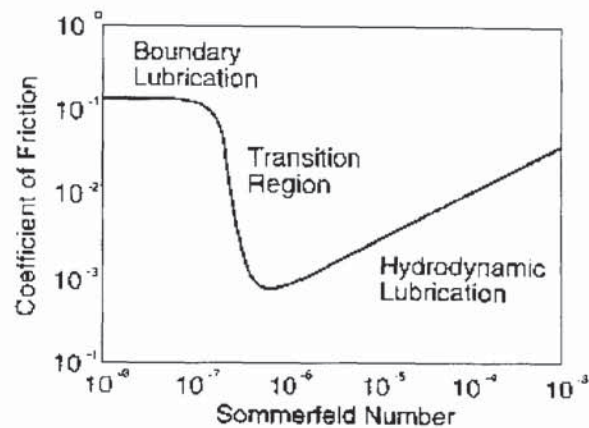
where L is a sample dimension

Boundary lubrication is defined as that in which the sliding surfaces are separated by a very thin film of lubricant, so that the chemical and physical natures of the surfaces and the lubricant are of major importance. The thin film between the solid surfaces usually contains only one or two layers of lubricant molecules. In contrast, the opposing two solid materials are completely separated by fluid in the case of fluid-film lubrication. As a result, the friction becomes very low and the wear of the solid materials is often negligible. Solid-film lubrication arises with the use of extreme pressure additives in the boundary lubrication situation, at high temperatures to form a solid film. PTFE is a commonly used solid-film lubricant which exhibits uniquely low friction under almost any environmental conditions because of its inertness to chemical reagents and its high temperature resistance.

Experiments on lubrication of metal surfaces as a function of Sommerfeld number produce the Stribeck curve as shown in figure 7.1. At high Sommerfeld number, the surfaces are lubricated by hydrodynamic lubrication and there is no contact between the surfaces. As the Sommerfeld number reduces the surfaces get closer and the

coefficient of friction increases. If the lubricant is capable of adsorbing on the surfaces or has additives that adsorb on the surface, the Stribeck curve makes a transition to boundary lubrication. In boundary lubrication, the coefficient of friction is lower than for dry friction and the lubrication is provided by molecular monolayers adsorbed to the surfaces.

Figure 7.1 Typical Stribeck curve for metal surfaces



7.3 Coefficient of Friction

A variety of methods have been suggested for testing the friction and wear of polymeric materials. The principle for determining the coefficient of friction (μ) is the same among the different methods in that it is the measurement of the ratio of frictional force to the normal load applied on the sample in the frictional motion. However, it is often difficult to determine the value of μ for medical devices due to their complicated shape. In addition, these biomaterials may exhibit frictional profiles different to those of *in vitro* tests when inserted into the body, due to various interactions with proteins and cells present in the body.

7.4 Measurement of Coefficient of Friction of Contact Lenses

During blinking there is sliding motion between the eyelid and the surface of the eye, which is lubricated by the tear film. When a contact lens is placed on the eye, the surface of the contact lens will influence the blinking process and this will affect the

comfort of contact lens wear. To study the consequences of contact lens wear both on patient comfort and the process of blinking, it is useful to study the group of related phenomena which are summarised under the general heading "biotribology". This term usefully describes the various factors that affect the lubrication and sliding friction of the contact lens in the eye.

Kalachandra¹²³ measured the coefficient of friction between two poly(MMA) contact lenses in the presence of various ophthalmic polymer solutions. The surface tension and the contact angle on the poly(MMA) were found to be independent of the viscosity of the polymer solutions used, and the contact lens system operated as a system of boundary lubrication. The results are shown in table 7.1 below where it can be seen that PVA has the lowest coefficient of friction. The effects of these polymer solutions on μ may depend on the chemical structure, conformation, and adsorption characteristics of the polymer as well as the surface characteristics of the sliding surface and the load and speed used.

Table 7.1 Surface chemistry and frictional properties of ophthalmic polymer solutions

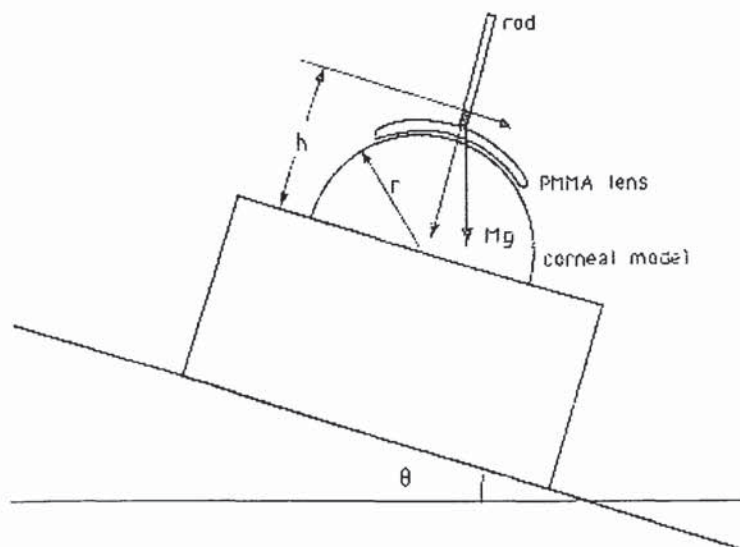
Ophthalmic Polymer	Coefficient of friction	Surface Tension dynes/cm	Contact angle on poly(MMA)
Methyl Hydroxy Ethyl Cellulose	0.234	50.0	42
Hydroxy Propyl Methyl Cellulose	0.191	48.0	40
Hydroxy Butyl Methyl Cellulose	0.187	64.7	36
Carboxy Methyl Cellulose	0.162	62.5	46
Chondroitin Sulphate	0.152	59.0	46
Dextran	0.147	55.0	45
Methyl Cellulose	0.131	58.0	42
Poly(vinyl methyl ether)	0.119	46.0	30
Polyvinyl Pyrrolidone	0.117	55.0	33
Polyvinyl Alcohol	0.109	46.0	43

The evaluation of lubricity between a RGP contact lens and a corneal model has been determined using the sliding angle method as shown in figure 7.2¹²⁴. A surface treated contact lens attached to a rod is first placed on the outer surface of a corneal model prepared from a PVA hydrogel in the shape of a hemisphere. To study the effect of different lubricants between the corneal model and a lens, different solutions can be added to the interfacial region. The stage carrying the test sample and the hemisphere is gradually inclined and the angle θ at which the contact lens sample starts to slide is carefully determined by the scale provided to the stage. The μ value between the contact lens and the opposing surface can be calculated by equation 7.2

$$Mgh \sin \theta = r\mu (Mg \cos \theta + a) \quad \text{Equation 7.2}$$

where r is the radius of the hemispheric test surface, g is the gravitational acceleration and h is the distance between the centre of the test sample and the centre of the hemisphere. $Mg \cos \theta$ corresponds to the normal load of the test sample against the hemisphere, while $Mgh \sin \theta$ corresponds to the frictional moment at the beginning of the sliding. The constant a in the equation is an additional factor resulting mainly from the surface tension of the liquid film between the two solid materials, which always exists in this experimental arrangement.

Figure 7.2 Determination of the static coefficient of friction between a RGP contact lens and a corneal model



The measurement of the friction and lubricity properties of soft contact lenses has been investigated by Nairn and Jiang³⁹. The equipment used consisted of a pad attached to a cantilever arm that is made from two crossed cantilever beams. The position of the cantilever can be adjusted vertically and it is this position that determines the normal force. A disc is attached to a rotating stage and as the disc rotates, the sliding motion exerts a frictional force on the pad. The normal and frictional forces cause deflections of the relatively compliant beam and the magnitude of these are measured optically by the use of lasers. By use of this equipment, the lubrication effectiveness of some commercially available ophthalmic solutions was investigated as was the difference between the front and back surface of the contact lens.

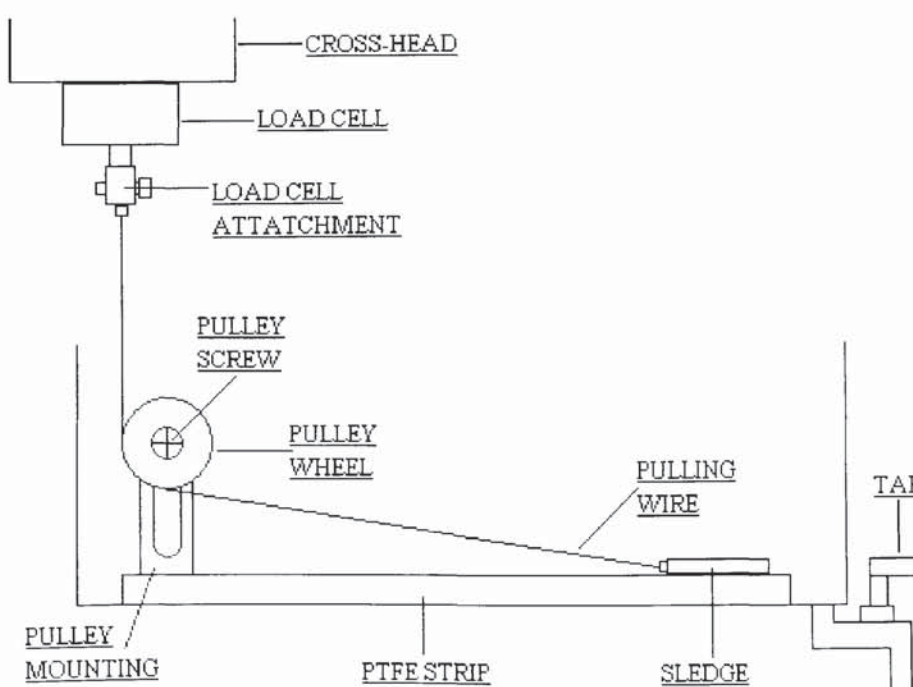
The coefficient of friction for a Sequence contact lens while sliding on a polycarbonate disc was measured both in the dry and lubricated situation. All the solutions used provided some lubrication, lowering the value of the coefficient of friction. It was suggested that contact lens lubrication is that of the boundary type that is also close to the transition to hydrodynamic lubrication. For a range of solutions the order of lubrication effectiveness was found to be the same as the trend in the magnitude of the viscosity of the solutions i.e. higher viscosity provides more lubrication. It was therefore concluded that in order to develop improved ophthalmic solutions viscosity must be increased without affecting other properties or, solutions must be developed that provide better lubrication at low viscosities.

This investigation also found reproducible differences in the coefficient of friction of the two surfaces of contact lenses which are probably due to processing methods. The posterior surface is the surface that rests on the cornea while the anterior surface is exposed to the tear fluid and is in contact with the eyelid during blinking. It was observed that the coefficient of friction of the anterior surface was consistently greater than that for the posterior surface. During contact lens wear, there is more sliding motion on the anterior surface of the lens and it is likely the magnitude of this friction will determine the comfort during wear for a particular lens type.

7.5 Development of Equipment for Measuring Coefficient of Friction of Contact Lenses

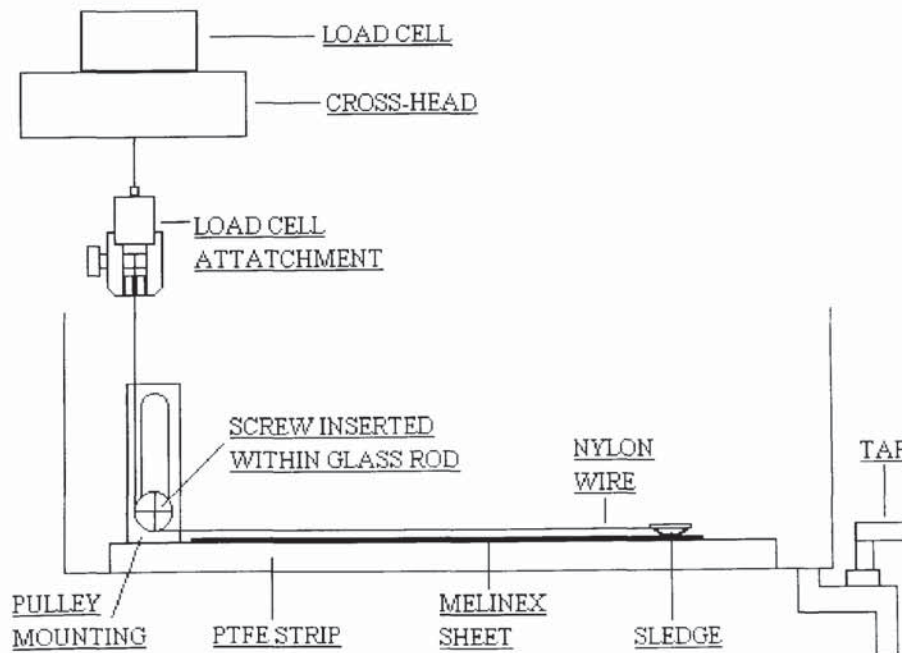
In order to measure the coefficient of friction of contact lenses, an attempt was made to modify apparatus for the measurement of this property for materials in sheet form which is used in conjunction with a mechanical testing tensometer. The equipment is shown schematically in figure 7.3. The resistance encountered during the sliding of the steel sledge over the sheet sample is measured as the force exerted on the load cell which is situated upon the tensometers cross-head. This allows the coefficient of friction of the material to be calculated. The sled supplied with the equipment was made of stainless steel and was much too large and heavy to be used for hydrogel materials. The sled pulling wire was also made of steel and was fed through an adjustable pulley wheel which was felt to be a system which was by no means frictionless. As the weight of the components that were physically moved by the tensometer was high, it was necessary that the larger 100N load cell was fitted to the cross-head. Contact lenses possess coefficients of friction which may be too small for this higher capacity, less sensitive load cell to detect. It was therefore necessary to modify the equipment substantially in order for contact lenses to be tested accurately.

Figure 7.3 Schematic diagram of original testing equipment



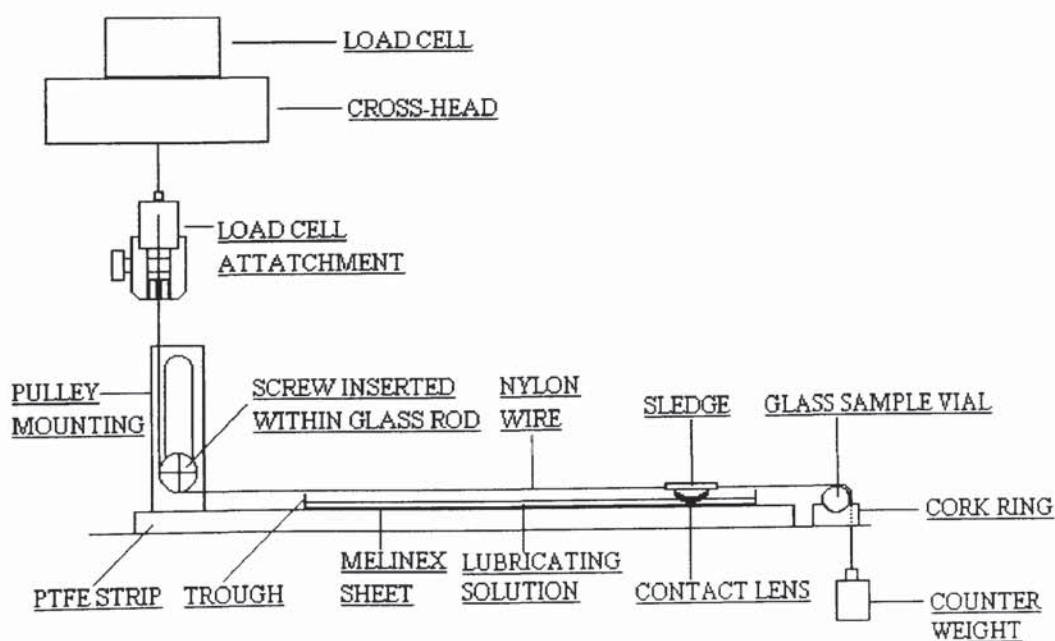
Since the pulling wire and pulley wheel system displayed a high degree of frictional resistance the equipment will produce overestimated values for the coefficient of friction of a sample. These components were therefore replaced with a system that could achieve sled movement with minimal friction force. Nylon sliding on glass has long been considered to be a system that shows almost friction-less behaviour. The pulley was therefore removed from its housing and a glass tube was then fixed in its place. Thin nylon wire was then attached to the load cell of the tensometer and the edge of the sledge. The large metal sledge was also replaced with a much lighter sled that was in fact a plastic mould used in the manufacture of contact lenses. The contact lens is placed on the outside of the hemisphere so that it sits on the mould in a similar way as it would sit on the eye during wear. The lower mass of this sledge also enabled the experiment to be carried out using the smaller load cell which also has increased sensitivity. Finally the PTFE strip was found to be unsuitable for frictional studies of hydrogel materials and so polyethylene terephthalate (Melinex) sheets were placed upon the PTFE strip. This material is more suitable to measurements of this type and a new sheet can be employed for each experimental sample.

Figure 7.4 Schematic diagram of 1st modification of testing equipment



The majority of the apparatus is situated within a large tank that allows a lubricating solution to be added to the system before testing begins. However as the equipment has been modified for the measurement of small samples the volume of lubricating solution required to fill the tank is large and would cause substantial hydrodynamic drag effects. The tank was therefore removed and a smaller plastic trough was placed on to the PTFE strip. The Melinex sheet is then cut to the size of the trough and placed inside it before testing begins. In this way only a small amount of lubricating solution is required for testing and drag effects are maintained at a negligible level. During initial investigations it was discovered that the sledge was much too light to give smooth motion and constant friction results. The friction level was so low that the slightest movement in the cross-head resulted in uncontrolled movement of the sledge in the forward direction. It was therefore decided to attach another piece of nylon to the other end of the sledge and hang a counterweight over the end of the apparatus via another glass cylinder. This would keep the pulling wire under tension at all times so that the forward movement of the sledge will always be controlled giving constant coefficients of friction during motion. The final modified equipment design is illustrated schematically in figure 7.5.

Figure 7.5 Schematic diagram of final modification of testing equipment



7.6 Multipurpose Solutions

7.6.1 Introduction

The recent introduction of a range of multipurpose solutions offers for the first time the prospect of a simple care system for soft contact lenses. While these solutions may not produce the best cleaning results, the replacement of the complicated hydrogen peroxide and chlorine based systems with a more user friendly system is proving popular. As these products should improve compliance and therefore reduce the incidence of complications, these solutions will be beneficial to a large number of patients.

7.6.2 Components

Multipurpose solutions contain three components: an antimicrobial agent, a buffer system and sometimes a surfactant. There are two antimicrobial agents, polyquartermium 1 and polyhexamethylene biguanide (PHMB). Both are high molecular weight polymeric compounds and, at physiological pH, possess cationic charges and hydrophobic groups. These agents are collectively referred to as polycationics or polyquaternary ammonium compounds which is simplified to polyquats. These compounds have a high molecular weight and are too large to penetrate the hydrogel matrix and build up to toxic levels.

All the antimicrobial agents used in ophthalmic products are produced by ICI chemicals and are supplied under such trade names as Cosmocil CQ, Vantocil 1B and Baquacil SB, which have been used as preservatives in cosmetic agents and as swimming pool disinfectants. However, manufacturers have adopted their own names for PHMB and particular formulations of PHMB, such as Bausch & Lomb who use Dymed and Allergan who use TrisChem. The difference between the PHMB containing products is the concentration of PHMB and the combination of buffers and surfactants used.

Polyquats bind to negatively charged phospholipids found in the bacterial cell membrane and, once bound electrostatically the hydrophobic portion of the molecule becomes associated with the internal core of the bilayer membrane causing its disruption. *In vitro* studies show that the presence of surfactants enhances this effect¹²⁵. This mode of action of the polyquats appears to be similar to that of lysozyme, the naturally occurring antibacterial protein found in tears. For ophthalmic applications, the high antibacterial potency of these agents in comparison with conventional ophthalmic antimicrobial agents is important. PHMB is effective in the 0.00003-0.0001% range and at these levels the risk of adverse ocular reactions is minimised.

The other polyquat used is polyquaternium 1, which is named Polyquad by Alcon who also have a patent on its use in ophthalmic products. Polyquaternium 1 is a polyionene since the positively charged groups form an integral part of the polymer backbone. Also, like PHMB it was originally used as a preservative agent in cosmetic products. It has a higher molecular weight than PHMB and has been formulated with a citrate buffer system.

PHMB and polyquaternium 1 have a tendency, at high concentration to adhere to negative charges on the surface of soft contact lens materials. As a result, manufacturers have now formulated these agents with buffers or surfactants that either compete for the charge sites on the surface of the lens (tris buffer in Complete), or bind to the charges on the polymer (citrate buffer in Opti-1). In addition, the negatively charged citrate groups may also bind electrostatically to positively charged proteins such as lysozyme and lactoferrin, and facilitate their removal from the lens.

The presence of a buffer also increases the effectiveness of the antimicrobial agents. The boric acid/borate system used in ReNu, for example enhances the efficacy of PHMB which enables the product to be formulated with a lower concentration of PHMB than is used in other solutions. This combination constitutes the basis for the patent protection this product possesses.

In addition to antimicrobials and buffers, some of the multipurpose solutions contain surfactants. Often a high molecular weight ethylene oxide-propylene oxide block copolymer is used for this purpose. In ReNu an uncharged quaternary version of this compound, known as a poloxamine is used at a particular hydrophilic/hydrophobic balance which is protected by patent. These surfactants not only clean the contact lens of proteinaceous material and solubilise lipoidal debris, but may also adhere to the contact lens surface and increase its wettability. It has been claimed by Bausch & Lomb that the poloxamine surfactant in ReNu increases the wettability of the lens which in turn increases the comfort of lens wear. There is certainly evidence to suggest that poloxamers absorb hydrogel surfaces and reduce both bacterial and protein adherence. However, this has yet to be demonstrated in a clinical setting or be directly related to levels of ocular comfort.

In contrast to the solutions that contain high molecular weight surfactants, Complete contains a low molecular weight surfactant, tyloxapol. However in practice, low molecular weight materials may have an increased risk of irritating the eye. They can cross the corneal glycocalyx more readily, stimulate the nerve endings within the cornea and may lead to ocular discomfort.

7.6.3 Materials

The multipurpose solutions that were selected for investigation cover a range of variations currently available on the commercial market. Table 7.2 shows the concentration of components for each of the solutions investigated. The selection includes two examples that use each of the different types of antimicrobial agents or preservatives, that are used for this particular application. All the solutions also contain edetate disodium as a preservative and are all formulated to be isotonic. Three of the solutions also contain surfactants with each of these being different in both type and relative sizes of the molecules.

Table 7.2. Composition of multipurpose solutions investigated

Name	Company	Preservative and Buffer	Surfactant	Other
Complete	Allergan	Polyhexamethylene biguanide 0.0001%	Tyloxapol 0.025%	disodium edetate 0.05% NaCl
Opti-1	Alcon	Polyquad (polidronium chloride) 0.0011% Sodium citrate		disodium edetate 0.05% NaCl
Opti-1+	Alcon	Polyquad (polidronium chloride) 0.0011% Sodium citrate	Pationic Tetronic (PEO/PPO)	disodium edetate 0.05% NaCl
ReNu	Bausch & Lomb	Dymed (polyaminopropyl biguanide) 0.00005% Boric acid/sodium borate	Poloxamine 1%	disodium edetate 0.1% NaCl

7.6.4 Methods

The coefficient of friction of an Acuvue contact lens was determined using the above multipurpose solutions as lubricants. The viscosity values of the solutions were determined in order to correlate with the value for the coefficient of friction. A possible correlation between the coefficient of friction and surface tension was also investigated. Values for surface tension were obtained in both the dynamic and static states and all methodologies can be found in Chapter 2. These methods were also used to investigate the physical properties of saline and compare its behaviour to that of the multipurpose solutions.

7.6.5 Results

The results obtained during the investigation of the properties of artificial tear solutions are shown in table 7.3. The figures quoted are an average of at least five determinations and the standard deviations were found to be less than 5% for all the properties investigated.

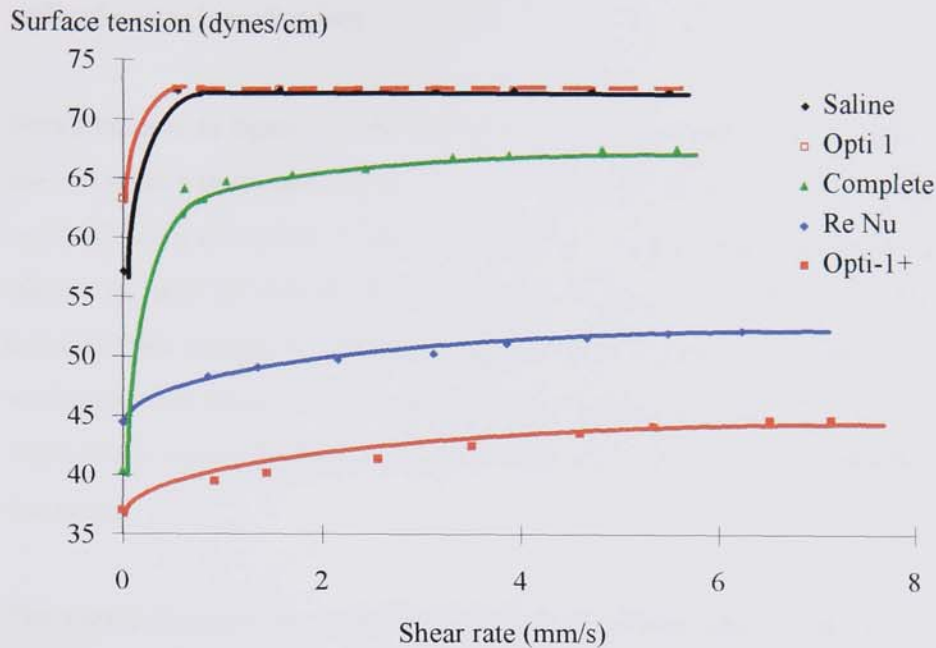
Table 7.3 Biotribology and surface chemistry results for multipurpose solutions

Multipurpose Solution	Viscosity (Centipoise)	S.S.T. (Dynes/cm)	D.S.T. (Dynes/cm)	Static Friction	Kinetic Friction
Saline	1.00	57.1	72.5	0.54	0.28
Complete	1.08	40.4	67.7	0.45	0.14
Opt-1	1.08	63.3	72.6	0.46	0.27
Opti-1+	1.11	37	44.8	0.44	0.15
ReNu	1.30	44.5	52.2	0.41	0.25

7.6.6 Discussion

Cleaning solution formulations are generally used in a dynamic cleaning system and contain surfactants which lower the surface tension of the solution. The surface tension of these solutions is usually calculated at the equilibrium state, which is not applicable to the effective surface tension in the dynamic state. It is therefore desirable to measure the surface tension of a solution in both the dynamic and static states. The efficiency of such solutions can be less than expected because of the low diffusion rate of the surfactant into the dynamically expanding interface. This can cause an increase in the surface tension of the solution which can approach that of water¹²⁶. A good surfactant for dynamic cleaning applications will present the same surface tension in the static and dynamic state. Therefore a graph showing both the static surface tension and the dynamic surface tension for each solution is plotted as shown in figure 7.6

Figure 7.6. Static surface tension values and, dynamic surface tension as a function of rate of bubble formation for multipurpose contact lens solutions



As shown in figure 7.6 when the surface tension for each solution is plotted against the rate of bubble formation (expressed in mm/s), its value reaches a constant with the increase in bubble rate. This equilibrium value will depend upon the concentration of surfactant in the surface of the expanding bubble. In two of the multipurpose solutions, and saline, the dynamic surface tension reached an equilibrium level at least 10 dynes/cm above the value of the static surface tension. This indicates that the solutions do not show good surfactant tendencies as they behave in a non-ideal manner. Saline and Opti-1 show very similar dynamic surface tension in the region of that of pure water, which correlates well with the fact that these solutions contain no surfactant components.

The three surfactant containing solutions display two different types of behaviour depending on the type of surfactant that is present within their formulations. Opti-1+ contains an ethylene oxide-propylene oxide copolymer similar to the poloxamine surfactant that is used in the ReNu formulation. These two solutions both display more ideal surfactant behaviour in that the value for the dynamic surface tension is only slightly higher than that of the static surface tension. However the Complete solution,

which also contains a surfactant, has a dynamic surface tension that is considerably greater than the static surface tension. This surfactant which is very different in both nature and molecular weight, must therefore be less efficient than the other larger molecular weight surfactants.

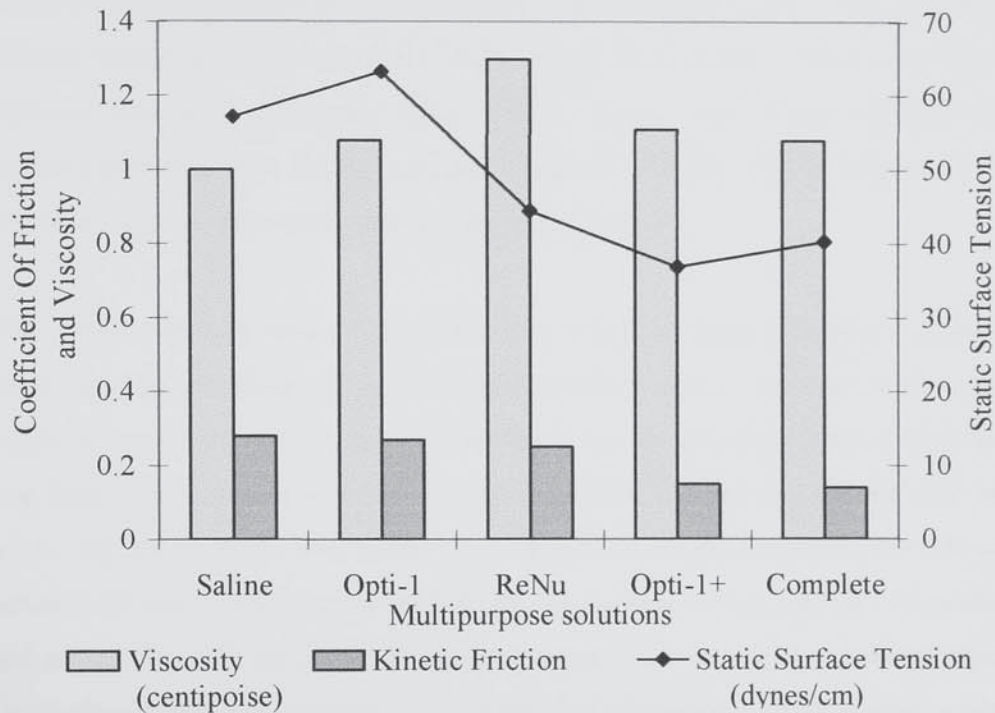
With reference to figure 7.6, the multipurpose solutions that contain surfactants display one common behavioural trend. In the dynamic situation, as shear rate is increased a constant increase in surface tension is observed. The greatest increase is between the static state and the lowest rate of bubble formation in the dynamic state. The two solutions that contain no surfactant show a large rise in surface tension between the static state and dynamic state with the lowest shear rate. However no increase in the value of the surface tension is observed with any further increase in the rate of bubble formation.

The values obtained for the static coefficient of friction were found to be very similar for all the multipurpose solutions examined. These values do not seem to correlate with any other property whose value was obtained during this investigation. However the values for the kinetic coefficients of friction are much smaller, having a value 50% less than the static state. This is as expected since the static force of friction and its coefficient are greater than the kinetic force of friction and its coefficient. The remainder of this discussion will concentrate only on results obtained for the coefficient of friction in the kinetic situation.

The viscosity of the multipurpose solutions are very similar being slightly higher in value than that of saline. The values obtained for the viscosity of each multipurpose solution appears to correlate with the molecular weight of the surfactants and additives within the solutions. ReNu contains the surfactant of highest molecular weight, which is reflected in its high viscosity value. Opti-1+ contains a similar surfactant with a slightly lower molecular weight and consequently its viscosity is slightly lower in value. Complete contains low molecular weight surfactants and so its viscosity is influenced predominantly by the high molecular weight preservative within its formulation. Opti-1 does not contain any surfactant and so its viscosity is again controlled by the high

molecular weight preservative this solution contains and so both solutions have similar viscosity values which are slightly higher than saline.

Figure 7.7 *Biotribology properties and surface tension values for a range of multipurpose contact lens solutions*



The values for the coefficient of friction in the kinetic state follow a trend that may be expected, given the values obtained for the surface tension and viscosity for each of the multipurpose solutions as shown in figure 7.7. The surface tension values of both saline and Opti-1 are high in both the dynamic and static state, as are the coefficients of friction. ReNu has relatively low surface tension values but a high viscosity which ultimately leads to the higher than expected value for the coefficient of friction. Opti-1+ has both low surface tension values and low viscosity values giving a very low coefficient of friction. Complete has low values for both viscosity and the coefficient of friction seen with this solution, however although its static surface tension value is low, its surface tension in the dynamic state is high. This unexpectedly seems to indicate the surface tension in static state has a greater influence on the coefficient of friction than the dynamic surface tension.

7.6.7 Conclusion

The coefficient of friction of a contact lens sliding on a surface was determined while the system was lubricated by a number of contact lens multipurpose solutions. The highest frictional values were obtained when saline was used as the lubricant. This is unsurprising as saline contains no surfactant and no viscosity agent. The coefficient of friction seems to follow the same trend as the static surface tension although the viscosity also has an influential effect. There are also clear effects of surface active agents which adsorb at the lens material surface, modifying interfacial properties and lowering both surface tension and coefficient of friction.

The results obtained during this study were similar to those obtained in a previous study into the coefficient of friction of soft contact lenses. However in the previous study, the coefficient of friction of a lens when measured in the presence of Complete was found to be similar in value as that with ReNu, which was not the case in this work. In the previous investigation, the samples were not soaked in the lubricating solution for any length of time prior to the experimental investigation. Thus there is not enough time for any surfactant present within a solutions formulation to adhere to the surface of the lens and reduce the coefficient of friction. In the present work, the lenses were soaked for at least 24 hours in the lubricating solution and this allows the surfactant to adhere and lower the coefficient of friction.

7.7 **Artificial Tear Solutions**

7.7.1 Introduction

When a contact lens sits on the eye in contact with the cornea, the front surface of the lens will be coated with a tear layer. The importance of the tear film in maintaining contact lens comfort is generally accepted but not understood in any detail. Similarly, the design and assessment of the efficacy of preparations for the relief of dry eye is carried out on a largely empirical basis. Improvements in technologies for the *in vitro* assessment of these phenomena would assist in improving the understanding of the

natural environment. This will allow the design of care solutions that more effectively relieve the symptoms of dry eye.

7.7.2 The Precorneal Tear Film

It is essential for good visibility and the well-being of the exposed ocular tissue that the cornea and the conjunctiva be covered with a thin, continuous fluid film, the precorneal tear film. The precorneal tear film has several functions the most important being to maintain the optical integrity of the cornea. The tear film keeps the cornea and conjunctiva moist and also provides nutrients to the cornea. It acts as an antibacterial defence mechanism for the cornea and conjunctiva by producing immunoproteins and also removes debris by means of a mechanical flushing system.

The precorneal tear film is made up of three layers: the superficial lipid layer, the middle aqueous layer and the mucoid layer. The superficial layer which consists of lipids, reduces the evaporation rate of the tear film, prevents tear strip overflow and lubricates the lid allowing smoother lid movement over the eye. The aqueous layer performs the functions of washing the eye, and providing a defence mechanism as well as aiding oxygen uptake for corneal metabolism. The mucin layer adheres to the microvilli of the corneal epithelium and functions as a wetting agent by providing a hydrophilic surface for the remaining tear layers.

7.7.3 Tear Film Abnormalities

In clinical practice, tear film abnormalities lead to conditions ranging from mild irritation to severe debilitation. There are five basic abnormalities of the tear film¹²⁷

- Deficient Aqueous.
- Decreased production by goblet cells results in mucin deficiency.
- Impaired lipid production.
- Impaired lipid function.
- Disruption of the corneal epithelial surface.

7.7.4 Tear Substitutes

There has been a specific interest in the formulation of eye-drops for the relief of irritated eyes for over 200 years. Initially these products were known as eye waters, later as eye slaves and more recently as eye-drops. The major and most important component of tear substitutes is water. The exposed surface of the eye must be covered with water, otherwise tissue damage will occur. Thus, all artificial formulations are dilute aqueous solutions of electrolytes and polymeric ingredients. Tear substitutes contain high molecular weight polymers added to saline solution to prolong the duration of the drop. An ideal tear substitute should duplicate the physiological role of the natural tear film and be compatible with normal tears. Relief from mucin and aqueous deficiencies is essential. Ideally a mucin compatible hydrophilic tear layer should be formed, the lipid layer should be maintained, and tear volume should be increased. The types of polymers commonly used in these applications are as follows.

Substituted cellulose ethers contain viscosity increasing agents that aid in increasing contact time. They exist as colloids that form optically clear solutions upon dissolving in water which have a refractive index similar to that of the cornea. They can be sterilised by heat as even though they coagulate at high temperatures they resume a solution form on cooling. Methylcellulose, the most commonly used cellulose ether, has a viscosity of 4000 centipoise and it is used in concentrations up to 1%. When the concentration is greater than 2% the solution is classified as an ointment. Hydroxyethyl cellulose and hydroxypropyl cellulose are also frequently used and they are less viscous and so cause less of a problem with lid crusting.

Polyvinyl alcohol (PVA) is an excellent wetting agent that also increases solution viscosity but this is considerably less viscous than methylcellulose. It lowers the surface tension of water and increases the contact time of a solution. It is easily sterilised by autoclaving or filtration as temperature does not affect its clarity or cause it to coagulate. It produces solutions which are transparent with a refractive index similar to that of water.

Other polymers including polyethylene glycol, polyvinyl pyrrolidone and derivatives of poly ethylene oxide can also be used to increase the viscosity of solutions. They have been claimed to act as artificial mucus and adhere to the corneal epithelium, thus increasing its surface energy.

Since body fluids and cells contain various electrolytes, it is important that tear substitutes should also contain salts at a similar level. An excess or deficiency of these salts may induce water movement across cell membranes by osmosis. This water transport into and out of the tissue may have an adverse effect upon it. The most common electrolyte used in tear substitutes is sodium chloride although potassium chloride is also employed.

Preservatives must be included in the formulation of multi-dose eye-drop bottles as directed by the Food and Drug Administration (FDA). Also, some of the preservatives are highly surface active and so can be detrimental to tear film stability. Commonly used preservatives include benzalkonium chloride and polymeric preservatives such as polyquat and dymed. The sodium salt of edectic acid is often included in the formulations because its presence often enhances the bactericidal activity of the preservative.

Other additives included in the formulation of artificial tear solutions include nutrients such as vitamins and occasionally, pharmaceutically active ingredients.

7.7.5 Materials

A number of commercially available artificial tear solutions were employed as lubricating agents in measurements to determine the coefficient of friction of a particular contact lens type. The products are a broad selection of currently available artificial tear solutions the compositions of which are shown in table 7.4.

Table 7.4 Compositions of artificial tear solutions investigated

Name	Producer	Polymer	Preservative	Disodium Edetate	Buffer	Other
Hypotears	Ciba Vision	PVA 1%	Benzalkonium Chloride 0.01%	Quantity Unknown	HCl NaOH	PEG 400
Liquifilm Tears	Allergan	PVA 1.4%	Benzalkonium Chloride 0.005%	0.015%	Hypo- tonic	
Vitaleyes	Ciba Vision	HPMC 0.04%	Benzalkonium Chloride 0.001%	0.01%	Boric Acid Borax	Vit A Vit B
Tears Naturale	Alcon	HPMC 0.3%	Benzalkonium Chloride 0.01%	0.05%		Dextran 70
Optrex	Optrex	HPMC 0.3%	Benzalkonium Chloride 0.01%		Boric Acid Borax	
Viva	Vision Pharmceu.	Polysorbate 0.5%		Quantity Unknown	Citric Acid	Vit A NaCl

7.7.6 Methods

The coefficient of friction of an Acuvue contact lens was determined using the above tear substitutes as lubricating solutions. The viscosity value of the artificial tear solutions was also determined in order to correlate the values with coefficient of friction results. The viscosity values also enable the type of lubrication that occurs to be identified by means of a plot of the coefficient of friction versus Sommerfeld number to produce a Stribeck curve. A possible correlation between the coefficient of friction and surface tension was also investigated. Values for surface tension were

obtained in both the dynamic and static states and all methodologies can be found in Chapter 2.

7.7.7 Results

The results obtained during the investigation of the properties of artificial tear solutions are shown in table 7.5. The figures quoted are an average of at least five determinations and the standard deviations were found to be less than 5% for all the properties investigated.

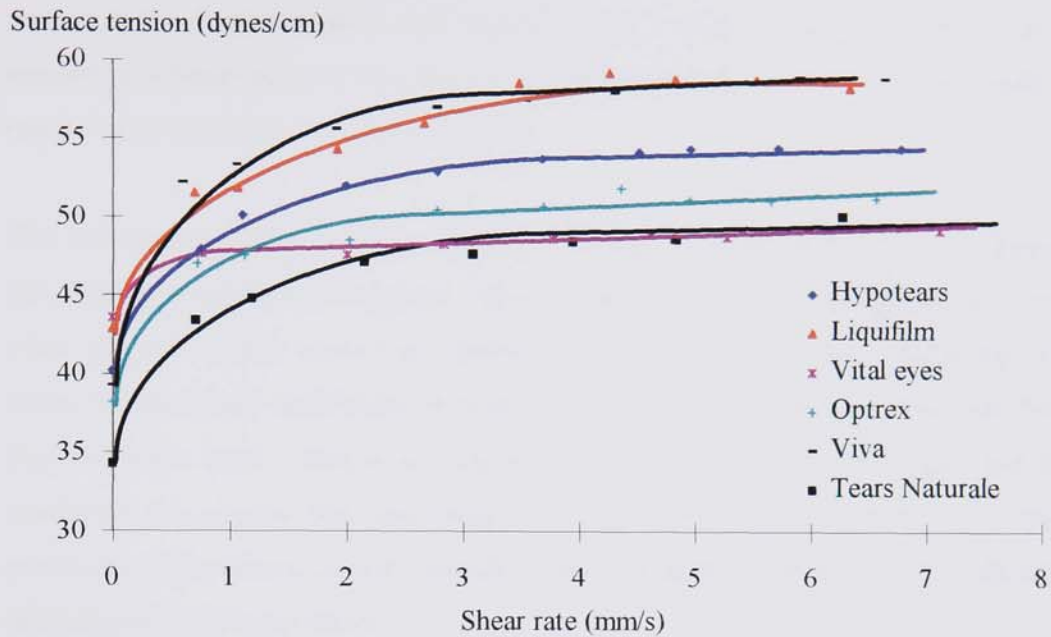
Table 7.5. Biotribology and surface chemistry results for artificial tear solutions

Tear Substitute	Viscosity (Centipoise)	Static Tension (Dynes/cm)	Dynamic Tension (Dynes/cm)	Static Friction	Kinetic Friction
Vital Eyes	6.75	43.6	49.3	0.40	0.25
Liquifilm	4	42.9	58.4	0.43	0.24
Hypotears	2.5	40.2	54.6	0.45	0.22
Viva	1.75	39.3	59.0	0.42	0.19
Optrex	5	38.2	51.4	0.45	0.22
Tears Nat.	4.25	34.3	49	0.44	0.15

7.7.8 Discussion

The surface tension of solutions is usually calculated at the equilibrium state, which is not the same as the effective surface tension in the dynamic state. It is therefore desirable to measure the surface tension of a solution in both the dynamic and static states. The low diffusion rate of the surfactant into the dynamically expanding interface can cause an increase in the surface tension of the solution which can approach that of water. Therefore a graph showing both the static surface tension and the dynamic surface tension for each solution is plotted as shown in figure 7.8

Figure 7.8. Static surface tension values and, dynamic surface tension as a function of rate of bubble formation, for tear substitutes



As shown in figure 7.8 when the surface tension for each solution is plotted against the rate of bubble formation (expressed in mm/s), its value reaches a plateau with the increase in bubble rate. The equilibrium value will depend upon the effective concentration of surfactant in the solution, which is the concentration of surfactant in the surface of the expanding bubble. In all the solutions with the exception of Vital eyes, the dynamic surface tension reached an equilibrium level 10-20 dynes/cm above the value of the static surface tension. This indicates that the solutions do not show good surfactant tendencies as they behave in a non-ideal manner.

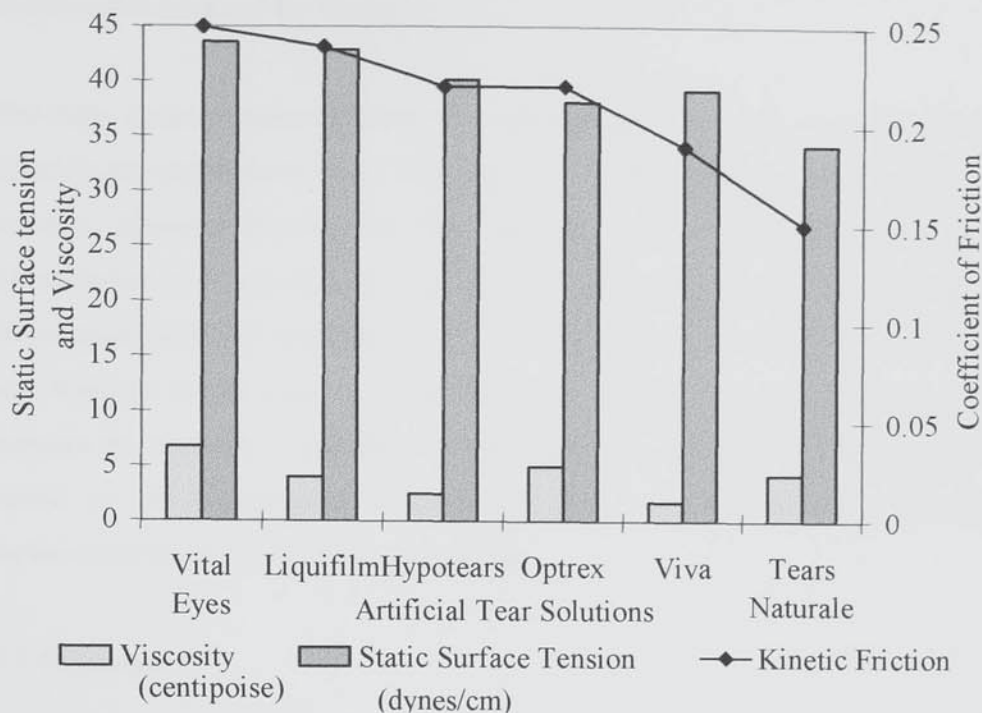
The magnitude of the difference between the surface tension in the dynamic as opposed to the static state appears to be influenced by the amount and type of polymer used to increase the solutions viscosity. Liquifilm and Hypotears both contain polyvinyl alcohol and the difference between the two surface tension measurements is very similar. The magnitude of this difference is slightly higher for Liquifilm but this solution contains slightly more PVA. Tears Naturale, Vital Eyes and Optrex all contain HPMC as the viscosity increasing agent. Tears Naturale and Optrex both

contain the same amount of HPMC and the magnitude of the different value of surface tension in the dynamic and static states is also the same within experimental error. Vital Eyes however has a much lower concentration of HPMC and thus the surface tension in the dynamic state is only slightly higher than that in the static state. Viva contains a different polymer and has the greatest difference in the value of the surface tension measured in the two different states.

The values obtained for the static coefficient of friction were found to be very similar for all the tear substitutes examined. These values do not seem to correlate with any other property whose value was obtained during this investigation. However the values for the kinetic coefficients of friction are much smaller, having a value 50% less than the static state. This is as expected since the static force of friction and its coefficient are greater than the kinetic force of friction and its coefficient. The remainder of this discussion will concentrate only on results obtained for the coefficient of friction in the kinetic situation.

The kinetic coefficient of friction results seem to correlate well with the surface tension results in the static state as shown in figure 7.9. Vital Eyes has the highest static surface tension and the highest coefficient of friction and is closely followed by Liquifilm which has slightly lower values of both these quantities. Hypotears has a significantly lower surface tension value which is reflected in the considerable reduction in the coefficient of friction that is observed with this solution. Viva possesses a slightly lower static surface tension which results in a larger than expected decrease in the coefficient of friction with this solution when compared to Hypotears. The static surface tension for Optrex is further decreased, however the coefficient of friction is much larger than would be expected given the values observed in the other solutions. Finally Tears Naturale has by far the lowest static surface tension value which gives rise to the extremely low coefficient of friction obtained when this solution is used as the lubricant.

Figure 7.9 Biotribology properties and surface tension values for a range of artificial tear solutions



The results indicate that viscosity may also influence the value of the coefficient of friction observed when artificial tear solutions are employed as lubricants during the sliding motion of a contact lens. Vital Eyes and Liquifilm have surface tension values that are the same, within experimental error, and so the reduced coefficient of friction value that Liquifilm has may be due to its reduced viscosity when compared to Vital Eyes. As the value of the coefficient of friction falls, a decrease is seen in both the viscosity and static surface tension for both Hypotears and Viva. However for Optrex although a slight decrease in surface tension is seen, a large increase in the viscosity of this solution is seen with respect to Viva. This increased viscosity could therefore be responsible for the high coefficient of friction value which is comparable to that of Hypotears.

Comparing Hypotears to Liquifilm, both these solutions contain PVA to increase viscosity although there is 40 % more present in Liquifilm. This difference in PVA content is responsible for the similar difference in viscosity values which is again approximately 40%. It must also be noted that Viva has an unusually low viscosity which may be explained by the fact that unlike the other solutions which are for the treatment of dry eye, this is a comfort solution for use with contact lens wear that

contains a different polymer to increase the solutions viscosity. This very low viscosity value gives rise to the low coefficient of friction value which accentuates the high friction value obtained for Optrex.

The static surface tension and kinetic coefficient of friction values obtained for Tears Naturale are significantly lower than the results obtained for any other artificial tear solution. However the viscosity value obtained for this solution is surprisingly high. The inclusion of a surfactant (dextran 70) within this solutions formulation gives rise to the unusual properties displayed by this solution when compared to the other artificial tear solutions in this study. The surfactant can adsorb onto the hydrogel surface to increase the materials wettability. In this way, Tears Naturale produces results very similar to the multipurpose solutions that also contain surfactants, although the surfactant level within this solution is higher.

7.7.9 Conclusion

The coefficient of friction of a contact lens sliding on a surface was determined while the system was lubricated by a number of artificial tear solutions. The coefficient of friction again seems to follow the same trend as the static surface tension with viscosity having an influential effect. There are also clear effects of surface active agents which adsorb at the lens material surface, modifying interfacial properties and lowering both static surface tension and kinetic coefficient of friction.

7.8 Chapter Conclusions

The coefficient of friction for a sliding contact lens lubricated by both multipurpose solutions and artificial tear solutions was determined by a novel and reproducible method. For both types of solutions, the value of the kinetic coefficient of friction for a contact lens appears to be controlled mainly by the static surface tension of the lubricating solution. However, viscosity also has a major influence and extremities in its value can change the coefficient of friction value to a level that may be unexpected given the static surface tension a solution may have. The effect of viscosity is not linear and is dependent on the type of polymer used to increase a solutions viscosity.

The highest frictional values were obtained when saline is used as the lubricant and this is expected given that it contains no surfactant and no viscosity agent. The addition of additives that increase viscosity, affects the coefficient of friction and this is illustrated by the results for Hypotears and Liquifilm. Both these artificial tear solutions contain PVA to increase viscosity although there is 40% more in Liquifilm which is reflected in its increased viscosity value. As these solutions have similar surface tension values, the increased coefficient of friction that Liquifilm possesses when compared to Hypotears is due to its increased viscosity agent content.

A greater reduction in the coefficient of friction of soft contact lenses can be achieved by the inclusion of a surfactant within the formulation of the solution used as a lubricant. The nature of hydrogel structure allows surfactant molecules to adsorb onto the surface of the contact lens. However for this to occur, the contact lens must be allowed to soak in the solution containing the surfactant for some time.

The results illustrate the reproducibility of this method for the measurement of the frictional characteristics of contact lenses. However, the magnitude of the value for the coefficient of friction obtained by this method is substantially overestimated. This is a consequence of the use of the counter weight to keep the pulling wire between the sledge and the load cell taut. The determination of the true coefficient of friction of the contact lens therefore becomes a difficult and complicated calculation. Calibration of the equipment is difficult as experimental determinations of this property for hydrogel contact lenses have been extremely limited. The equipment was therefore calibrated to results obtained in a previous study³⁹ with materials of this type. Although the results in this particular study are not believed to be totally reliable, they are the only source of results for this type of experiment which allows our equipment to be calibrated. The method can distinguish between different lubricating solutions and values obtained correlate well with those obtained from other surface characterisation techniques. The method also provides an excellent basis for the study of frictional properties of *ex vivo* contact lenses to explore various patient, lens and material combinations.

CHAPTER 8

CONCLUSIONS

AND

SUGGESTIONS FOR

FURTHER WORK

8.1 Conclusions

A fundamental if poorly understood characteristic of hydrogel materials is their tendency to dehydrate significantly at ambient humidity and temperature. Wearers of thin, high water content lenses are particularly prone to certain complications, apparently indicating the increased effect of dehydration as a consequence of increasing water content and decreasing lens thickness. This manifests itself as “corneal desiccation staining” which is one of the clinical problems impeding the development of successful hydrogel materials for extended wear applications. The extensive amount of literature devoted to this subject has attempted unsuccessfully to find correlations between changes in the water content of hydrogels during wear and, various lens wear conditions. The extent of dehydration is controlled by a number of factors although their precise contribution is unclear.

Although dehydration of contact lenses does occur, a number of authors have concluded that corneal staining cannot be correlated with the degree of dehydration of the lens. Corneal desiccation is controlled by the ability of water to move through a contact lens. It has been determined that the initial rate of evaporation of water from various lenses was in the same range regardless of material type or water content and was the same rate as the evaporation of pure water. The same rate of evaporation for high and low water content lenses indicates that dehydration of water can not be the single cause of corneal staining, since high water content lenses suffer more from these complications than lenses of low water content.

It has been suggested that materials containing a high proportion of water with the properties of bulk water are more susceptible to lens dehydration and hence induce corneal staining, compared to materials with high proportions of water in the bound state. Therefore an investigation was carried out to evaluate the effect of different water binding characteristics on the ability of a material to induce corneal staining. Results from a clinical study into corneal staining levels for a number of different contact lenses were compared to the relative proportions of free and bound water in the materials.

For the hydrogel contact lenses examined, the proportion of water existing in the bound state was found to be dependent on the swelling medium used. The contact lenses were divided into two groups, those which were cleaned using a multipurpose solution during the 1 month wear period and those cleaned using a peroxide based system. When the lenses cleaned with the multipurpose solution were soaked in the same solution prior to evaluation by DSC a correlation was identified. Lens materials with higher proportions of bound water were found to induce less corneal staining than materials with lower amounts of bound water. When the lenses cleaned in the peroxide based system are divided in groups based on the water contents this trend is again observed. However this correlation only exists for DSC measurements for the materials after swelling in water as peroxide gives misleading results.

It must be noted that large patient to patient variations were found for the extent of corneal staining observed for each particular lens type as shown in appendix 1. This is probably due to variations in the concentrations of lipids and proteins in the tears of each patient studied. Higher solute concentrations lower water activity which in turn results in greater lens dehydration. However, despite the variations, the large number of patients wearing each type of lens will produce results showing the typical staining levels encountered for average tear compositions.

Dehydration of hydrogel contact lenses during wear does occur, although this cannot be the main cause of corneal staining. It can be reasonable to expect that for two materials of similar water content, the material with the higher proportion of water existing in the bound state will dehydrate to a lesser degree than a material with a lower proportion of bound water. However it has been observed that the rate of evaporation of water from lenses is the same regardless of lens material and water content, and is the same as that in pure water. To account for this and the results in this work, it can be concluded that corneal staining associated with lens dehydration occurs by the following process. The evaporation of water from tears between blinks lowers the activity of water at the lens/tear interface and the water activity gradient between the surface and the lens interior gives rise to the transport of water towards the interface. Thus a steeper gradient, or a larger amount of water with a high activity (i.e. free water) in the lens will lead to higher levels of corneal staining.

The potential of using hydrogels as a moisture absorbing device within glass vials containing pharmaceutical products has been investigated. For this application a successful material must absorb and retain all moisture in the low humidity environment within the vial. Hydrogels have a high affinity for water and their widespread use in the biomaterials field indicates the absence of possible toxicity problems. A hydrogel material will be dehydrated prior to use and must continue to perform the desired function over a substantial period of time to increase the shelf-life of the product.

A range of hydrogel copolymers were dehydrated and their moisture absorbency profiles over a period of time were examined by dynamic vapour sorption. The equilibrium capacity is reached relatively quickly and depends on the total water content and the relative proportion of this water that exists in the bound state. For materials with similar water contents, the moisture absorption is greatest for the material with the higher proportion of water in the bound state. Absorption capacity must be maximised to enable the size of the desiccant hydrogel implant within the product vial to be minimised.

The simple hydrogel copolymers produced for this application have adequate moisture absorbency but suffer from undesirable mechanical properties. The materials are employed in the dehydrated state for this particular application and it was found that the initial hydrogels produced were extremely brittle in this state. Although the incorporation of monomers to increase flexibility in the dehydrated state resulted in polymers with improved properties, the flexibility of the polymer was still not considered sufficient to allow easy mechanical processing. Also substantial dimension changes were observed as the sample absorbed moisture.

Interpenetrating polymer network technology was employed to increase flexibility in the dehydrated state and improve dimensional stability as the hydrogel absorbs moisture. A polyurethane polymer is added to the hydrogel monomer mixture prior to the polymerisation process. As incorporation increases the water content of the resulting copolymer decreases while a dramatic increase in mechanical properties is observed. However, the absorbed moisture capacity decreases only slightly and the

materials containing an interpenetrant retain a significant amount of moisture when humidity is lowered back to zero, a property not observed in the conventional hydrogels.

Hydrogel materials have displayed the necessary properties for use in this particular application and an ideal formulation will incorporate the following points. A simple hydrogel based on a highly hydrophilic monomer would produce a high EWC polymer and methacrylic acid can also be added to the system to increase the water content further. Copolymerisation with other monomers can manipulate the hydrogels water binding properties such that the proportion of water existing in the bound state is maximised. Finally a small percentage of polyurethane interpenetrant is added to the system to impart a degree of flexibility to the hydrogel in the dehydrated state and improve dimensional stability during the hydration process.

For the production of contact lenses within group II of the F.D.A. classification (EWC>55%, non-ionic), the monomer most commonly used to provide such high levels of hydrophilicity is N-vinyl pyrrolidone. This monomer is relatively unreactive in free radical copolymerisation, producing polymers with local domains of the same chemical type. Polymers with this block-type structure are more susceptible to biochemical and biological deposition than polymers with small alternating monomer sequences. Another monomer acryloylmorpholine has a similar structure and hydrophilicity level as NVP. When these monomers are copolymerised with HEMA, they produce hydrogels with comparable physical properties. However, the sequence distribution of the AMO copolymer is much improved when compared to the NVP copolymer, having a narrower distribution of sequence lengths. This is due to the higher rate of reaction that AMO has in polymerisation reactions, which is a result of the formation of resonance stabilisation structures which lower the activation energy of the reaction.

The advantages of replacing NVP with AMO for the production of high EWC hydrogel soft contact lenses is the reduced level of protein and lipid absorption that these materials display which is a consequence of their improved sequence distributions. All conventional, high water content hydrogels display relatively poor

mechanical properties due to the large amount of water within the polymer. Attempts to improve mechanical properties without affecting other properties will be made with copolymers of AMO because of the advantages it presents.

The effects on the physical properties and surface energies of hydrogels incorporating monomers with the potential to carry a positive charge was investigated. It is hoped that the inclusion of such monomers will result in the formation of weak electrostatic bonds between the main chains in the resulting copolymer. It is desirable that this results in an increase in the mechanical properties of the copolymer without having a detrimental effect on its water binding and surface properties. However, the evaluation of improvements in mechanical properties will be difficult as increased incorporation of monomers with charged groups will be accompanied by an increase in the EWC and consequently a decrease in mechanical properties. Therefore all investigations were performed using a basic composition of AMO:HEMA at 70:30. This composition produces a hydrogel with a very high water content and any increase in water content due to incorporation of charged monomers will be small. This enables any increase in mechanical properties to be observed.

The charged monomers investigated were NVI, DMAEA, DMAEMA, 4-VP and PNO which were each incorporated at a number of levels up to 10% by weight. The most significant effect is the dramatic increase in EWC observed as charged monomer content increases. This increase in hydrophilicity is a consequence of the greater polarity that the charge induces. In the majority of copolymers produced, the increase in total water present is achieved by an increase in both the free and bound water proportions. However in the NVI copolymers the increased water content is attributed to a rise in the amount of water present in the bound state. This enables the production of hydrogels with a greater proportion of water existing in the bound state. As discussed previously it is this particular characteristic which is expected to decrease the incidence of corneal staining that occurs in wearers of high EWC contact lenses.

The increased water content that occurs as charged monomer content becomes greater is accompanied by an expected decrease in mechanical properties for each of the systems investigated. The magnitude of this decrease is large for all the charged

monomers with the notable exception of the copolymers containing NVI. In hydrogel polymers any water existing in the free state acts as an internal plasticiser which makes the polymer more flexible, reducing stiffness. In the copolymers containing the other charged monomers the increase in free water content results in the significant reduction in initial modulus. Conversely as NVI content is increased, no increase in free water content occurs and consequently a reduction in initial modulus is not observed.

The surface free energy of the dehydrated hydrogels remains relatively unaffected by the incorporation of increasing amounts of charged monomers. In this state the surface energy is totally dominated by the dispersive component with the polar component having a value approximately equal to zero. This is due to hydrophobic group expression at the air interface and the orientation of the hydrophilic groups towards the polymer bulk. In the hydrated situation, the surface free energy is dominated by a large polar component, with a dispersive component much reduced compared to the dehydrated situation. As the incorporation of basic, potentially cationic monomers is raised, the polar component of the surface free energy increases, while the dispersive component remains unaffected. The contact angle hysteresis is dependent on the ability of the carbon main chain to rotate pendant groups to the most thermodynamically favourable position. This has been shown to be dependent on both the size of the pendent group and the presence of any methyl groups upon the α -carbon atom.

The incorporation of monomers with the potential to carry a positive charge has offered some potential benefits especially in the case of NVI. Although mechanical properties did not increase with its incorporation in the AMO:HEMA copolymer they did not decrease either which is encouraging given the significant increase in total water content. It was therefore decided to incorporate an additional monomer in the system which would have the potential to carry a negative charge. It is hoped that the opposite charges situated upon the polymer main chains will interact electrostatically with each other increasing the inter-chain attractive forces and improving the materials mechanical properties.

All investigations were performed again using a AMO:HEMA 70:30 copolymer, so as to minimise increases in water content. In all compositions the positively charged monomer selected for incorporation was NVI because of the advantages it displayed over the other cationic monomers investigated. A range of monomers with the potential to carry a negative charge were incorporated in the copolymer and the effect on the physical properties of the material was investigated. The monomers investigated were MAA, ITA and SPI.

With the incorporation of equal proportions of two monomers of opposite charge, the amount of water in the AMO:HEMA copolymer generally increases. This would be expected given the increase in the number of hydrophilic sites, however the increase is due mainly to an increase in the proportion of water existing in the free state. As the presence of charged groups would be expected to increase the proportion of bound water, it may be concluded that weak bonds are being formed between monomers of opposite charge. This conclusion is further supported by the increased initial modulus observed for this situation. The addition of equal ratios of monomers of opposite charge has very little effect on the magnitude of both the dispersive and polar components of the surface free energy in both the hydrated and dehydrated states. The inclusion of these charge carrying monomers would be expected to increase the polar component of the surface free energy in the hydrated state. However as this is not observed the results can be interpreted as further evidence for the interaction of monomers of opposite charge, which prevents the hydrophilic groups from presenting themselves at the surface.

When the proportion of one particular charge type is increased to a level higher than that of the opposite charge, an increase in the total water content of the copolymer is observed. This unsurprisingly indicates that the presence of an excess amount of one charge type raises the hydrophilicity of the resulting material. The magnitude of the increase is dependent on the polar and steric effects of each particular monomer. With the rise in water content there is a decrease in the mechanical properties, the magnitude of which is related to the change in EWC. In the hydrated state as the proportion of one charge type is increased to an excess, the polar component of the surface free energy increases while the dispersive component is relatively unaffected. The polar

groups of the monomer of excess charge type have no groups of opposite charge to interact with and therefore present themselves at the surface during hydration which causes the observed increase in polar character.

As the incorporation of monomers of opposite charge, at a specific ratio, is increased the total amount of water in the AMO:HEMA copolymer is relatively unaffected. However there is an increase in the amount of water in the bound state and a decrease in the amount of water existing in a free state. As the ratio was in favour of one of the charged monomers the increase in bound water is expected given the increase in polar charged sites. A dramatic increase in the initial modulus is also observed although the tensile strength of the resulting copolymer remains unaffected. As the modulus of the material is a measure of its stiffness, it can be concluded that ionic bonds are formed between monomers carrying opposite charge. As the incorporation level of the monomers at an unequal ratio is increased, the polar component of the surface free energy increases while the dispersive component is unaffected. The polar groups of the monomer of excess charge type do not have monomers of opposite charge with which to interact and so present themselves at the surface during complete hydration and increase the polar nature of the surface.

During blinking there is sliding motion between the eyelid and the surface of the eye, which is lubricated by the tear film. When a contact lens is placed on the eye, the surface of the contact lens will influence the blinking process and this will effect the comfort of contact lens wear. To study the consequences of contact lens wear both on patient comfort and the process of blinking, it is useful to study the group of related phenomena which are summarised under the general heading "biotribology". This term usefully describes the various factors that affect the lubrication and sliding friction of the contact lens in the eye.

The coefficient of friction for a sliding contact lens lubricated by both multipurpose solutions and artificial tear solutions was determined by a novel and reproducible method. For both types of solutions, the value of the kinetic coefficient of friction for a contact lens appears to be controlled mainly by the static surface tension of the lubricating solution. However, viscosity also has a major influence and extremities in

its value can change the coefficient of friction value to a level that may be unexpected given the static surface tension a solution may have. The effect of viscosity is not linear and is dependent on the type of polymer used to increase a solutions viscosity.

The highest frictional values were obtained when saline is used as the lubricant and this is expected given that it contains no surfactant and no viscosity agent. The addition of additives that increase viscosity will affect the coefficient of friction. A large reduction in the coefficient of friction of soft contact lenses can be achieved by the inclusion of a surfactant within the formulation of the solution used as a lubricant. The nature of hydrogel structure allows surfactant molecules to adsorb onto the surface of the contact lens. However for this to occur, the contact lens must be allowed to soak in the solution containing the surfactant for some time.

The results illustrate the reproducibility and accuracy of this method for the measurement of the frictional characteristics of contact lenses. The method can distinguish between different lubricating solutions and values obtained correlate well with those obtained from other surface characterisation techniques. The method provides an excellent basis for the study of frictional properties of *ex vivo* contact lenses to explore various patient, lens and material combinations.

8.2 Suggestions For Further Work

Although it has been shown that the water structuring within hydrogel soft contact lenses directly influences the extent of corneal staining found in patients wearing such lenses, more clinical data will increase the confidence in this argument. It would also be interesting to study the dehydration characteristics of a variety of soft contact lenses using dynamic vapour sorption apparatus. This will enable the verification of reports that all hydrogel contact lenses dehydrate at the same rate which was found to be equal to that of pure water. It will also be desirable to investigate the differences between worn and unworn lenses with this technique and the consequences of adsorption of proteins, lipids and phospholipids.

Hydrogel materials in the dehydrated state have displayed the necessary properties to allow their use as pharmaceutical packaging agents with desiccating properties. The number of materials whose moisture absorbency characteristics were investigated by DVS was strictly limited. It would be interesting to examine a wider range of compositions for this application and to investigate such factors as porosity and volume-surface area relationships.

The consequences of incorporation of a pair of charged monomers of opposite charge on the physical properties of the resulting copolymer has been investigated. Although the desired increase in mechanical properties was achieved, it is unknown what effect the charged monomer content will have on protein and lipid adsorption levels. It would therefore be useful to measure these properties for such materials as encouraging results could allow the incorporation of such monomers in high EWC contact lenses. Incorporation of NVI alone in hydrogel contact lenses should also be investigated further as this monomer increases the proportion of water existing in the bound state which may lead to lower levels of corneal staining.

A technique for measuring the coefficient of friction of contact lenses has been established which produces reproducible results and is sensitive enough to detect changes in compositions of solutions used for lubricating purposes. It would be interesting to measure this property for a range of contact lens materials and to investigate differences between worn and unworn lenses. This could also be extended to look at the consequences of different concentrations of adsorbed species. The effect of charged groups at the surface of the material should also be evaluated. As contact lenses dehydrate during wear they become less comfortable to the wearer. It is therefore desirable to see if these changes can be measured by coefficient of friction measurements of hydrogel contact lenses at different hydration levels.

REFERENCES

1. Wichterle, O. and Lim, D., Hydrophilic gels for biological use, *Nature*, 185, 117-118, (1960)
2. Sperling, L.H., *Interpenetrating polymer networks and related materials*, Plenum press, New York (1981)
3. Jeronimidis, G., *Natural composite materials, advances in materials science and engineering*, Ed. Cahn, R.W., Pergamon Press (1989)
4. Andrade, J.D., *Hydrogels for medical and related applications*, ACS symposium series, 31, (1976)
5. Wichterle, O., *Hydrogels*, in *Encyclopedia of Polymer Science and Technology*, Mark, H. and Gaylord, N., Eds., Interscience, New York, 15, 273, (1971)
6. Ratner, B.D., *Biomedical applications of hydrogels, a review and critical appraisal*, in *Biocompatibility of Clinical Implant Materials*, Vol. 2, Williams, D.F., Ed., CRC Press, Boca Raton, FL, 145, (1981)
7. Tighe, B.J., *Hydrogel materials: the patents and the products (Parts I and II)*, *Optician*, 17, 197, 5202 and 5207, (1989)
8. Corkhill, P.H., Fitton, J.H. and Tighe, B.J., *Towards a synthetic articular cartilage*, *J. Biomater. Sci. Polymer Edn.*, 4, 6, 615-630, (1993)
9. Roorda, W.E., Boddle, H., de Boer, A.G. and Junginger, H.E., *Synthetic hydrogels as drug delivery systems*, *Pharm. Wk. Bul. (Sci)*, 12, 165-189, (1988)
10. Park, G.B., *Burn wound coverings - a review*, *Biomat. Med. Dev. And Art. Org.*, 6, 29-37, (1978)
11. Pedley, D.G., Skelly, P.J. and Tighe, B.J., *Hydrogels in biomedical applications*, *Bri. Polym. J.*, 12, 99-110, (1980)
12. Frommer, M.A. and Lancet, D., *Freezing and non-freezing water in cellulose acetate membranes*, *J. Appl. Polym. Sci.*, 16, 1295-1303, (1972)
13. Pedley, D.G. and Tighe B.J., *Water binding properties of hydrogel polymers for reverse osmosis and related applications*, *Br. Polym. J.*, 11, 130-136, (1979)
14. Stillinger, F.H., *Water revisited*, *Science*, 209, 451-457, (1980)
15. Saenger, W., *Structure and dynamics of water surrounding biomolecules*, *Annu. Rev. Biophys. Chem.*, 16, 93-114, (1987)
16. Taniguchi, Y. and Horigome, S., *The states of water in cellulose acetate membranes*, *J. Appl. Polym. Sci.*, 19, 2743-2748, (1975)

17. Corkhill, P.H., Jolly, A.M., Ng, C.O. and Tighe, B.J., Synthetic hydrogels 1: Hydroxyalkyl acrylate and methacrylate copolymers - water binding studies. *Polymer*, 28, 1758-1766, (1987)
18. Roorda, W.E., Bouwstra, J.A., de Vries, M.A. and Junginger, H.E., The thermal analysis of water in poly(HEMA) hydrogels, *Biomaterials*, 9, 494-499, (1988)
19. Sung, Y.K., Gregonis, D.E., Jhon, M.S. and Andrade, J.D., Thermal and pulse NMR analysis of water in poly(2-hydroxyethyl methacrylate), *J. Appl. Polym. Sci.*, 26, 3719-3728, (1981)
20. Hatakeyama, T., Yamauchi, A. and Hatakeyama, H., Studies on bound water in poly(vinyl alcohol) hydrogel by DSC and FT-NMR, *Eur. Polym. J.*, 20, 61-64, (1984)
21. Yamada-Nosaka, A., Ishikiriyama, K., Todoki, M. and Tanzawa, H., H-NMR studies on water in methacrylate hydrogels 1., *J. App. Polym. Sci.*, 39, 2443-2452, (1990)
22. Quinn, F.X., Kampff, E., Smyth, G. and McBrierty, V.J., Water in hydrogels 1. A study of water in poly(N-vinyl-2-pyrrolidone/methyl methacrylate) copolymer, *Macromolecules*, 21, 3191-3198, (1988)
23. Quinn, F.X., Smyth, G. and McBrierty, V.J., Water in hydrogels 2. A study of water in poly(hydroxyethyl methacrylate), *Macromolecules*, 21, 3198-3204, (1988)
24. Quinn, F.X., McBrierty, V.J., Wilson, A.C. and Friends, G.D., Water in hydrogels 3. Poly(hydroxyethyl methacrylate)/saline solution systems, *Macromolecules*, 23, 4576-4581, (1990)
25. McBrierty, V.J., Quinn, F.X., Keely, C., Wilson, A.C. and Friends, G.D., Water in hydrogels 4. Poly(N-vinyl-2-pyrrolidone-methyl methacrylate)/saline systems, *Macromolecules*, 25, 4281-4284, (1992)
26. Carles, J.E. and Scallan, A.M., The determination of the amount of bound water within cellulosic gels by NMR spectroscopy, *J. App. Polym. Sci.*, 17, 1855-1865, (1973)
27. Peschier, L.J.C., Bouwstra, J.A., de Bleyser, J., Junginger, H.E. and Leyte, J.C., Water mobility and structure in poly(2-hydroxyethyl methacrylate) hydrogels by means of the pulsed field gradient NMR technique, *Biomaterials*, 14, 945-952, (1993)
28. Roorda, W.E., de Bleyser, J., Junginger, H.E. and Leyte, J.C., Nuclear magnetic resonance relaxation of water in hydrogels, *Biomaterials*, 11, 17-23. (1990)

29. Mathur, A.M. and Scranton, A.B., Characterisation of hydrogels using nuclear magnetic resonance spectroscopy-review, *Biomaterials*, 17, 547-557, (1996)
30. Luprano, V., Ramires, P., Montagna, G. and Milella, E., Non-destructive characterisation of hydrogels, *J. Mater. Sci. Mater. Medicine*, 8, 175-178, (1997)
31. Koda, S., Yamashita, K., Iwai, S., Nomura, H. and Iwata, M., Ultrasonic investigation of the states of water in hydrogels, *Polymer*, 35, 5626-5629, (1994)
32. Shinyashiki, N., Matsumura, Y., Miura, N., Yagihara, S. and Mashimo, S., Dielectric study of water structure in polymer solution, *J. Phys. Chem.*, 98, 13612-13615, (1994)
33. Sakamoto, T., Nakamura, H., Uedaira, H. and Wada, A., High-frequency dielectric relaxation of water bound to hydrophilic silica gels, *J. Phys. Chem.*, 93, 357-366, (1989)
34. Mashimo, S., Kuwabara, S., Yagihara, S. and Higasi, K., Dielectric relaxation time and structure of bound water in biological materials, *J. Phys. Chem.*, 91, 6337-6338, (1987)
35. Pathmanathan, K. and Johari, P., Dielectric and conductivity relaxations in poly(hema) and of water in its hydrogels, *J. Polym. Sci.: Part B: Polymer Phys.*, 28, 675-689, (1990)
36. Gestblom, B., Dielectric relaxation time of bound water in biological materials, *J. Phys. Chem.*, 95, 6064-6066, (1991)
37. Lee, H.B., Jhon, M.S. and Andrade, J.D., Nature of water in synthetic hydrogels 1. Dilatometry, specific conductivity and differential scanning calorimetry of polyhydroxyethyl methacrylate, *J. Colloid Interface Sci.*, 51, 225-231, (1975)
38. Jhon, M.S. and Andrade, J.D., Water and hydrogels, *J. Biomed. Mater. Res.*, 7, 509-552, (1973)
39. Nairn, J.B. and Jiang, T., Measurement of the friction and lubricity properties of contact lenses, ANTEC 95
40. Larsen, D.W., Huff, J.W. and Holden, B.A., Proton NMR relaxation in hydrogel contact lenses: correlation with *in vivo* lens dehydration data, *Current Eye Res.*, 9, 697-706, (1990)
41. Patel, S., Effects of lens dehydration on back vertex power, apical height and lens mass of high water content hydrogel lenses, *Int. Contact Lens Clin.*, 10, 38-42, (1983)

42. Mousa, G.Y., Callendar, M.G., Sivak, J.G. and Egan, D.J., The effects of the hydration characteristics of hydrogel lenses on the refractive index. *Int. Contact Lens Clin.*, 10, 31-37, (1983)
43. Fatt, I., Changes in dimensions of soft contact lenses while on the eye, *Optician*, 185, 11, 4782, (1983)
44. McNally, J.J., Chalmers, R.L. and Payor, R., Corneal epithelial disruption with extremely thin hydrogel lenses, *Clin. Exp. Optom.*, 70, 106-111, (1987)
45. Holden, B.A., Sweeney, D.F. and Seger, R.G., Epithelial erosions caused by thin high water content lenses, *Clin. Exp. Optom.*, 69, 103-107, (1986)
46. LaHood, D., Sweeney, D. and Holden, B.A., Overnight corneal edema with hydrogel, rigid gas permeable and silicone elastomer contact lenses. *Int. Contact Lens Clin.*, 15, 149-154, (1988)
47. Efron, N. and Young, G., Dehydration of hydrogel contact lenses *in vitro* and *in vivo*, *Ophthal. Physiol. Opt.*, 8, 253-256, (1988)
48. Fatt, I. and DiMartino, R.B., Water content of a hydrogel lens on the eye, *Optician*, 190, 19-22, (1985)
49. Brennan, N.A., Lowe, R., Efron, N. and Harris, M.G., In vivo dehydration of disposable (Acuvue) contact lenses, *Optom. Vision Sci.*, 67, 201-203, (1990)
50. Efron, N., Brennan, N.A., O'Brien, K.A. and Murphy, P.J., Surface hydration of hydrogel contact lenses, *Clin. Exp. Optom.*, 69, 219-222, (1986)
51. Cedarstaff, T.H. and Tomlinson, A., A comparative study of tear evaporation rates and water content of soft contact lenses, *Am. J. Opt. Physiol. Opt.*, 60, 167-174, (1983)
52. Hovding, G., The fluid content of hydrophilic contact lenses on the eye, *Acta Ophthalmol (Kbh)*, 61, 889-897, (1983)
53. Mirejovsky, D., Patel, A.S. and Young, G., Water properties of hydrogel contact lens materials: a possible predictive model for corneal desiccation staining, *Biomaterials*, 14, 1080-1088, (1993)
54. Brennan, N.A., Lowe, R., Efron, N., Ungerer, J.L. and Carney, L.G., Dehydration of hydrogel lenses during overnight wear, *Am. J. Opt. Physiol. Opt.*, 64, 534-539, (1987)
55. Pritchard, N. and Fonn, D., Dehydration, lens movement and dryness ratings of hydrogel contact lenses, *Ophthal. Physiol. Opt.*, 15, 281-286, (1995)
56. Martin, D.K., Water transport in dehydrating hydrogel contact lenses: Implications for corneal desiccation, *J. Biomed. Mater. Res.*, 29, 857-865, (1995)

57. Andrasko, G., Hydrogel dehydration in various environments, *Int. Contact Lens Clin.*, 10, 22-28, (1983)
58. Brennan, N.A. and Efron, N., Hydrogel lens dehydration: A material-dependent phenomenon?, *Contact Lens Forum*, 28-29, (1987)
59. Baker, D. and Tighe, B.J., Polymers in contact lens applications (VIII). The problem of biocompatibility, *Contact Lens J.*, 10, 3, 3-14, (1981)
60. Baier, R.E., Dutton, R.C. and Gott, V.L., Surface chemical features of blood vessel walls and of synthetic materials exhibiting thromboresistance. in *Advances in Experimental Medicine*, Vol. 7, Surface chemistry of biological surfaces, Plenum Press, New York, 235-260, (1970)
61. Andrade, J.D., Interfacial phenomena and biomaterials, *Medical Instrumentation*, 7, 110-120, (1973)
62. Coleman, D.L., Gregonis, D.E. and Andrade, J.D., Blood-materials interactions: The minimum interfacial free energy and the optimum polar/apolar ratio hypothesis, *J. Biomed. Mater. Res.*, 16, 381-393, (1982)
63. Ratner, B.D., Hoffman, A.S., Hanson, S.R., Harker, S.R. and Whiffen, J.D., Blood compatibility-water content relationships for radiation grafted hydrogels, *J. Polym. Sci. Polym. Symp.*, 66, 363-375, (1979)
64. Okano, T., Nishiyama, S., Shinohara, I., Akaike, T. and Sakurai, Y., Interaction between plasma protein and microphase separated structure of copolymers, *Polymer J. (Tokyo)*, 10, 223-228, (1978)
65. Smith, L., Doyle, C., Gregonis, D.E. and Andrade, J.D., Surface oxidation of cis-trans polybutadiene, *J. Appl. Polym. Sci.*, 26, 1269-1276, (1982)
66. Andrade, J.D., Smith, L.M. and Gregonis, D.E., The contact angle and interface energetics in *Biomedical Polymers*, Vol. 1, J.D. Andrade Ed., New York, Plenum, 249-292, (1985)
67. Young, T., On the cohesion of fluids, *Phil. Trans. Roy. Soc. (London)*, 95, 65-87, (1805)
68. Dupre, A., *Theorie mechanique de la chaleur*, Guthier Villars, Paris, 369, (1869)
69. Owens, D.K. and Wendt, R.C., Estimation of the surface free energy of polymers, *J. Appl. Polym. Sci.*, 13, 1741-1747, (1969)
70. Panzer, J., Components of solid surface free energy from wetting measurements, *J. Colloid and Interface Sci.*, 44, 142-161, (1973)
71. Hamilton, W.C., A technique for the characterisation of hydrophilic solid surfaces, *J. Colloid Interface Sci.*, 40, 219-222, (1972)

72. Hamilton, W.C., Measurement of the polar force contribution to adhesive bonding, *J. Colloid Interface Sci.*, 47, 672-675, (1974)
73. Fowkes, F.M., Determination of interfacial tensions, contact angles and dispersion forces in surfaces by assuming additivity of intermolecular interactions in surfaces, *J. Phys. Chem.*, 66, 382, (1962)
74. Tamai, Y., Makuuchi, K. and Suzuki, M., Experimental analysis of interfacial forces at the plane surfaces of solids, *J. Phys. Chem.*, 71, 4176-4179, (1967)
75. Adamson, A.W., Physical chemistry of surfaces, 3rd Edn., Wiley-Interscience, New York, N.Y., (1976)
76. Andrade, J.D., King, R.N., Gregonis, D.E. and Coleman, D.L., Surface characterisation of poly(hydroxyethyl methacrylate) and related polymers I. Contact angle methods in water, *J. Appl. Polym. Sci., Polym. Symp.*, 66, 313-336, (1979)
77. Holly, F.J. and Refojo, M.F., Wettability of hydrogels I. Poly(2-hydroxyethyl methacrylate), *J. Biomed. Mater. Res.*, 9, 315-322, (1975)
78. Morra, M., Occhiello, E. and Garbassi, F., On the wettability of poly(2-hydroxyethyl methacrylate), *J. Colloid Interface Sci.*, 149, 84-91, (1992)
79. Corkhill, P.H., Novel Hydrogel Polymers, Ph.D. Thesis, Aston University, (1988)
80. Anseth, K.S., Bowman, C.N. and Brannon-Peppas, L., Mechanical properties of hydrogels and their experimental determination-review, *Biomaterials*, 17, 1647-1657, (1996)
81. Trevett, A.S. and Tighe, B.J., The characterisation of mechanical properties of soft contact lenses, *British Contact Lens Association Transactions, Annual Clinical Conference, Glasgow*, 57-61, (1990)
82. LaPorte, R.J., *Hydrophilic Polymer Coatings for Medical Devices: Structure/Properties, Development, Manufacture and Applications*, Technomic Publishing Company, Lancaster, P.A., (1997)
83. Ikada, Y. and Uyama, Y., *Lubricating Polymer Surfaces*, Technomic Publishing Company, Lancaster, P.A., (1993)
84. Alfrey, T. and Goldfinger, G., The mechanism of copolymerisation, *J. Chem. Phys.*, 12, 205-209, (1944)
85. Mayo, F.R. and Lewis, F.M., Copolymerisation I. A basis for comparing the behaviour of monomers in copolymerisation; the copolymerisation of styrene and methyl methacrylate, *J. Am. Chem. Soc.*, 66, 1594-1601, (1944)

86. Ashraf, N., Sequence distributions in free radical polymerisations, Ph.D. thesis, Aston University, (1993)
87. Alfrey, T. and Price, C.C., Relative reactivities in vinyl copolymerisation, *J. Polym. Sci.*, 2, 101-106, (1947)
88. Varma, I.K. and Patnaik, S., Copolymerisation of 2-hydroxyethyl methacrylate with alkyl acrylate, *Eur. Polym. J.*, 12, 259-261, (1976)
89. Harwood, L.M. and Moody, C.J., *Experimental Organic Chemistry*, Blackwell Scientific Publications, London, (1989)
90. Trevett, A.S., The Mechanical Properties of Hydrogel Copolymers, Ph.D. Thesis, Aston University, (1991)
91. Martin, D.K. and Holden, B.A., Forces developed beneath hydrogel contact lenses due to squeeze pressure, *Phys. Med. Biol.*, 30, 635, (1986)
92. Rubenstein, R.Y., *Simulation and the Monte Carlo Method*, John Wiley & Sons, New York, N.Y., (1981)
93. Fatt, I., A predictive model for dehydration of a hydrogel contact lens in the eye, *J. Brit. Contact Lens Assoc.*, 12, 15-31, (1989)
94. Mirejovski, D., Patel, A.S. and Rodriguez, D.D., Effect of proteins on the water and transport properties of various hydrogel contact lenses, *Curr. Eye Res.*, 10, 187-196, (1991)
95. Kohler, J.E. and Flanagan, G.W., Clinical dehydration of extended wear lenses, *Int. Contact lens Clin.*, 12, 152-161, (1985)
96. McCarey, B.E. and Wilson, L.A., pH, osmoalinity and temperature effects on the water content of hydrogel contact lenses, *Contact Intraocul. Lens Med. J.*, 8, 158-167, (1982)
97. Carney, L.G. and Hill, R.M., Hydrogen ion concentration of human tears: effects of prolonged eye closure, *Arch. Ophthalmol. (Paris)*, 36, 835-838, (1976)
98. Fatt, I. and Chaston, J., Temperature of a contact lens on the eye, *Int. Contact Lens Clin.*, 7, 195-198, (1980)
99. Terry, J.E. and Hill, R.M., Human tear osmotic pressure: Diurnal variations and the closed eye, *Arch. Ophthalmol.*, 96, 120-122, (1978)
100. Osborn, G.N. and Zantos, S.G., Corneal desiccation staining with thin high water content contact lenses, *CLAO J.*, 14, 81-85, (1988)
101. Brennan, N.A., A simple instrument for measuring the water content of hydrogel lenses, *Int. Contact Lens Clin.*, 10, 357-362, (1983)

102. Fatt, I., A new procedure for measuring a water transport characteristic of dehydrating hydrogels - how this characteristic controls dehydration of the lens in the eye, *Int. Contact Lens Clin.*, 17, 144-150, (1990)
103. Peniche, C., Cohen, M., Vaquez, B. and San Roman, J., Water sorption of flexible networks based on 2-hydroxyethyl methacrylate - triethyleneglycol dimethacrylate copolymers, *Polymer*, 38, 24, 5977-5982 (1997)
104. Hyde, T. and Gladden, L., Simultaneous measurement of water and polymer concentration profiles during swelling of poly(ethylene oxide) using magnetic resonance imaging, *Polymer*, 39, 4, 811-819 (1998)
105. Maffezzoli, A., Luprano, A., Montagna, G. and Nicolais, L., Ultrasonic characterisation of water sorption in poly(2-hydroxyethyl methacrylate) hydrogels, *J. Appl. Polym. Sci.*, 67, 823-831 (1998)
106. Ma, J.J., Franklin, V.J., Tonge, S.R. and Tighe, B.J., Ocular compatibility of biomimetic hydrogels, *Poster presented at BCLA 9th Annual Clinical Conference*, Torquay, May, (1994)
107. Artoni, G., Gianazza, E., Zanoni, M., Gelfi, C., Tanzi, M.C., Barozzi, C., Ferruti, P. and Righetti, P.G., Fractionation techniques in hydro-organic environment II. Acryloylmorpholine polymers as matrix for electrophoresis in hydro-organic solvents, *Analytical Biochemistry*, 137, 420-428, (1984)
108. Tighe, B.J. and Gee, H., Kelvin contact lenses, U.S. Patent 4,430,458, (1984)
109. Ma, J.J., Novel hydrogel polymers, Ph.D. thesis, Aston University, (1995)
110. Feil, H., Bae, Y.H., Feijen, J. and Kim, S.W., Mutual influence of pH and temperature on the swelling of ionizable and thermosensitive hydrogels, *Macromolecules*, 25, 5528-5530, (1992)
111. Khare, A.R. and Peppas, N.A., Investigation of hydrogel water in polyelectrolyte gels using differential scanning calorimetry, *Polymer*, 34, 22, (1993)
112. Jar, P-Y. and Wu, Y.S., Effect of counter-ions on swelling and shrinkage of polyacrylamide based ionic gels, *Polymer*, 38, 10, (1997)
113. Baker, J., Stephens, D., Blanch, H. and Prausnitz, J., Swelling equilibria for acrylamide based polyampholyte hydrogels, *Macromolecules*, 25, 1955-1958, (1992)
114. Tong, Z. and Liu, X., Swelling equilibria and volume phase transitions in hydrogels with strongly dissociating electrolytes, *Macromolecules*, 27, 844-848, (1994)

115. Zhou, W., Yao, K. and Kurth, M., Studies of cross-linked poly(AM-MSAS-AA) gels I. Synthesis and characterisation, *J. Appl. Polym. Sci.*, 64, 1000-1007, (1997)
116. Zhou, W., Yao, K. and Kurth, M., Studies of cross-linked poly(AM-MSAS-AA) gels II. Effects of polymerisation conditions on the water absorbency. *J. Appl. Polym. Sci.*, 64, 1009-1014, (1997)
117. Lee, W. and Wu, R., Superabsorbent polymeric materials II. Swelling behaviour of cross-linked poly[sodium acrylate-co-3-dimethyl (methacryloyloxyethyl) ammonium propane sulphonate] in aqueous salt solution, *J. Appl. Polym. Sci.*, 64, 1701-1712, (1997)
118. Knoesei, R., Ehrmann, M. and Galin, J., Poly(ammonium sulfopropylbetaine)s 5. Interactions in dilute aqueous solution with low molecular weight salts or zwitterions and with poly(electrolyte)s, *Polymer*, 34, 9, 1925-1932, (1993)
119. Baker, J., Blanch, H. and Prausnitz, J., Swelling properties of acrylamide based ampholytic hydrogels: comparison of experiment with theory, *Polymer*, 36, 5, 1061-1069, (1995)
120. Fushimi, H., Ando, I. and Iijima, T., States of water in cationically charged poly(vinyl alcohol) membranes, *Polymer*, 32, 2, 241-248, (1991)
121. French K.A., Novel cationic polymers for use at biological interfaces, Ph.D. thesis, Aston University, (1996)
122. Ikada, Y., Suzuki, M. and Tamada, Y., Polymer surfaces possessing minimal interaction with blood components, in *Polymers as Biomaterials*, Shalaby, S., Hoffman, A., Ratner, B. and Horbett, T., eds, Plenum, New York, 135-147, (1984)
123. Kalachandra, S. and Shah, D.O., Polymers as ophthalmic lubricating agents, *Mat. Res. Soc. Symp. Proc.*, 110, 463-469, (1989)
124. Ichijima, E., Kobayashi, H., Ikada, Y., Akita, J. and Ikeuchi, K., An estimation method for the friction between a contact lens and corneal models, *Japanese Soc. Biomater. Prep.*, 95, (1989)
125. Franklin, V., Tonge, S. and Tighe, B.J., Disclosure - the true story of multipurpose solutions, *Optician*, 5500, 25-28, (1995)
126. Janule, V.P., On-site surface and wetting tension measurements of water based coatings and substrates, *Pigment and Resin Technology*, 24, 1, (1995)
127. Holly, F.J., Artificial tear formulations, *Int. Ophthalmol. Clin.*, 20, 171, (1980)

Appendix I

Corneal Staining and Water Binding Data for Hydrogel Contact Lenses

Stain scores and physical properties of contact lenses cleaned with ReNu

Lens	Stain Score	Standard Deviation	EWC %	Centre Thickness mm
Medalist 66	0.90	1.5	66	0.10
Focus	0.59	0.6	55	0.10
Surevue	0.85	1.0	58	0.11
Rythmic	1.50	1.4	73	0.15
Precision	0.80	0.7	74	0.14

Percentage of EWC present as bound water after soaking in the following solutions

Lens	ReNu %	Saline %	Water %	Packing Solution %
Medalist 66	40.39	48.06	44.52	47.18
Focus	54.87	70.89	78.36	71.89
Surevue	41.60	53.78	61.22	49.36
Rythmic	33.25	44.27	38.47	43.78
Precision	34.00	43.07	40.73	44.43

Stain scores and physical properties of contact lenses cleaned with Peroxide

Lens	Stain Score	Standard Deviation	EWC %	Centre Thickness mm
Z6	1.10	1.37	38	0.06
DR40	0.75	0.78	40	0.06
Classic	0.50	0.67	42	0.06
Surevue	1.10	2.30	58	0.11
Excelens	1.20	1.09	64	0.12
ES70	0.82	1.14	70	0.14
Rythmic	1.00	1.00	73	0.15

Percentage of EWC present as bound water after soaking in the following solutions

Lens	Peroxide %	Saline %	Water %	Packing Solution %
Z6	77.47	82.85	80.37	82.79
DR40	53.60	73.44	62.28	81.00
Classic	76.90	80.60	77.86	80.57
Surevue	80.88	53.78	61.22	49.36
Excelens	63.89	51.38	41.31	56.20
ES70	38.13	44.36	36.57	43.11
Rythmic	36.14	44.27	38.47	43.78

Appendix II

Sequence Distributions for Hydrogel Copolymers

Computer simulated sequence distribution of HEMA:AMO (70:30) copolymer

70% of Monomer A=HEMA

30% of Monomer B=AMO

$r(AB) = 3.79$

$r(BA) = 0.21$

```
00X00000000000X00X0000000000000X00000000000000000000
X000000000000X00X0X00000X0000000000000000000000000000
00X0000000000000X00000000000000X00000000000000000000
000000000000000000000000000000X0000X0000000X0X00000
000000000X0000X00000000000000X0X00X0000000000000000
0000000X000X000X0X0000000000X0000X0X0X00000000X0
00000X000000000000XX000000000000000000000000X000X00
0000X000000X00000000000000X0000X000000X00X0000000
00X000000000000000000000X00000X000000000000000000
00000X00000000000000000000000000X0000000000000000
0000000000000X0000X00000000000X000X00000000000000
00000000000000X00000000X0000000X00000000000000X0X0
X000000XX00000000X00000000000X0X000000000000X0000
00000000000XX0000000000000000000000X0000X000000000
00000000000000000000000000000X00XX0000X0X000000000
0000000000000X000000X000000000000000000XX0X0X00000
0000000000XX00X00X00XX0000X0X0000000000XX00X00000X
0X00X0000000X0000000000X000000000000X00000000000
00X0000XX000X00X00X00X00000000000000X0000X0X0000
0000X000X000X00000000000000000000000000000000XX00
X00X00000000X0000000000X000000X0000000000X000000
00000000X0000X0X0000000X000X0000000X000X0000000
00X000X00XX0XX000X0X0000XXX00X0000X0X0000000X000
00000000X0X00000X0X000000XXX00X000000000000000X00
XX000000X000XX0000000X0000000X00X0XX0X000X0000X0
000X0000000000000000X00X00X0X0XX00XX0000000X00XX0X
00000X0X00X0X0X0X0000X0X00000X000000X0X0X000000X
X000000X00000000X00X00000X0X00XX0000X0X0000XX000
X0X0000000X0XXX0XXXX000X0000X0X000X000000X000X00
0XX000XXX00000X000000X00X0XX0X0X0000X00X00000000
00X0X00X00X00000XX0000X00X0XX00000000XX0000XX0X
000X0XX00XX00X0X0X00X0000X00XX0X0XXX000X0X00X00X
00XX0X00X0000X00X00XX00X0000000X000X0000XXXXX0X00
X0XX000000X00XX000X00XXXXX0X0000XX0000XX0XXX00X00
000XX0000X000000000XXXX00XX0000X0XXX0000XX00X00X0
0XXX0X0000XXXX0X00X0XXX0XX0XX0X00XXXXX0XX00X0XX0
X00X00XXX0XX0X00X0X0X00XX0X00XXXXXXX0XXX00XXXXXX
00XXXXXXXXXXXXXXXXXXXXXXXXXXXXXXXXXXXXXXXXXXXXXXXXXXXX
XXXXXXXXXXXXXXXXXXXXXXXXXXXXXXXXXXXXXXXXXXXXXXXXXXXXXXXX
XXXXXXXXXXXXXXXXXXXXXXXXXXXXXXXXXXXXXXXXXXXXXXXXXXXXXXXX
XXXXXXXXXXXXXXXXXXXXXXXXXXXXXXXXXXXXXXXXXXXXXXXXXXXXXXXX
XXXXXXXXXXXXXXXXXXXXXXXXXXXXXXXXXXXXXXXXXXXXXXXXXXXXXXXX
```

The simulation represents polymerisation to 100% conversion

In the simulated copolymer HEMA is represented by O and AMO by X

The simulated copolymer contains 1400 HEMA units and 600 AMO units

Sequence Distributions

Length	HEMA	AMO
1	73	214
2	62	44
3	24	12
4	31	3
5	9	3
6	17	1
7	10	1
8	9	0
9	2	0
10	7	0
11	4	0
12	6	0
13	4	0
14	3	0
15	3	0
16	3	0
18	1	0
20	1	0
21	3	0
23	1	0
27	4	0
31	1	0
35	1	0
45	1	0
222	0	1

Computer simulated sequence distribution of HEMA:NNDMA (70:30) copolymer

70% of Monomer A=HEMA

30% of Monomer B=NNDMA

$$r(AB) = 1.56$$

$$r(BA) = 0.34$$

00000X000X000000000X00X000000X00XX0X000000X000X0
000000000XXX00X00XX000X0000X0X0X0000X0000X000X000X00
00000X0X000X000000000X0X0X0X0000000000X000XX0000
000XX00XX0000000000000000000000000X00XXX00X0000000000000
0X00X0000X00X00000000XX00000000X0000000X000X00X0X
X0000000X00000000000000X000X0000X0000000X0X000X0000
00X00000000X0X00X000XX00000X00X0000000X000X00X00
000000000000000X00000000000X0000X0X000000X000X000
0X000000000X00000000000X00000000000X00X00X000000
0X0X0X000X0X0X000000X000000000X0000000XX0X000000
00000000X0X0000X00X00X0000X0X00X00000000X0X00X00
X00000X00000X00XX000X0X0X000X000X000000XX000X0000
00000X0X00000000000000XX0X0X000000XX00X0X000000X0
X0000000000000000X000X0X00X0000000XX0X0X00X00000
00000X00000000000000XX000X0000000000000000000000X0X0X
000X0X0000000X00000X0000X00000000X0000000000000000
0X00XX000000X000000X000X0000000X00X0X000X0000X00
X0X0X000XXX0X00X000000000XX0X00X000X00X000000000X
0000000X000000X0XXX00000X000000X00X00X000X0000X0
0000X0000X0X00XXX0X00X0X000X000X0000X00X00X0XX0
0000000X0000X000000000000000X0XX0000000XX000XXXX
00000000000X000X0000000X00XX0X00XX0X0X00000X0000
00000X000000XX00X000X000X0X00000X00X00000000X0X
0000XX00X000XX000X00XX0X000X0000000XX0000X0X0000
000X0000000000X0000X000X0X0X00000000X0X0000X000X
000X000000XX000X0X000X00000000XX0000000000XX00X000
XXX000X0000X0X000X00X0XX000X000000X00X000X00X0X00
00X0X000XX00X0000000XX00X0X0X00XX0X0XX000X0XX000
X0X000X000X000000000X00X00000X0X000000XX00000X0X
0X0X00X000X000X0X0XXX000X000000X0000X000X000X00X
0XX00000X0000X0X00XX00X0X0X0XX0000X000X00X0X000X
000XX0X0000XX00X000X0X000X00X000X0XX0X0XX0XX00X0
0000X0XXXX0X000000X00X00X00X000XX000X0000XX000000
0000X00X00X0X0000X0000000000XXXX0X0X00000000000000
00000X0X0000X0XXX0XXX00000XX00X0XX0000X0X00000X00
00X0X0000X00X00X00X00XXXX00000000XXX0XX00X0XX00000
0X0X0X0XXX000000000XXXXX0XX000X0X0X00X0XXXXXX0X
00000X0X0X000X00X0X00X0XX00X00XXX00X00XXXX0X0000
000X0X0X0000X00X0X000X0XXXX0X0XXX00XX0XX0XXX00XX
00000XX0X0XXX00XX00X0X0X0XX00XXXX000XXXX0XXXXXXX
X0XX0X0XXX0XXXXXXXXXX0X0X00X0XXXXXXXXXXXXXXXXXXXXX
XXXXXXXXXXXXXXXXXXXXXXXXXXXXXXXXXXXX

The simulation represents polymerisation to 100% conversion

In the simulated copolymer HEMA is represented by O and NNDMA by X
The simulated copolymer contains 1400 HEMA units and 600 NNDMA units

Sequence Distributions

Length	HEMA	NNDMA
1	130	319
2	83	60
3	67	15
4	31	9
5	20	1
6	18	1
7	18	0
8	10	1
9	9	0
10	5	1
11	5	0
12	3	0
14	2	0
15	2	0
16	2	0
17	1	0
18	2	0
51	0	1

Computer simulated sequence distribution of HEMA:NVP (70:30) copolymer

70% of Monomer A=HEMA

30% of Monomer B=NVP

$$r(AB) = 4.43$$

$$r(BA) = 0.04$$

00X00000000000000000000000000000000X00000X00X0X000000000
X0000000000000000X000X000X0X000000000X00X00000000000
X000X
000X00000000000000
00X00X0000X000000000000000000000000X00X00000X0000000000X
X0000000000X00000X000X000000000X000X0000X00X0000
00000000X0000000000000000000X00X000000000000000X00000
00X00000000000X000000X0000000000000000X000X0000000
X00000000X00000000000X000000X0000X000XX000000000
X00000000X00000000000000000000000000000000000000X0000
00X00000X000X00000000X0X00000000000000000000000000X0000
X0000000000000X0000000000000000X00X0000000X0000000
00000000X00000000000000000000000000000000000000X0X0
0X00000000X00000X000000X00000000000000000000000000000
X0X0X0000X0000000000000000X0000000X0X0000000000000X
00000X00000X00000000000000000000000000000000000000XX0X0X
00000000000X000XX00000X00X00000X000000X0X000000X
0000X00000X00000000000X0X0X0000000000X0000000X00
00000000000000000000000000000000X0X000000X0000000000X
0000000X00000000X0000X0000X0000X00X0000X00X0000
00X00X0X00X
000X000X00000X000000X0X00000000X000X00X00000000
0000000000000000X000X0X0000X0000X0X0000X0000000000X
00000000X0X00X000X00X0000X00X0X0X0000000X00X00000
00000000X00XX00X00X000X0XX0X00X000000X0X000000X0
000000X00X000000X000X00X000X000XX0000XX0X00X000X
0X000X0X0XX0X0X00000X0X0X0X0XX0X0XXX00XX0X0X0X00
X0X0X00XX000X0X0000XX0X00X0X0X0X0X0XX0XXX00000X
0X0X0X0X0XX
XX
XX
XX
XX
XX
XX
XX

The simulation represents polymerisation to 100% conversion

In the simulated copolymer HEMA is represented by O and NVP by X

The simulated copolymer contains 1400 HEMA units and 600 NVP units

Sequence Distributions

Length	HEMA	NVP
1	75	244
2	37	19
3	27	1
4	23	1
5	19	0
6	16	0
7	12	0
8	8	0
9	5	0
10	7	0
11	6	0
12	3	0
13	8	0
14	3	0
15	2	0
16	3	0
17	2	0
18	1	0
19	2	0
21	1	0
23	1	0
25	1	0
28	1	0
32	1	0
33	1	0
46	1	0
311	0	1

Appendix III

Water Binding Data for Hydrogel Copolymers

Copolymer Composition	Equilibrium Water Content %	Freezing Water Content ‰	Bound Water Content ‰
AMO-HEMA 70:30	69.6±0.5	56.1±0.5	13.5±0.5
AMO:HEMA:NVI 70:30:2½	71.1±0.5	55.7±0.5	15.4±0.5
AMO:HEMA:NVI 70:30:5	71.8±0.5	53.4±0.5	18.4±0.5
AMO:HEMA:NVI 70:30:7½	72.2±0.5	55.4±0.5	16.8±0.5
AMO:HEMA:NVI 70:30:10	72.5±0.5	54.9±0.5	17.6±0.5
AMO:HEMA:DMAEMA 70:30:2½	74.3±0.5	60.5±0.5	13.8±0.5
AMO:HEMA:DMAEMA 70:30:5	75.9±0.5	58.1±0.5	17.8±0.5
AMO:HEMA:DMAEMA 70:30:7½	72.4±0.5	61.6±0.5	10.8±0.5
AMO:HEMA:DMAEMA 70:30:10	78.8±0.5	58.4±0.5	20.4±0.5
AMO:HEMA:DMAEA 70:30:2½	72.3±0.5	58.3±0.5	14.0±0.5
AMO:HEMA:DMAEA 70:30:5	75.4±0.5	61.6±0.5	13.8±0.5
AMO:HEMA:DMAEA 70:30:7½	76.8±0.5	62.8±0.5	14.0±0.5
AMO:HEMA:DMAEA 70:30:10	78.2±0.5	61.9±0.5	16.3±0.5
AMO:HEMA:PNO 70:30:2½	71.7±0.5	53.6±0.5	18.1±0.5
AMO:HEMA:PNO 70:30:5	72.6±0.5	54.3±0.5	18.3±0.5
AMO:HEMA:PNO 70:30:7½	72.6±0.5	54.9±0.5	17.7±0.5
AMO:HEMA:PNO 70:30:10	73.3±0.5	56.6±0.5	16.7±0.5
AMO:HEMA:4-VP 70:30:2½	68.6±0.5	52.5±0.5	16.1±0.5
AMO:HEMA:4-VP 70:30:5	68.5±0.5	50.9±0.5	17.6±0.5
AMO:HEMA:4-VP 70:30:7½	68.7±0.5	54.2±0.5	14.5±0.5
AMO:HEMA:4-VP 70:30:10	67.4±0.5	50.0±0.5	17.4±0.5

Copolymer Composition	Moles Of Water / Mole Of Polymer	Moles Of Free Water / Mole Of Polymer	Moles Of Bound Water / Mole Of Polymer
AMO-HEMA 70:30	17.7	14.2	3.5
AMO:HEMA:NVI 70:30:2 ¹ / ₂	18.6	14.6	4.0
AMO:HEMA:NVI 70:30:5	19.0	14.1	4.9
AMO:HEMA:NVI 70:30:7 ¹ / ₂	19.2	14.7	4.5
AMO:HEMA:NVI 70:30:10	19.3	14.6	4.7
AMO:HEMA:DMAEMA 70:30:2 ¹ / ₂	22.0	17.9	4.1
AMO:HEMA:DMAEMA 70:30:5	24.2	18.5	5.7
AMO:HEMA:DMAEMA 70:30:7 ¹ / ₂	20.2	17.2	3.0
AMO:HEMA:DMAEMA 70:30:10	28.7	21.3	7.4
AMO:HEMA:DMAEA 70:30:2 ¹ / ₂	20.0	16.1	3.9
AMO:HEMA:DMAEA 70:30:5	23.5	19.2	4.3
AMO:HEMA:DMAEA 70:30:7 ¹ / ₂	25.4	20.7	4.7
AMO:HEMA:DMAEA 70:30:10	27.5	21.8	5.7
AMO:HEMA:PNO 70:30:2 ¹ / ₂	19.1	14.3	4.8
AMO:HEMA:PNO 70:30:5	19.8	14.8	5.0
AMO:HEMA:PNO 70:30:7 ¹ / ₂	19.6	14.8	4.8
AMO:HEMA:PNO 70:30:10	20.2	15.6	4.6
AMO:HEMA:4-VP 70:30:2 ¹ / ₂	16.6	12.7	3.9
AMO:HEMA:4-VP 70:30:5	16.4	12.2	4.2
AMO:HEMA:4-VP 70:30:7 ¹ / ₂	16.4	12.9	3.5
AMO:HEMA:4-VP 70:30:10	15.4	11.4	4.0

Copolymer Composition	Equilibrium Water Content %	Freezing Water Content %	Bound Water Content ‰
AMO-HEMA-NVI-ITA 70:30:3 ³ / ₄ :1 ¹ / ₄	70.3±0.5	54.3±0.5	16.0±0.5
AMO-HEMA-NVI-ITA 70:30:3 ¹ / ₃ :1 ² / ₃	70.9±0.5	54.6±0.5	16.3±0.5
AMO-HEMA-NVI-ITA 70:30:2 ¹ / ₂ :2 ¹ / ₂	67.8±0.5	52.7±0.5	15.1±0.5
AMO-HEMA-NVI-ITA 70:30:1 ² / ₃ :3 ¹ / ₃	68.2±0.5	55.7±0.5	12.5±0.5
AMO-HEMA-NVI-ITA 70:30:1 ¹ / ₄ :3 ³ / ₄	67.3±0.5	55.9±0.5	11.4±0.5
AMO-HEMA-NVI-ITA 70:30:5 ¹ / ₆ :1 ¹ / ₆	72.5±0.5	56.2±0.5	16.3±0.5
AMO-HEMA-NVI-ITA 70:30:2 ¹ / ₂ :5	71.1±0.5	54.2±0.5	16.9±0.5
AMO-HEMA-NVI-ITA 70:30:3 ¹ / ₃ :6 ² / ₃	71.4±0.5	54.2±0.5	17.2±0.5
AMO-HEMA-NVI-ITA 70:30:5:10	70.5±0.5	50.5±0.5	20.0±0.5
AMO-HEMA-NVI-SPI 70:30:4:1	74.0±0.5	56.0±0.5	18.0±0.5
AMO-HEMA-NVI-SPI 70:30:3 ³ / ₄ :1 ¹ / ₄	74.1±0.5	54.0±0.5	20.1±0.5
AMO-HEMA-NVI-SPI 70:30:3 ¹ / ₃ :1 ² / ₃	73.1±0.5	55.4±0.5	17.7±0.5
AMO-HEMA-NVI-SPI 70:30:2 ¹ / ₂ :2 ¹ / ₂	74.6±0.5	59.1±0.5	15.5±0.5
AMO-HEMA-NVI-SPI 70:30:1 ² / ₃ :3 ¹ / ₃	76.3±0.5	61.5±0.5	14.8±0.5
AMO-HEMA-NVI-SPI 70:30:1 ¹ / ₄ :3 ³ / ₄	73.5±0.5	56.7±0.5	16.8±0.5
AMO-HEMA-NVI-SPI 70:30:1:4	75.5±0.5	66.4±0.5	9.1±0.5
AMO-HEMA-NVI-MAA 70:30:3 ³ / ₄ :1 ¹ / ₄	78.1±0.5	60.2±0.5	17.9±0.5
AMO-HEMA-NVI-MAA 70:30:3 ¹ / ₃ :1 ² / ₃	74.5±0.5	59.5±0.5	15.0±0.5
AMO-HEMA-NVI-MAA 70:30:2 ¹ / ₂ :2 ¹ / ₂	73.2±0.5	56.8±0.5	16.4±0.5
AMO-HEMA-NVI-MAA 70:30:1 ² / ₃ :3 ¹ / ₃	75±0.5	60.8±0.5	14.2±0.5
AMO-HEMA-NVI-MAA 70:30:1 ¹ / ₄ :3 ³ / ₄	75.1±0.5	60.9±0.5	14.2±0.5

Copolymer Composition	Moles Of Water / Mole Of Polymer	Moles Of Free Water / Mole Of Polymer	Moles Of Bound Water / Mole Of Polymer
AMO-HEMA-NVI-ITA 70:30:3 ³ / ₄ :1 ¹ / ₄	17.8	13.7	4.1
AMO-HEMA-NVI-ITA 70:30:3 ¹ / ₃ :1 ² / ₃	18.3	14.1	4.2
AMO-HEMA-NVI-ITA 70:30:2 ¹ / ₂ :2 ¹ / ₂	15.9	12.4	3.5
AMO-HEMA-NVI-ITA 70:30:1 ² / ₃ :3 ¹ / ₃	16.2	13.2	3.0
AMO-HEMA-NVI-ITA 70:30:1 ¹ / ₄ :3 ³ / ₄	15.6	13.0	2.6
AMO-HEMA-NVI-ITA 70:30:5 ⁵ / ₆ :1 ¹ / ₆	20.0	15.5	4.5
AMO-HEMA-NVI-ITA 70:30:2 ¹ / ₂ :5	18.5	14.1	4.4
AMO-HEMA-NVI-ITA 70:30:3 ¹ / ₃ :6 ² / ₃	18.7	14.2	4.5
AMO-HEMA-NVI-ITA 70:30:5:10	17.8	12.8	5.0
AMO-HEMA-NVI-SPI 70:30:4:1	21.5	16.3	5.2
AMO-HEMA-NVI-SPI 70:30:3 ³ / ₄ :1 ¹ / ₄	21.4	15.6	5.8
AMO-HEMA-NVI-SPI 70:30:3 ¹ / ₃ :1 ² / ₃	20.7	15.7	5.0
AMO-HEMA-NVI-SPI 70:30:2 ¹ / ₂ :2 ¹ / ₂	22.6	17.9	4.7
AMO-HEMA-NVI-SPI 70:30:1 ² / ₃ :3 ¹ / ₃	24.9	20.1	4.8
AMO-HEMA-NVI-SPI 70:30:1 ¹ / ₄ :3 ³ / ₄	21.6	16.7	4.9
AMO-HEMA-NVI-SPI 70:30:1:4	24.1	21.2	2.9
AMO-HEMA-NVI-MAA 70:30:3 ³ / ₄ :1 ¹ / ₄	26.6	20.5	6.1
AMO-HEMA-NVI-MAA 70:30:3 ¹ / ₃ :1 ² / ₃	21.8	17.4	4.4
AMO-HEMA-NVI-MAA 70:30:2 ¹ / ₂ :2 ¹ / ₂	20.4	15.8	4.6
AMO-HEMA-NVI-MAA 70:30:1 ² / ₃ :3 ¹ / ₃	22.3	18.1	4.2
AMO-HEMA-NVI-MAA 70:30:1 ¹ / ₄ :3 ³ / ₄	22.4	18.2	4.2

Appendix IV

Tensile Data for Hydrogel Copolymers

Copolymer Composition	Initial Modulus MPa	Tensile Strength MPa	Elongation At Break %
AMO-HEMA 70:30	0.15±0.01	0.17±0.02	121±17
AMO:HEMA:NVI 70:30:2½	0.15±0.01	0.19±0.04	127±20
AMO:HEMA:NVI 70:30:5	0.16±0.01	0.22±0.02	131±12
AMO:HEMA:NVI 70:30:7½	0.14±0.01	0.22±0.05	154±30
AMO:HEMA:NVI 70:30:10	0.14±0.01	0.16±0.03	120±22
AMO:HEMA:DMAEMA 70:30:2½	0.15±0.01	0.12±0.02	85±16
AMO:HEMA:DMAEMA 70:30:5	0.14±0.01	0.17±0.02	120±17
AMO:HEMA:DMAEMA 70:30:7½	0.12±0.01	0.12±0.04	103±34
AMO:HEMA:DMAEMA 70:30:10	0.11±0.01	0.06±0.03	62±30
AMO:HEMA:DMAEA 70:30:2½	0.15±0.01	0.20±0.04	134±19
AMO:HEMA:DMAEA 70:30:5	0.14±0.01	0.11±0.02	86±17
AMO:HEMA:DMAEA 70:30:7½	0.12±0.01	0.14±0.03	115±23
AMO:HEMA:DMAEA 70:30:10	0.12±0.01	0.12±0.03	106±26
AMO:HEMA:PNO 70:30:2½	0.15±0.01	0.12±0.05	92±30
AMO:HEMA:PNO 70:30:5	0.13±0.01	0.15±0.07	118±29
AMO:HEMA:PNO 70:30:7½	0.14±0.01	0.13±0.02	103±14
AMO:HEMA:PNO 70:30:10	0.13±0.01	0.11±0.05	89±42
AMO:HEMA:4-VP 70:30:2½	0.14±0.01	0.15±0.01	117±8
AMO:HEMA:4-VP 70:30:5	0.14±0.03	0.13±0.02	108±30
AMO:HEMA:4-VP 70:30:7½	0.13±0.02	0.16±0.02	140±27
AMO:HEMA:4-VP 70:30:10	0.12±0.01	0.14±0.03	128±25

Copolymer Composition	Initial Modulus MPa	Tensile Strength MPa	Elongation At Break %
AMO-HEMA-NVI-ITA 70:30:3 ³ / ₄ :1 ¹ / ₄	0.20±0.02	0.19±0.03	98±21
AMO-HEMA-NVI-ITA 70:30:3 ¹ / ₃ :1 ² / ₃	0.21±0.01	0.19±0.03	84±18
AMO-HEMA-NVI-ITA 70:30:2 ¹ / ₂ :2 ¹ / ₂	0.23±0.01	0.19±0.05	87±22
AMO-HEMA-NVI-ITA 70:30:1 ² / ₃ :3 ¹ / ₃	0.24±0.01	0.20±0.05	84±21
AMO-HEMA-NVI-ITA 70:30:1 ¹ / ₄ :3 ³ / ₄	0.24±0.01	0.20±0.02	85±8
AMO-HEMA-NVI-ITA 70:30:5 ⁵ / ₆ :1 ⁴ / ₆	0.20±0.01	0.18±0.01	93±6
AMO-HEMA-NVI-ITA 70:30:2 ¹ / ₂ :5	0.28±0.01	0.20±0.03	72±8
AMO-HEMA-NVI-ITA 70:30:3 ¹ / ₃ :6 ² / ₃	0.34±0.01	0.19±0.02	49±6
AMO-HEMA-NVI-ITA 70:30:5:10	0.49±0.02	0.19±0.04	38±9
AMO-HEMA-NVI-SPI 70:30:4:1	0.16±0.01	0.17±0.03	104±17
AMO-HEMA-NVI-SPI 70:30:3 ³ / ₄ :1 ¹ / ₄	0.16±0.01	0.15±0.02	98±16
AMO-HEMA-NVI-SPI 70:30:3 ¹ / ₃ :1 ² / ₃	0.16±0.01	0.15±0.01	98±12
AMO-HEMA-NVI-SPI 70:30:2 ¹ / ₂ :2 ¹ / ₂	0.15±0.01	0.15±0.01	102±9
AMO-HEMA-NVI-SPI 70:30:1 ² / ₃ :3 ¹ / ₃	0.17±0.01	0.14±0.01	88±12
AMO-HEMA-NVI-SPI 70:30:1 ¹ / ₄ :3 ³ / ₄	0.16±0.01	0.15±0.02	84±14
AMO-HEMA-NVI-SPI 70:30:1:4	0.17±0.01	0.12±0.01	72±5
AMO-HEMA-NVI-MAA 70:30:3 ³ / ₄ :1 ¹ / ₄	0.15±0.01	0.16±0.03	112±23
AMO-HEMA-NVI-MAA 70:30:3 ¹ / ₃ :1 ² / ₃	0.17±0.02	0.18±0.01	113±11
AMO-HEMA-NVI-MAA 70:30:2 ¹ / ₂ :2 ¹ / ₂	0.17±0.01	0.21±0.04	122±10
AMO-HEMA-NVI-MAA 70:30:1 ² / ₃ :3 ¹ / ₃	0.15±0.01	0.16±0.02	99±19
AMO-HEMA-NVI-MAA 70:30:1 ¹ / ₄ :3 ³ / ₄	0.17±0.01	0.16±0.07	111±34

Appendix V

Surface Properties of Hydrogel Copolymers in the Dehydrated state

Copolymer Composition	Water Contact Angle	CH ₂ I ₂ Contact Angle	Dispersive Component Of Surface Energy (mN/m)	Polar Component Of Surface Energy (mN/m)
AMO-HEMA 70:30	86 _{±2}	32 _{±2}	41.9 _{±2}	1.5
AMO:HEMA:NVI 70:30:2 ¹ / ₂	90 _{±2}	31 _{±2}	43.6 _{±2}	0.6
AMO:HEMA:NVI 70:30:5	97 _{±2}	34 _{±2}	44.1 _{±2}	0
AMO:HEMA:NVI 70:30:7 ¹ / ₂	97 _{±2}	34 _{±2}	44.1 _{±2}	0
AMO:HEMA:NVI 70:30:10	99 _{±2}	35 _{±2}	44.2 _{±2}	0
AMO:HEMA:DMAEMA 70:30:2 ¹ / ₂	98 _{±2}	37 _{±2}	42.7 _{±2}	0
AMO:HEMA:DMAEMA 70:30:5	99 _{±2}	39 _{±2}	41.8 _{±2}	0
AMO:HEMA:DMAEMA 70:30:7 ¹ / ₂	100 _{±2}	41 _{±2}	40.9 _{±2}	0
AMO:HEMA:DMAEMA 70:30:10	101 _{±2}	41 _{±2}	41.2 _{±2}	0
AMO:HEMA:DMAEA 70:30:2 ¹ / ₂	101 _{±2}	36 _{±2}	44.2 _{±2}	0
AMO:HEMA:DMAEA 70:30:5	102 _{±2}	37 _{±2}	43.9 _{±2}	0.1
AMO:HEMA:DMAEA 70:30:7 ¹ / ₂	100 _{±2}	35 _{±2}	44.4 _{±2}	0
AMO:HEMA:DMAEA 70:30:10	104 _{±2}	38 _{±2}	43.9 _{±2}	0.2

Copolymer Composition	Water Contact Angle	CH ₂ I ₂ Contact Angle	Dispersive Component Of Surface Energy (mN/m)	Polar Component Of Surface Energy (mN/m)
AMO-HEMA-NVI-ITA 70:30:3 ³ / ₄ :1 ¹ / ₄	98±2	36±2	43.3±2	0
AMO-HEMA-NVI-ITA 70:30:3 ¹ / ₃ :1 ² / ₃	94±2	34±2	43.2±2	0
AMO-HEMA-NVI-ITA 70:30:2 ¹ / ₂ :2 ¹ / ₂	95±2	45±2	36.9±2	0.5
AMO-HEMA-NVI-ITA 70:30:1 ² / ₃ :3 ¹ / ₃	98±2	38±2	42.1±2	0
AMO-HEMA-NVI-ITA 70:30:1 ¹ / ₄ :3 ³ / ₄	97±2	31±2	45.7±2	0
AMO-HEMA 70:30	86±2	32±2	41.9±2	1.5
AMO-HEMA-NVI-ITA 70:30: ⁵ / ₆ :1 ¹ / ₆	100±2	40±2	41.5±2	0
AMO-HEMA-NVI-ITA 70:30:1 ² / ₃ :3 ¹ / ₃	98±2	38±2	42.1±2	0
AMO-HEMA-NVI-ITA 70:30:2 ¹ / ₂ :5	97±2	37±2	42.4±2	0
AMO-HEMA-NVI-ITA 70:30:3 ¹ / ₃ :6 ² / ₃	90±2	38±2	39.8±2	0.9
AMO-HEMA-NVI-ITA 70:30:5:10	80±2	36±2	38.1±2	3.9

Appendix VI

Surface Properties of Hydrogel Copolymers in the Hydrated State

Copolymer Composition	Air Contact Angle	Octane Contact Angle	Dispersive Component Of Surface Energy (mN/m)	Polar Component Of Surface Energy (mN·m)
AMO-HEMA 70:30	40 _{±2}	140 _{±2}	17.1 _{±2}	39.8 _{±2}
AMO:HEMA:NVI 70:30:2 ¹ / ₂	38 _{±2}	141 _{±2}	18.1 _{±2}	40.2 _{±2}
AMO:HEMA:NVI 70:30:5	34 _{±2}	147 _{±2}	17.9 _{±2}	43.1 _{±2}
AMO:HEMA:NVI 70:30:7 ¹ / ₂	35 _{±2}	147 _{±2}	17.2 _{±2}	43.1 _{±2}
AMO:HEMA:NVI 70:30:10	32 _{±2}	150 _{±2}	17.8 _{±2}	44.4 _{±2}
AMO:HEMA:DMAEMA 70:30:2 ¹ / ₂	39 _{±2}	144 _{±2}	15.9 _{±2}	41.8 _{±2}
AMO:HEMA:DMAEMA 70:30:5	38 _{±2}	147 _{±2}	15.3 _{±2}	43.1 _{±2}
AMO:HEMA:DMAEMA 70:30:7 ¹ / ₂	39 _{±2}	144 _{±2}	15.9 _{±2}	41.8 _{±2}
AMO:HEMA:DMAEMA 70:30:10	30 _{±2}	149 _{±2}	19.5 _{±2}	44.0 _{±2}
AMO:HEMA:DMAEA 70:30:2 ¹ / ₂	40 _{±2}	139 _{±2}	17.6 _{±2}	39.3 _{±2}
AMO:HEMA:DMAEA 70:30:5	39 _{±2}	147 _{±2}	14.6 _{±2}	43.1 _{±2}
AMO:HEMA:DMAEA 70:30:7 ¹ / ₂	35 _{±2}	148 _{±2}	16.8 _{±2}	43.6 _{±2}
AMO:HEMA:DMAEA 70:30:10	31 _{±2}	149 _{±2}	18.5 _{±2}	44.0 _{±2}

Copolymer Composition	Air Contact Angle	Octane Contact Angle	Dispersive Component Of Surface Energy (mN/m)	Polar Component Of Surface Energy (mN/m)
AMO-HEMA-NVI-ITA 70:30:3 ³ / ₄ :1 ¹ / ₄	37±2	149±2	15.2±2	44.0±2
AMO-HEMA-NVI-ITA 70:30:3 ¹ / ₃ :1 ² / ₃	34±2	144±2	19.2±2	41.8±2
AMO-HEMA-NVI-ITA 70:30:2 ¹ / ₂ :2 ¹ / ₂	42±2	141±2	15.2±2	40.2±2
AMO-HEMA-NVI-ITA 70:30:1 ² / ₃ :3 ¹ / ₃	36±2	144±2	17.9±2	41.8±2
AMO-HEMA-NVI-ITA 70:30:1 ¹ / ₄ :3 ³ / ₄	33±2	152±2	16.5±2	45.2±2
AMO-HEMA 70:30	40±2	140±2	17.1±2	39.8±2
AMO-HEMA-NVI-ITA 70:30:5 ¹ / ₆ :1 ⁴ / ₆	37±2	147±2	15.9±2	43.1±2
AMO-HEMA-NVI-ITA 70:30:1 ² / ₃ :3 ¹ / ₃	36±2	144±2	17.9±2	41.8±2
AMO-HEMA-NVI-ITA 70:30:2 ¹ / ₂ :5	33±2	151±2	16.9±2	44.8±2
AMO-HEMA-NVI-ITA 70:30:3 ¹ / ₃ :6 ² / ₃	27±2	152±2	20.0±2	45.2±2
AMO-HEMA-NVI-ITA 70:30:5:10	26±2	153±2	20.2±2	45.6±2